

https://dspace.org/

Metabolites and lipoproteins profiles of a cohort of Pancreatic Ductal Adenocarcinoma patients and associated immune responses

Elebo, Nnenna

2022

https://hdl.handle.net/10539/35658

Downloaded from a DSpace repository. https://dspace.org/

Metabolites and lipoproteins profiles of a cohort of Pancreatic Ductal Adenocarcinoma patients and associated immune responses.



Nnenna Elebo

A thesis submitted in fulfilment of the requirement for the Degree of Doctor of Philosophy

DEPARTMENT OF SURGERY, FACULTY OF HEALTH SCIENCES,
UNIVERSITY OF WITWATERSRAND, JOHANNESBURG.

JULY 2022

DECLARATION

I, Nnenna Elebo declare that this thesis entitled "Metabolites and lipoproteins profiles of a cohort of Pancreatic Ductal Adenocarcinoma patients and associated immune responses" is my own unaided work. It is being submitted for the Degree of Doctor of Philosophy in the University of Witwatersrand, Johannesburg. It has not been submitted before for any degree or examination at any other university.



Nnenna Elebo

12th July, 2022

Date

DEDICATION

To my late Dad and brothers, I know you all are watching from above and hope I made you all proud.

To all the mothers, it is possible.

To my husband, my pillar and support, we did it!

PUBLICATIONS AND PRESENTATIONS

Publications arising from the study

- **Elebo N**., Fru P., Omoshoro JAO., Candy G and Nweke E.E (2020): Role of different immune cells and metabolic pathways in modulating the immune response in pancreatic cancer (Review). Molecular Medicine Reports 2020, 22, 4981. doi: http://dx.doi.org/10.3892/mmr.2020.11622 **Review Paper**

- **Elebo N**., Omoshoro JAO., Fru P., Devar J, De Wet van Zyl C., Vorster B.C., Smith M., Cacciatore S., Candy G and Nweke E.E (2021): Serum Metabolomic and Lipoprotein Profiling of Pancreatic Ductal Adenocarcinoma Patients of African Ancestry. Metabolites 2021, 11, 663. https://doi.org/10.3390/metabo11100663 **Original Paper**

Awards

- Postgraduate Merit Award University of Witwatersrand 2019-2021
- 3rd Prize Winner, Student Category, Bert Myburgh Research Forum November 2020

Local Conferences – Oral Presentations

- **Nnenna Elebo**, Jones Omoshoro-Jones, Pascaline Fru, John Devar, Smith M, Stefano Cacciatore, Geoffrey Candy, Ekene Nweke. *Metabolic profiling of a cohort of Pancreatic Ductal Adenocarcinoma (PDAC) patients of African descent using ^{1}H NMR spectroscopy analysis*. Bert Myburgh Research Forum, Department of Surgery, University of Witwatersrand, 25th November 2020.
- **Nnenna Elebo**, Jones Omoshoro-Jones, Pascaline Fru, John Devar, Christiaan De Wet van Zyl, Chris Vorster, Smith M, Stefano Cacciatore, Geoffrey Candy, Ekene Nweke. *Serum metabolomic profiling of a cohort of Pancreatic Ductal Adenocarcinoma (PDAC) patients of African descent using NMR spectroscopy analysis.* 48th Surgical Research Society of Southern Africa, Virtual Congress, 9-10th July, 2021.
- **Nnenna Elebo**, Jones Omoshoro-Jones, Pascaline Fru, John Devar, Christiaan De Wet van Zyl, Chris Vorster, Smith M, Stefano Cacciatore, Geoffrey Candy, Ekene Nweke. *Metabolomic and Lipoprotein Profiling of Pancreatic Ductal Adenocarcinoma Patients of African Ancestry.* School of Clinical Medicine (SOCM) Biennial Research Day. 30th September 2021.

- **Nnenna Elebo**, Jones Omoshoro-Jones, Pascaline Fru, John Devar, Christiaan De Wet van Zyl, Chris Vorster, Smith M., Stefano Cacciatore, Geoffrey Candy, Ekene Nweke. *Metabolites levels correlate to tumour stage and survival in Pancreatic Ductal Adenocarcinoma patients.* Metabolomics South Africa (MSA) Virtual Symposium, 20th-21st October 2021.
- **Nnenna Elebo**, Jones Omoshoro-Jones, Pascaline Fru, John Devar, Smith M, Stefano Cacciatore, Geoffrey Candy, Ekene Nweke. *Serum metabolomic profiling of a cohort of Pancreatic Ductal Adenocarcinoma (PDAC) patients of African descent using NMR spectroscopy analysis.* Bert Myburgh Research Forum, Department of Surgery, University of Witwatersrand, 24th November 2021.
- **Nnenna Elebo**, Jones Omoshoro-Jones, Pascaline Fru, John Devar, Smith M, Stefano Cacciatore, Geoffrey Candy, Ekene Nweke. *Serum metabolomic profiling of a cohort of Pancreatic Ductal Adenocarcinoma (PDAC) patients of African descent using NMR spectroscopy analysis.* Molecular Biosciences Research Thrust (MBRT) Virtual Postgraduate Research Day, University of Witwatersrand. 9th December 2021.
- **Nnenna Elebo**, Jones Omoshoro-Jones, Pascaline Fru, John Devar, Smith M, Geoffrey Candy, Ekene Nweke. *Expression of immune cell markers in a pilot cohort of South African Pancreatic Ductal Adenocarcinoma patients.*49th Surgical Research Society of Southern Africa, Hybrid Meeting 8-9th July, 2022.

<u>International Conferences – Poster Presentations</u>

- **Nnenna Elebo**, Jones Omoshoro-Jones, Pascaline Fru, John Devar, Christiaan De Wet van Zyl, Chris Vorster, Smith M, Stefano Cacciatore, Geoffrey Candy, Ekene Nweke. *Metabolomic profiling of a cohort of Pancreatic Ductal Adenocarcinoma (PDAC) patients of African descent using ^{1}H NMR spectroscopy analysis*. 14th Congress of the European-African Hepato Pancreato Biliary Association Virtual Congress, 15-17th September 2021, Spain.
- **Nnenna Elebo**, Jones Omoshoro-Jones, Pascaline Fru, John Devar, Christiaan De Wet van Zyl, Chris Vorster, Smith M, Stefano Cacciatore, Geoffrey Candy, Ekene Nweke. *Metabolites Levels Correlate to Tumour Stage and Survival in Pancreatic Ductal Adenocarcinoma Patients.* 15th Congress of the International Hepato Pancreato Biliary Association World Congress, 30th March -2nd April 2022, New York City.
- **Nnenna Elebo**, Jones Omoshoro-Jones, Pascaline Fru, John Devar, Christiaan De Wet van Zyl, Chris Vorster, Smith M, Stefano Cacciatore, Geoffrey Candy, Ekene Nweke.

Expression of immune markers in South African Pancreatic Ductal Adenocarcinoma patients. 15th Congress of the International Hepato Pancreato Biliary Association World Congress, 30th March -2nd April 2022, New-York City.

SUMMARY

Pancreatic Ductal Adenocarcinoma (PDAC) is one of the most fatal cancers with the poorest 5- year survival rate of 9%. PDAC is usually asymptomatic at the early stage and most patients are diagnosed at the advanced stage. The discovery of biomarkers at the resectable stage could be vital in improving the survival rate as well as improving the treatment strategies. This study aimed to identify metabolites and lipoproteins as well as associated immune cells/markers and their possible roles in PDAC. Following informed consent, blood samples were collected from 34 PDAC patients consisting of 22 resectable, 8 locally advanced and 4 metastatic pancreatic cancers (RPC, LAPC and MPC respectively) and 6 chronic pancreatitis patients at Chris Hani Baragwanath Academic Hospital. Six healthy volunteers were included, and the blood was processed into serum, plasma, and peripheral blood mononuclear cells (PBMCs). Nuclear Magnetic Resonance (NMR) spectroscopy, LipoScale test and Spectrophotometric assays were conducted on serum. A lipoprint assay was carried out to determine lipoprotein parameters and the lipid concentrations of each subtype. Multi-colour flow cytometric immunophenotyping and real-time PCR analyses were used to assess the immune cell markers. Data analysis was done using the R software and R studio and the Wilcoxon and Kruskal–Wallis rank-sum tests were used to compare differences in numerical covariates. Spearman's rank test was used to calculate the correlation coefficient (rho) between variables and the Wald test was used to calculate the statistical significance (*p*-value) of the differences between the Kaplan–Meier survival curves. In this study, the results showed elevated levels of glycine and lactate with worsening tumour stage. Decreased ethanol and 3-hydroxybutyrate concentrations were independently associated with longer survival time, irrespective of tumour stage. Abnormal lipoprotein associated with dysregulated lipid metabolism was detected. Glucose, lactate and some lipoproteins were directly linked to inflammatory markers. Furthermore, PDAC severity is associated with elevated levels of ROS. PDAC patients with CD4/CD8 ratio of less than 1 survived longer (Hazard Ratio = 3.572 *p*-value = 0.049). In this study identified novel metabolites such as 3-hydroxybutyrate and ethanol as well as $CD8^+$ T-cells were shown to be associated with patients' survival. Furthermore, evaluating the lipoprotein profiles might be vital in predicting prognosis and informing treatment decisions. This study showed that the integration of metabolomics, lipoproteins, and immune cell networks can contribute to a better understanding of the biology of PDAC in the population group.

ACKNOWLEDGEMENT

Thank you

- Lord for your Grace, I would not be where I am now if not for your unconditional love, mercy, and unmerited favour.

- Hon Benjamin Onwurolu, you are my soulmate and confidant, you always believe in me even when I don't, thank you for the financial and emotional support.

- Somma, Muna and Unoaku, my lovely daughters thank you for your love and for being my greatest cheerleaders.

- My family: my mom, sisters and brothers thank you all for your fervent prayers and support.

- Dr Nweke, words cannot express my gratitude for academic mentorship and support. Thank you for pushing me to be the best version of myself.

- Prof Candy, Dr Fru, and Dr Jones thank you all for your mentorship, advice, assistance and encouragement. I got the best supervisors.

- My colleagues and friends in the Surgery department lab, I appreciate all of you for your wonderful contributions towards the success of my study.

TABLE OF CONTENTS

DECLARATION ii
DEDICATION iii
PUBLICATIONS AND PRESENTATIONS iv
SUMMARY vii
ACKNOWLEDGEMENT viii
LIST OF TABLES xiv
LIST OF ABBREVIATIONS xvi
CHAPTER I: INTRODUCTION AND LITERATURE REVIEW 1
1.1 The Pancreas 1
1.1.1 Location of the Pancreas 2
1.1.2 Functions of the Pancreas 2
1.1.3 Diseases of the Pancreas 2
1.2 Pancreatic Ductal Adenocarcinoma (PDAC) 3
1.2.1 Risk Factors of PDAC 3
1.2.2 Diagnosis of PDAC 4
1.2.3 Classification of PDAC 4
1.2.4 Treatment of PDAC 5
1.3 The Immune System 6
1.3.1 Role of immune cells in Pancreatic Ductal Adenocarcinoma 6
1.3.2 Metabolic Pathways and their influence on the immune response in PDAC 10
1.4 Treatment development involving metabolic regulation in PDAC 19
1.5 Study Rationale 21
1.6 Aim 22
1.7 Objectives 22
CHAPTER II: DEMOGRAPHICS AND CLINICAL CHARACTERISTICS OF THE COHORT OF PANCREATIC DUCTAL ADENOCARCINOMA PATIENTS 23
2.1 Introduction 23
2.2 Demographics as risk factors in Pancreatic Ductal Adenocarcinoma 23
2.3 Clinical Presentation Patterns of Pancreatic Ductal Adenocarcinoma 24
2.3.1 Laboratory patterns associated with PDAC 25
2.4 Maladies associated with some of these symptoms 28
2.5 Methods 29

2.5.1 Patients recruitment and Clinical Data Collection....29
2.5.2 Statistical Analysis....30
2.6 Results....30
2.7 Discussion....35
2.8 Conclusion....36
CHAPTER III: SERUM METABOLOMIC AND LIPOPROTEIN PROFILING OF PANCREATIC DUCTAL ADENOCARCINOMA PATIENTS OF AFRICAN ANCESTRY....37
3.1 Introduction....37
3.1.1 Altered Metabolites Expression in Pancreatic Ductal Adenocarcinoma....37
3.2 Lipoproteins and their roles in cancer....39
3.2.1 Abnormal Lipoprotein (Lipoprotein X) in clinical pathologies....40
3.3 Materials and Methods....41
3.3.1 Sample Collection and Processing....41
3.3.2 Serum Sample Preparation for NMR analysis....42
3.3.3 Lipid Extracts Preparation....42
3.3.4 Nuclear Magnetic Resonance Spectroscopic Analysis....42
3.3.5 Nuclear Magnetic Resonance Profiling....43
3.3.6 Lipoprint Low-Density Lipoprotein Assay....43
3.3.7 Statistics and Data Analysis....44
3.4 Results....45
3.4.1 Metabolic and Lipoprotein Signatures in the Different Tumour Stages....45
3.4.2 Perturbed Metabolites and Patient Survival....49
3.4.3 Impact of Raised Bilirubin Levels on Metabolites and Lipoproteins in PDAC....51
3.4.4 Role of Lipoproteins in Monitoring Cholestatic Jaundice Treatment in PDAC....53
3.4.5 Detection of Lipoprotein X in Pancreatic Ductal Adenocarcinoma Patients....54
3.4.6 Impact of Diabetes and Inflammation on Metabolites and Lipoproteins Levels....55
3.5 Discussion....57
3.6 Conclusions....61
CHAPTER IV: THE EXPRESSION OF IMMUNE CELL MARKERS IN A COHORT OF PANCREATIC DUCTAL ADENOCARCINOMA PATIENTS OF AFRICAN ANCESTRY....62
4.1 Introduction....62
4.1.1 The Immune system and associated cells....62

4.1.2 Effector Immune Cells in Pancreatic Ductal Adenocarcinoma 63
4.1.3 Immune system in tumour progression 65
4.1.4 Immunosuppression in PDAC 66
4.2 Oxidative Stress and role in Pancreatic Ductal Adenocarcinoma 66
4.2.1 Reactive oxygen species (ROS) 67
4.3 Materials and Methods 69
4.3.1 Sampling and Processing Overview 69
4.3.2 Reactive oxygen species (ROS) analysis using DEPPD 70
4.3.3. Immunophenotyping using flow cytometry 70
4.3.4 Gene expression analysis of immune-related markers 75
4.4 Results 77
4.4.1: Impact of elevated ROS levels in Pancreatic Ductal Adenocarcinoma 77
4.4.2: Altered immune cell marker populations in the different tumour stages. 77
4.4.3 Impact of CD4/CD8 Ratio on Patient Survival 83
4.4.4 Gene expression of immune markers 84
4.4.5 Correlation of the ROS, Immunophenotyping and PCR Values 85
4.5 Discussion 86
4.6 Conclusion 89
CHAPTER V: CORRELATION OF THE CLINICAL DATA, METABOLITES, ROS, AND IMMUNE CELL MARKER LEVELS TO HYPOTHESIZE POSSIBLE RELATIONSHIPS 90
5.1: Introduction 90
5.2 Methods 90
5.2.1 Statistics and Data Analysis 90
5.3 Results 91
5.3.1 Correlation of clinical parameters with the Immune cell markers and ROS 91
5.3.2 Correlation of Metabolites with immune cell markers 92
5.3.3 Correlation of lipoproteins with immune cell markers 93
5.4 Discussion 94
5.5 Conclusion 95
CHAPTER VI: OVERALL CONCLUSION AND PROSPECTS 96
6.1 Introduction 96
6.2 Overall Conclusion and future work 96

6.3 Study Limitations 97
SUPPLEMENTARY TABLES 132
SUPPLEMENTARY FIGURES 154
APPENDIX A: TURNITIN REPORT 156
APPENDIX B: ETHICS CLEARANCE CERTIFICATE 158
APPENDIX C: STUDY INFORMATION DOCUMENT (HEALTHY CONTROLS) 159
APPENDIX D: STUDY INFORMATION DOCUMENT (PDAC/CP PATIENTS) 161
APPENDIX E: INFORMED CONSENT 163
APPENDIX F: PERMISSION TO CONDUCT RESEARCH 164

LIST OF FIGURES

Figure 1.1: Diagram of the pancreas showing the three main sections 1
Figure 1.2: The interaction between the metabolic pathways and the immune cells network ..7
Figure 1.3: Metabolic pathways dysregulated in PDAC 11
Figure 2.1: Boxplot of Total Bilirubin across all the groups with p-values 33
Figure 3.1: Nuclear Magnetic Resonance experiments 46
Figure 3.2: Boxplots showing the comparison of the concentration of metabolites.....48
Figure 3.3: Impact of tumour stages and metabolites concentration on patient survival 51
Figure 3.4: Measurement of Lipoprotein concentration in patient groups 53
Figure 3.5: Impact of cholestatic jaundice on lipoproteins.....54
Figure 3.6: Detection of Lipoprotein X in a LAPC 9 patient. 55
Figure 3.7: Inflammation status in patient groups. 56
Figure 3.8: Correlation of Glucose and Inflammatory markers.....57
Figure 4.1: Overview of Sample Size and Processing.....69
Figure 4.2: Spectrophotometric ROS Assay of PDAC and Control Groups. 77
Figure 4.3: Flowjo Layout profile of the immune cell markers populations. 79
Figure 4.4: Flowjo Layout profile of CD16 neutrophils cell marker populations 80
Figure 4.5: Boxplots showing the comparison of the percentages of the immune cells.....82
Figure 4.6: Boxplots showing the comparison of NKTs and NKs subsets.....82
Figure 4.7: Principal Component Analysis (PCA) of immunophenotyping datasets.. 83
Figure 4.8: Impact of CD4/CD8 on Patients' survival. Kaplan–Meier survival curves 84
Figure 4.9: Graphical representation of the immune marker by gene expression. 85
Figure S1: Correlation of Lactate with Cholangitis in PDAC patients.....154
Figure S2: Comparison of Immunophenotyping and Real-Time PCR.....155

LIST OF TABLES

Table 1.1: Immune cells and their role in pancreatic cancer. 18
Table 1.2: Metabolic pathways with their potential roles 20
Table 2.1. Demographic and clinicopathological features of PDAC and CP. 31
Table 2.2: Liver Function Tests of the CP and PDAC groups. 32
Table 2.3: Haematological parameters of the PDAC and CP groups. 34
Table 2.4: Blood chemistry of the PDAC and CP patient groups. 34
Table 3.1: Survival Analysis using Wald Test to assess the Metabolites in 47
Table 3.2 Survival Analysis using Wald Test to assess the Lipoprotein parameters 49
Table 3.3: Survival Analysis using Wald Test to assess the Metabolites 50
Table 4.1: Immune cells of both the innate and adaptive immune system 62
Table 4.2: A table showing the optimized titrated volumes of Antibodies. 73
Table 4.3: Percentage population of Immune cell makers in PDAC 81
Table 4.4: Correlation of ROS with immune cell markers. 86
Table 5.1: Correlation of CD4+ T cells with Liver Function Tests of PDAC groups. 91
Table 5.2: Correlation of CD4/CD8 ratio with Liver Function Tests of PDAC groups. 91
Table 5.3: Correlation of Liver Function Tests with $CD8^+$ T cells 92
Table 5.4: Correlation of Liver Function Test and Immune cell marker $CD57^+$ NKTs. 92
Table 5.5: Correlation of Lipoproteins and Immune cell marker $CD57^+$ NKTs 93
Table S1: List of the quantified signal and their relative assignment and multiplicity. 132
Table S2: Correlation of concentration of lipid extracts with the stages of PDAC. 132
Table S3: Selected metabolites ratios and their catalysing enzymes 133
Table S4: Correlation of metabolites ratios with the stages of PDAC 133
Table S6: Survival Analysis using Wald Test to assess the Metabolic Ratios 134
Table S7: Survival Analysis using Wald Test to assess the Lipoproteins 134
Table S8: Comparison of the Full Blood Count of N versus AB Clusters 135
Table S9: Comparison of the Blood chemistry of N versus AB components 135
Table S10: Comparison of the Liver function tests of N versus AB components. 135
Table S11: Comparison of the metabolite concentration of N versus AB clusters. 136
Table S12: Comparison of the lipid extracts concentration of N versus AB clusters. 136
Table S13: Comparison of the metabolite concentration ratios of N versus AB clusters. 137
Table S14: Comparison of the metabolite concentration ratios of N versus AB clusters 137
Table S15: Correlation of metabolites with GlycA, GlycB, CRP, and Albumin. 139

Table S16: Correlation of lipid extracts with GlycA, GlycB, CRP, and Albumin. 140
Table S17: Correlation of metabolite concentration ratios with GlycA, GlycB, CRP. 141
Table S18: Correlation of lipoproteins with GlycA, GlycB, CRP, and Albumin.....141
Table S19: Comparison of Metabolites of T2DM and Non-T2DM PDAC patients 141
Table S20: Comparison of Lipoproteins of T2DM and Non-T2DM PDAC patients.....143
Table S21: Comparison of Lipid Extracts of T2DM and Non-T2DM PDAC patients 143
Table S22: Comparison of Metabolic Ratios of T2DM and Non-T2DM PDAC patients....144
Table S23: Comparison of Metabolites of PDAC patients with High and Low GPS 144
Table S24: Comparison of Lipoproteins of PDAC patients with High and Low GPS.....145
Table S25: Comparison of Lipid Extracts of PDAC patients with High and Low GPS.....146
Table S26: Comparison of Metabolic Ratios of PDAC patients with High and Low GPS..147
Table S27: 6-colour Flow Cytometry Immunophenotyping Panel 147
Table S28: 6-colour Flow Cytometry Immunophenotyping FMO Panel 148
Table S29: Comparisons of LAPC01, LAPC02 and RPC01 150
Table S30: Correlation of Metabolites and Immune cell marker CD57+ NKTs in PDAC ..151
Table S31: Correlation of Metabolites and Immune cell marker CD3+ CD56- NKTs 152
Table S32: Correlation of Lipid Extracts and Immune cell marker CD57+NKTs in PDAC153

LIST OF ABBREVIATIONS

Abbreviations	Full meaning
ALP	Alkaline phosphatase
ALT	Alanine transaminase
AST	Aspartate transaminase
Akt	Protein Kinase B
CP	Chronic Pancreatitis
COX2	cyclooxygenase 2
CRP	C-reactive protein
EUS-BD	Endoscopic ultrasound-guided Biliary Drainage
FAO	Fatty acid oxidation
FAS	Fatty acid synthesis
FDR	False discovery rate
HDL	High-density lipoprotein
IDL	Intermediate-density lipoprotein
INR	International normalised ratio
LCAT	Lecithin-cholesterol acyl transferase
LDHA	Lactate dehydrogenase A
LFT	Liver Function Tests
LpX	Lipoprotein X
LDL	Low-density lipoprotein
RPC	Resectable Pancreatic Ductal Adenocarcinoma
GPS	Glasgow Prognostic Score
GGT	Gamma glutamyl transferase
GSH	Glutathione
GlycA	N-acetylglucosamine
GlycB	N-acetylneuraminic acid
HDAC	Histone deacetylases
HIF	Hypoxia-inducible factor
LAPC	Locally Advanced Pancreatic Ductal Adenocarcinoma
MAPK	Mitogen-activated protein kinase
MDSC	Myeloid-derived suppressor cells
MHC	Major Histocompatibility Class
MPC	Metastatic Pancreatic Ductal Adenocarcinoma
NCCN	National Comprehensive Cancer Network
NKTs	Natural Killer T-lymphocyte cells
NKG2D	Natural Killer group 2-member D
NOESY	Nuclear 55 Overhauser Effect SpectroscopY
NMR	Nuclear magnetic resonance
PAM	Partition around medoids
PD-1	Programmed cell death
PDAC	Pancreatic Ductal Adenocarcinoma
PFAA	Plasma free amino acids
PPP	pentose phosphate pathway
PTBD	Percutaneous Transhepatic Biliary Drainage
P13K	Phosphoinisitide-3-Kinase
PKM2	Phosphoglycerate Kinase

RPC	Resectable Pancreatic Ductal Adenocarcinoma
ROS	reactive oxygen species
Rho	Correlation coefficient
sMICA	Soluble MHC class 1 chain-related molecule A
STAT3	Signal transducer and activator of transmission 3
TAM	Tumour-associated macrophages
Tregs	Regulatory T-lymphocytes
TCA	Tricarboxylic acid
TNF-α	Tumour necrosis factor-alpha
T2DM	Type 2 Diabetes Mellitus
VLDL	very-low density lipoprotein

CHAPTER I: INTRODUCTION AND LITERATURE REVIEW

This chapter provides relevant background on the pancreas, the different immune cells, and their roles in pancreatic cancer, it also highlighted the individual metabolic pathways in pancreatic cancer and how they enable transitions in immune cells. Additionally, the potential of targeting metabolic pathways for effective therapeutic strategies is discussed.

1.1 The Pancreas

The pancreas is a large, flattened peer shaped abdominal organ that converts the food we eat into fuel for body cells. It secretes enzymes to assist digestion and regulate glucose levels in the body. The pancreas has 3 main sections as shown in **Figure 1.1** which are:

1. The head section: This is the wide part of the pancreas located towards the right side of the abdomen and is connected to the duodenum through the pancreatic duct. The uncinate process is a part of the gland found underneath the head of the pancreas. Of note, over 85% of pancreatic tumours are found in this region hence the name Pancreatic Ductal Adenocarcinoma (PDAC) (Herlea et al., 2020; Ryan et al., 2014).
2. The middle section: This is made up of the neck and body. This is the region between the head and the tail. Both the superior mesenteric artery and superior mesenteric veins cross behind the body of the pancreas which supplies blood to and from the pancreas. Tumour metastases also occur in organs along these veins.
3. The tail section is the thin tip found at the end of the pancreas and is located at the left side of the abdomen which is close to the spleen.

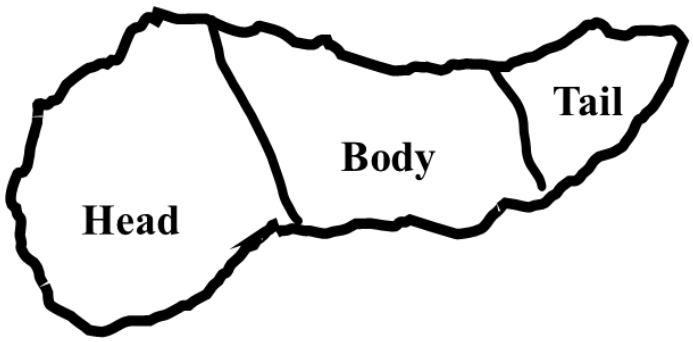


Figure 1.1: Diagram of the pancreas showing the three main sections: head, body and tail. Adapted from (Cesmebasi et al., 2015)

1.1.1 Location of the Pancreas

The pancreas is located behind the stomach and across the spine. Due to its concealed location, most of the tumours of the pancreas cannot be detected early (Sarantis et al., 2020). It is surrounded by other organs such as the spleen found at the tail end of the pancreas, the small intestine wrapped around the wide end of the pancreas, liver and gall bladder located very close to the pancreas. Symptoms of PDAC only start appearing when the tumour begins to interfere with the function of the pancreas or other nearby organs. Also, the pancreas is well supplied by blood which would provide a rich supply of nutrients and glucose to the developing tumour. Finally, the head of the pancreas is located at the juncture where the stomach meets the small intestine, and this is where the stomach releases partially digested food into the intestine while the pancreas releases digestive enzymes.

1.1.2 Functions of the Pancreas

The pancreas plays a dual role in the body, which are the endocrine and exocrine functions.

- Endocrine System functions: The pancreas secretes two hormones which are insulin and glucagon that are vital in regulating glucose levels. Insulin is secreted by the pancreas to reduce blood glucose when it's too high while glucagon is secreted when glucose levels are low.
- Exocrine System functions: The pancreas secretes enzymes that work with the bile and the gall bladder to break down proteins, fats and carbohydrates for proper digestion and absorption. Enzymes produced by the pancreas for digestion include lipases, amylases, trypsin and chymotrypsin.

1.1.3 Diseases of the Pancreas

1. Type 2 Diabetes Mellitus (T2DM): This results from the endocrine system dysfunction when the pancreas doesn't produce enough insulin to maintain the blood glucose levels.
2. Pancreatitis: This is the inflammation of the pancreatic tissue, which occurs when enzymes prematurely work in the pancreas before they are secreted into the duodenum. Acute pancreatitis is most commonly caused by gallstones blocking the main pancreatic duct, which can last for a few days or become chronic (known as chronic pancreatitis) and last for years.

3. Pancreatic Cancer: This condition is caused by cancerous cells in the pancreas, which grow and proliferate uncontrollably. Pancreatic cancer originating from the endocrine glands is less common and usually referred to as pancreatic neuroendocrine tumours (PNET). PDAC presents earlier than other types of pancreatic cancer because it can obstruct the bile flow (Antonello et al., 2009).

1.2 Pancreatic Ductal Adenocarcinoma (PDAC)

Pancreatic cancer is the 3rd leading cause of cancer-related deaths in both men and women combined with a 5-year survival of about 11% (Siegel et al., 2022). PDAC is the most common type of pancreatic neoplasm, which accounts for more than 85% of pancreatic cancer cases worldwide (Ryan et al., 2014). It exhibits a glandular pattern structurally similar to that of the ductal epithelial cells (Polireddy and Chen, 2016). PDAC has non-specific symptoms at its early stages causing it to remain undetected till late stages, usually locally advanced or metastatic with a significantly worse prognosis (Sarantis et al., 2020). The lack of early diagnostic markers for pancreatic tumorigenesis and progression may delay detection for up to 20 years (Yachida et al., 2010).

1.2.1 Risk Factors of PDAC

Risk factors of PDAC include environmental factors such as extreme alcohol consumption and excessive smoking, inherited genetic factors and demographic factors such as age, sex and ethnicity. The rate of PDAC is greater in the black population than in other races (Khawja et al., 2015; Yadav et al., 2011). Excessive alcohol consumption could predispose the pancreas to inflammation (Wang et al., 2016). Smokers have a greater chance of developing PDAC compared to non-smokers and this could be due to the release of carcinogens by the degradation of tobacco (Bosetti et al., 2012), which could in the long-run, affect inflammatory response and cell proliferation (Pandol et al., 2012). Diabetes mellitus and obesity are also risk factors for PDAC (Mizrahi et al., 2020) because they induce inflammatory states which promote the development of genomic irregularities and initiation of carcinogenesis (Andersen et al., 2017).

1.2.2 Diagnosis of PDAC

Some of the symptoms of PDAC include weight loss, anorexia, abdominal pain and jaundice (Mizrahi et al., 2020), which are usually observed at the advanced stage of the disease and are connected to the location of the tumour such as the head of the pancreas (Hart and Chari, 2019). A physical examination of the abdomen region would reveal abnormal lumps and liver function tests will then be carried out to check for bile blockage or hyperbilirubinaemia. Following suspicious findings computed tomography (CT) and magnetic resonance imaging (MRI) would be used to provide detailed images of the pancreas and bile ducts (Unger et al., 2018). To confirm the diagnosis, Endoscopic Retrograde Cholangiopancreatography (ERCP), Magnetic Resonance Cholangiopancreatology (MRC), and Percutaneous Transhepatic Cholangiopancreatology (PTC) are used for imaging and bile duct obstruction treatment (McGuigan et al., 2018).

1.2.3 Classification of PDAC

According to the National Comprehensive Cancer Network (NCCN) guidelines, PDAC can be classified into resectable, borderline resectable, locally advanced, and metastatic disease via a contrast-enhanced triple phased CT scan of the abdomen (Tempero et al., 2019). In Resectable Pancreatic Adenocarcinoma (RPC), the tumour has not invaded any vessel. When the tumour has invaded the portal vein to greater than 90° but less than 180º, it is referred to as borderline Pancreatic Adenocarcinoma in which case neoadjuvant chemotherapy may be necessary before surgery (Grossberg et al., 2020). The locally Advanced Pancreatic Adenocarcinoma (LAPC) group includes cases where the tumour had invaded the superior mesenteric artery and/or portal vein to more than 180°. Lastly, the metastatic Pancreatic Adenocarcinoma group (MPC) have the tumour already spread to other organs such as the liver (Soweid, 2017). The liver is the most common site for pancreatic metastases before moving to other distant organs such as the lungs and abdomen (Tsilimigras et al., 2021). The metastatic pattern of PDAC is greatly influenced by the lymphatic and mesenteric vein as well as the seed-soil compatibility, which contributes to organ specificity, hence most (85%) of the cancer cells migrate from the pancreas to the liver which is where the local microenvironment is favourable (Houg and Bijlsma, 2018).

PDAC is a highly heterogenic disease, and various attempts have been undertaken to define distinct subtypes to stratify patients towards personalized treatment strategies (Moffitt et al., 2015). Examples include pancreatic progenitor, squamous, ADEX and immunogenic as

described by Bailey and colleagues (Bailey et al., 2016). Other common subtypes include classical, basal-like, exocrine-like, stroma normal or activated among others (Collisson et al., 2019; Roa-Peña et al., 2019).

1.2.4 Treatment of PDAC

Upon diagnosis, the disease is stratified enabling the doctors to decide the best treatment option for the patient. Some of the treatment options available are:

1. Surgery: Resection is the removal of tumour by surgery which depends on the size and location of the tumour, tumour metastasis and health status based on the clinical investigation of the patient. Some of the surgery procedures carried out include:
    - Whipple procedure: This is a surgical procedure also known as pancreaticoduodenectomy and is commonly used to remove tumours from the head and body of the pancreas. In some cases, parts of the small intestine, bile duct, gall bladder and lymph nodes near the pancreas are removed while the remaining parts are re-attached to the small intestine for digestion.
    - Distal pancreatectomy: This is surgery that is used to treat cancer found in the tail and body of the pancreas. It is used to remove the tail and a portion of the body of the pancreas, as well as the spleen.
    - Total pancreatectomy: This is carried out when the tumour has spread throughout the pancreas. It is carried out to remove the entire pancreas, gall bladder, part of the stomach, small intestine, and spleen.
2. Chemotherapy: This is an anti-cancer drug injected through the vein or taken orally. These drugs enter the bloodstream and reach almost all areas of the body making this treatment useful for cancers whether they have spread or not. Some of the chemotherapeutic drugs used in pancreatic cancer include gemcitabine, 5-Fluorouracil and FOLFIRINOX. Chemotherapy can be used as follows:
    - Neoadjuvant chemotherapy: This is chemotherapy given before surgery to shrink the tumour so that it can be removed with less extensive surgery. It is often used to treat cancers that are too big to be removed by surgery such as borderline resectable PDAC. A combination of gemcitabine and S-1 (tegafur/ gemeracil/otreracil) have been recommended for borderline resectable PDAC before surgery (Kurata et al., 2021).
    - Adjuvant chemotherapy: This is used after surgery to kill cancer cells that have been left behind or have spread to other parts of the body. The adjuvant standard of care

for fit PDAC patients is the modified FOLFIRINOX (5-Fluorouracil, oxaliplatin and irinotecan) while gemcitabine plus nab-paclitaxel is for the unfit ones which are patients with cumulative impairment of various physiological systems (Mas et al., 2020).

3. Radiotherapy: Radiation therapy uses high-energy x-rays or particles to kill cancer cells. Radiation might be given after surgery but it is usually given along with chemotherapy and referred to as chemoradiotherapy (Liermann et al., 2020).

1.3 The Immune System

The immune system, which comprises the innate and adaptive immune system, protects the host from foreign pathogens, including cancer cells (Ghesquière et al., 2014). The innate immune system includes antigen-presenting cells, which phagocytose invading pathogens and present antigenic determinants with the major histocompatibility complex proteins (MHC)-II to $CD4^+$ T cells. Granulocytes, mast cells, dendritic cells (DCs), macrophages and natural killers (NK) cells are also innate immune cells (Hato and Dagher, 2015). The adaptive immune system is regulated and comprised mainly of B and T cells, which are usually activated when the innate immune system cannot eliminate the pathogens and provide long-lasting immunity (Inman et al., 2014).

1.3.1 Role of immune cells in Pancreatic Ductal Adenocarcinoma

The dysfunctional immune system in pancreatic cancer has been shown to promote tumour growth. The pancreatic cancer microenvironment has been identified to serve a vital role in tumour growth and the therapeutic response (Inman et al., 2014). Pancreatic cancer cells are enveloped in rich stroma, comprising both cellular and acellular components, including the extracellular matrix, fibroblasts, myofibroblasts, growth factors, cytokines, pancreatic stellate cells, and immune cells (von Ahrens et al., 2017). Dendritic cells, NK cells, $CD8^+$ and $CD4^+$ T cells are some of the immune cells reported to be activated to inhibit tumour growth and progression in PDAC (An et al., 2020) (**Figure 1.2**). Regulatory T cells (T-regs), tumour-associated macrophages (TAM), myeloid-derived suppressor cells (MDSCs) and tumour-associated neutrophils have also been reported to promote tumour growth and progression, as well as suppressing antitumoral responses (Martinez-Bosch et al., 2018).

MDSCs suppress immunity by inhibiting T-cell activation via the sequestration of cysteine, thereby reducing the availability of the amino acids tryptophan and arginine, which are

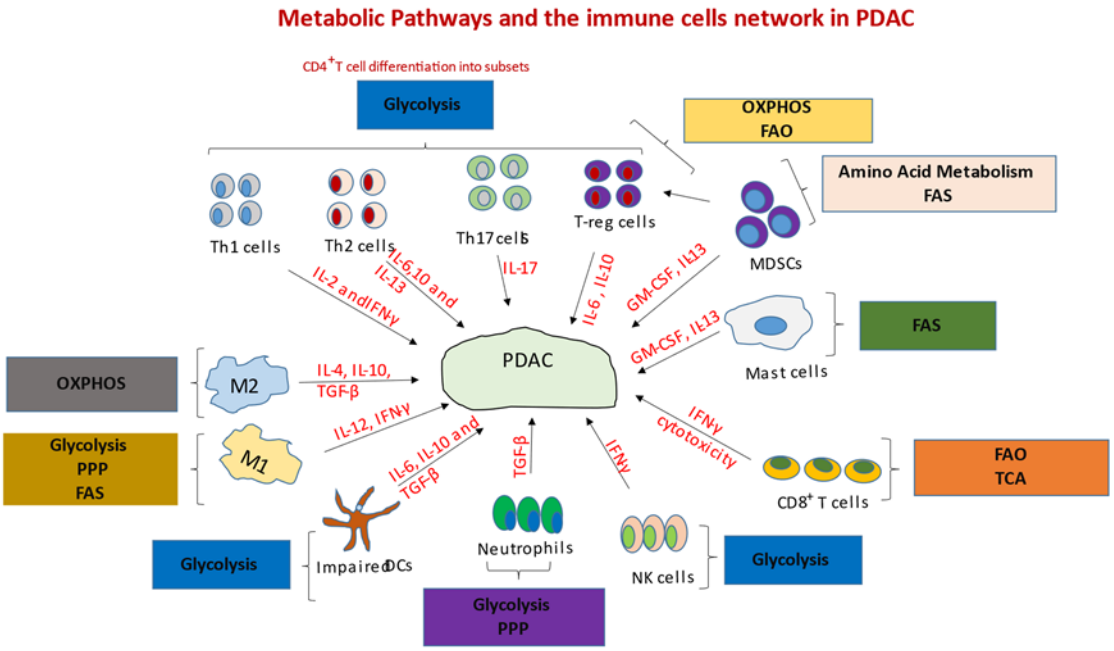


Figure 1.2: The interaction between the metabolic pathways and the immune cells network in PDAC. The immune network comprises the complex interactions between the innate immune cells, adaptive immune cells and pancreatic cancer cells. Immunity in PDAC is greatly influenced by cytokines and chemokines released by the tumour cells such as IL-6 and IL-10 as well as those released by the immune cells such as IL-4, IL-13 and IFN-γ. Metabolic pathways also serve an important role in the reprogramming of these immune cells, either by activating, inhibiting or polarising these immune cells. For instance, the switch from M1 to M2 macrophages is greatly influenced by FAO and TCA cycle. Enhanced glycolysis is necessary for T-cell differentiation into their subsets; Th1, Th2, Th17 and T-regs. PDAC, pancreatic ductal adenocarcinoma; PPP, pentose phosphate pathway; TCA, tricarboxylic acid; FAS, fatty acid synthesis; FAO, fatty acid oxidation; OXPHOS, Oxidative Phosphorylation; IFN-γ, Interferon-gamma; TGF-β, Transforming growth factor Beta; GM-CSF, Granulocyte-macrophage colony-stimulating factor; M1, pro-inflammatory macrophage; M2, anti-inflammatory macrophage; NK cells, Natural killer cells; DCs, Dendritic cells; MDSC, myeloid-derived suppressor cells; T-Reg, Regulatory T-cells; Th1, T helper cells 1; Th2, T helper T-cells 2; Th17, T helper T-cells 17, IL, Interleukin.

required for protein translation by T cells and reactive oxygen species (ROS) production (De Sanctis et al., 2016). A previous study illustrated that the growth factor granulocyte-macrophage colony-stimulating factor, secreted by pancreatic tumours, promoted the early recruitment of MDSCs (Bayne et al., 2012; R. Li et al., 2020). MDSCs inhibit the immune functions of effector T (T-eff) cells and NK cells, while the function of T regulatory (T-regs) are promoted (Padoan et al., 2019; Pergamo and Miller, 2017). Elevated MDSCs levels in pancreatic cancer were shown to be a poor prognostic factor associated with elevated T-regs and T helper (Th)2 cytokines levels (Wörmann et al., 2013). Using peripheral blood mononuclear cells (PBMCs) harvested from blood samples collected from 131 patients, flow

cytometric analysis revealed that both MDSC and T-reg levels were significantly elevated in patients with pancreatic cancer (Gabitass et al., 2011).

Macrophages switch their differentiation from M1 (proinflammatory) to M2 (anti-inflammatory) phenotypes in the presence of stimuli, such as the cytokines IL-10, IL-4, and TGF-β, which are secreted from the PDAC microenvironment (Cruz et al., 2020; Rhee, 2016). TAMs are macrophages initially recruited to the site of tumour formation in response to the chemotactic factors released by pancreatic cancer cells, and they promote tumour progression by suppressing antitumor immune responses and stimulating the vascularization and metastasis of cancer cells (Mielgo and Schmid, 2013; Pathria et al., 2019). This has been demonstrated using immunohistochemistry to identify inflammatory cells by evaluating the expression of proangiogenic and polymphangiogenic molecules, VEGFA and VEGFC, produced by macrophages in pancreatic cancer (Costache et al., 2015). Furthermore, TAMs were shown to regulate pancreatic intraepithelial neoplasia progression by being the main source of IL-6 in *Kras*^{G12D}-mutations, thereby promoting cancer development (Otto et al., 2021). Elevated levels of TAMs and M2 polarized TAMs were also shown to be associated with a worse prognosis in pancreatic cancer by promoting lymphatic metastasis by lymphangiogenesis (Liang et al., 2022).

$CD8^+$ T-cells play an important role in PDAC progression (Goulart et al., 2021). It has been shown that increased levels of $CD8^+$ T cells led to favourable clinical outcomes and the improved survival of patients with PDAC (Liu et al., 2016). The effect of $CD4^+$ T cells depends on their differentiation into their subtypes, T helper cell type (Th)1, Th2 and Th17, and T-regs (Saravia et al., 2019). $CD8^+$ T cells are compromised in human pancreatic cancer due to the degradation of MHC-1 molecules by enhanced autophagy, which leads to immune evasion and the inhibition of antitumor activity (Kim et al., 2012; Yamamoto et al., 2020). Both cytotoxic and helper T cells were found to be impaired by the influence of immunosuppressive cytokines, which promoted Th2 responses and led to tumour growth (Dadey et al., 2020). A meta-analysis study of 833 PDAC patients showed that the upregulation of $CD8^+$ and $CD4^+$ T cells predicted an improved prognosis in PDAC (Tang et al., 2021). A decrease in the levels of T-eff cells was suggested to be associated with the progression from a premalignant to the malignant stage in PDAC because it was associated with reduced tumour growth (Carstens et al., 2017; Kim et al., 2012). In addition, elevated levels of Th1 cells contributed to a good clinical outcome because they produce IFN-γ and TNF-α, which promote anticancer activities by activating cytotoxic T cell responses, as well as antigen-presenting cells (J. Lee et al., 2021).

The role of Th17 cells in pancreatic cancer is not completely understood because it depends on the cancer type, tumour stage and location (Saka et al., 2020; Zou and Restifo, 2010). Previous studies have revealed that an increased level of Th17 cells in murine pancreatic cancer inhibited tumorigenesis, leading to improved survival (Gnerlich et al., 2010), while in another study, elevated levels of Th17 cells in pancreatic tumour tissues and blood samples of patients was indicative of its involvement in invasion and metastasis (He et al., 2002, 2011). Th2 cells exhibit a tumour-promoting function in pancreatic cancer, and this was suggested to be the result of the upregulated levels of Th2 cytokines, such as IL-13, IL-10 and IL-6, found in the plasma of patients with pancreatic cancer (Goulart et al., 2021). T-regs depend on oxidative phosphorylation and fatty acid oxidation (FAO) for ATP upon activation (Macintyre et al., 2014); this permits T-regs to survive under tumour conditions in contrast to T-eff cells, which are impaired due to insufficient glucose production (Lochner et al., 2015). T-regs suppress immune responses via the secretion of IL-10 and TGF-β to produce an immunosuppressive environment (Arjomandnejad et al., 2021).In pancreatic cancer, T-regs were found to be involved in the early infiltration of preinvasive lesions, promoting tumour growth and progression (Dadey et al., 2020; Martinez-Bosch et al., 2018).

Cytotoxic lymphocyte-associated antigen-4 (CTLA-4) is a receptor found on T-regs that produces inhibitory signals upon interaction with its ligands, CD80 and CD86, on antigen-presenting cells. They inhibit the formation of the immune synapse between $CD4^+$ T cells and the antigen-presenting cells, which normally promotes the release of cytokines for cancer cell destruction (Van Coillie et al., 2020). In patients with pancreatic cancer, a large number of T-regs in circulation was associated with the advancement of the disease (Kunk et al., 2016). The chances of successful surgical resection and survival rate post-resection were also shown to be associated with the decreased levels of T-regs in patients with pancreatic cancer (Yamamoto et al., 2012). Additionally, increased numbers of mast cells were identified to be associated with metastasis and reduced survival in human pancreatic cancer (Longo et al., 2018).

The pancreatic cancer microenvironment releases tumour-derived factors, such as IL-6 and VEGF, which promote DC impairment by reprogramming the immune cell response from a Th1 type to a Th2 type, thereby promoting cancer development (Giovanelli et al., 2019; Ochi et al., 2012). One previous study reported that the elevated levels of DCs and NK cells in PDAC were associated with a prolonged or improved survival rate (Van Audenaerde et al., 2018).

The immune system uses NK cells to target cancer cells, which inhibits their growth, and a decreased level of NK cells was suggested to be associated with the advancement of pancreatic cancer (Janakiram et al., 2017). These findings were observed by determining the serum levels of soluble MHC class 1 chain-related molecule A (sMICA) and NK group 2-member D (NKG2D) in the NK cells of patients with pancreatic cancer using immunohistochemistry. Elevated levels of sMICA were found in patients with advanced pancreatic cancer and were correlated with the downregulation of NKG_2D expression, implying decreased levels of NK cells (Duan et al., 2011). Mast cells are commonly known for their role in allergies; however, in PDAC, elevated levels of mast cells were also associated with tumour progression (Aponte-López and Muñoz-Cruz, 2020; Cai et al., 2011).

1.3.2 Metabolic Pathways and their influence on the immune response in PDAC

The function and differentiation of immune cells are influenced by metabolism (Pearce and Pearce, 2017). **Figure 1.2** shows some of the metabolic pathways and the immune cell network in PDAC. Metabolism involves a series of chemical reactions that sustain life by converting food to energy and building blocks for larger compounds, such as proteins, lipids and nucleic acids (Odegaard and Chawla, 2013). The chemical reactions involved in metabolism are structured into pathways. Metabolites are end-products of metabolism, which are generated by living organisms during their life cycles and could reflect the function of the organism (Odegaard and Chawla, 2013).

The excessive growth of the extracellular matrix in PDAC as a result of the dense stroma leads to the formation of barriers against the immune system, drug delivery, oxygen and nutrients (Hosein et al., 2020). Hence the cells develop mechanisms that alter the typical metabolic pathways that supply nutrients, to survive (Stopa et al., 2020). Although immunotherapy promotes antitumor activities by reprogramming and enhancing immune response (Li et al., 2020), the function and differentiation of immune cells are greatly influenced by metabolism, hence the combination of both could be a more effective treatment option (Li et al., 2019). Metabolic pathways can either promote or inhibit immune cell functions, which could be essential in further understanding the immune response and in identifying novel therapeutic options to treat immune dysfunction in numerous types of diseases, including cancer.
The next section will describe some of the metabolic pathways and metabolites that are affected by pancreatic cancer (**Figure 1.3**).

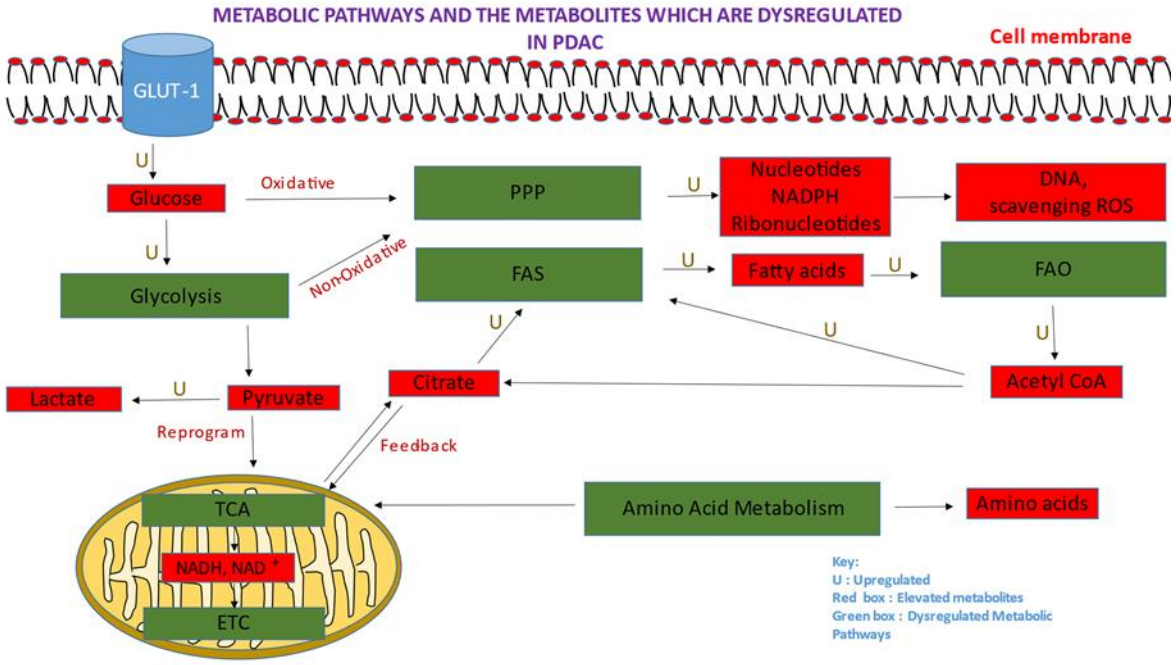


Figure 1.3: Metabolic pathways dysregulated in PDAC. The GLUT-1 transporter is upregulated in PDAC, which increases glucose uptake and glycolysis and promotes the flux of their intermediates into other metabolic pathways, such as the PPP. Glucose is metabolized into pyruvate, which feeds into the TCA cycle. Metabolic reprogramming of tumour cells restructures the TCA cycle and produces a high amount of lactate. The dysregulated FAS pathway contributes to the generation of building blocks for membrane synthesis. The fatty acids produced are oxidized via FAO to Acetyl CoA, which feeds back into the TCA cycle to generate NADH and NAD+ and stimulates the electron transport chain to produce more ATP for the PDAC cells. In PDAC cells, both oxidative and non-oxidative phases of the PPP are upregulated to generate NADPH for scavenging ROS and nucleotides for DNA synthesis. Amino acid metabolism feeds into the TCA cycle to meet the high metabolic demands of the tumour cells. Red represents upregulated metabolites and green represents dysregulated metabolic pathways. PDAC, pancreatic ductal adenocarcinoma; GLUT-1, glucose transporter 1; PPP, pentose phosphate pathway; TCA, tricarboxylic acid; FAS, fatty acid synthesis; FAO, fatty acid oxidation; NADH, nicotinamide adenine dinucleotide; NADPH, nicotinamide adenine dinucleotide phosphate; ROS, reactive oxygen species; U, upregulated.

Glycolysis

Glucose uptake and glycolysis are activated in pancreatic cancer cells, and their intermediates are fed into other biosynthetic pathways, such as the pentose phosphate pathway (PPP) (Yao et al., 2020). Glycolysis involves a series of enzymatic steps, whereby glucose is metabolized to pyruvate and then finally to lactate to yield ATP and other substrates for other metabolic pathways (O'Neill et al., 2016; Palmer et al., 2015). Glycolytic enzymes, such as hexokinase, enolase and phosphoglycerate kinase (PKM2), among others, were found to be overexpressed in pancreatic cancer, promoting tumour growth and metastasis (Chung et al., 2008; Yang et al.,

2020). The expression of hypoxia-inducible genes in pancreatic cancer cell lines (MiaPaca-2 and Pcl-43) under different conditions was investigated, and hexokinase was identified to be upregulated (Natsuizaka et al., 2007). PKM2 and lactate dehydrogenase A (LDH-A) have been linked with more aggressive tumours and poor survival in pancreatic cancer (Mohammad et al., 2016). Glycolysis in pancreatic cancer was revealed to promote lactate production, tumour growth and protein glycosylation (Cameron et al., 2018; Li et al., 2019; O'Neill et al., 2016). Hexokinase 2 has been shown to regulate lactate production and promote tumour growth and metastasis in PDAC (Anderson et al., 2016). Although glycolysis is less energy efficient compared with the tricarboxylic acid (TCA) cycle, it is preferred by cancer cells as it produces ATP faster, occurs independently of mitochondrial function and conserves nutrients for lipids, amino acids and nucleic acid biosynthesis (O'Neill et al., 2016). This phenomenon is known as the Warburg effect (Vander Heiden et al., 2009; Warburg et al., 1927) and in PDAC, leads to increased lactate production, which alters the tumour stroma interface, thereby increasing invasiveness (Colegio et al., 2014). Elevated lactic acid levels were identified to lead to a decreased pH in the tumour microenvironment, which inhibited cytotoxic T cell function and promoted tumour growth and progression (Choi et al., 2013).

M1 macrophages are characterized by enhanced glycolysis, while M2 macrophages exhibit decreased levels of glycolysis (Mills and O'Neill, 2016). M1-polarized macrophages are highly glycolytic due to the increased stimulation of the fructose-2,6-biphosphatase enzyme (Nonnenmacher and Hiller, 2018), which produces nitric oxide and TNF-α (Murray et al., 2014), and exhibit IL-12 and IL-23 phenotypes, while M2-polarised macrophages exhibit an IL-10 phenotype (Liu et al., 2018). T-cells require large amounts of glucose and glutamine catabolism for nucleotide and lipid synthesis, which are essential for cell growth (Lim et al., 2020). However, in their resting or naïve state, they require small amounts of glucose, amino acids and fatty acids for the sustenance and maintenance of energy (Li and Zhu, 2018).

Glycolysis is necessary for differentiating $CD4^+$ T cells into their effector subsets, as well as maintaining a proper balance between protective and suppressive immunity (DuPage and Bluestone, 2016; Michalek et al., 2011). Glycolysis is essential for T-eff cell activation and function because they require high metabolic flux (Herbel et al., 2016). T-eff cells are activated by the mTOR signalling pathway and hypoxia-inducible factor-α transcription factors, which promote glycolysis and amino acid metabolism but use FAO for ATP production (Waickman and Powell, 2012). The mTOR signalling pathway is highly involved in metabolism, altering the expression of key pathways such as glycolysis (Ersahin et al., 2015; Mao and Zhang, 2018).

T-eff subsets, such as Th17, Th1 and Th2, require elevated levels of glycolysis following activation (Michalek et al., 2011). Macintyre and colleagues (Macintyre et al., 2014) demonstrated that glucose transporter (GLUT)-1 was essential for $CD4^+$ T cell activation and effector function by examining the GLUT transporter family to determine their roles in glucose uptake and metabolism in T cells. The study also revealed that the levels of T-eff cells were elevated in GLUT-1 transgenic mice, which depend solely on glucose metabolism (Michalek et al., 2011). Increased levels of glycolysis were also found to be required for activated B cells to contribute to the immune response (Jellusova, 2020). In addition, activated neutrophils were identified to depend on glucose for ATP production via glycolysis (Rodríguez-Espinosa et al., 2015).

Dendritic cells are usually found in tissues that are in contact with external environmental systems (Dallal et al., 2002; Liu, 2016). They process and present antigens on the cell surfaces for T cells to respond to (Liu, 2016). In addition, DCs regulate the immune response by regulating the polarization of T cells to Th1, Th2 or Th3 subtypes following the stimulation by cytokines (Ito et al., 2001). Enhanced glycolysis occurs in DCs, which enables them to generate sufficient ATP and intermediates to perform the immune system functions. Krawczyk and colleagues (Krawczyk et al., 2010) demonstrated that DCs undergo maturation by Toll-like receptor signalling, and this occurred by the metabolic conversion from oxidative phosphorylation to aerobic glycolysis following the upregulation of fatty acid synthesis (FAS). The rapid induction of glycolysis was also essential for the activation and function of DCs (Everts et al., 2014).

Tricarboxylic acid cycle (TCA cycle)

The TCA cycle is a series of reactions that occur in the matrix of the mitochondria and involves the oxidation of Acetyl CoA to generate NADH and $FADH_2$, which are then converted to ATP via the electron transport chain **(Figure 1.3**) (Martínez-Reyes and Chandel, 2020). The TCA cycle was found to be dysregulated in PDAC, in which increased levels of pyruvate from glycolysis were reduced to lactate and fed into the TCA cycle to generate citrate for FAS (Reyes-Castellanos et al., 2020). Metabolites such as fumarate, succinate and D2-hydroxyglutarate were reportedly upregulated in cancer cells as a result of the dysfunction of the enzymes, fumarate dehydrogenase, succinate dehydrogenase and isocitrate dehydrogenase (Laurenti and Tennant, 2016). Elevated levels of these metabolites have been shown to increase ROS levels which, in turn, activated signalling pathways, such as P13K/AKT/mTOR, which

promote carcinogenesis (Nogueira and Hay, 2013; Waitkus et al., 2018). Macrophages are proinflammatory when there is a shift towards glycolysis and FAS, promoting the production of IL-β and TGF-β. Conversely, macrophages are polarized towards the anti-inflammatory state when there is a shift towards the Krebs cycle and FAO (Rodríguez-Prados et al., 2010). Increased citrate synthase activity was observed in PDAC upon measuring the activity in the tissues of patients with pancreatic cancer (Schlichtholz et al., 2005a); citrate synthase catalyses the reaction between Acetyl CoA and oxaloacetate to produce citrate, which is a substrate for membrane lipid synthesis (Swierczynski et al., 2014). Although pancreatic cancer has been associated with elevated citrate synthase levels, increased citrate production inhibits phosphofructokinase (PFK)2 (Halabe Bucay, 2009). PFK2 is a promoter of PFK1, an enzyme that catalyses the conversion of fructose-6-phosphate to fructose-1,6-biphosphate in the presence of ATP, thereby controlling glycolysis in cancer cells. M2 macrophages, which are observed in PDAC, utilize oxidative phosphorylation to support their metabolic demands and have an uninterrupted Krebs cycle (Amedei et al., 2014; O'Neill et al., 2016).

Pentose Phosphate Pathway (PPP)

The PPP consists of two phases, oxidative and non-oxidative, both of which were revealed to be upregulated in pancreatic cancer (Swierczynski et al., 2014). The major products of the oxidative phase of PPP are nucleotides and NADPH, while the non-oxidative phase generates ribonucleotides for DNA synthesis, which is mediated by transketolase and transaldolase enzymes (Patra and Hay, 2014). The mRNA expression levels of transketolase were reported to be upregulated in the pancreatic cancer cell lines, Panc-1, MiaPaca-2 and CaPan-1 (Liu et al., 2010). In addition, a previous study revealed that the activation of the non-oxidative phase of the PPP in pancreatic cancer promoted resistance to gemcitabine treatment (Shukla et al., 2017). Macrophages are polarized towards an M2 phenotype when the PPP is inhibited, thus indicating the importance of the PPP in the pro-and anti-inflammatory response of macrophages, as shown in **Figure 1.2**. Screening of 199 human kinases for their potential roles in immunoregulation revealed that the sedoheptulose kinase (SHK) enzyme, which limits the PPP, served an important role in macrophage polarization (Haschemi et al., 2012). In addition, the results proved that SHK enzyme downregulation was essential for the M1 reprogramming in macrophages. The PPP was found to be highly activated in lipopolysaccharide-activated macrophages due to the induction of the pyruvate kinase isoenzyme M2, which is an enzyme that diverts glycolytic intermediates to other biosynthetic pathways (Palsson-McDermott et al., 2015).

Amino acid Metabolism

L-type amino acid transporter (LAT-1) transports large amino acids, such as tryptophan, phenylalanine, tyrosine and histidine, among others (Fernandez-Zapico et al., 2019). LAT-1 was shown to be overexpressed in PDAC and was linked to angiogenesis and tumour cell proliferation (Altan et al., 2018). The breakdown of tissue proteins to branched-chained amino acids was revealed to be one of the early consequences of pancreatic cancer, thus, it may be used as a potential biomarker (Commisso et al., 2013). For example, leucine, isoleucine and valine are branched-chain essential amino acids (Ananieva and Wilkinson, 2018), which were reported to be elevated in pancreatic cancer because they are an alternative source of organic molecules that can fuel the TCA cycle. Whole-body protein breakdown associated with elevated BCAA levels might be an early event in PDAC development (Mayers et al., 2014).

Exosomes derived from the tumour microenvironment were also identified to enhance the proliferation of pancreatic cancer cells by supplying metabolites, such as proteins, nucleic acids and amino acids (Yao et al., 2020; Zhao et al., 2016). Due to poor vascularization, pancreatic tumours do not have a sufficient supply of glutamine; instead, they use micropinocytosis to engulf extracellular proteins, which are subsequently degraded in lysosomes to release glutamine and other amino acids (Kamphorst et al., 2015). PDAC is characterized by a low expression of glutamate dehydrogenase and the overexpression of glutamic oxaloacetic transaminase for the conversion of glutamine-derived aspartate to oxaloacetate in the cytoplasm, which is then further converted to malate and finally into pyruvate (Son et al., 2013). Glutamine regulates the balance between T-eff cells and T-regs; however, in the PDAC microenvironment, the transporter protein, alanine-serine-cysteine transporter 2, was found to be deficient, leading to the diminished generation and function of Th17 and Th1 cells (Singer et al., 2018), hence promoting T-reg formation.

Upon activation, T cells consume a large amount of arginine and tryptophan to generate memory T cells by switching from glycolysis to oxidative phosphorylation, which activates antitumor activities (Sinclair et al., 2013). Amino acids produce derivatives that support cancer growth and progression; for example, in the PDAC microenvironment, the overexpression of indoleamine-2,3-dioxygenase (IDO) and arginase depleted tryptophan and arginine, thereby suppressing T cell proliferation and activating T-reg differentiation (Pilotte et al., 2012). Glutamate conversion into α-ketoglutarate by glutamate dehydrogenase was shown to promote

cancer growth because it served as an anaplerotic intermediate for the TCA cycle and provided nitrogen for non-essential amino acid biosynthesis (Cluntun et al., 2017).

Lipid Metabolism (Fatty Acid Oxidation and Fatty Acid Synthesis)

- Fatty Acid Oxidation (FAO)

  FAO serves as a source of energy for the proliferation and survival of cancer cells (De Oliveira and Liesa, 2020). FAO is an alternative source of Acetyl CoA that enters the TCA cycle for ATP production and energy (Figure 1.2) (O'Neill et al., 2016). In another study, it was shown that ATP production in PDAC relies more on FAO rather than Glycolysis (Lee et al., 2020). Pancreatic tumours and cell lines have been shown to overexpress the cyclooxygenase (COX)2 enzyme, which was identified to be associated with the invasiveness and metastasis of the disease (Nzeako and Gores, 2002). COX2 catalyses the rate-limiting step in arachidonate metabolism to produce prostaglandin (Asano et al., 2002). The PDAC microenvironment was discovered to release endothelial growth factors, tumour promoters and cytokines, which induced COX2 expression (Molina et al., 1999). Dubois and colleagues (DuBois et al., 1994) showed that transforming growth factor-α and tumour promoter tetradecanoyl phorbol acetate stimulates the production of eicosanoids, such as COX2, in rat intestinal epithelial cell culture. Increased expression of COX2 plays a major role in the overproduction of PGE_2, which inhibits immune response in malignant tissues and apoptosis as well as induction of proliferation and angiogenesis (Dannenberg and Subbaramaiah, 2003; Sato et al., 1997). FAO was also indicated to serve an important role in regulating the balance between T-eff cells and suppressive T-regs, as it was observed to promote the generation of T-regs while inhibiting T-eff cell polarization (Michalek et al., 2011). FAO also enhanced the activation and maintenance of memory $CD8^+$ T cells (O'Sullivan et al., 2014).

- Fatty Acid Synthesis (FAS)

  Products derived from other cell metabolic pathways, such as glycolysis, the TCA cycle and PPP are used by cells to generate lipids for cellular growth in the FAS pathway (O'Neill et al., 2016). In pancreatic cancer, FAS involves the upregulation of ATP citrate lyase, Acetyl CoA carboxylase, fatty acid synthase (FASN), Acetyl CoA synthetase, stearoyl CoA desaturase, polyunsaturated fatty acids, monounsaturated fatty acids (MUFA) and saturated fatty acids (Swierczynski et al., 2014). Some plasma lipids, such as very-low-density lipoproteins, were also shown to be elevated, while

low-density lipoprotein, high-density lipoprotein and 3-hydroxybutyrate were decreased in patients with PDAC (Zhang et al., 2012). ATP-citrate lyase, an enzyme that converts citrate to Acetyl CoA which is a precursor for FAS, was also revealed to be upregulated in PDAC (Hatzivassiliou et al., 2005).

Deregulated FAS in PDAC, such as the biogenesis of fatty acids due to the overexpression of FASN, reportedly promoted cancer progression via resistance to chemotherapy (Tadros et al., 2017). Following resection, FASN levels are decreased in the majority of patients with PDAC, suggesting that elevated levels of FASN may be associated with poor survival and gemcitabine unresponsiveness via enhanced estrogen receptor stress (Guillaumond et al., 2015; Tadros et al., 2017). Another enzyme that serves an essential role in FAS is acyl CoA synthetase, which converts long-chain fatty acids to acyl CoA, a critical step in phospholipid and triglycerol biosynthesis (Coleman et al., 2002). Stearoyl-CoA desaturase-1 was demonstrated to exert an important role in the pathogenesis of PDAC by regulating the production of MUFAs (Macášek et al., 2012). Alcohol and tobacco-related carcinomas, such as PDAC, have also been shown to overexpress the aldo-keto reductase family 1B10 (AKR1B10) enzyme, which catalyses the production of aldehyde and NADPH from alcohol and $NADP^+$ (Chung et al., 2012). AKR1B10 is essential in FAS by regulating the stability of Acetyl CoA carboxylase, which can catalyse the biosynthesis of malonyl CoA, a FASN substrate. Fatty acids are esterified to phospholipids, which are required for membrane formation, and this pathway was indicated to be the most abundant in advanced pancreatic cancer (Swierczynski et al., 2014). Cholesterol uptake was also identified to be elevated in PDAC, as pancreatic cancer cells are highly dependent on cholesterol (Guillaumond et al., 2015). A summary of the discussed metabolic pathways and how they influence immune cells is presented in **Table 1.1.**

Table 1.1: Immune cells and their role in pancreatic cancer as well as the pathways through which they perform their functions.

Immune Cells	**Immune Cell in PDAC**	**Pathways Involved in PDAC**	**Immune Cell functions in PDAC**	**References**
Macrophages	i. Switch from M1 to M2 macrophages due to cytokines such as IL-10 and TGF-β ii. Tumour-associated macrophages: Releases growth factors such as VEGF and expresses PD-L1 (binds to programmed cell death on the surface of activated T cells).	TCA cycle and Fatty acid oxidation	Immunosuppression Angiogenesis Tumour cell metastasis Inhibits Tcell activation	(Sideras et al., 2014) (Chen et al., 2019)
T-cells	$CD8^+$T-cells suggest a better prognosis and favourable clinical outcome in PDAC. $CD4^+$T-cells • Th1 promotes anti-cancer • Th2 cells secrete cytokines such as IL-13 and IL-10 • Th17 could be pro or anti tumourigenic • T-regs i. Secretion of IL-10 and TGF-β ii. CTLA-4 are receptors on T-regs that produce inhibitory signals.	Fatty acid Oxidation, TCA cycle Glycolysis Oxidative Phosphorylation and Fatty Acid Oxidation	Phagocytosis and inhibition of tumour growth Inhibition of tumourigenesis Promotes tumour growth and tumorigenesis Immunosuppression Inhibition of tumour growth Immunosuppression and tumour growth Inhibition of immunology synapse and destruction of infected cells Impairs T cell activation and finally leads to T cell death	(Fukunaga et al., 2004; Masugi et al., 2019; O'Sullivan et al., 2014) (O'Neill et al., 2016; Wörmann et al., 2013) (De Monte et al., 2011) (Gnerlich et al., 2010; He et al., 2011) (Daniel et al., 2019; Sakaguchi et al., 2010) (Macintyre et al., 2014)
Dendritic cells	Decreased levels correlate to poor survival rate in PDAC	Glycolysis and Pentose Phosphate Pathway	Antigen presentation	(Chang et al., 2016; Yamamoto et al., 2012)
Mast cells	Mast cells promote tumour progression. Elevated levels correlate with metastasis in human PDAC.	Fatty Acid synthesis	Angiogenesis and Metastasis	(Cai et al., 2011; Longo et al., 2018; Ribatti, 2016)
Natural Killer cells	Decreased levels correlate to a worse prognosis in PDAC	Glycolysis	Produces cytokines for cancer cell destruction	(Duan et al., 2011; Lin et al., 2017)
MDSC	MDSC levels in PDAC correlate to increased levels of cytokine IL-13 and T-regs	Amino acid metabolism, Fatty acid synthesis	Immunosuppression and Inhibition of T cell activation	(Gabitass et al., 2011; Gabrilovich, 2017; Ostrand-Rosenberg, 2010)

1.4 Treatment development involving metabolic regulation in PDAC

Recent treatment developments involving TCA inhibition in PDAC include phase II and III clinical trials investigating a TCA cycle inhibitor delimitate, also known as CPI-613® (ClinicalTrials.gov.nos. NCT03435289 and NCT03504423). The combination of CPI-613 with gemcitabine, nab-paclitaxel and FOLFIRINOX has been explored for unresectable, locally advanced and metastatic PDAC (Alistar et al., 2020; Philip et al., 2019). These clinical studies demonstrated that CPI 613 can be safely administered with gemcitabine and nab-paclitaxel at doses up to 1500 m/g^2 and further studies are still ongoing. In addition, the P13K-AKT-mTOR signalling pathway controls cell cycle, survival, metabolism and motility in cancer (O'Donnell et al., 2018). Hence, studies targeting mTOR inhibition such as phase I and II clinical trials (ClinicalTrials.gov.no. NCT03362412) investigating Sirolimus and Metformin (ClinicalTrials.gov.no. NCT02048384), which are mTOR inhibitors, for the treatment of patients with advanced pancreatic cancer (Bever et al., 2020; Jin and Zhao, 2020) could be very vital in novel therapy development. A combination of metabolic regulation and chemotherapy could be more effective than the use of chemotherapy alone. A recent ongoing study on metastatic PDAC patients monitoring cholesterol disruption using Atorvastatin, Ezetimibe and Repatha, which are cholesterol-reducing drugs in combination with Folfirinox (ClinicalTrials.gov.no. NCT04862260) to modulate AKT signalling. This regulates proliferation and migration, hence inhibiting tumourigenesis (Kumar and Mandal, 2021). The aggressive and unresponsive nature of pancreatic cancer highlights a requirement for an improved understanding of the mechanism of progression to provide effective therapeutic targets. Immunotherapy is a growing and promising treatment strategy in cancer; however, in pancreatic cancer, it is clear that further studies are required to investigate its effectiveness.

The dysregulated interaction between the immune system and metabolic pathways in pancreatic cancer could provide greater insight into this disease. Furthermore, understanding these interactions may enable the development of effective therapeutic options that might increase the survival rate of patients. Targeting these pathways to enhance or elicit an immune response would be beneficial. Several studies have investigated the potential of targeting metabolic pathways and the effect on immune response in carcinogenesis, which is summarized in **Table 1.2**. Future studies to determine these effects in pancreatic cancer and discover new targets may prove favourable.

Table 1.2: Metabolic pathways with their potential roles as effective immunotherapeutic strategies

Metabolic Pathways	Prospective immunotherapy Strategies	References
Glucose Metabolism	• Targeting inhibition of tumour cells derived lactate on human T-cells as it enhances T-cell proliferation and cytotoxicity activities of NK and CD8 T-cells.	(Brand et al., 2016)
	• The use of PD-1 blocking antibodies promotes antitumor activities by enhancing T-cell proliferation via glycolysis inhibition and FAO promotion.	(Patsoukis et al., 2015)
	• Inhibition of key glycolytic enzymes such as lactate dehydrogenase A (LDHA) and Pyruvate Kinase Isoenzyme 2 (PKM2) correlates to the reduction of the infiltration of MDSC and promotion of $CD8^+$ T-cells, NK and T-cells.	(Liu et al., 2015; Mohammad et al., 2016)
Lipid metabolism	• Targeting the inhibition of COX2 and suppression of its metabolite prostaglandin E2 (PGE2) using Paeonol exerts anticancer effects by inhibiting the reprogramming from M1 to M2 macrophages.	(Kalinski, 2012; Li et al., 2014; Wang et al., 2021)
	• FAO inhibition in myeloid-derived suppressor cells enhances T-cell function and decreases cytokine production.	(Arina and Bronte, 2015; Hossain et al., 2015)
	• Immunosuppression of MDSCs via regulation of metabolic pathway involved in the transformation of amino acids to PGE_2 to inhibit lipid accumulation.	(Yan et al., 2019)
Amino Acid Metabolism	• Inhibition of Indoleamine -2,3-dioxygenase (IDO) to promote T cell proliferation and response.	(Yu et al., 2018)
	• Inhibition of glutamine metabolism using Aminooxyacetate (AOA) to mediate cytotoxicity in tumour cells.	(Korangath et al., 2015)
	• Targeting LAT-1 and amino acid pathways using SM-88 or anti-LAT-1 antibodies promotes tumour growth inhibition via disruption of protein synthesis and activation of DCs and T-cells.	(Altan et al., 2018; Fernandez-Zapico et al., 2019)
	• Blockade of adenosine production through the inhibition of CD39 and CD73 promotes anti-cancer activity by activating DC maturation and T-cells and NK cells activation.	(Allard et al., 2017, 2020; Leone and Emens, 2018)

PD-1: Programmed cell death, NK: Natural killer cells, FAO: Fatty Acid Oxidation, MDSC: Myeloid-derived suppressor cells, COX2: cyclooxygenase-2

1.5 Study Rationale

Worldwide, pancreatic cancer is estimated to cause over 460,000 deaths and about 496,000 cases annually (Sung et al., 2021). Progression of the disease and subsequent metastasis result in difficulty in treating PDAC. Hence the need for more investigation of underlying molecular underpinnings especially in under-studied patient groups. Although patients of African descent have an elevated risk and poor survival rates of PDAC, there is little molecular and clinical information for this group.

Due to the aggressiveness of the PDAC and its resistance to treatment options such as chemotherapy and radiotherapy, there is an urgent requirement for sensitive and specific biomarkers for disease detection. Clinical biomarkers such as CA-19-9 are being used by clinicians in triaging PDAC patients and to predict their prognosis (Ballehaninna and Chamberlain, 2012). However, most of them are not efficient because they cannot detect the disease at the onset and cannot be used to competently evaluate patients at the time of admission. CA-19-9 lacks sensitivity and specificity because they are not usually elevated at the onset of PDAC and may also be overexpressed in various inflammatory conditions (Scarà et al., 2015). Metabolites are altered in PDAC and have shown potential as biomarkers in several studies (Zhang et al., 2013). Although PDAC patients of African descent have a higher incidence and poorer prognosis (Siegel et al., 2022), this group of patients are under-represented in published studies. To date, to our knowledge, there has been no published study investigating the alteration of metabolites in this patient group. This study aims to assess small metabolites as potential diagnostic and prognostic markers in patients of African ancestry. Considering that the immune system is known to play a pivotal role in both PDAC progression and treatment, it is envisaged that the expression of immune cells in the different stages of PDAC can help elucidate the function of the immune system during tumorigenesis. These expression levels can be influenced by metabolic processes that are known to be dysregulated during PDAC progression. Thus, deciphering the complex relationship between the immune response in PDAC and metabolism would provide an avenue to identify relevant networks and pathways that may influence PDAC progression. This may result in more understanding of this disease and highlight potential therapeutic options.

1.6 Aim

This study aimed to demonstrate the expression of metabolites and lipoproteins in a cohort of PDAC patients as well as identify the levels of immune markers and the possible associations in the progression of PDAC in a cohort of patients.

1.7 Objectives

- To describe the demographic and clinicopathological characteristics of patients with different stages of PDAC.
- To identify dysregulated metabolites and lipoproteins in different groups of PDAC; resectable (RPC), locally advanced (LAPC) and metastatic (MPC) patients and compare with the controls: chronic pancreatitis (CP) and healthy controls (HC) using Nuclear Magnetic Resonance spectroscopy.
- To determine lipoprotein parameters: HDL, LDL, and VLDL, particle number, size, and lipid concentration of each subtype using Lipoprint assay.
- To determine levels of the reactive oxygen species (ROS) in PDAC and control groups using Spectrophotometric assay.
- To determine the expression of selected immune markers by immunophenotyping and gene expression analysis.
- To correlate clinical data, metabolites, ROS, and immune cell marker levels and hypothesize possible relationships.

In this thesis, a description of the demographic and clinicopathological features of the patient cohort used in this study is provided chapter II. In chapter III, the serum metabolomic and lipoprotein profiles of these patients are reported. In chapter IV, the expression of immune cell markers was assessed and in chapter V, all the data from the various analyses: demographics and clinical, metabolomics and lipoproteins, reactive oxygen species, immunophenotyping, and PCR datasets are integrated using statistical tools.

CHAPTER II: DEMOGRAPHICS AND CLINICAL CHARACTERISTICS OF THE COHORT OF PANCREATIC DUCTAL ADENOCARCINOMA PATIENTS

2.1 Introduction

Although risk factors often influence the development of cancer, most do not directly cause cancer. For early diagnosis of PDAC, the development of an integrated system including demography, clinical information and, screening methodologies might be more sensitive and specific (Poruk et al., 2013). The low incidence of this disease makes the screening of the general population impractical and thus early detection of PDAC difficult (Singhi et al., 2019). International guidelines on early detection of PDAC recommend targeted screening of those whose risk of developing the disease is greater than 5% (Canto et al., 2013). Prediction models developed for PDAC incorporating data on age, sex, race, risk factors and clinical investigations were shown to reach an AUC of 0.85 in envisaging high-risk patients as well as early detection of the disease (Pereira et al., 2020). The main cause of PDAC is not known but a person with an average risk of PDAC has about a 1% chance of developing the disease (Rawla et al., 2019). This study summarises some demographics and provides an overview of the presentation patterns of PDAC in a black African cohort.

2.2 Demographics as risk factors in Pancreatic Ductal Adenocarcinoma

Information about the demography and risk factors may bring about more improved lifestyle and health care choices, thereby improving the diagnosis, prognosis and subsequent treatment and management strategies. Demographic features such as age, gender, and race/ethnicity have been implicated in PDAC occurrence.

Age: The evaluation of age at the onset or diagnosis of the disease has been shown to help further inform risk assessment of developing PDAC, especially where medical records or databases of family history are not available. The risk of developing PDAC increases with age (Brune et al., 2010). Most people who develop PDAC are older than 45 years. Approximately 90% of people with PDAC are older than 55 years while about 70% are older than 65 years (Malvezzi et al., 2016).

Sex: Pancreatic cancer has a slight male predominance, and this could be due to lifestyle and habits differences between both sexes (Siegel et al., 2022). However, recent statistics estimates for 2022 on African Americans/Black people showed that 3,040

men and 3,300 women will die from pancreatic cancer (Giaquinto et al., 2022). The female sex might positively predict response to FOLFIRINOX in metastasised PDAC patients (Hohla et al., 2014). The female gender was shown to be associated with elevated CA19.9 levels which were more responsive to FOLFIRINOX (Hohla et al., 2014).

- **Race/ethnicity**: PDAC prevalence and outcomes vary considerably between races and ethnic groups. African Americans are more likely to develop PDAC than Caucasians (Silverman et al., 2003). This could be a combination of genetic and socio-economic reasons affecting early detection, and treatment (Siegel et al., 2021). These differences in pancreatic cancer incidences between races can be ascribed to increased risk factors such as diet, alcohol, smoking and overweight (Rawla et al., 2019).

2.3 Clinical Presentation Patterns of Pancreatic Ductal Adenocarcinoma

Although most PDAC patients are symptomatic at presentation, symptoms are usually non-specific which leads to a delay in the time of prognosis between presentation and diagnosis (Grossberg et al., 2020). PDAC has been associated with symptoms such as weight loss, abdominal pain, jaundice, new on-set T2DM, bloating, nausea, vomiting, steatorrhea, changes in bowel movements, pruritus, lethargy, back and shoulder pain (Porta et al., 2005). However, other clinical signs such as epigastric mass and ascities are much less common. However, these symptoms manifest at an advanced stage (Keane et al., 2014). Loss of volume due to skeletal muscle and adipose wasting is described as an early sign of PDAC growth (Danai et al., 2018; Sah et al., 2019). Since there is no diagnostic system for PDAC, the development of some or most of the symptoms listed above along with T2DM and recurrent chronic pancreatitis could strongly suggest a predisposition to pancreatic cancer (Vujasinovic et al., 2020).

T2DM is a risk factor of PDAC that is characterised by hyperinsulinemia, insulin resistance and pancreatic β- cell dysfunction (Chatterjee et al., 2017). PDAC has a complex and bidirectional relationship with T2DM (Li et al., 2012). Approximately 1% of diabetic patients over 50 years will be diagnosed with pancreatic cancer within 3 years of the ailment onset (Andersen et al., 2017). However, about 50% of the patients will have developed T2DM within 1-2 years before their diagnosis of PDAC which could be an early sign of the tumour (Chari et

al., 2008). Chronic pancreatitis is an inflammatory condition of the pancreas that is usually irreversible and leads to exocrine and endocrine dysfunction (Gardner et al., 2020).
Several serum markers for pancreatic cancer have been evaluated, the most useful is carbohydrate antigen 19-9 (CA 199-9). CA 19-9 sensitivity is closely related to tumour size, location, stage and resectability (Kared et al., 2016). Several markers have emerged from clinical studies, but none have better sensitivity than CA 19-9. Recent studies show that combining CA19-9 with metabolites detection in blood samples could be useful in early prognosis (Fahrmann et al., 2019). Clinical parameters are vital in the diagnosis and management of PDAC (Varghese et al., 2021).

2.3.1 Laboratory patterns associated with PDAC

Haematological Parameters: Red blood cell (RBC) count, white blood cell (WBC) count, and haemoglobin (Hb) concentration are highly regulated with vital clinical importance (Kelada et al., 2012). Abnormal values outside the normal ranges could be indicative of disorders or other diseases such as cancer. The reduction of total lymphocytes in the blood is the main immunologic change in PDAC (Fogar et al., 2006). Circulating lymphocytes tend to decrease as PDAC progresses (Miyazawa et al., 2021; Wachsmann et al., 2012). Elevated Red blood cell count or distribution width (RWD) is directly related to oxidative stress by affecting the RBC membrane and glycoproteins. Hence, high RWD levels could be an indication of a nutrient deficiency such as iron, folate or vitamin B-12 resulting from anaemia which is a symptom of PDAC. In pancreatic cancer patients, RWD plays a vital role in understanding the stages of the disease and the development of postoperative complications which would help determine surgery time and neoadjuvant treatment plan (Yilmaz et al., 2014).

International normalised ratio (INR) is a test used to measure the time it takes for blood to clot. Patients with elevated INR values have shorter thrombosis times (Epstein et al., 2012). Activation of coagulation, inflammation and angiogenesis affect the morbidity and mortality of patients with pancreatic cancer (Nakchbandi and Löhr, 2008). Anticoagulant therapy may represent a useful strategy to improve the prognosis of pancreatic cancer patients (Mandalà and Tondini, 2011). Due to the negative effect of prolonged INR on survival, coagulation assays such as INR tests could be used to provide foresight about the outcome.

Although pH and CO_2 are not usually considered classical laboratory tests required in PDAC diagnosis they are considered for research study purposes. The pH of tumours is significantly lower than that of healthy tissues and this may be due to anaerobic glycolysis in tumours (Gatenby and Gillies, 2004). Additionally, CO_2 levels are reduced in cancer cells because they secrete lactic acid instead of breaking down glucose to CO_2 as described in Warburg effects (Vander Heiden et al., 2009).

Liver Function Tests: Also referred to as hepatic panels are used to check how well the liver is working by monitoring the levels of enzymes and proteins made or cleared by the liver. They might be raised if there is a blockage in the bile duct. Liver function tests also measure the bilirubin and albumin levels in the blood.

- Hyperbilirunaemia: Bilirubin is a breakdown product of haemoproteins that is taken up from plasma into liver hepatocytes where it is conjugated to glucuronic acid and the conjugated form is excreted into bile (Creeden et al., 2021). Elevated bilirubin levels in the liver may damage the liver cells causing liver dysfunction or failure. Causes of hyperbilirubinemia in PDAC patients are due to obstruction of the extra-hepatic biliary tree by a head tumour, blockage of the intrahepatic bile duct due to tumour metastases (Vogel et al., 2015), and massive infiltration of the liver by tumour metastases resulting in non-cirrhotic liver failure (Levitt and Levitt, 2014). Elevated conjugated bilirubin in PDAC could be due to reflux bilirubin glucuronides into plasma due to intra or post-hepatic obstruction (Vogel et al., 2015). Bilirubin levels are usually the first measured in patients presenting with jaundice such as PDAC patients. Patients with high bilirubin levels lose the prognostic significance of inflammatory immune biomarkers in PDAC (Aziz et al., 2019). Bilirubin can freely move into the brain and cause neurotoxicity which in turn affects survival in patients with PDAC leading to a poor prognosis (Feng et al., 2018).

  Other consequences of hyperbilirubinemia include coagulopathy which occurs due to derangement of homeostasis resulting in excessive bleeding or impaired clot formation usually monitored by INR test, acute kidney injuries caused by prolonged elevated bilirubin levels which results in renal tubules damage thereby affecting the nephrons and secondary biliary cirrhosis which is long-term damage to the liver caused by unresolved obstructive jaundice.

- Alkaline phosphatase (ALP): These are enzymes found in both the liver and bone which play an important role in breaking down proteins. Higher levels of ALP may indicate a blocked duct, liver damage or disease. Serum bilirubin and ALP levels are potential laboratory tests for distinguishing between the benign and malignant causes of jaundice (Pasanen et al., 1993).
- Gamma-glutamyl transferase (GGT): Elevated levels of these enzymes might be indicative of bile duct damage or liver disease. GGT remains the most widely used marker of alcohol abuse, levels typically rise after heavy alcohol intake that has continued for several weeks (Carter et al., 2019).

  Clinically, cholestatic jaundice can be diagnosed when the ratio of total bilirubin to conjugated bilirubin is greater than 50% and there are elevated levels of other clinical liver parameters such as alkaline phosphatase (ALP) and gamma-glutamyl transferase (GGT) (Tripathi and Jialal, 2020).
- Alanine transaminase (ALT): These are enzymes that convert proteins into energy for the liver cells. When the liver is damaged or infected, ALT is released into the bloodstream hence there are increased levels.
- Aspartate transaminase (AST): They are present at low levels in the blood. Increased AST levels may indicate liver damage or disease.

  Both ALTs and ASTs are usually normal at the early stage of PDAC, prolonged and untreated obstructive jaundice might cause liver damage or injury which in turn leads to elevated transaminases levels.
- Hypoalbuminemia: Albumin (Alb) is one of the most abundant blood plasma proteins produced in the liver and maintains the oncotic pressure of the systemic circulation (Feng et al., 2018). Lower serum Albumin concentration could be because of the production of IL-6 which regulates albumin production by hepatocytes (Barber et al., 1999). There is usually slight or no hypoalbuminemia in the early stages of PDAC, but as the disease progresses, Alb levels drop significantly and could serve as an indicator of the prognosis of the disease in combination with CRP levels (Zhang et al., 2020).
- An acute-phase protein known as C-reactive protein (CRP) is produced by the liver as part of the systemic inflammatory response. The prognostic role of CRP has been shown to correlate inversely with survival (Szkandera et al., 2014).

- Urea and Electrolytes (U and E): Electrolyte disorders are usually associated with worse outcomes in cancer. U and E measure the alteration in urea and electrolytes such

as sodium, calcium, magnesium, and potassium levels (Berardi et al., 2019). In PDAC it is very essential to check for U and E before surgery or chemotherapy because these blood tests show how well the kidneys are working. Waste chemicals called urea and creatinine are produced by the body. Our kidneys remove them from our blood and get rid of them in our urine.

2.4 Maladies associated with some of these symptoms

(1) Cholestatic Jaundice: Cholestasis is the stagnation in bile flow usually caused by obstruction or functionally impaired hepatocytes. It can be classified into intrahepatic or extrahepatic cholestasis depending on the level of obstruction (Bhandari and Toouli, 2006). In PDAC, extrahepatic cholestasis occurs due to the obstruction of the extrahepatic bile duct outside the liver. Major constituents of bile are bilirubin and bile acids. Retention of excess bilirubin in the hepatocytes manifests as jaundice which is a yellowish pigmentation of the skin and sclera (Chen et al., 2018). Clinically cholestatic jaundice is marked by elevated bilirubin and serum alkaline phosphatase levels (Tripathi and Jialal, 2020). PDAC patients develop cholestasis via malignant biliary obstruction which occurs when the flow of bile from the liver is reduced or blocked leading to elevated bilirubin levels (Ćwiklińska et al., 2020). Over 70% of pancreatic cancer patients have some level of cholestasis at the time of their diagnosis (Kruse, 2010) which has been linked to abnormal LDL originating from the reflux of bile lipoprotein into the plasma (Phatlhane and Zemlin, 2015). Cholestasis can be relieved by decompression using plastic or metal stents which could be carried out via Endoscopic Retrograde Cholangio Pancreatography (ERCP) (Boulay and Parepally, 2014) and might result in complications (Donelli et al., 2007). However, complications associated with biliary stents occur in about 10-30% of cases, which are accompanied by recurrent jaundice and in some cases might develop cholangitis (Donelli et al., 2007). Thus, second-line methods such as Percutaneous Transhepatic Biliary Drainage (PTBD), Endoscopic Ultrasound-guided Biliary Drainage (EUS-BD) and surgical bypass may also be carried out (Boulay and Parepally, 2014).

(2) Cholangitis: This is characterised by inflammation and infection of the bile duct system through elevated biliary obstruction and infection (Zimmer and Lammert, 2015). Some of the presenting symptoms of cholangitis are right upper abdomen pains, fever and jaundice. Cholangitis in PDAC patients is associated with stent occlusion and recurrent

biliary obstruction, hence should be considered in the treatment plan (Darnell et al., 2021). Preoperative cholangitis has been statistically associated with increased postoperative morbidity and mortality levels in some cancers (Wang et al., 2018).

In this study, the demographics and clinicopathological parameters were described and comparisons were made between the PDAC and control groups.

2.5 Methods

2.5.1 Patients recruitment and Clinical Data Collection

The study was approved by the University of Witwatersrand Human Research Ethics Committee (Medical) (Study number—M190681). All participants gave written informed consent. Patient clinical data were collected using the REDCap v9.0 (Harvey, 2018). Sample and data collection were conducted between March 2019 and March 2020. The sampling site was the Hepatopancreatobiliary Unit at Chris Hani Baragwanath Academic Hospital, Soweto Johannesburg, South Africa and sample processing was done at the Department of Surgery, Faculty of Health Science, University of the Witwatersrand.

Only patients with clinically and histologically proven PDAC were recruited for this study. The inclusion criteria considered patients from 18 years old and above, of African ancestry, and diagnosed with one of the three stages of PDAC. African ancestry in this cohort was established from the recruited patients who self-reported to belong to one of the ethnic groups of South Africa. Patients undergoing chemotherapy at the time of the study were excluded. Stratification into resectable (RPC), borderline resectable, locally advanced (LAPC), and metastatic (MPC) disease was conducted with a contrast-enhanced triple-phased CT-scan of the abdomen following the National Comprehensive Cancer Network (NCCN) guidelines (Tempero et al., 2019). For this study, both resectable and borderline resectable were categorized as RPC. In this group, the tumour either had not invaded any vessel or had invaded the portal vein to 90°, in which case neoadjuvant chemotherapy may have been necessary before surgery. The LAPC group included cases where the tumour had invaded the superior mesenteric artery and/or portal vein to more than 180°. Lastly, in the MPC, the tumour had spread to other organs such as the liver (Soweid, 2017). Chronic Pancreatitis (CP) patients and healthy volunteers (HC) enlisted from the University of Witwatersrand, also of African ancestry, were recruited as the control arm of the study. All the patients recruited in this study

were age-matched. To be eligible, all the healthy participants confirmed that they were in good health and were not taking any regular medication. Clinical parameters such as haematological, blood chemistry and liver function tests were obtained from the patients' file and National Health Laboratory Service (NHLS) website.

2.5.2 Statistical Analysis

The Wilcoxon and Kruskal–Wallis rank-sum tests were used to compare differences in numerical covariates (e.g., age). Fisher's exact test was used to assess differences between categorical variables (e.g., gender). The Wald test was used to calculate the statistical significance (*p*-value) *p*-values < 0.05 were considered significant. To account for multiple testing, a false discovery rate (FDR) of <10% was applied.

2.6 Results

Six CP and thirty-four patients with PDAC, including 22 with Resectable Pancreatic Adenocarcinoma (RPC), 8 with Locally Advanced Adenocarcinoma (LAPC) and 4 with Metastatic Adenocarcinoma (MPC), were recruited. Six healthy controls (HC) were age-matched using Kruskal Wallis test (*p*-value = 0.134). The demographic features and comorbidities of the patients with PDAC and CP were reported in **Table 2.1**. The demographic features were matched across the four patient groups (i.e., CP, RPC, LAPC and MPC). About 50% ($n = 21$) of the patients are smokers (≥1 packet a day) and 18 patients are alcohol consumers (>100 g of alcohol, which corresponds to six bottles of beer, per day). Only 6 out of 44 patients are HIV positive. Although the clinical treatment data of these patients are not available, most of them have CD4 counts >350 cells/µl. The frequency of cholestatic jaundice was statistically significant, with a high prevalence in PDAC patients while being absent in all of the CP patients. Of note, five of the PDAC patients developed cholangitis, an inflammation of the bile duct system often caused by bacterial infection, and this was higher in patients with more advanced stages of PDAC. As an expected consequence of cholestatic jaundice, raised bilirubin values were observed in PDAC groups compared to the CP group, as reported in **Table 2.2** and shown in **Figure 2.1**.

Table 2.1. Demographic and clinicopathological features of Pancreatic Ductal Adenocarcinoma patients compared to Chronic Pancreatitis.

Feature	HC (*n* = 6)	CP (*n* = 6)	RPC (*n* = 22)	LAPC (*n* = 8)	MPC (*n* = 4)	*p*-value
HIV status						0.831
Negative, *n* (%)	6 (100.0)	5 (83.3)	19 (86.4)	6 (75.0)	4 (100.0)	
Positive, *n* (%)	0 (0.0)	1 (16.7)	3 (13.6)	2 (25.0)	0 (0.0)	
Gender						0.286
female, *n* (%)	3 (50.0)	0 (0.0)	8 (36.4)	2 (25.0)	2 (50.0)	
male, *n* (%)	3 (50.0)	6 (100.0)	14 (63.6)	6 (75.0)	2 (50.0)	
Smoking						0.450
no, *n* (%)	6 (100.0)	1 (16.7)	12 (54.5)	4 (50.0)	2 (50.0)	
yes, *n* (%)	0 (0.0)	5 (83.3)	10 (45.5)	4 (50.0)	2 (50.0)	
Alcohol						0.962
no, *n* (%)	4 (66.67)	3 (50.0)	13 (59.1)	4 (50.0)	2 (50.0)	
yes, *n* (%)	2 (33.33)	3 (50.0)	9 (40.9)	4 (50.0)	2 (50.0)	
Age, median (IQR)	37 (24-54)	51 (46-57)	63 (50-67)	56 (48-62)	56 (46-70)	0.439
Obstructive jaundice						0.013
no, *n* (%)	6 (100.0)	6 (100.0)	8 (36.4)	2 (25.0)	1 (25.0)	
yes, *n* (%)	0 (0.0)	0 (0.0)	14 (63.6)	6 (75.0)	3 (75.0)	
Cholangitis						0.145
no, *n* (%)	6 (100.0)	6 (100.0)	20 (90.9)	7 (87.5)	2 (50.0)	
yes, *n* (%)	0 (0.0)	0 (0.0)	2 (9.1)	1 (12.5)	2 (50.0)	
T2DM						0.322
no, *n* (%)	6 (100.0)	3 (50.0)	16 (72.7)	7 (87.5)	4 (100.0)	
yes, *n* (%)	0 (0.0)	3 (50.0)	6 (27.3)	1 (12.5)	0 (0.0)	
Hypertension						0.560
no, *n* (%)	6 (100.0)	6 (100.0)	17 (77.3)	6 (75.0)	4 (100.0)	
yes, *n* (%)	0 (0.0)	0 (0.0)	5 (22.7)	2 (25.0)	0 (0.0)	

Healthy Controls (HC) are not included in statistical analysis IQR: interquartile range; T2DM: Type 2 Diabetes Mellitus; CP: chronic pancreatitis; RPC: Resectable Pancreatic Ductal Adenocarcinoma; LAPC: Locally Advanced Pancreatic Ductal Adenocarcinoma; MPC: Metastatic Pancreatic Ductal Adenocarcinoma.

Table 2.2: Liver Function Tests of the Chronic Pancreatitis and Pancreatic Ductal Adenocarcinoma groups.

Feature	* Physiological Range	CP Median	RPC Median	LAPC Median	MPC Median	*p*-Value	FDR
Total Protein (g/L)	60–78	66.0	59.0	66.0	69.0	0.289	0.330
Albumin (g/L)	35–52	36.5	30.0	27.0	32.5	0.361	0.361
Total Bilirubin (µmol/L)	5–21	5.0	154.0	120.0	58.0	0.006	0.030
Conjugated Bilirubin (µmol/L)	0–3	2.0	141.0	112.5	45.0	0.008	0.030
Alanine transaminase (U/L)	10–40	18.0	88.0	29.5	38.0	0.051	0.082
Aspartate transaminase (U/L)	15–40	28.5	104.0	55.0	75.0	0.019	0.052
Alkaline phosphatase (U/L)	53–128	74.0	615.0	337.0	314.5	0.025	0.052
Gamma-glutamyl transferase. (U/L)	<68	61.5	751.0	301.0	483.0	0.151	0.201

FDR: false discovery rate; CP: chronic pancreatitis; RPC: Resectable Pancreatic Ductal Adenocarcinoma; LAPC: Locally Advanced Pancreatic Ductal Adenocarcinoma; MPC: Metastatic Pancreatic Ductal Adenocarcinoma. *Physiological range calculated by Bio Analytical Research Corporation South Africa (https://www.barcsa.co.za/test-directory/test-reference-ranges/), Accessed on 6th September 2021.

Although not statistically significant, the PDAC groups also displayed the typical profile associated with cholestatic jaundice, including increased alkaline phosphatase and gamma-glutamyl transferase activity and a lesser increase in the transaminase enzymes, when compared to the CP patients. Interestingly, T2DM tended to be more frequent amongst CP patients when compared to PDAC patients, although statistical significance was not achieved. From the routinely collected clinical data, no statistical significance was observed for routine haematological (**Table 2.3**), however an increase in levels was observed in white cell count, platelet count and INR while a decline was seen in haematocrit, haemoglobin, prothrombin time and red cell count when comparing the PDAC and CP groups. There was also no statistical significance observed for chemistry parameters (**Table 2.4**) between the PDAC and CP groups. The marker, CRP, was not included because the data was not collected, however, inflammatory status was assessed by comparing the reactive oxygen species (ROS) levels of the PDAC and CP groups in chapter 4.

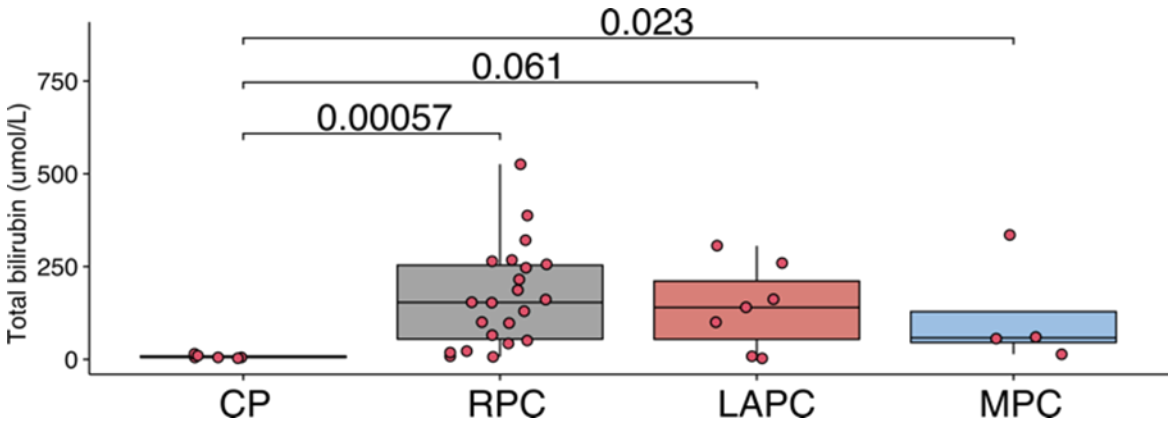


Figure 2.1: Boxplot of Total Bilirubin across all the groups with p-values. Showing statistically significant higher values of Total Bilirubin in PDAC groups RPC, LAPC and MPC compared to CP using the Wilcoxon Rank Sum test. Higher values of bilirubin may be due to bile obstruction, which might cause damage to the liver. CP: Chronic pancreatitis; RPC: Resectable Pancreatic Ductal Adenocarcinoma; LAPC: Locally Advanced Pancreatic Ductal Adenocarcinoma; MPC: Metastatic Pancreatic Ductal Adenocarcinoma.

Table 2.3: Haematological parameters of the Pancreatic Ductal Adenocarcinoma and Chronic Pancreatitis patient groups.

Feature	CP median [IQR]	RPC median [IQR]	LAPC median [IQR]	MPC median [IQR]	*p*-value	FDR
Haematocrit	0.385 [0.282 0.455]	0.316 [0.281 0.367]	0.303 [0.244 0.325]	0.339 [0.304 0.373]	0.482	0.620
White cell count (/L^9)	6.83 [6.153 8.182]	8.89 [6.91 12.4]	10.845 [7.927 11.037]	9.905 [4.225 17.31]	0.484	0.620
Haemaglobin (g/DL)	12.7 [9.6 14.6]	10.25 [9.475 11.525]	9.4 [7.825 10.775]	10.95 [10 11.6]	0.507	0.620
Platelet count (/L^9)	245 [222.75 339.25]	372.5 [313 502.75]	436.5 [324.25 497]	358 [317.75 405.25]	0.206	0.594
Prothrombin time	12.1 [11.675 12.9]	13.2 [12.5 15.2]	14.35 [13.025 14.525]	14.2 [13.525 16.05]	0.151	0.594
INR	0.935 [0.927 0.975]	1.08 [1 1.175]	1.165 [1.048 1.183]	1.165 [1.122 1.317]	0.038	0.414
MCV (fL)	92.25 [88.525 93.275]	93 [88 98.3]	89.45 [87.675 91.675]	91.25 [86.75 95.15]	0.647	0.684
MCH (pg)	30.05 [28.25 31.325]	30.2 [28.9 32.5]	29.95 [28.825 30.825]	28.5 [27.85 29.2]	0.260	0.594
MCHC (g/dl)	32.3 [31.75 33.15]	33.4 [32.2 33.8]	33.1 [31.725 33.575]	31.05 [30.8 31.775]	0.312	0.594
MPV (fL)	10.3 [9.2 10.5]	10.5 [9.6 10.9]	10.4 [9.675 11.2]	10.9 [10.575 11.225]	0.324	0.594
Red cell count (/L^12)	4.09 [3.018 4.878]	3.49 [2.99 3.83]	3.325 [2.538 3.852]	3.77 [3.425 4.095]	0.684	0.684

IQR: Interquartile range. FDR: False Discovery Ratio, CP: chronic pancreatitis; RPC: Resectable Pancreatic Ductal Adenocarcinoma; LAPC: Locally Advanced Pancreatic Ductal Adenocarcinoma; MPC: Metastatic Pancreatic Ductal Adenocarcinoma INR: International Normalised Ratio, MCV: Mean Corpuscular Volume, MCH: Mean Corpuscular Hemoglobin, MCHC: Mean Corpuscular Hemoglobin concentration, MPV; Mean Platelet Volume

Table 2.4: Blood chemistry of the Pancreatic Ductal Adenocarcinoma and Chronic Pancreatitis patient groups.

Features	CP median [IQR]	RPC median [IQR]	LAPC median [IQR]	MPC median [IQR]	p-value	FDR
Sodium (mmol/L)	138 [135.5 139.75]	137 [135 140]	135.5 [129.5 137.5]	139.5 [138.5 141]	0.295	0.889
Potassium (mmol/L)	4.05 [3.7 4.4]	3.7 [3.4 4.1]	3.55 [3.275 4.075]	3.7 [3.125 4.3]	0.659	0.889
Chloride (mmol/L)	97.5 [97 101.75]	96 [93 97]	93.5 [89.75 96.5]	90.5 [88.75 93]	0.127	0.889
Bicarbonate (mmol/L)	19.5 [18.25 20.75]	23 [17 25]	20 [19.75 21.5]	24.5 [18.5 30.25]	0.800	0.889
Anion gap (mmol/L)	24.5 [20.75 26.75]	26 [19 30]	23 [22 26.25]	29.5 [25.75 33]	0.445	0.889
Calcium (mmol/L)	2.26 [2.198 2.382]	2.2 [2.11 2.31]	2.105 [1.978 2.235]	2.135 [2.128 2.148]	0.403	0.889
Magnesium (mmol/L)	0.865 [0.83 0.885]	0.79 [0.68 0.9]	0.77 [0.682 0.885]	0.78 [0.72 1.16]	0.800	0.889
Inorganic Phosphate (mmol/L)	1.18 [1.13 1.32]	1.06 [0.96 1.2]	1.085 [0.995 1.278]	1.14 [1.098 1.367]	0.477	0.889
Urea (mmol/L)	4 [3.45 5.45]	4 [2.2 5.5]	3.5 [2.075 7.125]	4.35 [3.05 6.325]	0.945	0.645
Creatinine (µmol/L)	90 [64.25 130]	71 [58 95]	64.5 [48 79.75]	76.5 [72.75 80.25]	0.585	0.889

IQR: Interquartile range, FDR: False Discovery Ratio, CP: chronic pancreatitis; RPC: Resectable Pancreatic Ductal Adenocarcinoma; LAPC: Locally Advanced Pancreatic Ductal Adenocarcinoma; MPC: Metastatic Pancreatic Ductal Adenocarci

2.7 Discussion

PDAC remains a devastating malignancy with a very poor survival rate. Early detection of this disease will play a vital role in treatment strategies. Integration of demographic, clinical information, imaging, surgical and systemic therapies could be useful in developing novel strategies thereby improving prognosis.

Impact of Demographics

Although the features such as age, sex, smoking, and alcohol consumption were not statistically distinguished across the groups, this study confirms that PDAC is more prevalent in males than females and this could be due to lifestyle habits such as excessive alcohol consumption and smoking (Huang et al., 2021).

Hyperbilirubinemia in PDAC

PDAC patients present with obstructive jaundice (Aziz et al., 2019) hence it was statistically altered across the groups in this cohort. Furthermore, MPC had the highest cholangitis, although not statistically significant and this could be due to the sample size. In this study, cholangitis could be due to stent treatment and recurrent biliary obstruction as most of the PDAC patients have undergone the treatment, and about 10% required additional stenting or other forms of treatment (Darnell et al., 2021). In this study, total and conjugated bilirubin levels were significantly distinguished across the groups as expected due to the obstruction of the bile flow by the tumour. Other liver function test parameters such as GGT and AST exceeded the normal physiological threshold although not statistically distinguished across the groups. Hence, this study confirms that PDAC is associated with increased levels of total and conjugated bilirubin as well as other liver parameters such as ALP and GGT, as observed in similar studies (Aziz et al., 2019; Maringhini et al., 1993).

The Effects of other diseases in Pancreatic Ductal Adenocarcinoma

In this study, T2DM, hypertension and HIV were not statistically distinguished across the groups, this could be because most PDAC patients have been undergoing treatment for the various maladies and sample size limitation. Although T2DM is a risk factor for PDAC, studies have shown that pancreatic cancer-associated diabetes is of recent onset (Pannala et al., 2009). CP and T2DM are risk factors for PDAC, however, in this study T2DM was more prevalent in CP. The prevalence of T2DM in CP might be caused by fibro-inflammatory destruction (Hart

et al., 2016). CP is an inflammatory disease that replaces the pancreatic organ with fibrotic tissue (Braganza et al., 2011). Beta-cell dysfunction and loss as well as insulin resistance are the effects of T2DM in patients with CP (Olesen et al., 2020).

2.8 Conclusion

This study confirms that PDAC presents as obstructive jaundice characterised by elevated bilirubin levels. Most of the demographics and clinicopathological features could not be distinguished across the groups and this could be due to sample size which might result in type 2 errors, especially with subgroup analyses. Hence, the need for the establishment of other biomarkers that could be more specific in a validation study with a larger cohort is an endeavour that is already under consideration as part of postdoctoral work.

CHAPTER III: SERUM METABOLOMIC AND LIPOPROTEIN PROFILING OF PANCREATIC DUCTAL ADENOCARCINOMA PATIENTS OF AFRICAN ANCESTRY

3.1 Introduction

Pancreatic Ductal Adenocarcinoma (PDAC) is one of the most fatal cancers, primarily due to its late-stage presentation and resistance to therapy (Yao et al., 2020). Over the past two decades, the number of deaths caused by pancreatic cancer has doubled to over 441,000 cases globally (Klein, 2021). Although there is very little biological information on PDAC in the African population, they have been shown to have increased incidence and mortality, attributed to a combination of social (such as excessive smoking and alcohol intake) and genetic factors (Khawja et al., 2015; Silverman et al., 2003; Yadav and Lowenfels, 2013).

As a hallmark of cancer, tumour cells reprogram their metabolism, such as promoting glycolysis to maintain cell survival and increase proliferation rate (Hanahan and Weinberg, 2011; Tennant et al., 2010; Warburg et al., 1927) as described in Chapter 1. Metabolites are products of metabolism that navigate important biological functions such as energy conversion (Cacciatore et al., 2017; Labbé et al., 2019) and signalling (Elebo et al., 2021; Lu and Thompson, 2012). Blood metabolite concentrations can reflect the metabolic adaptation of tumour or highlight the host response to the tumour (Moore et al., 2019). For cancer cells to grow, multiply and metastasize they undergo abnormal metabolism to fulfil their high energy requirement (Schlichtholz et al., 2005). These metabolites are obtained from the blood or supplied by stromal cells. Abnormal metabolism could be seen in the overexpression of some metabolite transporters in cancer cells (El Ansari et al., 2018; Ma et al., 2019).

3.1.1 Altered Metabolites Expression in Pancreatic Ductal Adenocarcinoma

PDAC develops in a nutritional-deficient and hypoxic microenvironment characterized by poor angiogenesis and a large amount of dense connective tissue, hence they actively scavenge extracellular proteins (Kamphorst et al., 2015). Tumour cells reprogram their metabolism to survive in these hostile conditions and maintain their elevated proliferation rate, which is not exhibited by normal cells (Tennant et al., 2010) explained in Chapter 1. Due to these changes, specific metabolites may appear in the patient's serum that can be used as biomarkers. Previous

studies have shown the value of metabolomics analyses to detect PDAC (Kobayashi et al., 2013).

Metabolomics is a multidisciplinary omics science which is an analytical profiling technique for identifying, measuring and comparing a large number of metabolites present in biological samples (Emily Grace Armitage et al., 2017) thus promoting the identification of biomarkers that could be potential targets for the development of new therapies in PDAC. These biomarkers could be metabolites, small molecules which are products or intermediates of metabolism and signalling molecules. Dysregulated metabolism results in alteration in the number of metabolites, understanding the patterns of changes in metabolites could give an insight into the functional changes that occur due to the disease (Bathe et al 2010). Several metabolites such as leucine, valine, isoleucine, tyrosine, lysine, creatinine, triglycerides, and 3-hydroxybutyrate are dysregulated in PDAC (OuYang et al., 2011). In this sense, Nuclear Magnetic Resonance (NMR) spectroscopy was shown to be a powerful technique for the high-throughput analysis of blood samples (Bertini et al., 2012; Cacciatore et al., 2021). NMR is a versatile and efficient tool used to identify and quantify a wide range of metabolites and lipoproteins in a biological sample usually within a micro-molar range (Dunn et al., 2005). It has been used to investigate the serum metabolome of patients with PDAC to distinguish between malignant and benign diseased states (Bathe et al., 2011; Michálková et al., 2018, 2021; OuYang et al., 2011).

Metabolomics studies using NMR could be untargeted and have been found useful in identifying disease-associated biomarkers (Lusczek et al., 2013) as well as distinguishing between pancreatic cancer and benign hepatobiliary disease (Bathe et al., 2011). The carbohydrate fragment of N-acetylglucosamine (GlycA) is a composite NMR-based signal corresponding to changes in glycoprotein circulation (Otvos et al., 2015). This signal arises from the N-acetyl methyl groups of N-acetylglucosamine and N-acetylgalactosamine residues located on the glycan branches of plasma proteins; α1-acid glycoprotein, α1-antitrypsin, α1-antichymotrypsin, haptoglobin and transferrin (Eke G Gruppen et al., 2015). GlycA and N-acetylneuraminic acid (GlycB) are associated with common inflammation markers such as tumour necrosis factor-alpha (TNF-α), C-reactive protein (CRP), interleukin-6 (Eke G. Gruppen et al., 2015; Otvos et al., 2015) among others hence could be used as an inflammatory marker in PDAC.

3.2 Lipoproteins and their roles in cancer

Lipoproteins are cholesterol-rich particles that are complex endogenous aggregations of lipids and proteins synthesized in the liver. Their major role is the transportation of water-insoluble biological lipids such as triglycerides, phospholipids, and cholesterols (Feingold and Grunfeld, 2000) to their respective destination. They are classified into chylomicrons, very low-density lipoprotein (VLDL), low-density lipoprotein (LDL), and high-density lipoprotein (HDL) based on their densities (Jonas and Phillips, 2008). Cancer cells are rapidly dividing and have high requirements for cholesterols such as LDL which are cholesterol-rich particles and have been found to play important role in the prostate, colon, and adrenal gland cancers (Guan et al., 2019).

Lipoproteins are constantly changing in their composition and physical structure as the peripheral tissues take up various components leaving behind remnants that are returned to the liver. Free cholesterols, cholesterol esters and phospholipids are the main constituents of lipoproteins (Kwiterovich, 1998). Not much is known about the effect of lipoprotein on pancreatic cancer, hence the need for such studies.

1) Chylomicrons are ultra-low-density lipoproteins that consist of phospholipids, cholesterol, and apolipoprotein B48. Their main function is to transport triglycerides and fat-soluble vitamins from the intestines to other locations in the body such as the heart muscle, skeletal muscle and adipose tissues. The transfer of the triglycerides and cholesterol esters to the tissues depletes the protein aggregates leaving behind remnant chylomicrons which are taken up by the liver.

2) Low-density lipoprotein: These are lipoproteins involved in the distribution of cholesterol manufactured in the liver to the extrahepatic tissues and cells (Patel and Kashfi, 2022). Optimal levels of LDL-C are less than 100mg/dL while levels greater than 160 mg/dL are considered elevated (Stein et al., 2004). The uptake of cholesterol into the cells occurs via the binding of lipoproteins to the LDL receptors on the cell surface. LDL is then taken into the cells and broken down to free cholesterols and amino acids. Diseases associated with LDL are characterized by elevated cholesterol levels which are not efficiently disposed of from the blood. Elevated LDL-C levels have been associated with poor prognosis in breast, colorectal and prostate cancers (Liao et al., 2015; Magura et al., 2008; Rodrigues dos Santos et al., 2014).

3) Very low-density lipoprotein: The liver secretes VLDL which transports triglycerides to the other tissues and lipolyzed to IDL after entering the bloodstream.

They are finally converted to LDL by hepatic lipase in the liver for clearance and this process is known as the endogenous lipid pathway (Smelt, 2010). Very low-density lipoprotein contains apoE while LDL doesn't. Elevated levels of VLDL-cholesterol were observed in the metabonomic alterations from pancreatic intraepithelial neoplasia (PanIN) to PDAC hence, could be used as a biomarker for early diagnosis of the disease (Lin et al., 2016).

4) High-density lipoprotein: These are small spherical lipid-protein complexes with densities ranging from 1.06 to 1.21 g/ml. High-density lipoprotein transports excess cholesterol from the body tissues back to the liver where the cholesterol is broken down to bile acids and is then excreted. They are composed of an outer layer made up of free cholesterols, phospholipids and apolipoproteins (Apo) covering a hydrophobic core consisting of triglycerides and cholesterol esters. Apo A-I is synthesized in the liver and constitutes 60% of the protein content of HDL which is responsible for the antiatherogenic effect of HDL (Kwiterovich, 1998). Other apolipoproteins found in HDL particles include; Apo A I-IV, Apo C and Apo E. Decrease in HDL-C has been reported in metastatic liver cancer (Jiang et al., 2006). Chronic inflammation has been shown to reduce HDL-cholesterol levels (Feingold and Grunfeld, 2000). Cholesterol elimination from cancer cells by HDL results in PDAC growth and development inhibition, as well as apoptosis (Bauer et al., 2021).

3.2.1 Abnormal Lipoprotein (Lipoprotein X) in clinical pathologies

Lipoprotein X (LpX) is an abnormal lipoprotein rich in phospholipids and unesterified cholesterol associated with cholestasis found in lecithin-cholesterol acyl transferase (LCAT) deficiency characterized by a low concentration of HDL (Ćwiklińska et al., 2020). Lipoprotein profile can be altered in cholestasis when tumour growth mechanically increases the pressure in the surrounding tissues causing the blockage of the bile duct (Yan et al., 2009). Plasma concentration of LpX correlates to serum bilirubin levels (Stepien et al., 2013). LpX appears in patients with obstructive jaundice and could be used as a marker for cholestasis (Amar et al., 2019) and compared with alkaline phosphatase (AP), γ-glutamyl transferase (GGT), and bilirubin levels (Sörös et al., 1998). Lipoprotein profile can be altered in cholestasis when tumour growth mechanically increases the pressure in the surrounding tissues causing the blockage of the bile duct (Yan et al., 2009).

Patients with severe obstructive cholestasis secondary to pancreatic cancer have been shown to have high LpX concentrations (Sivakumar et al., 2011). PDAC patients with obstructive cholestasis have elevated total and conjugated bilirubin levels as well as high LpX concentration (Sörös et al., 1998).

Characterization of Lipoprotein X

Lipoprotein X is a spherical particle 30-70 nm in diameter and is associated with LDL fraction which is isolated in a density gradient of 1.006-1.063 g/ml. Albumin contributes to about 40% of the protein content while Apo C makes up the rest. It is made up of 66% phospholipids, 22% cholesterol esters, 3% triglycerides and 6% proteins. The major bile acid component of LpX is lithocholic acid while lecithin is the major phospholipid and it is fractionated into LpX1, LpX2 and LpX3. Lipoprotein X has a diameter ranging from 30nm to70nm with a density similar to LDL and a size similar to VLDL (Ahsan et al., 2014).

Although very little is known about the role of LpX in PDAC, the detection of LpX may be vital because it could influence treatment methods. Routinely available biochemical laboratory tests do not usually indicate the presence of LpX, hence electrophoresis and biochemical analysis are implored. In this study, dysregulated metabolites and lipoproteins in different groups of PDAC; resectable (RPC), locally advanced (LAPC) and metastatic (MPC) patients were identified compared to control groups: chronic pancreatitis (CP) and healthy controls (HC). Furthermore, the identified altered metabolites and lipoproteins were evaluated to show potential links with several maladies such as cholestasis and inflammation and parameters such as tumour aggressiveness and patient survival.

3.3 Materials and Methods

3.3.1 Sample Collection and Processing

Blood samples were collected during fasting by venepuncture in two separate clear vacutainer tubes (BD Biosciences, Franklin Lakes, NJ, USA) with coagulant EDTA (purple lid) and without anti-coagulant (red lid). The blood was processed to serum by centrifuging at 3000 rpm, 4 °C for 10 min after allowing it to clot for 30–60 min at room temperature. Plasma was then isolated after gravity separation for 30-60 min at room temperature followed by centrifugation at 3000 rpm, 4ºC for 30 min. The sample was processed within 2 h of collection and aliquoted (200 µl) in single-use vials, which were stored at -80 °C until needed. NMR

analysis was carried out at the Centre for Human Metabolomics, North-West University, Potchefstroom 2531, South Africa.

3.3.2 Serum Sample Preparation for NMR analysis

Three hundred microliters of thawed serum samples were aliquoted into a microcentrifuge tube and followed by 300 µL of a solution containing 0.75 M potassium phosphate buffer (pH 7.4), 5.81 mM of trimethylsilyl-2,2,3,3-tetradeuteropropionic acid (TSP; Sigma-Aldrich, St. Louis, MO, USA) and a trace amount of sodium azide dissolved in deuterium oxide. Samples were vortexed to ensure complete homogeneity and a final volume of 540 µL of each sample was transferred to a 5 mm NMR tube (Wilmad Lab Glass, Vineland, NJ, USA) and analysed.

3.3.3 Lipid Extracts Preparation

Lipids were extracted using the protocol described by Lamiquiz-Moneo et al. (Lamiquiz-Moneo et al., 2019). Three hundred microliters of BUME (butanol: methanol—2:1) were added to 100 µL serum aliquots in glass GC vials followed by 300 µL DIPE (diisopropyl ether: ethyl acetate—3:1) and 300 µL H_2O. Samples were vortexed for 1 min after the addition of BUME and H_2O and incubated on a shaker for 10 min at room temperature after DIPE addition to allow for lipid extraction. The samples were then centrifuged at 4000 rpm for 5 min, after which the top layer was transferred to clean vials, dried under N_2 at 37 °C and then resuspended in 600 µL solution of $CDCl_3$:CD_3OD:D_2O (chloroform-d:methanol-d:water-d; 16:7:1, *v*/*v*/*v*) containing 1.18 mM TSP. Five hundred and forty microlitres of this final solution were then transferred to a 5 mm NMR tube (Wilmad Lab Glass) for analysis.

3.3.4 Nuclear Magnetic Resonance Spectroscopic Analysis

One-dimensional (1D) proton (^{1}H)-NMR spectra were acquired using different pulse sequences on a 500 MHz Bruker Avance III HD NMR spectrometer equipped with a triple-resonance inverse 1H probe head and x, y, and z gradient coils. A standard nuclear overhauser effect spectroscopy (NOESY) pulse sequence presat (noesygppr1d.comp) was used on both serum and lipid extract samples. On serum samples, NOESY was used to detect both signals of small metabolites and high-molecular-weight macromolecules such as lipoproteins. Additionally, a standard diffusion-edited (DIFF) pulse sequence (ledbpgppr2s1d) was used on serum samples to detect only high-molecular-weight macromolecules, such as lipoproteins. Pooled samples

were used as a quality control sample and were included in each batch for qualitative assessment of repeatability by overlaying the raw spectra.

3.3.5 Nuclear Magnetic Resonance Profiling

NMR spectroscopy was used to quantify a panel of 75 signals. The peaks of the identified metabolites were fitted by combining a local baseline and Voigt functions based on the multiplicity of the NMR signal (Marshall et al., 1997). The assignment of quantified signals is reported in **Table S1**. To validate the efficacy of the different deconvolution models, the root-mean-square deviation was determined. The absolute concentration of each metabolite was calculated according to the previously reported equation (Serkova et al., 2005). The number of protons contributing to the unknown signals was imputed to 1. The concentration of carbohydrates was also estimated by considering the equilibrium between their cyclic forms.
GlycA and GlycB signals were quantified by integrating the areas between 2.00 and 2.05 ppm and between 2.09 and 2.05 ppm, respectively, above a local baseline, aiming to remove the signal of lipoproteins. The Liposcale test (Biosfer TesLab, Reus, Spain) was then used to determine lipoprotein parameters, HDL, LDL, and VLDL particle number, size, and lipid concentration of each subtype (Mallol et al., 2015). Each DIFF spectrum in the range between 0.1 and 9.5 ppm, excluding the regions corresponding to the water signals between 4.40 and 5.00 ppm, was segmented into 0.001-ppm chemical shift bins, and the corresponding spectral areas under the curve, giving a total of 8800 variables.

3.3.6 Lipoprint Low-Density Lipoprotein Assay

Principle

Lipoprint LDL is an electrophoresis system that is capable of separating lipoprotein fractions and subfractions (usually from VLDL to HDL) in a fasting serum or plasma with a Total Cholesterol ≥100 mg/dL. Lipoproteins are stained with a lipophilic dye and separated using a high-resolution linear polyacrylamide gel. The dye binds proportionally to the relative amount of cholesterol in each lipoprotein (Muñiz, 1977). These prestained lipoproteins undergo electrophoresis and as the lipoprotein particles migrate through the gel matrix, they are resolved into separate bands according to their sizes. HDL migrates the farthest followed by LDL and then VLDL. Chylomicrons usually remain in the loading gel or above the stacking gel. The gel tubes are placed into a digital scanner to generate an image of the resolved lipoprotein bands.

Procedure

Separation of VLDL, LDL and HDL particles based on size was performed on frozen plasma samples (-80ºC) by using polyacrylamide 3% gel electrophoresis Lipoprint® kit (Quantimetrix Inc., Redondo Beach, California) following the manufacturer's instructions of Lipoprint® system users manual (Delaye et al., 2017). The electrolyte buffer solution was prepared by dissolving one vial of the buffer salts in 1200 ml of distilled water. Gel tubes were removed from the jar and placed in the preparation rack with the unfilled end facing upwards. 25 µl of the plasma samples was placed in each tube after which 200 µl of the lipoprint loading gel was added to each tube. A strip of parafilm was placed between the gel tubes and the preparation rack to avoid contamination. The loading gel was mixed carefully by inverting the preparation rack several times and photo polymerised for 30 mins. Gel tubes were removed carefully and were placed in an electrolyte buffer solution to undergo electrophoresis for 60 mins. The Lipoprint LDL System Template was then used to identify the lipoprotein subfractions present on the gel.

3.3.7 Statistics and Data Analysis

Statistical analysis and graphical illustrations of the data were generated in R (version 3.6.1) and R studio (version 1.1.456) software, using scripts developed in-house. Wilcoxon and Kruskal–Wallis rank-sum test was used to compare differences in numerical covariates (e.g., age and metabolite concentration). Fisher's exact test was used to assess differences between categorical variables (e.g., gender). Spearman's rank test was used to calculate the correlation coefficient (rho) between variables. The Wald test was used to calculate the statistical significance (*p*-value) of the differences between the Kaplan–Meier survival curves. Prognostic factors for overall survival were analysed using the Cox proportional hazard regression. *p*-values < 0.05 were considered significant. To account for multiple testing, a false discovery rate (FDR) of <10% was applied. FDR is the ratio of the number of false-positive classifications to the total number of positive classifications. The KODAMA algorithm (Cacciatore et al., 2017) was used to identify patterns that demonstrate metabolic phenotypes across all samples (Bray et al., 2017). The partition around medoids (PAM) clustering (Rayward-smith, V.J., 2006) was applied to the KODAMA scores using the silhouette algorithm 10 (Rousseeuw, 1987) to verify the obtained results. The silhouette median value was utilized to assess the ideal number of clusters, ranging from 2 to 10.

Using partial least-squares (PLS) analysis, regression was performed on DIFF spectra metabolic profiles. Furthermore, a 10-fold cross-validation was performed to evaluate the predictive efficacy of the model (Bertini et al., 2012). Both the goodness of fit parameter (R^2) and the predictive ability parameter (Q^2) were also calculated using standard formulas (Eriksson et al., 2003). The Q^2 value was calculated from the *p*-value to assess the performance of the PLS regression model (Szymańska et al., 2012). A *p*-value < 0.05 was regarded as significant.

3.4 Results

3.4.1 Metabolic and Lipoprotein Signatures in the Different Tumour Stages

In this study, a serum sample analysis of the cohort was conducted using NMR spectroscopy. Three different sets of NMR experiments were conducted to collect a broad range of information (**Figure 3.1**). To delineate the metabolic signatures of PDAC, the Spearman's rank correlation test was performed to link metabolic values to the different PDAC groups in the following rank order: HC=0, CP = 1, RPC = 2, LAPC = 3, and MPC = 4. A total of 75 signals were quantified from the NMR spectra of serum samples and lipid extracts, including 29 metabolites, 19 lipid classes, inflammatory markers, GlycA and GlycB, and 1 signal that correlated with protein concentration. The analysis of metabolites concentrations in serum samples (**Table 3.1**) and lipid extracts (**Table S2**) revealed that lactate, the end-product of glycolysis under anaerobic conditions, was strongly correlated with the disease stage (rho = 0.50; *p*-value < 0.001; FDR = 0.012). Although not significant, pyruvate, the precursor of lactate, showed a positive correlation with the tumour stage (rho = 0.28, *p*-value = 0.060, FDR=0.294). Lactate and glucose concentrations were not correlated (rho = 0.06; *p*-value=0.688). Furthermore, PDAC patients with cholangitis did not have the highest levels of lactate across the group. Hence, no significant correlation was observed between the elevated lactate levels and cholangitis as shown in **Figure S1**.

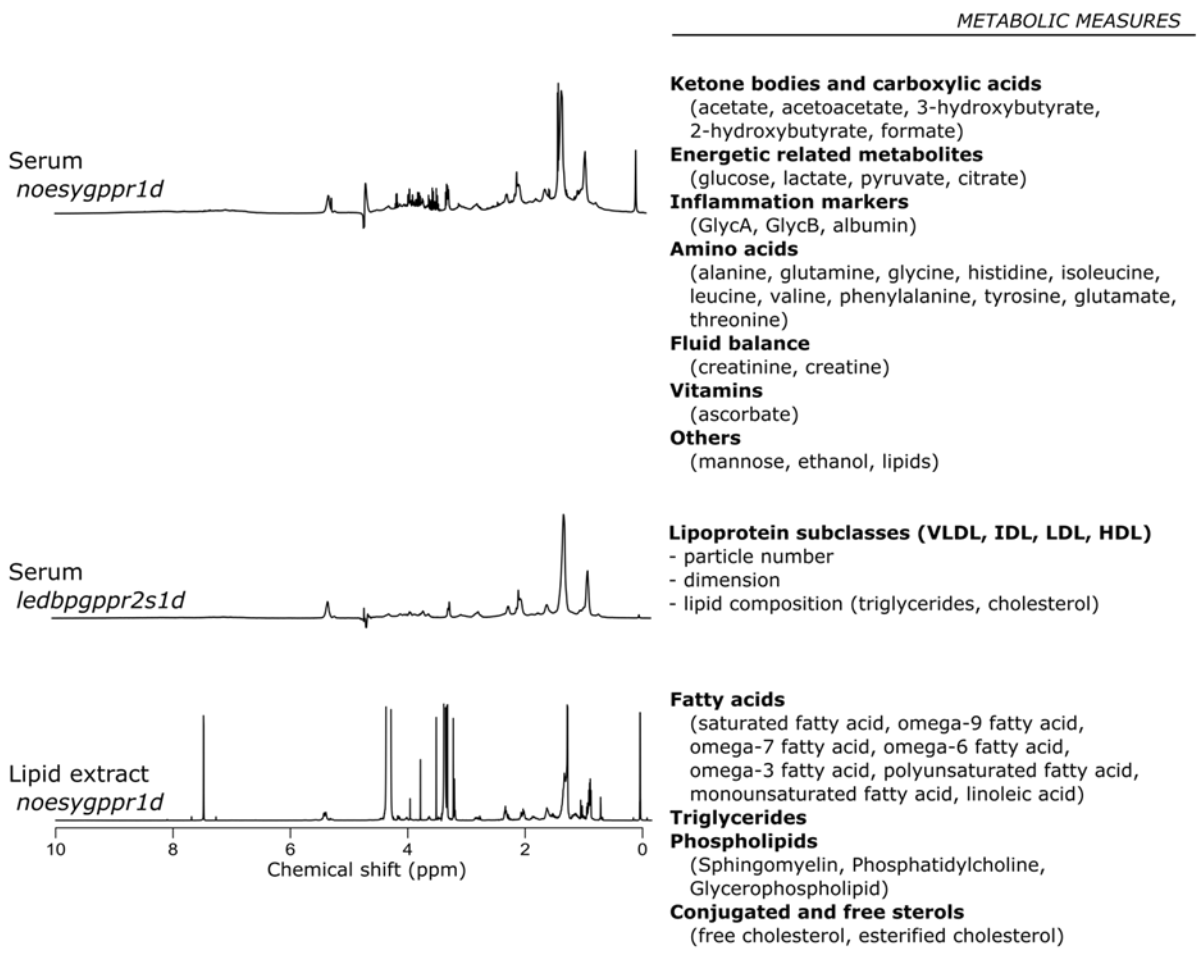


Figure 3.1: Nuclear Magnetic Resonance experiments showing their relative metabolic measures extracts such as metabolites, amino acids, vitamins, proteins, lipoproteins, fatty acids and fatty acid extracts.

Table 3.1: Correlation of concentration of metabolites with the stages of Pancreatic Ductal Adenocarcinoma.

Feature	rho	*p*-value	FDR
Formate	0.22	0.151	0.513
Unknown signal at 8.12 ppm	-0.01	0.941	0.995
Unknown signal at 8.07 ppm	0.3	0.043	0.235
Phenylalanine	0.32	0.030	0.235
Tyrosine	0.01	0.960	0.995
Unknown signal at 7.14 ppm	0.07	0.632	0.849
Histidine	-0.03	0.841	0.933
Glucose	0.13	0.406	0.767
Mannose	0.2	0.181	0.543
Unknown signal at 5.15 ppm	0.18	0.232	0.564
Unknown signal at 5.09 ppm	0.05	0.727	0.905
Unknown signal at 5.01 ppm	0.12	0.439	0.793
Ascorbate	-0.47	0.001	0.021
Threonine	0.16	0.282	0.600
Lactate	0.5	<0.001	0.012
Creatinine	-0.18	0.248	0.574
Creatine	0.08	0.582	0.811
Glycine	0.52	<0.001	0.012
Methanol	-0.19	0.202	0.543
Unknown signal at 2.55 ppm	-0.09	0.542	0.811
Citrate	0	0.997	0.997
Glutamine	-0.11	0.482	0.793
Pyruvate	0.28	0.060	0.278
Glutamate	0.24	0.115	0.450
Acetoacetate	0.1	0.529	0.811
Acetate	0.19	0.200	0.543
Alanine	-0.03	0.822	0.932
Unknown signal at 1.45 ppm	0.32	0.032	0.235
Unknown signal at 1.43 ppm	0.18	0.226	0.564
3-Hydroxybutyrate	0.11	0.467	0.793
Ethanol	0.04	0.804	0.932
Unknown signal at 1.16 ppm	0.15	0.339	0.692
Unknown signal at 1.14 ppm	-0.31	0.035	0.235
Unknown signal at 1.11 ppm	0.31	0.041	0.235
Unknown signal at 1.06 ppm	0.04	0.800	0.932
Valine	-0.2	0.182	0.543
Isoleucine	0.06	0.702	0.895
Leucine	-0.26	0.083	0.354
2-Hydroxybutyrate	0.3	0.046	0.235
Protein NH	-0.42	0.005	0.058
Unsaturated lipid -CH=CH-	-0.08	0.589	0.811
Lipid alpha-CH2	0.17	0.271	0.600
Cholesterol	0.02	0.912	0.989
Lipid =CH-CH2-CH=	-0.13	0.402	0.767
Glycorol phospholipid	0.07	0.658	0.861
Phospholipid	0	0.976	0.995
Lipid beta-CH2	-0.09	0.561	0.811
Lipid CH2	0.05	0.755	0.916
Lipid CH3	-0.1	0.500	0.796
GlycB	0.23	0.129	0.471
GlycA	0.11	0.453	0.793

Rho: spearman's correlation coefficient measures the strength of association between two variables; FDR: false discovery rate

A strong positive correlation with tumour stage was noted with the glycine concentration (rho = 0.52; *p*-value < 0.001, FDR = 0.012). On the other hand, ascorbate (rho = −0.47; *p*-value = 0.001, FDR = 0.021) seems to be depleted or present in a reduced concentration in patients with PDAC. A comparison of the concentrations of lactate, glycine, ascorbate, and pyruvate across the groups HC, CP, RPC, LAPC, and MPC is shown in **Figure 3.2.**

A selected number of ratios between metabolite concentrations was selected and associated with one or more enzymatic reactions (**Table S3**). The analysis of the metabolite ratios (**Table S4**) showed no association with disease stage. The lipoprotein parameters, including the size, number of particles and concentration of lipids (cholesterol and triglycerides) in the main classes of lipoproteins are very low-density lipoprotein (VLDL), intermediate-density lipoprotein (IDL), low-density lipoprotein (LDL) and high-density lipoprotein (HDL), were estimated using Liposcale test. Negative correlations of some parameters were reported, such as the number of HDL particles with disease stage (**Table 3.2**). Gamma-glutamyl transferase and the ratio between aspartate transaminase and alanine transaminase were not associated with the disease stage (result not included).

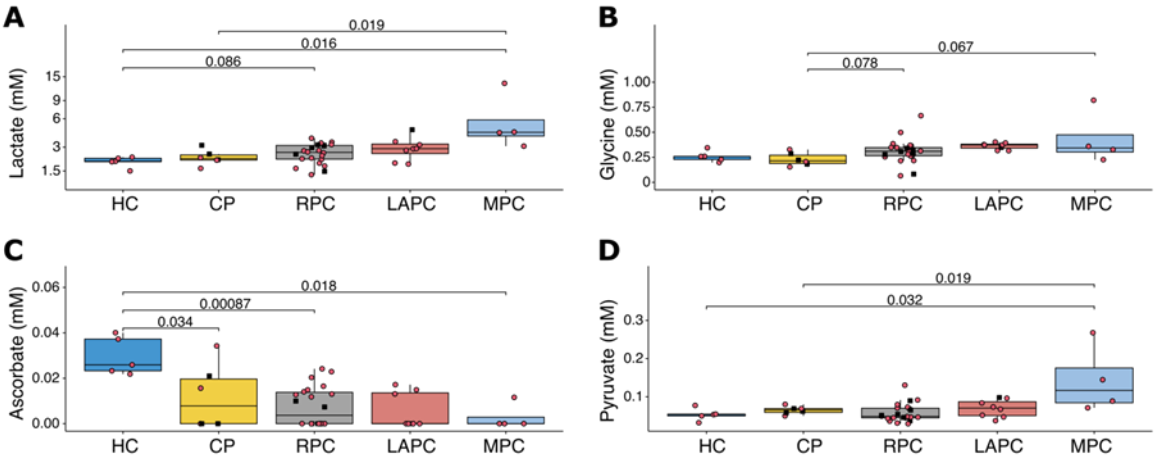


Figure 3.2: Boxplots showing the comparison of the concentration of metabolites (A) Lactate, (B) Glycine, (C) Ascorbate and (D) Pyruvate for HC, CP, RPC, LAPC, and MPC. Lactate is shown to be significantly elevated across the groups, glycine was also elevated in MPC when compared with CP. Ascorbate was significantly downregulated in CP, RPC, LAPC, and MPC when compared to HC, while pyruvate was significantly upregulated in MPC when compared to HC, CP, HC, RPC, and LAPC. Black squares represent patients with Type 2 Diabetes Mellitus. HC: Healthy controls; CP: Chronic Pancreatitis; RPC: Resectable Pancreatic Adenocarcinoma; LAPC: Locally Advanced Pancreatic Adenocarcinoma; MPC: Metastatic Pancreatic Adenocarcinoma.

Table 3.2 Correlation of concentration of lipoproteins with the stages of Pancreatic Ductal Adenocarcinoma.

Feature	rho	*p*-value	FDR
VLDL.C (nmol/L)	-0.07	0.667	0.754
IDL.C (nmol/L)	0.32	0.031	0.089
LDL.C (nmol/L)	0.22	0.151	0.230
HDL.C (nmol/L)	-0.38	0.011	0.046
VLDL.TG (nmol/L)	-0.03	0.840	0.910
IDL.TG (nmol/L)	0.28	0.060	0.139
LDL.TG (nmol/L)	0.3	0.043	0.112
HDL.TG (nmol/L)	-0.08	0.607	0.717
VLDL.P (nmol/L)	0.01	0.964	0.964
Large.VLDL.P.(nmol/L)	-0.13	0.404	0.500
Medium.VLDL.P (nmol./L)	-0.23	0.121	0.211
Small.VLDL.P.(nmol/L)	0.02	0.916	0.953
LDL.P (nmol/L)	0.26	0.080	0.161
Large.LDL.P.(nmol/L)	0.21	0.174	0.251
Medium.LDL.P.(nmol/L)	0.28	0.064	0.139
Small.LDL.P (nmol/L)	0.15	0.333	0.450
HDL.P (mol/L)	-0.39	0.008	0.046
Large.HDL.P (mol/L)	-0.35	0.019	0.072
Medium.HDL.P.(mol/L)	-0.39	0.008	0.046
Small.HDL.P.(mol/L)	-0.39	0.009	0.046
VLDL.Z (nm)	-0.22	0.139	0.225
LDL.Z (nm)	0.14	0.346	0.450
HDL.Z (nm)	0.34	0.024	0.077
Non.HDL.P.(nmol/L)	0.26	0.087	0.162
Total.P.HDL.P (nmol/L)	0.39	0.008	0.046
LDL.P.HDL.P (nmol/L)	0.39	0.008	0.046

Rho: spearman's correlation coefficient measures the strength of association between two variables; FDR: false discovery rate

3.4.2 Perturbed Metabolites and Patient Survival

After adjusting for age, the Wald test was used to identify the metabolites in serum samples as shown in **Table 3.3**, the lipid extracts (**Table S5**), the metabolite ratios (**Table S6**), and the lipoprotein parameters (**Table S7**) that correlated with the time of survival. Both 3-hydroxybutyrate (*p*-value = 0.015; FDR = 0.370) and ethanol (*p*-value = 0.002; FDR = 0.126) were independently correlated with the survival time in patients with PDAC. Cox hazard analysis showed that a statistically significant higher hazard ratio (HR) exists between the patients with the 20% highest concentration of ethanol compared to the rest (HR = 4.22 [95%CI: 1.44–12.32]; *p*-value = 0.009) and between the patients with 20% highest concentration of 3-hydroxybutyrate compared to the rest (HR = 2.88 [95%CI: 1.02–8.11]; *p*-value = 0.045). Gamma-glutamyl transferase and the ratio between aspartate transaminase and alanine transaminase were not associated with the survival time (result not included).

Table 3.3: Analysis using Wald Test to evaluate the association of Metabolites level with survival time in Pancreatic Ductal Adenocarcinoma Patients.

Features	*p*-value	FDR
Formate	0.657	0.964
Unknown signal at 8.12 ppm	0.169	0.792
Unknown signal at 8.07 ppm	0.237	0.810
Phenylalanine	0.615	0.964
Tyrosine	0.895	0.964
Unknown signal at 7.14 ppm	0.865	0.964
Histidine	0.707	0.964
Glucose	0.919	0.964
Mannose	0.186	0.792
Unknown signal at 5.15 ppm	0.549	0.964
Unknown signal at 5.09 ppm	0.900	0.964
Unknown signal at 5.01 ppm	0.312	0.842
Ascorbate	0.379	0.919
Threonine	0.347	0.886
Lactate	0.852	0.964
Creatinine	0.929	0.964
Creatine	0.692	0.964
Glycine	0.236	0.810
Methanol	0.431	0.964
Unknown signal at 2.55 ppm	0.527	0.964
Citrate	0.083	0.760
Glutamine	0.500	0.964
Pyruvate	0.826	0.964
Glutamate	0.591	0.964
Acetoacetate	0.089	0.760
Acetate	0.837	0.964
Alanine	0.945	0.964
Unknown signal at 1.45 ppm	0.036	0.606
Unknown signal at 1.43 ppm	0.160	0.792
3-Hydroxybutyrate	0.015	0.370
Ethanol	0.002	0.126
Unknown signal at 1.16 ppm	0.152	0.792
Unknown signal at 1.14 ppm	0.643	0.964
Unknown signal at 1.11 ppm	0.974	0.974
Unknown signal at 1.06 ppm	0.634	0.964
Valine	0.811	0.964
Isoleucine	0.512	0.964
Leucine	0.699	0.964
2-Hydroxybutyrate	0.181	0.792
Protein NH	0.791	0.964
Unsaturated lipid -CH=CH-	0.451	0.964
Lipid alpha-CH2	0.908	0.964
Cholesterol	0.059	0.752
Lipid =CH-CH2-CH=	0.270	0.810
Glycorol phospholipid	0.570	0.964
Phospholipid	0.159	0.792
Lipid beta-CH2	0.560	0.964
Lipid CH2	0.763	0.964
Lipid CH3	0.314	0.842
GlycB	0.269	0.810
GlycA	0.257	0.810

FDR: false discovery rate

Patients with 20% highest concentrations of ethanol and 3-hydroxybutyrate were grouped. This combined group showed significantly poorer survival than the remaining patients (HR = 5.87 [95%CI: 1.92–17.92]; *p*-value = 0.002). No correlation was observed between PDAC stages, lipid extracts, metabolite and lipoprotein levels, and survival time. **Figure 3.3** shows Kaplan–Meier plots of the survival time, segregated according to the value of ethanol, 3-hydroxybutyrate, and a combination of them, as described earlier.

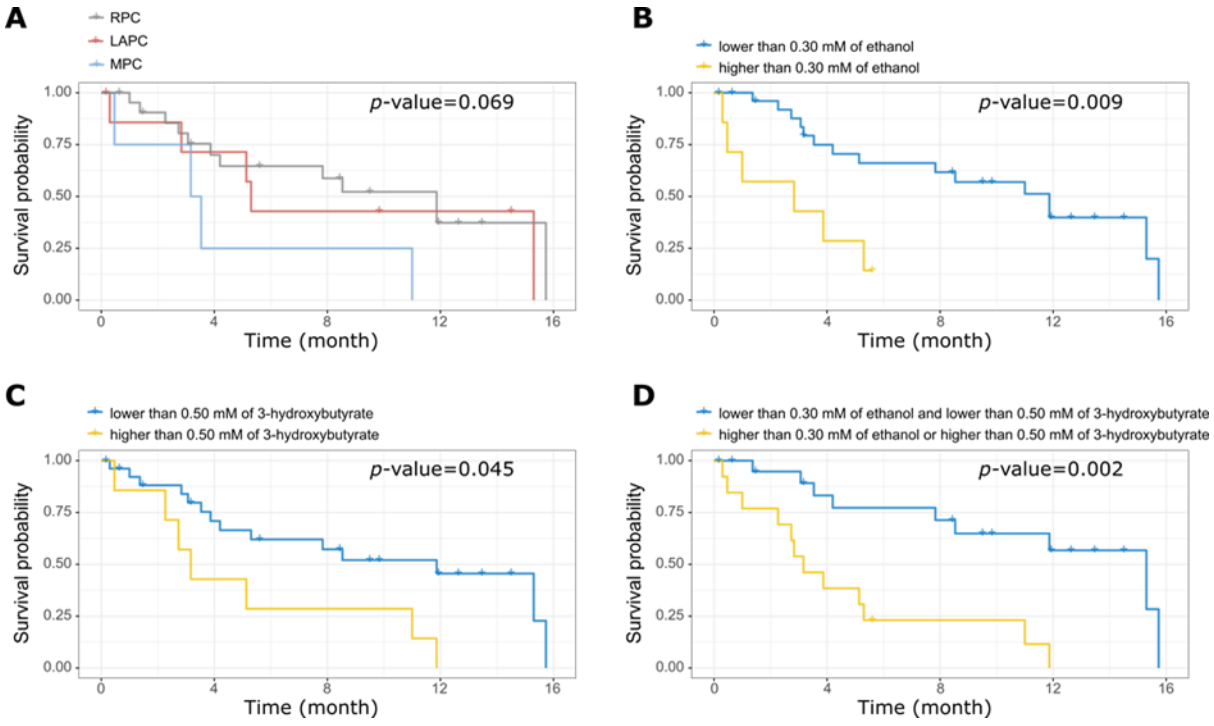


Figure 3.3: Impact of tumour stages and metabolites concentration on patient survival. Kaplan–Meier survival curves showing the effect of (A) Tumour stage, (B) Ethanol, (C) 3-hydroxybutyrate, and (D) combination of ethanol and 3-hydroxybutyrate with survival time. There was no significant link between tumour stages and patient survival. PDAC patients with low levels of both ethanol and 3-hydroxybutyrate survived longer. RPC: Resectable Pancreatic Adenocarcinoma; LAPC: Locally Advanced Pancreatic Adenocarcinoma; MPC: Metastatic Pancreatic Adenocarcinoma.

3.4.3 Impact of Raised Bilirubin Levels on Metabolites and Lipoproteins in PDAC

PAM clustering was performed on the KODAMA scores to identify any distinct lipoprotein phenotype (**Figure 3.4A**). Three distinct clusters were identified. All HC and CP patients were classified in the largest cluster (N). The lipoprotein parameters of the individuals classified in cluster N showed values similar to those of the general population. The patients classified in one of the other two clusters (A and B) showed an atypical lipoprotein profile. To verify if patients belonging to clusters A or B showed signs of cholestatic jaundice, as suggested by Lamiquiz-Moneo et al. (Lamiquiz-Moneo et al., 2019), the concentration of cholesterol ester and free cholesterol was evaluated in the lipid extracts (**Figure 3.4B**). The ratio between free cholesterol and cholesterol ester was used as a marker to identify the presence of an abnormal lipoprotein produced in patients with cholestatic jaundice (Ćwiklińska et al., 2020). **Figure 3.4C** shows that patients belonging to clusters A and B have a higher ratio indicative of the

possible presence of abnormal lipoprotein. Using the ratio between free cholesterol and cholesterol ester, a threshold of 0.45 was identified to discriminate clusters A and B from cluster N. All patients belonging to clusters A and B had values above 0.45. All patients belonging to cluster N had values below 0.45, except for three patients. Supervised PLS analysis was then performed to identify variance in the metabolic profiles of DIFF spectra associated with the ratio between free cholesterol and cholesterol ester; the resulting model demonstrated clear and robust discrimination between patient's ratio values below and above 0.45 (R2 = 0.81, 95% CI 0.81–0.86; Q2 = 0.70, 95% CI 0.69–0.72; *p*-value < 0.001). The cross-validated model was able to discriminate the two groups with an accuracy of 90%, a sensitivity of 93.75%, and a specificity of 87.50%.

Both A and B clusters showed atypical lipoprotein expression and were then grouped as "AB", to understand the effects of the altered ratio (free cholesterol/cholesterol ester) in lipoproteins, a comparison of the N versus AB clusters was performed for full blood count features (**Table S8**), blood chemistry features (**Table S9**) and liver function parameters (**Table S10**). As expected, most of the liver function parameters were significantly altered; total bilirubin (*p*-value = 0.003, FDR = 0.012), conjugated bilirubin (*p*-value = 0.006, FDR = 0.016) and aspartate transaminase (*p*-value = 0.009, FDR = 0.018) increased in clusters AB. Furthermore, some metabolites (**Table S11**), such as total protein (*p*-value < 0.001, FDR < 0.001), glutamine (*p*-value < 0.001, FDR = 0.007) reduced in concentration, whereas lipid levels (*p*-value < 0.001, FDR = 0.001) were elevated in clusters AB. Lipid extracts (**Table S12**), metabolite ratios (**Table S13**) and lipoproteins (**Table S14**) were significantly altered.

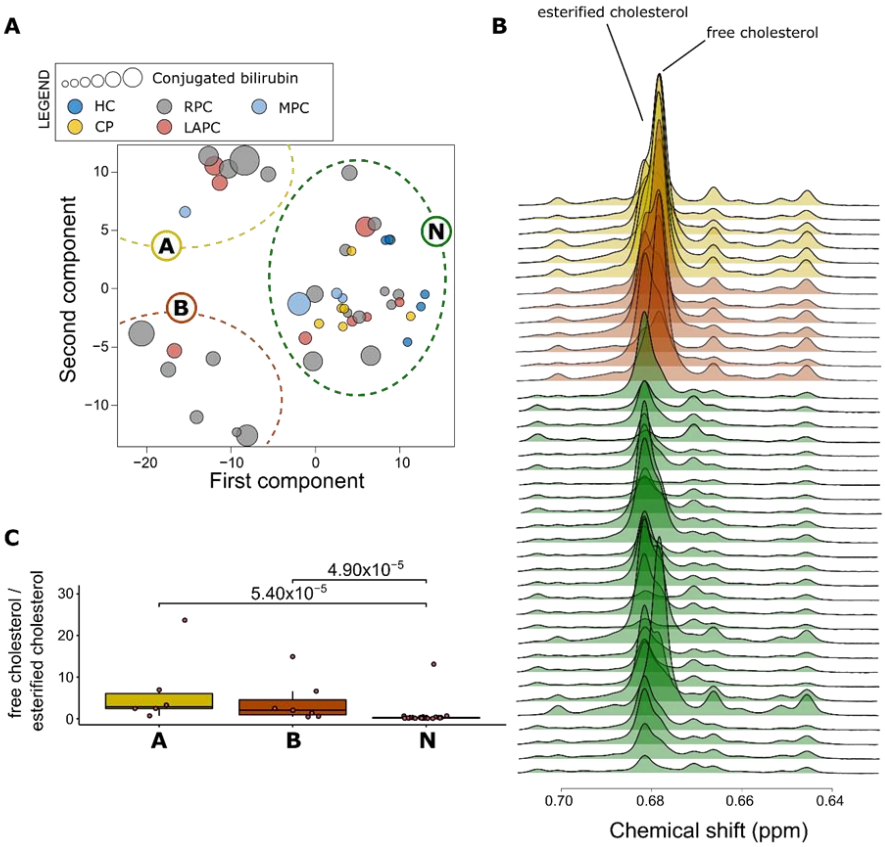


Figure 3.4: Measurement of Lipoprotein concentration in patient groups. (A) Lipoprotein particle concentrations were measured from the NMR spectra using the LipoScale test and were separated into 3 clusters. Cluster N, which is made up of all the controls and some PDAC patients, has a normal lipoprotein profile, while clusters A and B have atypical lipoprotein profiles with high bilirubin levels. (B) Spectra showing the abnormal lipoprotein profile associated with clusters A (yellow) and B (red) with a high concentration of free cholesterol, which could be indicative of an abnormal lipoprotein profile while cluster N (green) all have a normal lipoprotein profile; higher levels of esterified cholesterol, except for one outlier. (C) A boxplot of the ratio of free cholesterol to esterified cholesterol was calculated for the three clusters to comprehend the level of lipoprotein abnormality in the serum. Cluster N has the least ratio. PDAC: Pancreatic Ductal Adenocarcinoma.

3.4.4 Role of Lipoproteins in Monitoring Cholestatic Jaundice Treatment in Pancreatic Ductal Adenocarcinoma

The effects of increased bilirubin levels and its treatment with ERCP stent placement in PDAC were assessed using KODAMA (**Figure 3.5 (A)**). It showed that the treatment returns the lipid profile to normal except in the case of a patient that was treated one day before sample collection. Furthermore, we observed that some patients treated for cholestasis with either ERCP stent placement or percutaneous transhepatic biliary drainage (PTBD) still had unconjugated bilirubin levels greater than 100 (**Figure 3.5 (B)**). Using the ratio between free cholesterol and cholesterol ester, a threshold of 0.45 was identified to discriminate clusters A and B from cluster N. All patients belonging to clusters A and B had a value above 0.45 while

those in cluster N had values below 0.45, except 3 patients; 2 RPC patients classified in the cluster N that received cholestasis treatment 48 hours before blood collection showed a ratio value of 0.68 and 0.63, 1 MPC patient classified in the cluster N showed a value of 13.11.

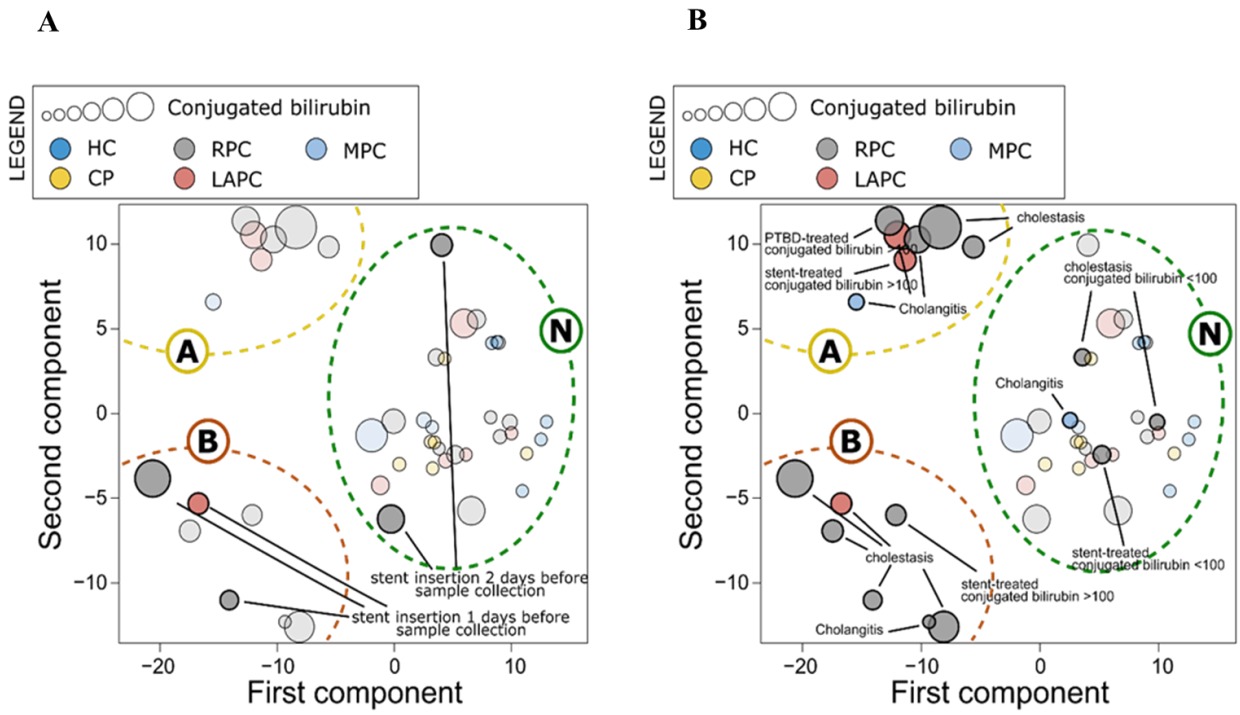


Figure 3.5: Impact of cholestatic jaundice on lipoproteins (A): Role of cholestatic jaundice on Lipoprotein profile. Most of the patients have been treated for cholestatic jaundice, but those that received their treatment 1day before sample collection had no difference in lipoprotein profile as they are still in transition while those that received their treatment 2 days before collection have almost normal lipoprotein profile. (B): Effect of Cholestatic jaundice treatment on Lipoprotein profile in PDAC patients. Most of the patients in the cluster (N) have been treated for cholestasis but have conjugated bilirubin<100 and few had cholangitis. Patients that fall in both groups A and B have also been treated with either PTBD or ERCP stent, but their conjugated bilirubin is greater than 100 and they have an atypical lipoprotein profile. ERCP: Endoscopic Retrograde Cholangiopancreatography, PTBD: Percutaneous transhepatic biliary drainage.

3.4.5 Detection of Lipoprotein X in Pancreatic Ductal Adenocarcinoma Patients

Low-density lipoprotein means particle diameter and LDL score as a proportion of small dense LDL particles to the whole LDL area were calculated. The amount of cholesterol in each band was calculated by multiplying the relative area of each band by the total cholesterol of the sample. Low-density lipoprotein-cholesterol was calculated as the sum of the cholesterol concentrations of all the LDL subfractions plus the Mid-bands A, B and C as shown in **Figure 3.6(A).** From the results, Total cholesterol and LDL-C increased in concentration while HDL-

C remained within the normal range in the PDAC patients. CP patients had increased levels of both Total cholesterol and HDL-C and reduced HDL-C levels. An abnormal lipoprotein band which could be LpX was observed in the middle section and is narrower in size than VLDL while the LDL is of intermediate size and lower concentration for this patient (Phatlhane and Zemlin, 2015) (**Figure 3.6(B)**). This would be confirmed in the validation study.

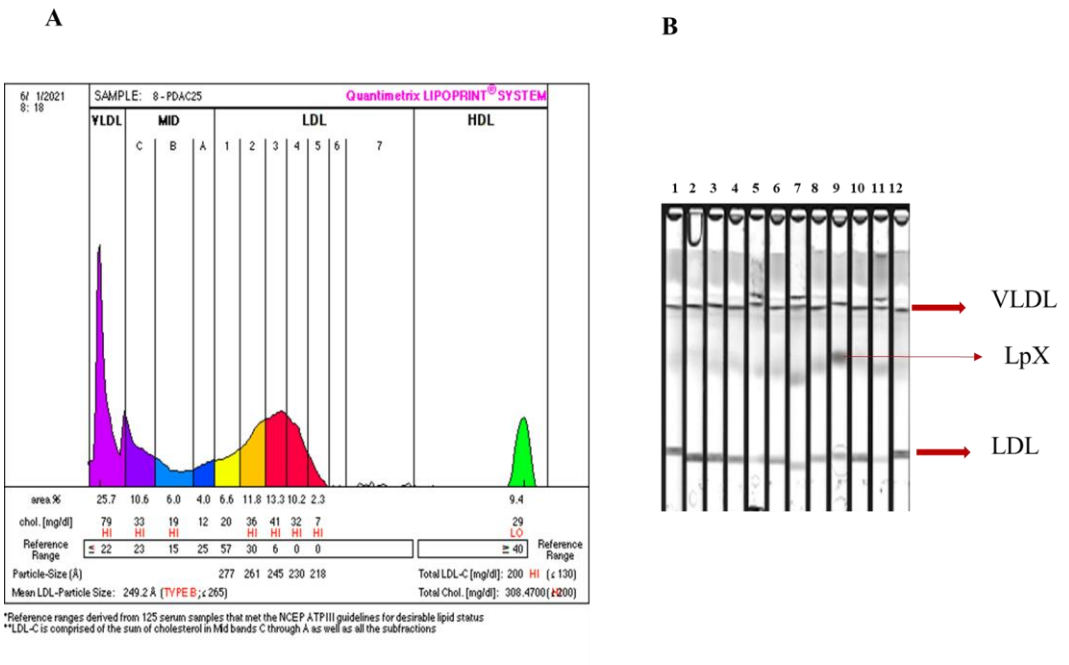


Figure 3.6: Detection of Lipoprotein X in a Locally Advanced Pancreatic Ductal Adenocarcinoma patients (LAPC 9). (A) An example of Quantimetrix Lipoprint Profile for LAPC 9 patient: The report was generated after running a Locally Advanced Pancreatic Ductal Adenocarcinoma sample, the result showed that there were elevated levels of Total Cholesterol and LDL-C with normal HDL-C levels. (B) Gel generated from the Quantimetrix Lipoprint: Lipoproteins were distinctively separated, and an abnormal lipoprotein band which might be LpX was observed in lane 9. LpX band was observed in the mid-region and is narrower than VLDL.

3.4.6 Impact of Diabetes and Inflammation on Metabolites and Lipoproteins Levels

To determine the impact of diabetes and inflammation on the metabolic signatures of PDAC patients and their link with the tumour stages, the serum metabolite concentrations between patients with and without T2DM were compared using Wilcoxon rank-sum test. With regards to patients with T2DM, no statistically significant difference between the CP and PDAC groups in the metabolite and lipoprotein concentrations was detected (results not included).

Then, the inflammatory status of the patients using both the Glasgow Prognostic Score (GPS) and the NMR inflammatory biomarkers, GlycA and GlycB were compared (**Figure 3.7A**). GPS is a cumulative inflammation-based cancer prognostic marker based on elevated serum CRP and decreased albumin concentration (McMillan, 2013). The percentage of patients with GPS

= 2 is higher in PDAC than in CP. The NMR inflammatory marker GlycA and GlycB were lower in HC compared to the pathology groups (**Figure 3.7B, C**). Slightly higher values of GlycA and GlycB were observed in CP compared to PDAC. Over 14% of the PDAC patients had cholangitis and showed only slightly higher values of CRP (*p*-value = 0.064), which were not significant. However, we identified metabolites (**Table S15**) such as glucose, lactate, histidine, phosphorous, lipid extracts (**Table S16**), glucose/lactate, threonine/glycine ratios (**Table S17**) and lipoproteins (**Table S18**) that correlated with inflammatory markers: GlycA, GlycB, CRP, and Albumin. Glucose was shown to correlate directly with GlycB (**Figure 3.8**).

Additionally, a comparison between T2DM and non-T2DM (**Tables S19-S22**), as well as between patients with high and low GPS (**Tables S23-26**) across the groups was carried out. No statistical significance was observed between T2DM and non-T2DM PDAC patients. Conversely, significant alterations in protein levels, most lipoprotein parameters, lipid extracts, and threonine/glycine ratios were observed between the high and low GPS PDAC patients.

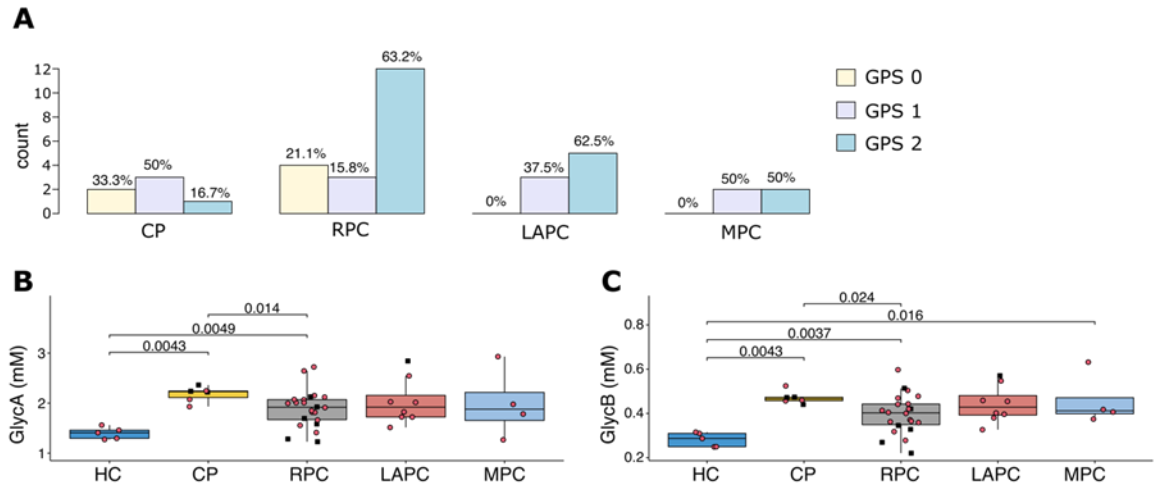


Figure 3.7: Inflammation status in patient groups (A) shows the inflammation levels of PDAC and CP groups using the Glasgow Prognostic Score (GPS), CP (6) has the least inflammation and PDAC (RPC:22; LAPC: 8; MPC: 4.) groups are all highly inflamed. GlycA (B) and GlycB (C) show the comparison of the inflammatory status of PDAC and control groups (HC and CP) using GlycA and GlycB biomarkers, respectively. There was no difference observed across the groups for both GlycA and GlycB levels except when compared with the HC. The black square boxes represent T2DM patients. T2DM: Type 2 Diabetes Mellitus; PDAC: Pancreatic Ductal Adenocarcinoma; HC: Healthy controls; CP: Chronic Pancreatitis; RPC: Resectable Pancreatic Adenocarcinoma; LAPC: Locally Advanced Pancreatic Adenocarcinoma; MPC: Metastatic Pancreatic Adenocarcinoma.

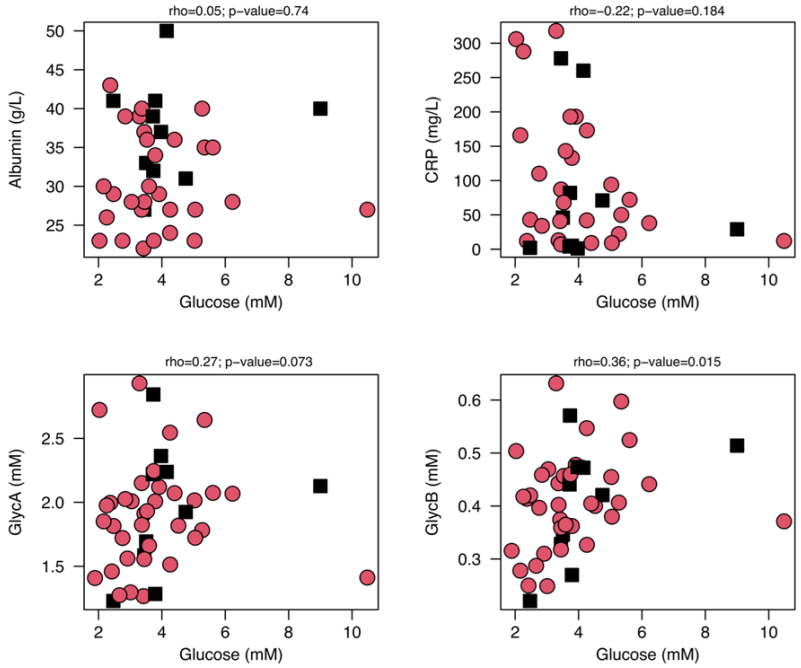


Figure 3.8: Correlation of Glucose and Inflammatory markers. GlycB has a positive correlation with glucose. Elevated glucose levels detected in the blood could be because of chronic inflammation decreasing insulin secretion and sensitivity. Black-square boxes represent PDAC patients with T2DM. There was no direct correlation between diabetes and the markers. The outlier could be a sample collected from a patient with high blood sugar levels after feeding. T2DM: Type 2 Diabetes, PDAC: Pancreatic Ductal Adenocarcinoma**.**

3.5 Discussion

PDAC has an almost equal number of new cases and deaths annually. Hence, there is a need for further investigation of underlying molecular underpinnings, especially in under-studied patient groups. Although patients of African descent have an elevated risk and poor survival rates of PDAC, there is little molecular and clinical information for this group. The combination of an analysis of metabolites and lipoproteins profiles with clinical parameters may improve management decisions and outcomes (Elebo et al., 2021). In this study, preliminary data showing metabolomic and lipoprotein perturbations in our patient group were observed at different stages of PDAC.

Metabolites are altered with PDAC severity

As the severity of PDAC increased from resectable to metastatic, there was an observed elevation of levels of lactate and glycine and reduced levels of ascorbate. Thus, these metabolite profiles could help to distinguish PDAC severity. In PDAC cells, there is an

increased uptake of glucose to produce lactate and ATP under aerobic conditions, a phenomenon known as the Warburg effect (Cao et al., 2020). Warburg effect promotes PDAC progression by providing a constant energy source for cellular growth and proliferation. Additionally, enhanced glycolysis leads to the generation of substrates such as pyruvate and, subsequently, lactate, which promotes tumour growth (McDonald et al., 2017) as discussed earlier in the Glycolysis section of **Chapter 1**. Furthermore, the correlation between glucose/lactate ratio with CRP, which was observed in this study, could suggest that glycolysis is elevated with inflammation.

Glycine is formed from 3-phosphoglycerate an intermediate of the glycolysis pathway (Mentch and Locasale, 2016), thus upregulated glycolysis could result in elevated glycine levels. Glycine is also the main substrate in glutathione and collagen production (Amelio et al., 2014; Xu et al., 2019), which are essential in PDAC progression. The activation of serine/glycine biosynthesis promotes tumorigenesis by delivering a single carbon for 1-carbon metabolism of proteins, lipids, nucleic acids, and other biological macromolecules to support tumour growth (Pan et al., 2021). Furthermore, this study observed that the Threonine/Glycine ratio has a direct association with albumin, inferring an increase in glycine levels with inflammation.

This study also showed a link between reduced levels of ascorbate (vitamin C) and the severity of PDAC. Oxidized ascorbate (dehydroascorbate) is transported into cells via glucose transporters, after which it is reduced to ascorbate using glutathione (Park et al., 2018). It acts as a pro-oxidant triggering reactive oxygen species activities, which inhibit a key glycolytic enzyme, Glyceraldehyde-3-Phosphate Dehydrogenase (GAPDH), in cancer cells (Yun et al., 2015). Reduced levels of ascorbate may imply deregulation of the glycolysis rate, resulting in the Warburg effect, which, in turn, may favour PDAC progression. This hypothesis is supported by various studies that have identified the therapeutic roles of ascorbate in PDAC. A combination of ascorbate and gemcitabine achieved a more significant tumour growth inhibition in the mouse model than gemcitabine alone; additionally, pharmaceutic doses of vitamin C act as a pro-oxidant and reduce tumour growth in mice xenografts (Chen et al., 2008; Polireddy et al., 2017). The anti-tumour effect was further observed when ascorbate inhibited epithelial-to-mesenchymal transition and, consequently, metastasis in both in vitro and in vivo models (Polireddy et al., 2017). The administration of ascorbate was also demonstrated to improve survival in a stage IV PDAC patient with little toxicity observed (Drisko et al., 2018).

Altered metabolites are linked to patient survival

Interestingly, this study showed that ethanol and 3-hydroxybutyrate (3-HB) might have a negative correlation with survival time and are independent of the disease stage. Several studies have contradictory results on the role of 3-hydroxybutyrate in pancreatic cancer (Mehta et al., 2017; OuYang et al., 2011). PDAC cells adapt their metabolism to the environment they are exposed to by utilizing the diverse fuels that are available (Sousa and Kimmelman, 2014). Excessive amounts of ketone bodies are usually found in individuals with diabetic ketoacidosis (DKA) or alcoholic ketoacidosis (AKA) (Laffel, 1999). This study suggests that high 3-HB levels could be linked to alcohol consumption or T2DM and not necessarily to the pathology. In DKA, a lack of insulin contributes to ketogenesis in the liver. DKA is also linked to an altered ratio of 3-HB to acetoacetate (Laffel, 1999), although there was no association with staging and survival in our cohort. One study showed that heavy alcohol consumption was a contributing risk factor of PDAC, especially in black women (Silverman et al., 2003). Although ethanol can either be an endogenous or exogenous metabolite, most of the patients in our cohort are heavy alcohol consumers. Indeed, it is well-known that high concentrations of ethanol inhibit lipolysis, while a substantial production of ketone bodies such as 3-hydroxybutyrate occurs with its decrease (Halperin et al., 1983). In liver cells, AKA causes a change in redox potential induced by alcohol and reduces oxaloacetate levels (Halperin et al., 1983). Although the mechanism leading to early deaths in PDAC patients who are alcohol consumers is unclear, one theory is that the use of 3-hydroxybutyrate by oxidative mitochondrial metabolism can induce the proliferation and migration of cancer cells (Sivakumar et al., 2011). In addition, ascorbate depletion in PDAC patients due to heavy alcohol consumption could both increase the glycolysis rate, thereby promoting the severity of the disease and inhibiting glycogen synthesis in the tumour microenvironment (Lim et al., 2018). The analysis of the metabolic profile could be used to understand the potential role of alcohol consumption in predicting patient outcomes.

Abnormal lipoprotein profiles may be linked to PDAC

Total bilirubin, conjugated bilirubin, alkaline phosphatase (ALP) and gamma-glutamyl transferase (GGT) are some of the parameters used to assess liver function but they can also be linked to liver diseases or injury (Méndez-Sánchez et al., 2017). Furthermore, chronic inflammation induces a variety of alterations in lipid metabolism, which are accompanied by an altered ratio of free cholesterol to cholesterol ester and associated with an abnormal lipoprotein profile (Ćwiklińska et al., 2020). This study confirms the previously reported

association between an atypical lipoprotein profile with cholestatic jaundice (Lamiquiz-Moneo et al., 2019), suggesting that the detection of abnormal lipoprotein profile might be used to identify cholestatic jaundice in PDAC patients. This study hypothesizes that altered lipid metabolism observed in PDAC patients could be due to the effects of cholestatic jaundice in these patients as observed by (Di Gangi et al., 2016).

In this study, the lipoprotein pattern of these patients was characterised by increased Total cholesterol, LDL-C, and a low HDL-C concentration. This was demonstrated by (Fellin and Manzato, 2019). LpX detected in this cohort was found to be at the same density range as LDL but with a wider diameter and has also been linked to cholestatic jaundice as a result of biliary obstruction (Fellin and Manzato, 2019). Unlike LDL-C which can be taken up by the liver, LpX can only be cleared by the spleen when cholestasis jaundice has been treated (Phatlhane and Zemlin, 2015). The presence of LpX has been shown to increase the activity of HMG-CoA reductase in the liver which promotes hepatic cholesterol synthesis (Walli and Seidel, 1984). LDL-C correlates to Total cholesterol which is usually associated with some types of cancer (Delimaris et al., 2007). Lipid derangements such as LpX have been shown to mediate hypercholesterolemia (Brandt et al., 2015). Cholesterol toxicity decreases by converting free cholesterols to non-toxic esters of fatty acids (Hashemi et al., 2017). Hence, low HDL-C levels combined with the increased cholesterol content observed in the PDAC patients could suggest reduced efflux mechanisms and increased esterification which utilises the enzyme LCAT (Georgila et al., 2019). Furthermore, cholesterol uptake disruption in combination with chemotherapy might be promising in PDAC metabolic therapy (Guillaumond et al., 2015). LDL-mediated tumourigenesis could also lead to elevated intracellular ROS levels which subsequently lead to inflammation (Patel and Kashfi, 2022).

Metabolic inflammatory markers could not distinguish patient groups

Although inflammation has emerged as an important player in pancreatic cancer development and progression (Shadhu and Xi, 2019), NMR inflammatory markers, GlycA and GlycB, were not able to discriminate between CP and PDAC. Although few PDAC patients developed cholangitis, which is an inflammation of the biliary tract, they presented a generally high level of inflammation, as expected. GlycA and GlycB were not able to stratify the patients based on the tumour staging. However, a fingerprint of the inflammatory processes was observed in the metabolic profile. Interestingly, the positive correlation between GlycB and glucose concentration could enrich the long-standing debate on the link between inflammation and

diabetes. The higher level of glucose detected in the blood could be due to the effect of chronic inflammation on decreasing insulin secretion and sensitivity (Nordmann et al., 2017).

3.6 Conclusions

This study demonstrated that obstructive jaundice, T2DM, and inflammation can contribute to defining the metabolic phenotype in PDAC, thus evaluating their patterns could help to predict prognosis, whereby patients at high risk of late-stage disease may benefit from better management decisions. The depletion of vitamin C in PDAC patients with a high alcohol consumption rate reiterates its therapeutic role. Furthermore, evaluating the lipoprotein profiles in patients could help to more accurately identify those with obstructive jaundice that may require urgent treatment; however, this has to be verified. Despite some of the statistically significant data, the small number of recruited patients in each stage might be a limitation. This pilot study is part of an ongoing project, and a future study would aim to validate these findings in a larger patient cohort.

CHAPTER IV: THE EXPRESSION OF IMMUNE CELL MARKERS IN A COHORT OF PANCREATIC DUCTAL ADENOCARCINOMA PATIENTS OF AFRICAN ANCESTRY

4.1 Introduction

Despite the recent advances in anti-cancer therapies, PDAC remains very difficult to treat. Immuno-inflammatory response plays a vital role in tumour growth and progression because PDAC patients exhibit immune dysfunction. Although PDAC is surrounded by immune cells, they induce an immunosuppressive and tumour-promoting microenvironment that propagates tumour growth (Chang et al., 2016). Hence a better understanding of these cells could help in the development of therapies targeting immune response in PDAC.

4.1.1 The Immune system and associated cells

The immune system which is made up of the innate and the adaptive system protects the host from pathogens and tumours (Inman et al., 2014). The innate immune system is pro-inflammatory, recruited to phagocytose invading pathogens by breaking them down to peptides. The peptides combine with major histocompatibility complex proteins II (MHC II) which then present it to CD4 T-cells which secret cytokines and chemokines to regulate the immune system. Granulocytes, mast cells, dendritic cells, macrophages and NK cells are some examples of innate immune cells. The adaptive immune system is regulatory and comprised mainly of B and T lymphocytes. They are usually activated when the innate immune system cannot eliminate the pathogens to provide long-lasting immunity. Below is Table 1 showing some immune cells and their functions.

Table 4.1: Immune cells of both the innate and adaptive immune system and their functions.

Immune cells	Immune Function
Dendritic cells	Presentation of antigens
Natural killer cells	Releasing cytotoxic molecules
Mast cells	Enhancing the permeability of blood vessels and promoting immune cell recruitment
Macrophages (M1 and M2)	Promotes T lymphocyte activation and initiates an immune response, wound repair and immunosuppression.
B lymphocytes	Secretion of antibodies
T lymphocytes (helper and cytotoxic)	Coordinate immune response and kills infected cells in the body

4.1.2 Effector Immune Cells in Pancreatic Ductal Adenocarcinoma

Adaptive immune cells carry out an immune function in response to a stimulus hence the name immune effector cells. Examples include NK cells, $CD8^+$T-cells and $CD4^+$T-cells which have been described in **Section 1.3.1**. At the early stages of PDAC, effector cells are present and activated. The cells of the adaptive immune system interact with the environment by displaying specificity, memory and heterogeneity in contrast to the innate immune cells. These functions are carried out by cells responsible for antigen recognition such as T lymphocytes which participate in cellular responses against intracellular pathogens.

T-lymphocytes: They are identified as CD3 which is a generic T-cell receptor that identifies all T-cells and has been demonstrated to be associated with increasing grade of tumour differentiation in PDAC thereby conferring a more favourable prognosis (Tewari et al., 2013). The specificity of CD3 antigen for T cells and its appearance at all stages of T cell development makes it an ideal T cell marker for both detection of normal T cells and T cell neoplasms. T-helper cells ($CD4^+$ and $CD8^+$ T cells) form large proportions of the $CD3^+$T cells involved in cell-mediated immunity (Yang et al., 2017). Alteration of either the number or the function of $CD4^+$ T cells and $CD8^+$ T cells will affect the immune conditions. Hence maintaining the balance between $CD4^+$ and $CD8^+$ T cells is critical for tumour immunity. The CD4/CD8 ratio is correlated with prognosis in several cancers including PDAC (Hernberg et al., 1996; Tímár et al., 2005; Wang et al., 2017).

- CD4: CD4 is a glycoprotein that serves as a co-receptor for T-cell receptor (TCR) and is found on the surface of immune cells such as T-helper cells, monocytes and dendritic cells. They modulate the functions of $CD8^+$ T-cells and B-cells. Naïve CD4 cells can differentiate into 3 subsets; 1) Th1 cells which activate macrophages and $CD8^+$T cells by secreting IL-2 and IFN-γ to support cell-mediated immune response. 2) Th 2 cells induce B-cell antibody class switching by secreting IL-4, IL-5, IL-6, IL-10 and IL-13 in PDAC (Bellone et al., 1999; Formentini et al., 2009), they have protumorigenic effects. 3) Th17 are subsets of $CD4^+$ T-cells that secrete IL-17A cytokine and have been shown to exhibit either pro or anti-tumour role in PDAC (Gnerlich et al., 2010; He et al., 2011). The switch from Th1 to Th2 correlates to poor survival in PDAC (Foucher et al., 2018).

- CD8: CD8 co-receptor is predominantly expressed on the surface of cytotoxic T-cells but can also be found on natural killer and dendritic cells. They attack tumour cells presenting tumour-associated antigen peptides with MHC class I on their surface (Wörmann et al., 2013).

Natural Killer (NK) cells: They are cytotoxic lymphocytes that play important roles in innate and adaptive immune system response against tumour by secreting cytokines such as IL-13, TNF-α and GM-CSF that do not require prior antigen exposure to facilitate their anti-tumour effect (Paul and Lal, 2017). They represent about 5-25% of circulating lymphocytes and express CD16, CD56 and CD57 markers in humans (Abel et al., 2018). NK cells can lyse cells that have become infected by a virus or intracellular pathogen and produce cytokines induced by inflammation to mediate protective immunity. Their cytotoxicity occurs through three processes which are; target cell recognition and contact, immunological synapse formation and then cancer cell death (Abel et al., 2018). NK cells have been associated with poor outcomes in PDAC because of their decreased activity (H. S. Lee et al., 2021). They are polarized towards tumour-promoting phenotype in PDAC by some mediators such as tumour cell-derived extracellular vesicles in the TME via the alteration of their functions, thereby evading recognition and promoting their elimination (Huber et al., 2020). Although neutrophils are vital components of the body's defence against diseases the uncontrolled release of its toxic substances may cause apoptosis as well as tissue scarring (Haslett et al., 1994). Hart and colleagues demonstrated that CD16 downregulated on cells undergoing apoptosis (Hart et al., 2000). Some markers of NK cells used in this study are described below.

- CD57: This marker is also known as the human natural killer cell (HNK-1) and is present in the late stages of differentiation of $CD4^{+}$T and $CD8^{+}$ T-cells (Brenchley et al., 2003). They have been shown to display cellular senescence, proliferation defects and elevated expression of ROS (Kared et al., 2016). Studies have shown that the expression of CD57 on $CD4^{+}$T and $CD8^{+}$ T-cells correlates with increased expression of cytolytic enzymes such as granzyme A and B as well as perforin which are mediators of anti-tumour immunity (Chattopadhyay et al., 2009). Conversely, Van den Hove and colleagues reported that over 40% of patients with untreated haematological malignancies displayed elevated expression of CD57 on CD4 and CD8 T-cells (Van den Hove et al., 1998). CD 57^{+} NK cells can up-regulate MHC class I and MHC class

II molecules on tumour cells through IFN-γ secretion to facilitate tumour-specific antigen recognition by T-lymphocytes (Höflich et al., 1998). Although CD57 is a very useful marker of NK cell maturation and identifying cytotoxic cells, it has been shown to have decreased replicative ability (Kared et al., 2016).

- CD56: They are known as the neural cell adhesion molecule (NCAM) which are members of the immunoglobulin family. NCAM can be used for the detection and targeting of primary tumours and metastases (Aletsee-Ufrecht et al., 1990). They are phenotypic markers of NK cells but can be expressed by monocytes, dendritic cells, gamma delta T-cells and alpha-beta T-cells (Van Acker et al., 2017). $CD56^{+}CD16^{-}$ NK subset has been reported to develop from metastatic PDAC following treatment with CTLA-4 (Frankel et al., 2010).
- CD16: They are human leukocytes found on the surface of NK cells, monocytes, neutrophils and macrophages. They participate in signal transduction and are identified as Fc receptors FcγRIII. CD16 is encoded by two genes termed FcyRIIIa and FcyRIIIb (Ravetch and Perussia, 1989). FcyRIIIa encodes a transmembrane form of CD16 and is expressed by macrophages and NK cells, whereas FcyRIIIb encodes a Phosphatidyl Inositol-linked molecule exclusively expressed by granulocytes (neutrophils). NK cells display $CD16^{+}$ $CD57^{+}$ phenotype with reduced cytotoxic activity and low levels of IFN-γ expression but produce increased levels of IL-10 in PDAC which is an immunoregulatory cytokine (Marcon et al., 2020).

4.1.3 Immune system in tumour progression

The immune system either protects the host from or activates it toward tumour progression through a process known as immunoediting (Schreiber et al., 2011). Immunoediting involves three phases: elimination, equilibrium, and escape. When immune cells destroy unstable premalignant tumour cells at the early stage, elimination occurs (Lisiecka and Kostro, 2016). If the elimination is not completely successful, the altered tumour cells that survive elimination and the host immune system go into equilibrium but when these unstable tumour cells accumulate in excess such that the immune elimination response is not sufficient, the tumour cells acquire resistance and escape mechanisms (Lisiecka and Kostro, 2016). These tumour cells are immuno-inflammatory and produce cytokines that promote tumour growth (Chang et al., 2016). Other inflammatory components include the mast cells, macrophages and

neutrophils. The immune response is insufficient to eliminate the cells that have been genetically altered by producing immunosuppressive signals.

4.1.4 Immunosuppression in PDAC

PDAC is a T-cell rich tumour. Although PDAC is surrounded by immune cells, immune response dysfunction occurs, inhibiting the immune effectors (Cassim and Pouyssegur, 2020). The innate and adaptive immune responses are released to destroy tumours but PDAC induces immunosuppression to prevent eradication by effector immune cells via the expression of PD-L1 (Basso et al., 2013; Panni et al., 2014). Pancreatic cancer cells downregulate the expression of MHC class I molecules by interfering with the antigen cross-presentation to effector T-cells (Garrido et al., 2017). PDAC cells evade immune surveillance, evasion via non-functional Fas receptors and abnormal expression of functional Fas ligand (Gaianigo et al., 2017). Immunosuppressive factors such as IL-10 and TGF-β promotes the excess flow of suppressive immune cells, which contributes to a systemic Th2 immune phenotype in PDAC (Mao et al., 2021). Patients suffering from diabetes for a long time are at great risk of PDAC because they have a dysfunctional immune system which leads to an immunosuppressive state (D'Marco et al., 2020).

4.2 Oxidative Stress and role in Pancreatic Ductal Adenocarcinoma

Oxidative stress can be defined as the imbalance between the production of oxidants (reactive oxygen species) and antioxidants (Bansal and Kaushik, 2019). Oxidative stress in biological systems may result from the overproduction of superoxide anion and hydroxyl radicals or nitric oxide (Jomova et al., 2012). They can alter major classes of biomolecules such as lipids, proteins, and nucleic acids by changing their structure and function (Nandi et al., 2019). This REDOX imbalance leads to the damage of the cell components such as lipids and proteins as well as the organs and ultimately the whole organism (Singh et al., 2019). Oxidative stress has been linked to several ailments such as neurodegenerative diseases (Liu et al., 2017) and cancer (Talib et al., 2020). Studies show that cancer cells are under increased oxidative stress compared to normal cells due to enhanced generation and accumulation of ROS-mediated reaction products in cancer cells. They can be detected in plasma and urine as well as overexpression of antioxidant enzymes in response to oxidative stress (Sosa et al., 2013). Oxidative stress occurs in cells when the generation of ROS overwhelms the cells' antioxidant

defence (Hayes et al., 2020). Oxidative stress stimulates pro-inflammatory cytokines such as IL-2 and IL-6 which promotes angiogenesis and tumour vascularization via the expression of vascular endothelial growth factor (VEGF) in PDAC cells (Martinez-Useros et al., 2017; Tang et al., 2005).

4.2.1 Reactive oxygen species (ROS)

ROS are highly reactive molecules with a single unpaired electron in their outermost shell of electrons and are grouped into 2: free oxygen radicals such as hydroxyl radical, superoxide, and non-radical ROS like hydrogen peroxide (H_2O_2) and hydroperoxide (Sies, 2017). They are among the main causes of PDAC instability and pathogenesis (Chen et al., 2021), and have been detected in many cancers because of their high metabolic rates (Sosa et al., 2013). NADPH oxidase is the major source of ROS in pancreatic cancer (Martinez-Useros et al., 2017). Although ROS have been shown to promote carcinogenesis they also have some biological functions such as stimulating cell proliferation and cell cycle progression (Harris and DeNicola, 2020). They also stimulate epidermal growth factor (EGF) and platelet-derived growth factor (PDGF), which in turn activate the enzyme tyrosine kinase resulting in the stimulation of downstream pathways such as phosphatidylinositol-3-kinase (P13K) AKT signalling (Lemmon and Schlessinger, 2010). ROS and pro-inflammatory cytokines are important factors involved in the pathogenesis of PDAC because ROS regulates the relationship between inflammation and pancreatic cancer by modulating the levels of inflammatory factors such as HIF-1alpha, chemokines, cytokines and growth factors (Aggarwal et al., 2019).

ROS mediate vital functions such as phagocytosis, antigen presentation and recognition in immune cells (Kennel and Greten, 2021). They also exert immunosuppressive effects on NK and T-cells, however, DCs require elevated ROS levels during cross-presentation to cytotoxic $CD8^+$T-cells (Oberkampf et al., 2018). ROS regulates the differentiation and effector functions of T-cell subsets. Elevated levels of ROS promote Th1 phenotype (Frossi et al., 2008) while decreased levels promote Th1 and Th17 phenotypes (Abimannan et al., 2016). Immune cells such as macrophages induce ROS production through the secretion of stimuli such as TNF- α. Upon inflammation, activated macrophages produce peroxinitrile radicals which promote tumour cell apoptosis (Castaneda et al., 2017).

Role of ROS in Metabolism

Metabolic alterations increase ROS intracellular levels, which promote tumour formation (Yasuda et al., 2021). Glycolytic enzymes Glyceraldehyde-3-phosphate dehydrogenase (GADPH) and Pyruvate kinase M2 (PKM2) are inactivated by oxidative stress. GADPH is a major oxidative target of ROS and these enzymes undergo a modification of their cysteine residues to cysteic acid thereby inhibiting their activity (Hwang et al., 2009; Muronetz et al., 2020). Intracellular ROS inhibits PKM2 and diverts glucose into PPP to generate reducing the potential for maintaining REDOX (Boese and Kang, 2021). In cancer cells, PKM2 plays a role in supporting cell survival by sustaining antioxidant responses under acute oxidative stress (Li et al., 2018,). AMP-activated protein kinase (AMPK) is activated by H_2O_2 (Kang et al., 2015). Other enzymes such as fumarate hydratase enhance ROS production via the activation of HIF1 factors (Sullivan et al., 2013). Fumarate covalently binds to GSH to form succinated glutathione (GSF), an alternative substrate of glutathione reductase that consumes NADPH to enhance ROS accumulation (Sullivan et al., 2013). NADPH is required to generate GSH for ROS detoxification (Anastasiou et al., 2011; Sullivan et al., 2016). GSH which is a tripeptide of cysteine, glycine, and glutamate can scavenge and reduce ROS (Bin et al., 2017). It is generated from PPP to disable cytochrome c and then released into the cytoplasm following an elevated ROS level (Boese and Kang, 2021).

Role of ROS in Pancreatic Ductal Adenocarcinoma

Pancreatic cancer cells accumulate more ROS (Cheung et al., 2020) and are antiapoptotic as a result of the elevated ROS levels (Park et al., 2017; Vaquero et al., 2004). ROS plays dual and opposing roles in PDAC depending on its concentration. It facilitates cancer progression at mild to moderate levels (Martinez-Useros et al., 2017) while excessive ROS production promotes the release of cytochrome c into the cytoplasm which mediates programmed cell death (Matilla, 2021). This is the main mechanism of many chemotherapies as seen in the use of a combination of gemcitabine and cannabinoid has been used to induce autophagy in PDAC cells via ROS-mediated mechanism (Sharafi et al., 2019). At the early stage of PDAC, elevated ROS levels cause DNA damage which results in cancer progression because of the gene mutation thus therapies targeting decreased ROS would be effective in preventing the initiation of pancreatic cancer (Zhang et al., 2016).

Conventional treatments have not been very successful in improving the survival rate of PDAC hence the need for the development of other novel therapies. The expression of immune cells can affect immune response during tumour progression and treatment. In this study, immune cell populations were quantified in the different PDAC groups in the patient cohort using immunophenotyping and gene expression analysis. ROS levels were also quantified in the patient groups.

4.3 Materials and Methods

4.3.1 Sampling and Processing Overview

Blood samples were collected and processed into serum as described in **Chapter 3, Section 3.3.1** above. An overview of the total number of patients recruited is shown in **Figure 4.1** below.

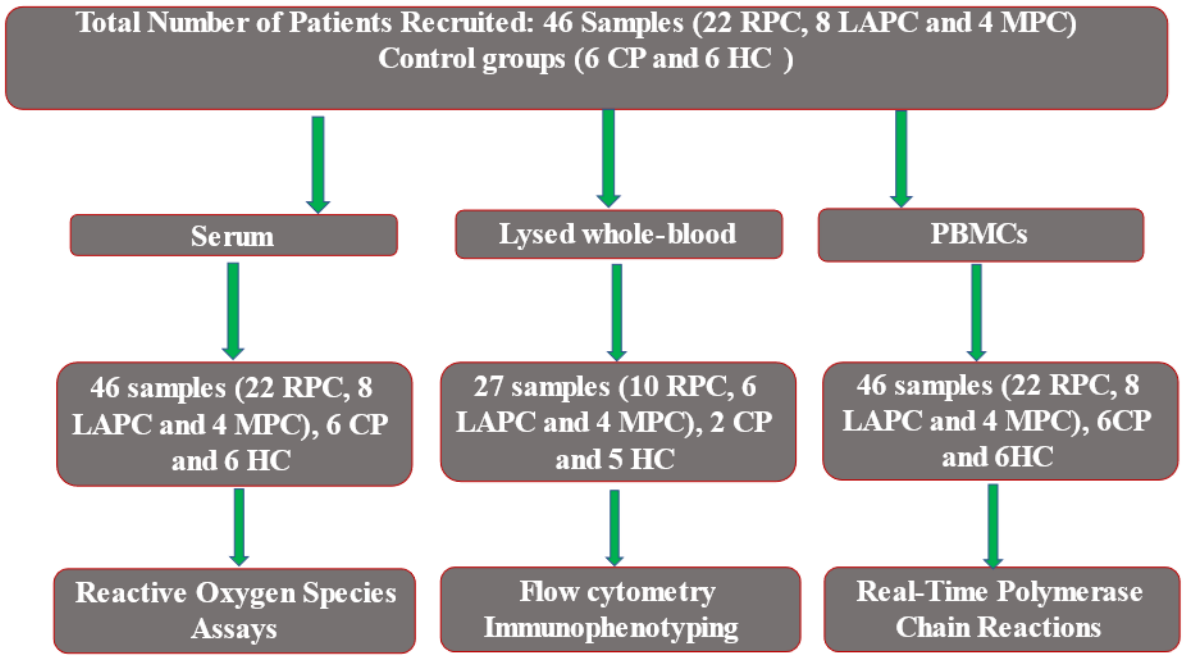


Figure 4.1: Overview of Sample Size and Processing. After Ethics approval and informed consent blood samples collected were processed into serum and PBMCs for ROS and Real-Time Polymerase Chain Reaction Analyses respectively. Whole blood was lysed to fix the white blood cells for Immunophenotyping assays. HC; Healthy controls, CP: Chronic Pancreatitis, RPC: Resectable Pancreatic Ductal Adenocarcinoma, LAPC; Locally Advanced Pancreatic Ductal Adenocarcinoma, MPC; Metastatic Pancreatic Ductal Adenocarcinoma.

4.3.2 Reactive oxygen species (ROS) analysis using N, N- diethyl -para-phenylenediamine

N, N- diethyl -para-phenylenediamine (DEPPD) sulphate is a compound that reacts with serum to form a long-lived cation. Under acidic conditions metal ions (Fe^{2+} and Fe^{3+}) contained within the serum samples are released from their transport proteins and catalyse the decomposition of hydroperoxides (Hayashi et al., 2007). Hydroperoxides decompose into alkoxy and peroxyl radicals, which convert N alkylated p-phenylenediamines into a coloured radical cation. This can be measured spectrophotometrically with absorbance being proportional to the number of hydroperoxyl compounds and thus the oxidative status of the sample can be determined.

One hundred and forty microlitres of 0.1M Sodium acetate buffer pH 4.8 was added to each allocated well of a 96-well plate. Five microlitres of serum samples (PDAC and controls) and standards (different concentrations of hydrogen peroxide solutions: 50, 25, 6.25, 3.13, 1.56, 0.78 and 0.39 µM) were added in duplicates. DEPPD and Iron sulphate were dissolved in 0.1M Sodium acetate buffer pH 4.8, respectively. 100 µl of the reagent mixture prepared at a ratio of 1:25 was then added to each well. The solution was incubated at 37 °C for 1 min. Colour development was recorded at 505 nm at 25 °C, every 15 secs for 30 repeats using FL 600 Microplate reader Multiscan Sky Microplate Spectrophotometer (Thermo Fisher Scientific, Massachusetts USA).

The R studio V1.3 software was used for statistical analysis. A standard curve of the standards was plotted to determine the concentration of the samples. Test for significant differences ($p<0.05$) between the PDAC samples and controls (healthy and chronic pancreatitis) was carried out using an unpaired non-parametric t-test such as the Wilcox test.

4.3.3. Immunophenotyping using flow cytometry

Principle

Flow cytometry is a technique that is used to analyse single cells by measuring the physical and chemical characteristics of their population (McKinnon, 2018). This technique helps to identify the lineage or hierarchy of cells using antibodies that detect markers or antigens on the cells hence the prefix immune. While some antigens are found only on one cell type others are found on different cell types. This laboratory method is used to identify the presence or absence of white blood cells (WBCs) based on the types of markers or antigens present on the cell's surface, nucleus, and cytoplasm. This technique requires the use of frozen lysed whole blood samples for flow cytometry immunophenotyping (Braudeau et al., 2021).

Sample processing

For immunophenotyping assays, a subset of twenty-seven samples (10 RPC, 6 LAPC, 4 MPC, 2 CP, and 5 HC) were used, due to limited resources, as shown in **Figure 4.1**. White blood cells were fixed by adding 1 ml of diluted BD FACS Lyse (BD Biosciences, New Jersey, United States) solution to 100µl of the whole blood sample from the purple capped vacutainer tube within 2 h of collection and allowed to stand at room temperature for 12-15 mins after which it was stored at -80ºC until analysis.

Plasma was then isolated by gravity separation from forty-six blood samples collected in the purple vacutainer tubes for 30-60 mins at room temperature followed by centrifugation at 3000 rpm, 4ºC for 30 mins, processed within 2 h of collection, and aliquoted (200 µl) in single-use vials, stored at -80 °C until needed.

Peripheral blood mononuclear cells (PBMCs) which are major cells in the human body immunity containing lymphocytes, monocytes and macrophages were separated using Ficoll-Paque™ (GE Healthcare, Illinois, United States) separation method. Blood samples were diluted 1:1 with plain Rosewell Park Memorial Institute (RPMI) media (Sigma-Aldrich Merck, Missouri, USA). The blood was carefully layered on Ficoll paque (GE Healthcare, Illinois, USA) which was added in the dark in a 2:1 ratio and then centrifuged at 3000 rpm for 30 mins RT (Decel=0). The white cloudy layer containing the PBMC was pipetted out into a 50ml falcon tube. The cells were washed by adding 30ml plain RPMI media to the cells and centrifuged at 2200 rpm for 10 mins (Decel=9). The supernatant was decanted and 5ml Ammonium Chloride Potassium or ACK (150 mM NH_4Cl, 10 mM $KHCO_3$, 0.1 mM EDTA pH 7.2) was added and allowed to stand for 5mins to get rid of red blood cells (RBC). RBCs and platelets were washed off by adding 15ml RPMI media and centrifuged at 1200 rpm for 10 mins (Decel=9). The cells were counted, and the concentration was between 1×10^5– 10^6 cells/mL. The cells were then resuspended in a freezing media [10% Dimethyl Sulphoxide (Sigma Aldrich, Missouri, USA), 90% Gibco Feval Bovine Serum FBS (Thermo Fischer Massachusetts, USA)]. The cell samples were aliquoted and stored at -80 °C until required for transcriptomic assays. Samples were only thawed once to preserve integrity.

Preparation of Antibodies and Titration experiment by flow cytometry

Antibodies required for immunophenotyping were titred to determine the optimal concentration of antibody that is required to give good separation between positive and negative populations and to determine the position of the negative population on the axis. Antibodies were optimized by titration to optimally stain lymphocytes populations and their

subpopulations using CD3 BD Horizon Brilliant™ Ultraviolet (BUV), CD4 Alexa flour and CD8 Brilliant Violet™ 605, CD56 PE Phycoerythrin Cyanine 7 (PECy7), CD57 BB515 while the granulocyte population was stained with CD16 PECy5. All antibodies were obtained from BD Biosciences, (New Jersey, United States).

Titration assay: Cryovials containing fixed white cells from whole blood were retrieved from a - 80°C freezer and thawed in a water bath at 37 °C for 2 mins. Five hundred microlitres of thawed samples (mixture of cells and FACS lyse) were transferred into BD polystyrene tubes (BD Biosciences, New Jersey, USA) and centrifuged at 1500 rpm for 5mins, supernatant was then decanted. Thawed cells were resuspended in 2ml of 1× PBS, washed once by centrifuging at 1500 rpm for 5 mins and supernatant was then decanted. A master mix of stain buffer and FC blocker was prepared by adding 1 µl of FC blocker to 50 µl of staining buffer and then vortexed briefly. Fifty microlitres of the master mix were added to the cells and resuspended. Doubling dilutions of the antibodies which are CD3/BUV496, CD4/AF700, CD8/BV605, CD16/PE-CY5, CD56/PE-CY7 and CD57/BB515 were prepared in the dark with a control tube without any antibody. Double the manufacturer's recommended volume of fluorescence-labelled antibody was added to tube 1 and 2-fold serial dilutions were done for a total of 8 tubes or concentrations. For example., if the recommended amount is 5 µl, 10 µl was added to 90 µl of 1×PBS. The content of tube **1** was mixed by pipetting and 50 µl was transferred subsequently across all tubes. Fifty microlitres of the antibody solution were then transferred to the washed fixed white blood cells in all tubes, mixed thoroughly, and incubated in the dark, at room temperature for 30 mins. Cells were washed by adding 1 ml of 1x PBS, resuspended, and centrifuged at 1500 rpm for 5 mins, with supernatant discarded. The stained cells were then resuspended in 300 µl staining buffer (1×PBS, 5%FBS, and 0.1%NaN_3), and 100,000 events were acquired on a flow cytometer (BD Biosciences, New Jersey, United States). **Table 4.2** below shows the antibodies and their optimised antibody volume.

Table 4.2: A table showing the optimized titrated volumes of Antibodies.

Antibody/Fluorochrome	Optimized volume (µl)
CD3 /BUV-496	1.00
CD4 /AF-700	1.25
CD8 /BV-605	1.0
CD16 /PE-Cy5	1.25
CD56 /PE-Cy7	1.5
CD57 /BB515	1.0

BUV: BD Horizon Brilliant™ Ultraviolet; BV: Brilliant Violet™; PE-CY: Phycoerythrin Cyanine; BB515: BD Horizon Brilliant™ Blue; CD: Cluster of differentiation.,

Multicolour Flow Cytometry for Immunophenotyping Analysis

Multicolour flow cytometry immunophenotyping analysis was then used to determine immune cell populations and frequency. A 6-colour panel as seen in **Table S27** was established to characterize heterogeneous cell populations in the PDAC stages and compared with the controls (CP and HC).

Fully stained samples and unstained samples were prepared from the thawed cells. Stained samples were prepared by adding antibodies in the dark at previously titrated volume and then incubated for 30 mins at room temperature. The cells were then washed with diluted Dulbecco's Phosphate Buffered Saline or PBS (Sigma Aldrich, Missouri, United States) at 1500 rpm for 5 min. Approximately 100,000 cells were acquired on BD LSRFortessa™ II flow cytometer (BD Biosciences, New Jersey, United States) for each sample at a threshold of 25,000 after the necessary quality controls using FACSDiva™ software version 5 (BD, Biosciences, New Jersey, United States). Basic quality control (QC) using BD cytometer setup and tracking (CST) beads, photo-multiplier tubes (PMT) voltage optimization, 8 Peak beads, compensation, and fluorescence minus one (FMO) were some of the controls used to ensure that valid and consistent data on the cytometer were as follows:

1. Cytometer Setup and Tracking: This is a control carried out using BD CS and T beads lot number; 11087 (BD Biosciences, New Jersey, USA) to provide a standardised method to perform quality control of the optics, electronics and fluidics of the instrument. They are also used for adjusting the detector voltage.
2. ExPhoto-Multiplier Tubes (PMT) voltages optimization using unstained and single stained cells was used to optimize applied voltage to exclude electronic noise and ensure that the stained cells were within the dynamic range of the instrument. This further ensures that the best quality data in each channel of the flow cytometer is obtained.

3. Basic Quality Control (Q.C) 8 Peak Beads (BD Biosciences, New Jersey, United States): These are designed for routine calibration of flow cytometers but can also be used for monitoring and correcting variations in longitudinal studies. These beads are used to determine the linearity and sensitivity of the system. The linearity of the instrument will determine if the logarithmic amps and PMTs are functioning properly while the sensitivity of the instrument detects any dye or light contamination. Hence the main function of the Q.C 8 peak beads was to ensure that the Mean Fluorescence Intensity (MFI) ranges are consistent and reproducible.

Method: One drop of Q.C 8peak bead (Lot number: 9121914) was added to 500µl of 1xPBS or sheath fluid. The beads were run at low on the flow cytometer. The most suitable peak was chosen, and the MFI range was calculated.

4. Compensation for spill-over was done using CompBeads (Anti-Mouse Ig, κ/Negative Control Compensation Particles Set; BD Biosciences, New Jersey, United States) to minimize spectral overlap between different fluorophores. The three rules of compensation are:
    - Controls need to be as bright or brighter than any sample, the compensation will be applied.
    - Background fluorescence should be the same for the positive and negative controls.
    - Compensation controls must match the exact experimental fluorochrome.

Method: A drop of negative and positive beads (Anti-Mouse Ig, κ/Negative Control Compensation Particles Set; BD Biosciences, New Jersey, United States) respectively was added to 50 µl of 1x PBS. The recommended pre-titrated volumes of antibodies were added to tubes in the dark and incubated for 30 mins. Beads were washed with 2 ml 1xPBS and centrifuged at 1500rpm for 5mins. The supernatant was decanted, and the pellet was resuspended in 300 µl of staining buffer. A total of 10,000 events were recorded on the flow cytometer.

5. Fluorescence Minus One (FMO): FMO controls are used to determine the cut-off point between background fluorescence and positive populations in multi-colour immunofluorescent experiments. They are very useful and therefore highly recommended where a positive cell population is presented as a smear instead of being distinctly separate from the negative population. The lack of distinction between positive and negative populations is heightened by the "spreading" of the negative

populations due to the contributions of fluorescence overlap compensation from multiple fluorochromes as described in **Table S28.**

Data and Statistical analysis: Data was analysed using FlowJo LLC version 10 (BD, Biosciences, New Jersey, United States) using Flow cytometry standard (FCS) files linked to the compensation controls from FACSDiva™ software. Cells were gated as singlets to exclude doublets using forward scatter height (FSC-H) and forward side scatter area (FSC-A) parameters. To discriminate white blood cells into lymphocytes, monocytes and granulocytes, forward side scatter (FSC) versus side scatter (SSC) was used. All populations were represented as percentages of parent populations. Cell differentiation included lymphocytes (CD3) and their subpopulations ($CD3^+CD4^+$, $CD3^+CD8^+$ $CD3^+CD16^+$, $CD3^+CD56^+$, $CD3^+CD57^+$) and granulocyte populations ($CD16^+$).

4.3.4 Gene expression analysis of immune-related markers

Total RNA Extraction

Total RNA was extracted from PBMCs isolated from the PDAC and control samples, using the TriReagent® (Sigma Aldrich, Missouri, United States). PBMC samples were thawed on ice for 5 mins and then centrifuged at 1500rpm for 5 mins. Two hundred and fifty microlitres of the TriReagent were added into the pellet, resuspended, and allowed to stand at room temperature for 5 min. Sixty microlitres of chloroform were added to samples and shaken vigorously until they turned milkish. Samples were then allowed to stand at room temperature for 10 min and then centrifuged at 12000xg for 15 min at 4ºC. The aqueous phase was transferred into a fresh tube, 150 µl of propanol was then added and allowed to stand for 5 mins at room temperature to separate the mixture into three phases and then centrifuged at 12000xg for 10 mins. After decanting the supernatant, the RNA pellet was washed with 250 µl of 75% ethanol, vortexed, and centrifuged at 7500xg for 8mins. Pellet was then air-dried for 5 mins after decanting the supernatant. The pellets were placed on a heat block at 55º-60ºC for 5min until the ethanol had evaporated. Thirty microlitres of RNA-free water was then added to the pellet and the mixture was resuspended and placed back on the heat block for about 5 mins followed by placement on ice. The quality of RNA was measured using a NanoDrop ND-1000 Spectrophotometer (Thermo Fischer Scientific, Massachusetts, United States), and A260/280 ratio > 1.8 was observed across all samples.

Complementary DNA (cDNA) Synthesis

cDNA synthesis was performed from 250 ng/µl of total RNA using the Photoscript® II First Strand cDNA synthesis Kit E6560S (New England BioLabs® Inc.), according to the manufacturers' instructions. Two microlitres of $d(T)_{23}VN$ (50 µM) were added to 10 µl of Photoscript II Reaction Mix (2x), after which 2 µl of Photoscript II Enzyme Mix (10x) was then added to the mixture. Two microlitres of RNA template were added followed by Nuclease free water to make up 20 µl and was then incubated at 42 ºC for 1hr, denatured at 85 ºC, and then allowed to cool down at 4 ºC.

Quantitative Real-time Polymerase Chain Reaction (RT-PCR)

Forty-six samples (RPC= 22, LAPC = 8, MPC = 4, CP=6 and HC=6) were included in this assay. The TaqMan® Fast Advanced Master Mix (Thermo Fischer, Massachusetts, United States) was used to perform singlet Real Time-PCR as per the manufacturers' instructions. Eight microlitres of Total PCR reaction mix volume were prepared by adding 5 µl Taqman gene expression master mix, 0.5 µl Taqman assay (target genes), and 2.5 µl nuclease-free water. The PCR reaction ran for 40 cycles including hold at 50ºC for 2 mins, polymerase activation at 95ºC for 10mins, denatured at 95ºC for 15 secs, and annealed at 60 ºC for 60 secs. The reference gene Microsomal Ribosomal Protein L19 (*MRPL19*) and target genes *CD8A*, *CD4*, *CD3*, *CD16/FCGRB*, *CD56/NCAM1* and *CD57/B3GAT* were obtained from Thermo Fischer Scientific, Massachusetts, United States. MRPL19 is a housekeeping gene used as a control because its expression doesn't change in pancreatic cancer (Mohelnikova-Duchonova et al., 2012). The MIQE guidelines were strictly adhered to (Bustin et al., 2009). The Quant Studio™ 1 Real-Time System (Thermo Fischer Scientific, Massachusetts, United States) was used to run the RT-PCR reactions.

Data Analysis

The $2^{-\Delta\Delta CT}$ method was used to calculate relative changes in gene expression using the Microsoft Excel® software. The RT-PCR data were analysed using GraphPad Prism™ software version 8 (GraphPad Software Inc, California, United States). A Shapiro-Wilk test was used to test for normality. Statistical analysis and graphical illustrations of the data were generated in R (version 3.6.1) and R studio (version 1.1.456) software using KODAMA. The data was non-parametric hence Wilcoxon and Kruskal–Walli's rank-sum test was used to compare differences between the controls (CP and HC) and PDAC groups (RPC, LAPC and MPC).

Spearman's rank test was then used to calculate the correlation coefficient (rho) between ROS, immunophenotyping and real-time PCR assays.

4.4 Results

4.4.1: Impact of elevated ROS levels in Pancreatic Ductal Adenocarcinoma

A spectrophotometric assay of ROS showed that there was no significant difference observed when the PDAC groups were compared with CP groups but when compared with HC there was significance. ROS levels was elevated in RPC (*p*-value= 0.003) and LAPC (*p*-value= 0.008) compared to HC group (**Figure 4.2).**

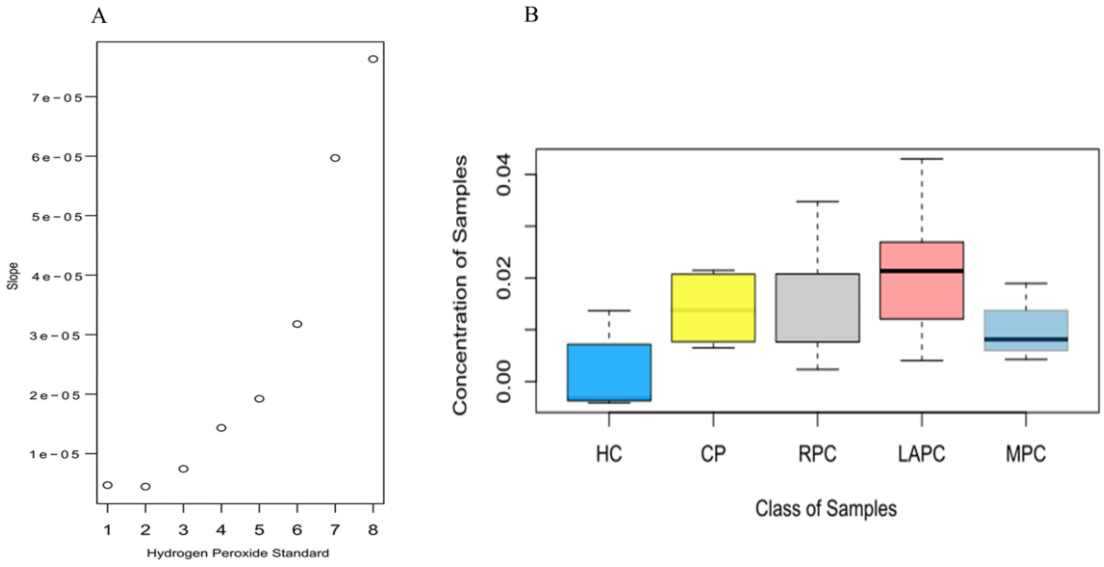


Figure 4.2: Spectrophotometric ROS Assay of PDAC and Control Groups. A Standard curve of hydrogen peroxide standards. B: Boxplot showing the comparison in ROS levels between the PDAC groups (RPC, LAPC, and MPC) and control groups (HC and CP). A significant change was observed when the PDAC groups RPC and LAPC were compared with HC groups. HC; Healthy controls, CP: Chronic Pancreatitis, RPC: Resectable Pancreatic Ductal Adenocarcinoma, LAPC; Locally Advanced Pancreatic Ductal Adenocarcinoma, MPC; Metastatic Pancreatic Ductal Adenocarcinoma

4.4.2: Altered immune cell marker populations in the different tumour stages.

The immune cell markers CD3, CD4, CD8, CD16, CD56 and CD57 were assessed in the lymphocytes and granulocytes cell populations. Cells were gated using forward versus side angle light scatter to identify lymphocytes, monocytes, and granulocytes with side scatter versus the various stained markers to confirm these populations. Lymphocyte gating was used to evaluate CD3 marker as well as their subsets $CD3^{+}CD4^{+}$, $CD3^{+}CD8^{+}$, $CD3^{+}CD16^{+}$, $CD3^{+}CD56^{+}$ and $CD3^{+}CD57^{+}$ (**Figure 4.3)**. Granulocyte gating was used to evaluate $CD16^{+}$.

The percentage of gated lymphocytes in leukocytes ranged from 3-24% in PDAC groups and 6-40% for the controls as described in **Table 4.3.** $CD16^+$ neutrophils were the most overexpressed in MPC, which might be undergoing apoptosis as evident from the formation of two populations in granulocytes and this is based on anecdotal evidence (**Figure 4.4**). The HC group had the highest percentage of lymphocytes and $CD3^+CD4^+$ T-cells. Conversely, the LAPC group showed the highest frequency of $CD3^+$ and $CD3^+CD8^+$ T-cells indicating that these immune cell markers were statistically altered when compared with the control group HC (**Figure 4.5)**. The results also indicated that patients with PDAC show a broad range of $CD3^-$ $CD56^+$ NK cells compared to the controls; HC and CP, however, few NK cells were found in such patients. This might not be due to the loss of markers $CD56^+$, $CD16^+$, and $CD57^+$ NKs but due to an increase in PDAC severity. Thus, the number of NK and NKT cells in the PDAC patients was found to be significantly smaller than that of the control groups (**Figure 4.6)**.

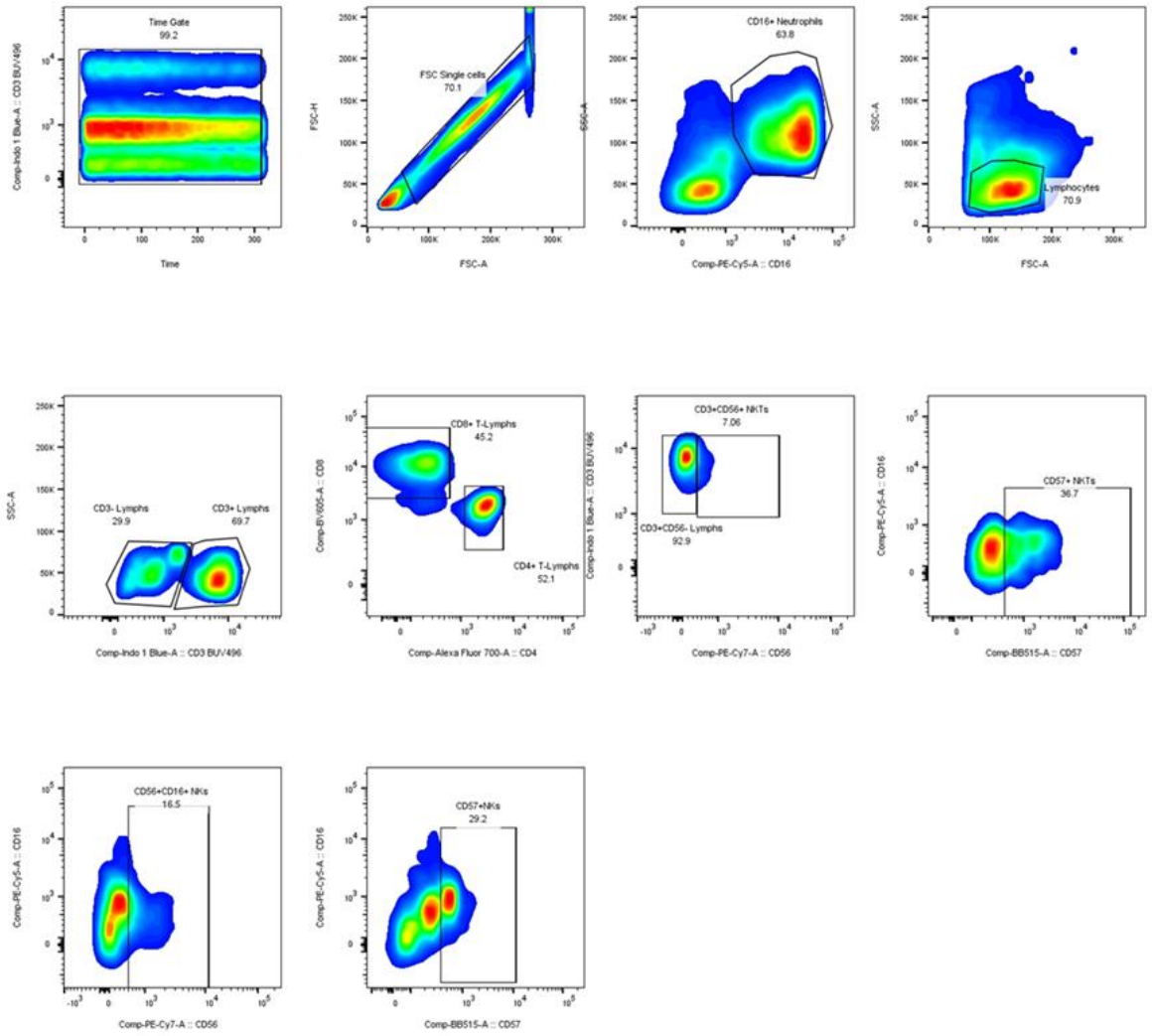


Figure 4.3: Flowjo Layout profile of the immune cell markers populations and subsets in LAPC9. The total cell events collected was 100,000. Cells were gated into Singlets (FSC-A versus FSC-H) and leukocytes (FSC-A versus SSC-A). Leukocytes were further gated into Not $CD16^+$ neutrophils and $CD16^+$ neutrophils (CD16 versus SSC-A). Lymphocytes were observed by gating Not $CD16^+$ neutrophils (FSC-A versus SSC-A) which were further gated to $CD3^-$ and $CD3^+$ (CD3 versus SSC-A). $CD3^+$ was then gated to: NKTs- $CD3^+$ $CD56^+$, $CD3^+$ $CD56^+$, $CD57^+$ and T-cells subsets; $CD3^+CD4^+$ and $CD3^+CD8^+$. $CD3^-$ was gated to NKs- $CD56^+CD16^+$. BUV: BD Horizon Brilliant™ Ultraviolet; BV: Brilliant Violet™; PE-CY: Phycoerythrin Cyanine; BB515: BD Horizon Brilliant™ Blue; CD: Cluster of differentiation., LAPC: Locally Advanced Pancreatic Ductal Adenocarcinoma.

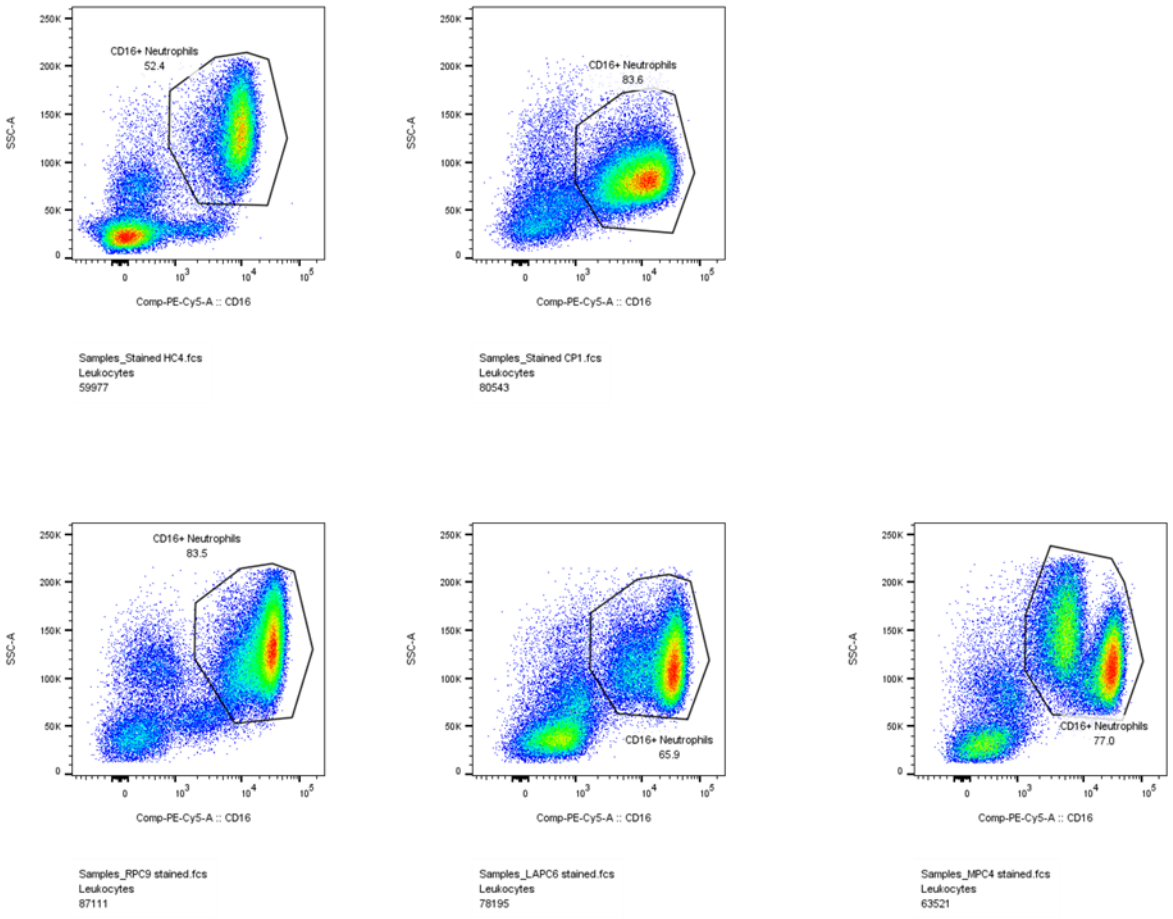


Figure 4.4: Flowjo Layout profile of CD16 neutrophils cell marker populations in the different groups (HC4, CP1, RPC9, LAPC6 and MPC4). The total cell events collected was 100,000. Cells were gated using CD16 versus SSC-Aand two separate populations were observed. The two populations gated as $CD16^{+}$ neutrophils became more distinct with the severity of the disease which implies it was more prevalent in LAPC and MPC groups when compared with the control groups. PE-CY: Phycoerythrin Cyanine; CD: Cluster of differentiation; HC: Healthy Controls; CP: Chronic Pancreatitis; RPC: Resectable Pancreatic Ductal Adenocarcinoma; LAPC: Locally Advanced Pancreatic Ductal Adenocarcinoma; MPC: Metastatic Pancreatic Ductal Adenocarcinoma.

Table 4.3: Percentage population of Immune cell makers in PDAC

	$CD16^+$ Neutrophils	Lymphocytes	$CD3^+$	NKTs	$CD57^+$ NKTs	$CD3^+CD56^-$	$CD4^+$	$CD8^+$	$CD56^+CD16^+$ NKs	$CD57^+$ NKs	MFI $CD57^+$ NKTs	MFI $CD57^+$ NKs	CD4:CD8
LAPC01	63.8	22.4	74.0	9.96	34.4	66.6	52.6	44.8	25.0	30.6	1014	631	1.174107
LAPC02	75.1	17.3	75.1	17.6	57.3	61.9	9.9	87.9	35.0	83.9	1740	2077	0.112628
LAPC03	67.5	20.1	74.2	15.8	52.5	62.4	12.0	85.6	34.9	75.7	1561	1894	0.140187
LAPC04	66.9	23.8	77.3	14.0	29.7	64.5	50.4	46.7	38.7	24.7	1186	681	1.079229
LAPC05	69.9	19.8	70.9	16.0	32.9	57.7	51.3	46.3	42.2	33.8	1064	713	1.107991
LAPC06	65.9	24.0	75.4	16.5	29.9	63.0	50.6	46.7	35.6	29.0	1077	707	1.083512
MPC01	89.8	3.02	39.7	10.0	57.4	35.7	63.2	33.6	28.3	47.8	1703	1802	1.880952
MPC02	89.6	3.31	38.9	9.64	58.7	35.2	67.6	30.4	24.7	46.9	1402	2194	2.223684
MPC03	88.4	3.79	42.0	11.4	51.8	37.0	63.4	34.5	22.0	50.5	1885	2624	1.837681
MPC04	77.0	8.86	39.5	32.1	82.8	26.8	43.0	53.0	38.3	55.3	3702	1881	0.811321
RPC01	85.7	3.09	49.9	29.6	37.5	35.1	21.1	77.4	76.3	49.3	861	616	0.27261
RPC02	58.6	12.0	34.2	37.7	65.0	20.2	33.0	47.1	29.0	42.8	1456	1146	0.700637
RPC03	83.5	5.38	58.9	16.2	36.3	49.4	24.5	73.7	21.6	43.5	936	691	0.332429
RPC04	72.6	9.86	48.1	14.3	48.7	41.3	32.3	53.9	31.6	46.3	1449	1087	0.599258
RPC05	72.2	9.51	49.3	14.7	52.5	42.0	34.4	53.8	32.5	40.5	1412	1021	0.639405
RPC06	70.2	10.8	52.8	11.0	51.3	47.0	33.2	54.2	36.4	49.7	1295	921	0.612546
RPC07	81.3	4.68	40.0	27.2	69.5	29.1	48.3	41.7	32.8	50.1	3451	620	1.158273
RPC08	80.9	5.01	42.2	27.9	64.4	30.4	45.4	43.6	24.0	50.8	2362	649	1.041284
RPC09	81.6	6.79	29.5	12.2	38.2	25.9	50.1	48.3	57.6	42.3	1536	2909	1.037267
RPC10	60.8	13.2	52.4	21.7	69.2	41.0	58.4	37.0	29.3	32.2	1872	1281	1.578378
CP01	83.6	6.19	44.7	98.2	46.9	0.8	5.0	50.75	96.5	77.9	7973	880	0.098522
CP02	52.5	16.6	59.0	93.5	65.9	3.8	26.1	30.75	85.9	84.3	17396	958	0.84878
HC01	68.4	25.9	68.0	90.7	17.4	5.2	66.6	24.4	17.3	31.6	15188	8925	2.729508
HC02	56.7	33.6	66.6	90.9	14.7	4.59	50.1	43.4	26.3	32.8	18008	6717	1.154378
HC03	48.0	38.5	45.3	91.6	4.41	2.65	54.2	37.8	26.8	41.6	5485	3801	1.433862
HC04	52.4	40.5	70.2	93.2	27.8	4.44	62.7	28.5	34.6	41.1	25772	2867	2.2
HC05	53.4	39.2	68.8	90.5	25.6	6.23	58.6	27.0	42.3	26.0	10838	4461	2.17037

LAPC: Locally Advanced Pancreatic Ductal Adenocarcinoma, MPC: Metastatic Pancreatic Ductal Adenocarcinoma, RPC: Resectable Pancreatic Ductal Adenocarcinoma, CP: Chronic Pancreatitis, HC: Healthy controls, NKTs: Natural killer T lymphocytes-cells, NKs: Natural killer cells, MFI; Median Fluorescence Intensity

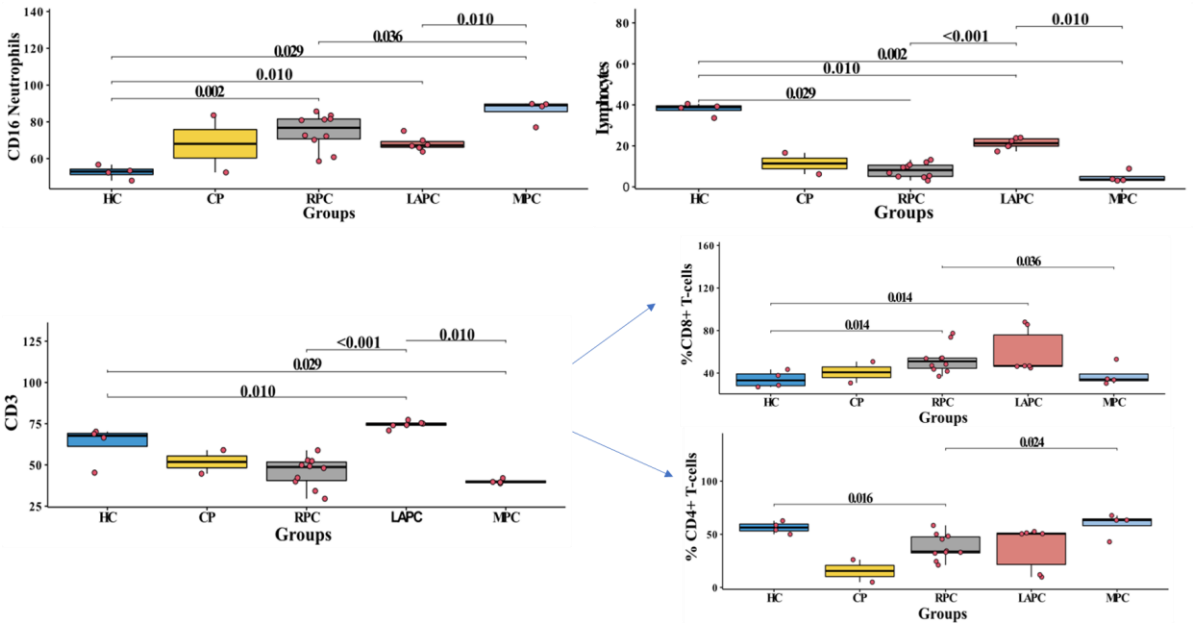


Figure 4.5: Boxplots showing the comparison of the percentages of the immune cell markers. (A) CD16 Neutrophils (B) Lymphocytes, (C) $CD3^+$ T cells (D1) $CD4^+$ T- cells and (D2) $CD8^+$ T- cells for HC, CP, RPC, LAPC, and MPC. $CD16^+$ Neutrophils and Lymphocytes showed significance when PDAC groups were compared with the HC and not CP. The percentage of $CD3^+$ was greatest in LAPC which was significant when compared with other PDAC and Control groups. $CD3^+$ and $CD8^+$ T- cells were significantly altered when RPC, LAPC, and MPC were compared with the HC. RPC: Resectable Pancreatic Adenocarcinoma; LAPC: Locally Advanced Pancreatic Adenocarcinoma; MPC: Metastatic Pancreatic Adenocarcinoma., HC: Healthy Controls.

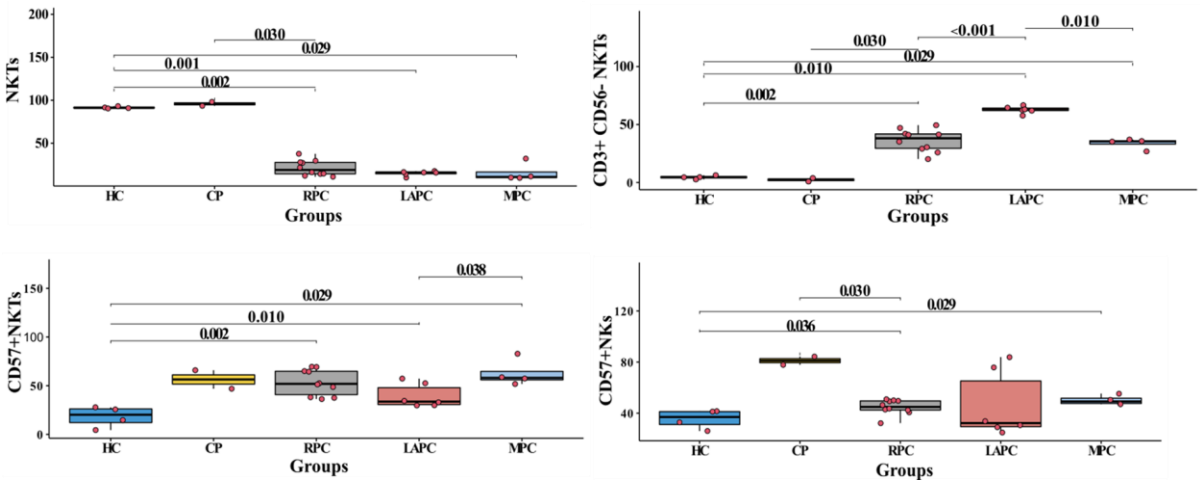


Figure 4.6: Boxplots showing the comparison of NKTs and NKs subsets. (A) NKTs (B) $CD3^+CD56^-$ NKTs (C) $CD57^+$ NKTs and (D) $CD57^+$: NKs for HC, CP, RPC, LAPC, and MPC. NKTs showed significance when PDAC groups were compared to HC except for RPC and CP. $CD3^+CD56^-$ NKTs and $CD57^+$ NKTs were significantly altered across the groups (MPC and LAPC, LAPC and RPC, RPC and CP) and when compared with HC. The PDAC groups only showed a statistical difference when compared with HC for $CD57^+$ NKs markers. Both NKTs and NKs decreased across the groups, hence downregulated levels of both $CD56^+$ and $CD57^+$ suggest poor prognosis in PDAC. RPC: Resectable Pancreatic Adenocarcinoma; LAPC: Locally Advanced Pancreatic Adenocarcinoma; MPC: Metastatic Pancreatic Adenocarcinoma., HC: Healthy Controls. NKs: Natural killer cells, NKTs: Natural Killer T lymphocytes cells.

Principal Component Analysis (PCA) of the data set was carried out using the R (version 3.6.1) and R studio (version 1.1.456) software. The MPC, CP and HC groups were shown to be separate clusters while RPC and LAPC were not distinctively separated except for three outliers RPC1, LAPC2, and LAPC3 as observed in **Figure 4.7.** To understand why the properties of these outliers were different from the rest of the group, a comparison of the outliers versus the rest of the groups was carried out for all the immune cell markers as shown in **Table S29.** Natural killer cells and NKT cells were significantly increased in the outliers compared to the rest of the groups.

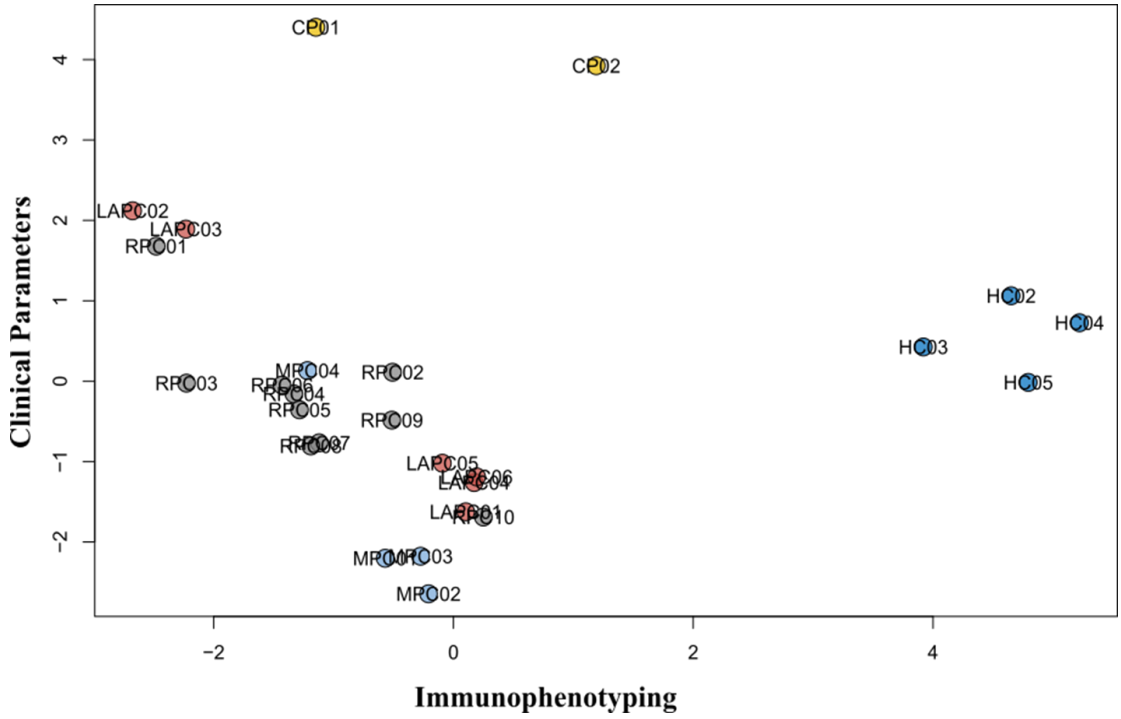


Figure 4.7: Principal Component Analysis (PCA) of immunophenotyping datasets. PCA was used to explain the variance-covariance structure of the variable data set through linear combinations of Immunophenotyping and Clinical parameters data sets to determine the pattern of separation. All the HC and CP were in separate clusters. LAPC, MPC and RPC were not distinctly separated with exception of the outliers LAPC02, LAPC03 and RPC01 RPC: Resectable Pancreatic Adenocarcinoma; LAPC: Locally Advanced Pancreatic Adenocarcinoma; MPC: Metastatic Pancreatic Adenocarcinoma., HC: Healthy Controls.

4.4.3 Impact of CD4/CD8 Ratio on Patient Survival

Kaplan–Meier survival curves were created using the R library "survival." The Wald test was used to calculate the *p*-values between survival curves. Prognostic factors for overall survival (OS) were analysed using the Cox proportional hazard regression. Statistically, CD4/CD8 ratio

was negatively correlated with OS and about four PDAC patients with CD4/CD8 less than 1 survived longer (HR = 3.572 *p*-value = 0.049) (**Figure 4.8**). There were no prognostic factors associated with a high CD4/CD8 ratio in this patient cohort, this might be due to the limited sample size. However, the role of CD4/CD8 ratio is controversial, several studies have shown that a high CD4/CD8 ratio had a worse prognosis in colorectal, breast and ovarian cancer (Diederichsen et al., 2003; García-Martínez et al., 2014; GIUNTOLI et al., 2009). No correlation was observed between other immune markers and survival time.

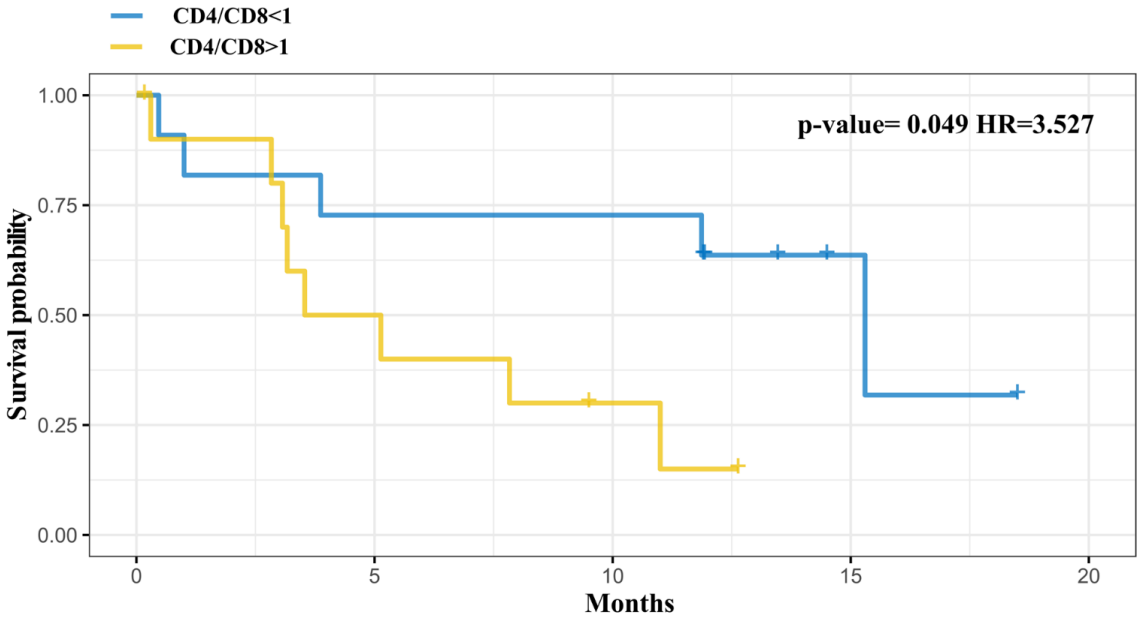


Figure 4.8: Impact of CD4/CD8 on Patients' survival. Kaplan–Meier survival curves showing the effect on CD4/CD8 ratio at threshold=1. Statistically, PDAC patients CD4/CD8<1 survived longer. This implies that elevated levels of $CD8^+$ T cells suggest a favourable prognosis. RPC: Resectable Pancreatic Adenocarcinoma; LAPC: Locally Advanced Pancreatic Adenocarcinoma; MPC: Metastatic Pancreatic Adenocarcinoma.

4.4.4 Gene expression of immune markers

Gene expression analysis showed no statistical difference observed when PDAC groups were compared with the control groups **(Figure 4.9)**. The CP group had the highest fold change for both *CD56* (2.68± 1.36) and *CD57* (49.22± 63.47). For the PDAC groups, RPC had the highest foldchange for *CD3*(30.47± 75.01) and *CD4* (11.75± 44.31). The LAPC group had the highest foldchange for *CD8* (3.86± 7.35) and *CD16* (51.69±108.9).

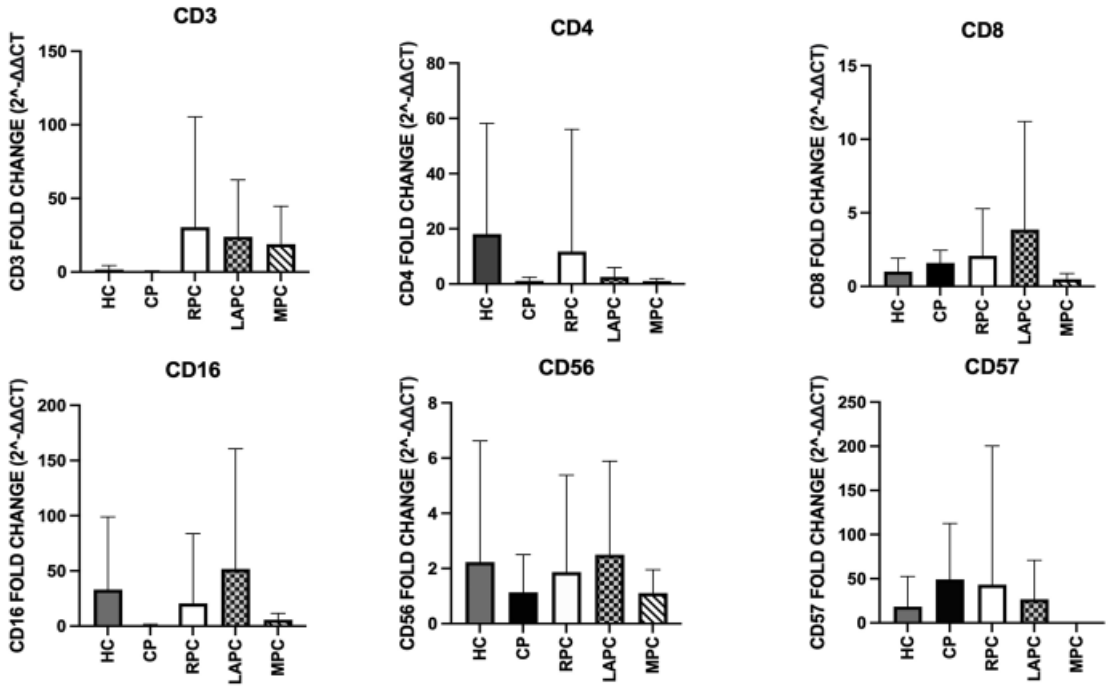


Figure 4.9: Graphical representation of the immune marker by gene expression. CD8, CD16, and CD56 genes were upregulated in LAPC. HC, RPC, and CP have the highest levels of CD4, CD3, and CD57 genes respectively. Although there was no statistical correlation or differences observed when comparing the PDAC groups with the control groups, Although not significant, we observed that patients with resectable PDAC had the highest foldchange for both CD4 (11.75 ± 44.31) and CD3 (30.47 ± 75.01) while patients with locally advanced PDAC had the highest fold change for CD8 (3.86 ± 7.35) and CD16 (51.69 ± 108.9) genes compared to metastatic PDAC patients.RPC: Resectable Pancreatic Adenocarcinoma; LAPC: Locally Advanced Pancreatic Adenocarcinoma; MPC: Metastatic Pancreatic Adenocarcinoma., HC: Healthy Controls

4.4.5 Correlation of the ROS, Immunophenotyping and PCR Values

A comparison of the immunophenotyping and PCR results showed that although there was no significant correlation, both methods showed strong similarities in the expression of $CD8^+$ immune markers (**Figure S2**) in different patient groups (RPC, LAPC, MPC, and HC). Additionally, NK cells, CD56 and CD57 were most upregulated in CP for both assays. The correlation of ROS and immune markers showed a strong positive correlation of $CD8^+$ T-cells and ROS levels. $CD4^+$ T-cells and CD4/CD8 ratio decreased with increased ROS levels (**Table 4.4**).

Table 4.4: Correlation of ROS with immune cell markers (immunophenotyping) in Pancreatic Ductal Adenocarcinoma.

Feature	rho	*p*-value	FDR
$CD16^+$ Neutrophils	0.19	0.373	0.441
Lymphocytes	-0.22	0.281	0.406
$CD3^+$	0.11	0.610	0.610
NKTs	-0.15	0.475	0.514
$CD57^+$ NKTs	0.39	0.056	0.128
$CD3^+$ $CD56^-$	0.36	0.075	0.140
$CD4^+$	-0.54	0.006	0.028
$CD8^+$	0.53	0.006	0.028
$CD56^+CD16^+$ NKs	0.21	0.319	0.415
$CD57^+$ NKs	0.33	0.106	0.172
MFI $CD57^+$ NKTs	-0.43	0.034	0.111
MFI $CD57^+$ NKs	-0.38	0.591	0.128
CD4:CD8	-0.58	0.003	0.028

Rho: spearman's correlation coefficient measures the strength of association between two variables; FDR: false discovery rate NKT: Natural Killer T lymphocytes cells, NKs: Natural killer cells

4.5 Discussion

PDAC tumour cells exhibit immunosuppressive characteristics (Foucher et al., 2018). Infiltrating immune cells may influence PDAC progression in diverse ways. Hence, the immune status could be essential in predicting the outcome and management of the disease. ROS can either be detrimental or beneficial for immune cell function and response (Kotsafti et al., 2020). In this study, the role of ROS and immune cell marker phenotype and genotype in PDAC progression were evaluated.

A low amount of ROS levels may be needed in PDAC progression

In this study, there was an observed elevation of ROS levels as PDAC progressed from RPC to LAPC. A mild concentration of ROS promotes cancer progression, while malignant cells induce antioxidant programs such as activation and stabilization of nuclear factor erythroid-derived 2 (Nrf2) to avoid programmed cell death. In response to elevated ROS levels, Kelch-like ECH-associated protein1 (Keap1), which is bound to Nrf2 becomes inactivated (Durand and Storz, 2017). Nrf2 then translocates to the nucleus and activates genes that mediate antioxidant programs (Durand and Storz, 2017). Hence in PDAC cells, ROS need to be kept at a threshold level that promotes proliferation but prevents senescence and cell death, this could

suggest a decrease in ROS levels at the MPC stage. ROS promote apoptosis and cancer cell survival depending on its' concentration and cancer cell type (Aggarwal et al., 2019).

$CD16^+$ neutrophils are upregulated with tumour severity

$CD16^+$ neutrophils (FcγRIIIb) were observed to be increased with the severity of the disease. Neutrophils can exert both pro and anti-tumoural functions which could depend on the type of tumour and microenvironment (Galdiero et al., 2018). Additionally, they exhibit functional plasticity depending on the expression of cell surface markers, cytokines and ROS (Yang et al., 2017). Although not statistically significant, ROS had a positive correlation with $CD16^+$ immune marker. Studies have shown that ROS production is vital in several neutrophil effector functions (Mackey et al., 2019). Neutrophils contribute to the destruction of cancer cells particularly upon treatment with cancer therapeutic antibodies, however, the existence of immature neutrophils in circulation mediates immunosuppression and subsequent metastasis (Mackey et al., 2019). Neutrophil apoptosis is associated with reduced responsiveness and inhibition of receptors activating effector function (Hart et al., 2000) and loses its ability to secrete granule enzymes on deliberate external stimulation (Haslett et al., 1994). $CD16^+$ neutrophils uniquely function as an inhibitor of antibody-dependent destruction of cancer cells, thereby identifying it as a potential target for enhancing the therapeutic efficacy of cancer therapeutic antibodies (Treffers et al., 2019).

$CD8^+$T-cells expression may inform PDAC prognosis

In this study, $CD8^+$ T-cells were most upregulated in LAPC while $CD4^+$T-cells were downregulated with tumour severity. $CD4^+$T cells alone were not statistically significant prognostic indicators except when combined with other immune markers similar to $CD8^+$ T cells as observed by Fukunaga and colleagues (Fukunaga et al., 2004). Additionally, no statistical alteration was recorded between $CD4^+$T-cells and tumour severity for HIV-positive PDAC patients in this cohort. Pancreatic cancer cells escape immunity by secreting cytokines such as IL-10 and TGF-β and immunosuppression as a result of these cytokines affects the immune function by inhibiting the infiltration of $CD4^+$ and $CD8^+$ T cells in the cancer cells (Fukunaga et al., 2004). This study confirms that CD4/CD8 ratio < 1 in the serum of PDAC patients suggests a favourable prognosis. Studies have shown that the $CD4^+/CD8^+$ ratio correlates with the prognosis of pancreatic cancer (Liu et al., 2017; Yang et al., 2017).

ROS may impact immune response in Pancreatic Ductal Adenocarcinoma

This study observed a significant negative and positive correlation between ROS and $CD4^+$, and $CD8^+$T immune cell markers, respectively. Elevated ROS levels inhibit T-cell function while low amounts stimulate T-cell activation or proliferation (Franchina et al., 2018; Sheng et al., 2010). Additionally, ROS is very vital in effector T-cell activation by promoting nuclear factor of activated T-cells (NFAT) dependent IL-2 expression in $CD4^+$ and $CD8^+$ T-cells (Sena et al., 2013). ROS have been shown to modulate $CD4^+$ T cell at G0/G1 phase of the cell cycle as a result of AMPK phosphorylation and mTOR inhibition (Previte et al., 2017). Conversely, stimulation of $CD8^+$ T-cells can induce ROS generation modulated by NADH-Oxidase 2 (NOX2) to produce IFN-γ for anti-tumour immunity (Bai et al., 2015).

Natural Killer cells may be linked to inflammation

This study observed that CP has the largest frequency of NK and NKT cells. NK cell activation is accompanied by the secretion of inflammatory cytokines thereby driving inflammation which restricts adaptive immune responses (Zitti and Bryceson, 2018). Additionally, T2DM which is also linked to inflammation (Donath and Shoelson, 2011) was shown to have more prevalence in CP patients, therefore might contribute to increased NK and NKT cells. $CD57^+$ and $CD56^+$ NKTs levels increased in CP patients when compared with HC. NK cells fail to survive or proliferate in a hypoxic microenvironment which contributes to the immune escape of NK cells in PDAC patients (Lim et al., 2019). NK cells excluded from PDAC tumours display downregulation of both $CD16^+$ and $CD57^+$ (Marcon et al., 2020). In the blood of PDAC patients, the downregulation of Natural killer Group 2D (NKG2D) reduces cytotoxicity, by lowering the levels of IFN-γ with elevated levels of IL-10, an immunoregulatory cytokine (Marcon et al., 2020). Decreased NKG2D levels stimulate impaired killing of the tumour cells by NK and NKT cells (Lim et al., 2019).

Elevated levels of NK cell markers, $CD56^+$ and $CD57^+$, correlate with favourable outcomes (S. Zhang et al., 2020). $CD56^+$ drives the maturation of NK cells and is weak in cytotoxicity but strong in the production of anti-tumour cytokines such as IFN-γ and TNF-α (Zhang et al., 2020), however, $CD16^+$ $CD56^+$ is a more matured and cytotoxic NK subset. $CD57^+$ is regarded as a marker of terminal differentiation which is less proliferative but more cytotoxic to tumour cells and could acquire IFN-γ when crosslinked with $CD16^+$ (Kared et al., 2018, 2016).

4.6 Conclusion

In this chapter, it was demonstrated that immune cells such as $CD8^+$ T and NK cells, could be essential in predicting prognosis in the PDAC cohort. This study showed that increased CD4/CD8 ratio correlated with poor survival. Therefore immune cells could be useful when predicting prognosis in PDAC. Evaluating the role of these immune cells as well as their interaction with ROS might be significant in developing novel therapeutic strategies. The small number of recruited patients in each stage is a limitation. However, several of these preliminary results are informative and worth exploring as well as validating in future studies with a larger cohort.

CHAPTER V: CORRELATION OF THE CLINICAL DATA, METABOLITES, ROS, AND IMMUNE CELL MARKER LEVELS TO HYPOTHESIZE POSSIBLE RELATIONSHIPS

5.1: Introduction

Over the decade, advances in diagnostic and treatment strategies for PDAC have made relevant but limited incremental progress in patient outcomes (Chang et al., 2016). Importantly, approaches aimed at specific immune targets or cells have been met with limited success chiefly due to immunoregulatory pathways within the PDAC microenvironment (Ho et al., 2020). New strategies for screening high-risk to detect pancreatic tumours at earlier stages are urgently required to make a clinically significant impact. A combination of biochemical and pathological parameters improves the prediction of survival in pancreatic cancer (Hank et al., 2022). Thus, the integration of both clinical and laboratory-based parameters may not only aid in identifying markers for the disease but further help to understand disease progression. In this chapter, correlation analyses of data already obtained in this study (including demographics, clinicopathological, metabolomics, lipoproteins, and immune markers) were conducted.

5.2 Methods

The patient data and results generated from the previous chapters were used to determine relationships and associations between the measured parameters. The methods used to obtain this data have been described in the **Chapters 3** and **4.**

5.2.1 Statistics and Data Analysis

Statistical analysis of the data was generated in R (version 3.6.1) and R studio (version 1.1.456) software using scripts developed in-house. Spearman's rank test was used to calculate the correlation coefficient (rho) between variables. To account for multiple testing, a false discovery rate (FDR) of <10% was applied. The KODAMA algorithm (Cacciatore et al., 2017) was used to identify patterns that demonstrate correlation across all the datasets.

5.3 Results

5.3.1 Correlation of clinical parameters with the Immune cell markers and ROS

The liver function parameter Gamma Glutaryl Transferase (GGT) showed a positive correlation with immune cell marker $CD4^+$ and CD4/CD8 ratio (**Tables 5.1 and 5.2).** Conversely, total bilirubin, conjugated bilirubin, aspartate transaminase, alkaline phosphatase and gamma glutaryl transferase were negatively correlated with elevated $CD8^+$ T cells (**Table 5.3)**. Additionally, Aspartate Transaminase and Gamma Glutaryl Transferase were statistically positively correlated with $CD57^+$ NKTs (**Table 5.4)**. There was no statistically significant correlation observed for either routine haematological or chemistry parameters with the immune cell markers. Furthermore, there was no statistical significance observed between ROS and clinical parameters as well as with maladies such as diabetes, cholangitis and HIV.

Table 5.1: Correlation of CD4+ T cells with Liver Function Tests of PDAC groups.

Feature	rho	*p*-value	FDR
Total Protein (g/L)	0.13	0.619	0.631
Albumin (g/L)	0.11	0.631	0.631
Total Bilirubin (µmol/L)	0.43	0.049	0.098
Conjugated Bilirubin (µmol/L)	0.45	0.041	0.098
Alanine transaminase (U/L)	0.35	0.116	0.155
Aspartate transaminase (U/L)	0.41	0.066	0.105
Alkaline phosphatase (U/L)	0.44	0.047	0.098
Gamma glutamyl transferase (U/L)	0.62	0.003	0.024

Rho: spearman's correlation coefficient measures the strength of association between two variables; FDR: false discovery rate

Table 5.2: Correlation of CD4/CD8 ratio with Liver Function Tests of PDAC groups.

Feature	rho	p-value	FDR
Total Protein (g/L)	0.21	0.408	0.466
Albumin (g/L)	0.11	0.635	0.635
Total Bilirubin (µmol/L)	0.44	0.049	0.090
Conjugated Bilirubin (µmol/L)	0.45	0.039	0.090
Alanine transaminase (U/L)	0.36	0.105	0.140
Aspartate transaminase (U/L)	0.42	0.056	0.090
Alkaline phosphatase (U/L)	0.47	0.033	0.090
Gamma glutamyl transferase (U/L)	0.64	0.002	0.019

Rho: spearman's correlation coefficient measures the strength of association between two variables; FDR: false discovery rate

Table 5.3: Correlation of Liver Function Tests with $CD8^+$ T cells of Pancreatic Ductal Adenocarcinoma groups.

Feature	rho	*p*-value	FDR
Total Protein (g/L)	-0.16	0.531	0.607
Albumin (g/L)	-0.02	0.932	0.932
Total Bilirubin (µmol/L)	-0.51	0.019	0.039
Conjugated Bilirubin (µmol/L)	-0.52	0.015	0.039
Alanine transaminase (U/L)	-0.38	0.088	0.118
Aspartate transaminase (U/L)	-0.48	0.029	0.046
Alkaline phosphatase (U/L)	-0.51	0.018	0.039
Gamma glutamyl transferase. (U/L)	-0.64	0.002	0.014

Rho: spearman's correlation coefficient measures the strength of association between two variables; FDR: false discovery rate

Table 5.4: Correlation of Liver Function Test and Immune cell marker $CD57^+$ NKTs in Pancreatic Ductal Adenocarcinoma groups.

Feature	rho	*p*-value	FDR
Total Protein (g/L)	0.04	0.883	0.883
Albumin (g/L)	-0.13	0.582	0.665
Total Bilirubin (µmol/L)	0.43	0.054	0.086
Conjugated Bilirubin (µmol/L)	0.43	0.049	0.086
Alanine transaminase (U/L)	0.36	0.112	0.149
Aspartate transaminase (U/L)	0.43	0.051	0.086
Alkaline phosphatase (U/L)	0.57	0.007	0.028
Gamma glutamyl transferase. (U/L)	0.57	0.006	0.028

Rho: spearman's correlation coefficient measures the strength of association between two variables; FDR: false discovery rate

5.3.2 Correlation of Metabolites with immune cell markers

Although not statistically significant, ascorbate showed a strong negative correlation with both $CD57^+$ NKTs and $CD3^+$ $CD56^-$ NK cells (**Table S30 and Table S31).** No statistical significance was observed for lactate, glycine and other metabolites with the immune cell markers (result not shown).

5.3.3 Correlation of lipoproteins with immune cell markers

Most lipoproteins parameters such as HCL-C, HDL-p, LDL-C, LDL-p, IDL-C, VLDL-C among others (**Table 5.5)** and lipid extracts (**Table S32**) were observed to be significantly altered with immune cell marker $CD57^+$ NKTs. Most HDL-C and particles were observed to show a negative correlation whereas LDL-C has the opposite. Furthermore, free cholesterols, phospholipids, triglycerides, linoleate among others were positively correlated with $CD57^+$ NKTs.

Table 5.5: Correlation of Lipoproteins and Immune cell marker $CD57^+$ NKTs in PDAC

Features	rho	*p*-value	FDR
VLDL cholesterol (nmol/L)	0.36	0.071	0.093
IDL. cholesterol (nmol/L)	0.56	0.003	0.010
LDL cholesterol (nmol/L)	0.31	0.129	0.152
HDL cholesterol (nmol/L)	-0.68	<0.001	0.001
VLDL triglyceride (nmol/L)	0.34	0.094	0.116
IDL triglyceride (nmol/L)	0.55	0.004	0.012
LDL triglyceride (nmol/L)	0.52	0.007	0.018
HDL triglyceride (nmol/L)	0.05	0.811	0.811
VLDL particle (nmol/L)	0.38	0.056	0.082
Large VLDL particle(nmol/L)	0.29	0.157	0.177
Medium VLDL particle (nmol/L)	0.2	0.328	0.355
Small VLDL particle(nmol/L)	0.38	0.057	0.082
LDL particle (nmol/L)	0.42	0.032	0.060
Large LDL particle (nmol/L)	0.41	0.039	0.068
Medium LDL particle (nmol/L)	0.47	0.015	0.031
Small LDL particle (nmol/L)	0.17	0.395	0.411
HDL particle (mol/L)	-0.72	<0.001	<0.001
Large HDL particle (mol/L)	-0.36	0.067	0.092
Medium HDL particle (mol/L)	-0.62	<0.001	0.002
Small HDL particle (mol/L)	-0.66	<0.001	0.001
VLDL size (nm)	-0.39	0.051	0.082
LDL size (nm)	0.49	0.011	0.025
HDL size (nm)	0.63	<0.001	0.002
Non-HDL particle (nmol/L)	0.44	0.025	0.052
Total particle / HDL particle (nmol/L)	0.67	<0.001	0.001
LDL particle / HDL particle (nmol/L)	0.68	<0.001	0.001

Rho: spearman's correlation coefficient measures the strength of association between two variables; FDR: false discovery rate

5.4 Discussion

PDAC remains cancer with a very poor prognosis and as the incidence is increasing, deaths from this cancer will continue to increase. PDAC is characterized by an aggressive nature. Through the statistical analysis, this study found some correlations between certain clinical and laboratory parameters analysed as described in previous chapters. These correlations may provide an avenue to explore several potential mechanistic pathways in PDAC progression.

Immune cell markers may be linked to liver malfunction

In this study, there was a negative correlation between $CD8^+$ T cells and some of the liver function parameters while $CD4^+$ T cells and CD4/CD8 ratio were directly linked to GGT. GGT is a marker for excessive alcohol and most of the patients in this study are heavy alcohol consumers. PDAC patients in this study have elevated bilirubin levels, reflecting an obstruction in the bile duct by the tumour. Immune balance and tolerance are essential in liver function activities (Kubes and Jenne, 2018). Obstructive jaundice suppresses T cell function via the production of insufficient bile within the biliary tract, thereby reducing the level of lymphocytes of the intestinal mucosa lamina propria including $CD8^+$ T cells (Chang et al., 2018) hence the inverse correlation with the total and conjugated bilirubin as well as GGT. Furthermore, GGT and ALP have been linked to cholestatic jaundice hence showing that a high proportion of $CD8^+$ T cells in the serum could be associated with long-term survival (Naito et al., 1998; Schumacher et al., 2001). Although very little is known about the impact of $CD4^+$ T-cells on the liver function activities of PDAC patients, this study suggests that there might be a potential link.

ALP and GGT, which are indicators of a blocked duct, were observed to have a positive correlation with $CD57^+$ NKTs. Although not much is known about the role of $CD57^+$ NKTs in PDAC, it may have pro-tumour effects. For example, decreased levels of ascorbate correlated with elevated $CD57^+$ NKTs. Ascorbate has been shown to promote anti-tumour activities (Polireddy et al., 2017) hence suggesting that $CD57^+$ NKTs may have an opposite effect as it was shown to be elevated with tumour severity.

Impact of immune cells on altered lipoproteins

This study demonstrated that lipoproteins were significantly altered with $CD57^+$ NKTs; LDL had a strong positive correlation with $CD57^+$ NKTs while HDL had a negative one. PDAC

patients display reduced HDL levels to prevent cholesterol depletion for tumour growth (Bauer et al., 2021). Additionally, most cholesterol derivatives such as linoleate, glycerophospholipids, and sphingomyelin among others were shown to have a positive correlation with elevated $CD57^+$ NKTs levels. High values of phospholipids and triglycerides have been associated with malignant pancreatic tissue growth (Notarstefano et al., 2020). Hypercholesterolemia is significantly linked to pancreatic cancer growth; LDL promotes proliferation, invasion, and metastasis via the activation of the STAT3 pathway which triggers inflammation (Jung et al., 2021). Hence, since the immune cell marker $CD57^+$ NKTs correlates positively with LDL and hypercholesterolemia which are known to play diverse roles in PDAC progression, it might further hint at its function as a pro-tumour immune marker.

5.5 Conclusion

This study confirmed that $CD8^+$T-cells may play a favourable prognostic role in tumour progression due to their relationship to certain clinical parameters and inflammatory markers. Future studies would need to further verify the mechanistic importance of these cells in processes such as inflammation. Also, the observed abnormal lipoprotein profile might be linked with $CD57^+$ NKTs, which could play a pro-tumour role in PDAC. However, validation of these results in a larger cohort is required in which studies such as those investigating the inhibition of $CD57^+$NKTs, and stimulation of $CD8^+$T-cells in PDAC are performed.

CHAPTER VI: OVERALL CONCLUSION AND PROSPECTS

6.1 Introduction

The incidence of PDAC continues to increase with very little improvement in the survival rate. This may be attributed to a combination of late diagnosis, its aggressive nature, and unresponsiveness to treatment. Studies have shown that black patients have the poorest prognosis. To our knowledge, this study is the first to evaluate clinical parameters, metabolites and lipoprotein levels, immune cell and inflammatory markers in a cohort of patients of African ancestry. These evaluated parameters have allowed for the identification of potential markers, a better understanding of the disease in this patient cohort, and plausible molecular mechanisms associated with the disease.

6.2 Overall Conclusion and future work

These preliminary findings and the geographical setting are unique for this type of study, which is generally lacking in the field. Despite the sample size challenges, we believe that these preliminary findings, although descriptive and exploratory, may provide relevant inputs for the design of a metabolomics pancreatic cancer project that can integrate the different pathways for better disease diagnosis, management, and treatment. Importantly, findings from this study highlight those alterations in serum metabolic profiles can result from the effects of cholestasis, alcohol intake, and inflammation. The integration of metabolomics, lipoproteins, and immune cell networks to better understand the biology of PDAC was also a highlight.

The demographic and clinicopathological characteristics of the patients played a vital role in the identification of altered metabolites and lipoproteins in different groups of PDAC. Glycolytic metabolites lactate and glycine could be potential prognostic biomarkers for the early diagnosis of PDAC and may be vital in improving the survival rate. Ethanol and 3-hydroxybutyrate may be important parameters to consider in pancreatic cancer management and treatment, especially in this cohort. Additionally, the declining levels of ascorbate as the tumour severity increases help to confirm its potential therapeutic potential. Therefore, it may be beneficial to combine its targeting with other metabolic pathways such as glycolysis.

Elevated bilirubin levels are associated with abnormal lipoprotein profiles in PDAC. This atypical lipoprotein correlates with increased total cholesterol levels and the detection of LpX. An extensive study on the quantification and role of LpX in PDAC could be pertinent in understanding the course of metastasis and identification of better management options. Also, targeting cholesterol inhibition and blockade from cancer cells could be crucial in developing anti-tumour effects.

Inflammation plays an important role in PDAC growth and progression as shown by the elevated levels of ROS in the patient cohort. ROS levels were also linked to the expression of some immune markers such as $CD8^+$ and $CD4^+$ T-cells, suggesting its role in immune response. Therefore, ROS inhibition could be efficient in impeding pancreatic cancer cell proliferation and possibly in modulating immune response. Furthermore, this study showed that effector immune cells could be essential in predicting the outcome and management of PDAC. Decreased levels of $CD8^+$ T-cells correlated with poor survival. Expansion and activation of $CD8^+$ T-cells could reduce toxicity and improve the anti-tumour effect in PDAC.

Finally, the correlation of clinical data, metabolites, lipoproteins, ROS, and immune cell marker levels hinted at potential links between these various parameters. For example, $CD57^+$NKTs were observed to be correlated to abnormal lipoprotein profiles in PDAC patients. Future mechanistic studies demonstrating this link may prove useful in further elucidating mechanisms associated with PDAC progression and help identify novel targets.

6.3 Study Limitations

While some exciting findings were observed, which allowed for a better understanding of the biology of PDAC in the patient cohort, this was not without limitations. The major limitation in this study was the sample size which needs to be expanded on in future research. There were setbacks regarding patient recruitment and sample collection. In our setting, most patients present late when they are frail and unable to consent or tend to refuse consent. Also, most patients go undiagnosed and so do not present at all thus reducing the number of potential patients. Additionally, COVID-19 has had a devastating impact that the healthcare system became overstretched. Another challenge was the availability of clinical information often experienced in most hospitals in South Africa. Thus, this has significantly affected patient recruitment, sample collection, and processing. Due to this limitation, the role of other maladies

such as T2DM, HIV, and cholangitis could not be adequately assessed in this study. The availability of financial resources due to limited funding also played a pivotal role in patient recruitment and some analyses conducted such as immunophenotyping. However, sample collection is ongoing to validate these findings in an increased sample size.

REFERENCES

Abel, A.M., Yang, C., Thakar, M.S., Malarkannan, S., 2018. Natural Killer Cells: Development, Maturation, and Clinical Utilization. Front Immunol 9, 1869. https://doi.org/10.3389/fimmu.2018.01869

Abimannan, T., Peroumal, D., Parida, J.R., Barik, P.K., Padhan, P., Devadas, S., 2016. Oxidative stress modulates the cytokine response of differentiated Th17 and Th1 cells. Free Radical Biology and Medicine 99, 352–363. https://doi.org/10.1016/j.freeradbiomed.2016.08.026

Aggarwal, V., Tuli, H.S., Varol, A., Thakral, F., Yerer, M.B., Sak, K., Varol, M., Jain, A., Khan, Md.A., Sethi, G., 2019. Role of Reactive Oxygen Species in Cancer Progression: Molecular Mechanisms and Recent Advancements. Biomolecules 9. https://doi.org/10.3390/biom9110735

Ahsan, L., Ossoli, A.F., Freeman, L., Vaisman, B., Amar, M.J., Shamburek, R.D., Remaley, A.T., 2014. Chapter 7 - Role of Lecithin: Cholesterol Acyltransferase in HDL Metabolism and Atherosclerosis, in: Komoda, T. (Ed.), The HDL Handbook (Second Edition). Academic Press, Boston, pp. 159–194. https://doi.org/10.1016/B978-0-12-407867-3.00007-X

Aletsee-Ufrecht, M.C., Langley, K., Rotsch, M., Havemann, K., Gratzl, M., 1990. NCAM: a surface marker for human small cell lung cancer cells. FEBS Letters 267, 295–300. https://doi.org/10.1016/0014-5793(90)80948-I

Alistar, A.T., Morris, B., Harrison, L., Bickenbach, K., Starker, L., Ginder, N., McIlwain, L., Luther, S., Pardee, T.S., Alpert, J., 2020. A single-arm, open-label, phase I study of CPI-613 (Devimistat) in combination with gemcitabine and nab-paclitaxel for patients with locally advanced or metastatic pancreatic adenocarcinoma. JCO 38, 4635–4635. https://doi.org/10.1200/JCO.2020.38.15_suppl.4635

Allard, B., Longhi, M.S., Robson, S.C., Stagg, J., 2017. The ectonucleotidases CD39 and CD73: Novel checkpoint inhibitor targets. Immunological Reviews 276, 121–144. https://doi.org/10.1111/imr.12528

Allard, D., Allard, B., Stagg, J., 2020. On the mechanism of anti-CD39 immune checkpoint therapy. J Immunother Cancer 8, e000186. https://doi.org/10.1136/jitc-2019-000186

Altan, B., Kaira, K., Watanabe, A., Kubo, N., Bao, P., Dolgormaa, G., Bilguun, E.-O., Araki, K., Kanai, Y., Yokobori, T., Oyama, T., Nishiyama, M., Kuwano, H., Shirabe, K., 2018a. Relationship between LAT1 expression and resistance to chemotherapy in pancreatic ductal adenocarcinoma. Cancer Chemotherapy and Pharmacology 81, 141–153. https://doi.org/10.1007/s00280-017-3477-4

Altan, B., Kaira, K., Watanabe, A., Kubo, N., Bao, P., Dolgormaa, G., Bilguun, E.-O., Araki, K., Kanai, Y., Yokobori, T., Oyama, T., Nishiyama, M., Kuwano, H., Shirabe, K., 2018b. Relationship between LAT1 expression and resistance to chemotherapy in pancreatic ductal adenocarcinoma. Cancer Chemotherapy and Pharmacology 81, 141–153. https://doi.org/10.1007/s00280-017-3477-4

Amedei, A., Niccolai, E., Prisco, D., 2014. Pancreatic cancer: Role of the immune system in cancer progression and vaccine-based immunotherapy. Human Vaccines & Immunotherapeutics 10, 3354–3368. https://doi.org/10.4161/hv.34392

Amelio, I., Cutruzzolá, F., Antonov, A., Agostini, M., Melino, G., 2014. Serine and glycine metabolism in cancer. Trends in Biochemical Sciences 39, 191–198. https://doi.org/10.1016/j.tibs.2014.02.004

An, Y., Liu, F., Chen, Y., Yang, Q., 2020. Crosstalk between cancer-associated fibroblasts and immune cells in cancer. Journal of Cellular and Molecular Medicine 24, 13–24. https://doi.org/10.1111/jcmm.14745

Ananieva, E.A., Wilkinson, A.C., 2018. Branched-chain amino acid metabolism in cancer. Curr Opin Clin Nutr Metab Care 21, 64–70. https://doi.org/10.1097/MCO.0000000000000430

Anastasiou, D., Poulogiannis, G., Asara, J.M., Boxer, M.B., Jiang, J., Shen, M., Bellinger, G., Sasaki, A.T., Locasale, J.W., Auld, D.S., Thomas, C.J., Vander Heiden, M.G., Cantley, L.C., 2011. Inhibition of Pyruvate Kinase M2 by Reactive Oxygen Species Contributes to Cellular Antioxidant Responses. Science 334, 1278. https://doi.org/10.1126/science.1211485

Andersen, D.K., Korc, M., Petersen, G.M., Eibl, G., Li, D., Rickels, M.R., Chari, S.T., Abbruzzese, J.L., 2017. Diabetes, Pancreatogenic Diabetes, and Pancreatic Cancer. Diabetes 66, 1103–1110. https://doi.org/10.2337/db16-1477

Anderson, M., Marayati, R., Moffitt, R., Yeh, J.J., 2016. Hexokinase 2 promotes tumor growth and metastasis by regulating lactate production in pancreatic cancer. Oncotarget 8, 56081–56094. https://doi.org/10.18632/oncotarget.9760

Aponte-López, A., Muñoz-Cruz, S., 2020. Mast Cells in the Tumor Microenvironment. Adv Exp Med Biol 1273, 159–173. https://doi.org/10.1007/978-3-030-49270-0_9

Arina, A., Bronte, V., 2015. Myeloid-derived suppressor cell impact on endogenous and adoptively transferred T cells. Current Opinion in Immunology 33, 120–125. https://doi.org/10.1016/j.coi.2015.02.006

Arjomandnejad, M., Sylvia, K., Blackwood, M., Nixon, T., Tang, Q., Muhuri, M., Gruntman, A.M., Gao, G., Flotte, T.R., Keeler, A.M., 2021. Modulating immune responses to AAV by expanded polyclonal T-regs and capsid specific chimeric antigen receptor T-regulatory cells. Molecular Therapy - Methods & Clinical Development 23, 490–506. https://doi.org/10.1016/j.omtm.2021.10.010

Asano, T., Shoda, J., Ueda, T., Kawamoto, T., Todoroki, T., Shimonishi, M., Tanabe, T., Sugimoto, Y., Ichikawa, A., Mutoh, M., Tanaka, N., Miwa, M., 2002. Expressions of Cyclooxygenase-2 and Prostaglandin E-Receptors in Carcinoma of the Gallbladder. Clin Cancer Res 8, 1157.

Aziz, M.H., Sideras, K., Aziz, N.A., Mauff, K., Haen, R., Roos, D., Saida, L., Suker, M., van der Harst, E., Mieog, J.S., Bonsing, B.A., Klaver, Y., Koerkamp, B.G., van Eijck, C.H., 2019a. The Systemic-immune-inflammation Index Independently Predicts Survival and Recurrence in Resectable Pancreatic Cancer and its Prognostic Value Depends on Bilirubin Levels: A Retrospective Multicenter Cohort Study. Annals of Surgery 270.

Aziz, M.H., Sideras, K., Aziz, N.A., Mauff, K., Haen, R., Roos, D., Saida, L., Suker, M., van der Harst, E., Mieog, J.S., Bonsing, B.A., Klaver, Y., Koerkamp, B.G., van Eijck, C.H., 2019b. The Systemic-immune-inflammation Index Independently Predicts Survival and Recurrence in Resectable Pancreatic Cancer and its Prognostic Value Depends on Bilirubin Levels: A Retrospective Multicenter Cohort Study. Annals of Surgery 270.

Bai, A., Moss, A., Rothweiler, S., Serena Longhi, M., Wu, Y., Junger, W.G., Robson, S.C., 2015. NADH oxidase-dependent CD39 expression by CD8+ T cells modulates interferon gamma responses via generation of adenosine. Nature Communications 6, 8819. https://doi.org/10.1038/ncomms9819

Ballehaninna, U.K., Chamberlain, R.S., 2012. The clinical utility of serum CA 19-9 in the diagnosis, prognosis and management of pancreatic adenocarcinoma: An evidence based appraisal. Journal of gastrointestinal oncology 3, 105–119. https://doi.org/10.3978/j.issn.2078-6891.2011.021

Bansal, A.K., Kaushik, K., 2019. Role of Oxidative Stress, Reactive Oxygen Species & Antioxidants in Male Reproductive Functions. Theriogenology Insight 9, 31–41. https://doi.org/10.30954/2277-3371.01.2019.7

Barber, M.D., Ross, J.A., Fearon, K.C.H., 1999. Changes in Nutritional, Functional, and Inflammatory Markers in Advanced Pancreatic Cancer. null 35, 106–110. https://doi.org/10.1207/S15327914NC352_2

Basso, D., Fogar, P., Falconi, M., Fadi, E., Sperti, C., Frasson, C., Greco, E., Tamburrino, D., Teolato, S., Moz, S., Bozzato, D., Pelloso, M., Padoan, A., De Franchis, G., Gnatta, E., Facco, M., Zambon, C.-F., Navaglia, F., Pasquali, C., Basso, G., Semenzato, G., Pedrazzoli, S., Pederzoli, P., Plebani, M., 2013. Pancreatic tumors and immature immunosuppressive myeloid cells in blood and spleen: role of inhibitory co-stimulatory molecules PDL1 and CTLA4. An in vivo and in vitro study. PLoS One 8, e54824. https://doi.org/10.1371/journal.pone.0054824

Bathe, O.F., Shaykhutdinov, R., Kopciuk, K., Weljie, A.M., McKay, A., Sutherland, F.R., Dixon, E., Dunse, N., Sotiropoulos, D., Vogel, H.J., 2011a. Feasibility of Identifying Pancreatic Cancer Based on Serum Metabolomics. Cancer Epidemiol Biomarkers Prev 20, 140. https://doi.org/10.1158/1055-9965.EPI-10-0712

Bathe, O.F., Shaykhutdinov, R., Kopciuk, K., Weljie, A.M., McKay, A., Sutherland, F.R., Dixon, E., Dunse, N., Sotiropoulos, D., Vogel, H.J., 2011b. Feasibility of Identifying Pancreatic Cancer Based on Serum Metabolomics. Cancer Epidemiol Biomarkers Prev 20, 140. https://doi.org/10.1158/1055-9965.EPI-10-0712

Bauer, R., Kuehrer, K.M., Udonta, F., Wroblewski, M., Ben-Batalla, I., Hassl, I., Körbelin, J., Röhrl, C., Unseld, M., Jauhiainen, M., Hengstschläger, M., Loges, S., Stangl, H., 2021. The HDL particle composition determines its anti-tumor activity in pancreatic cancer. https://doi.org/10.1101/2021.07.16.452627

Bayne, L.J., Beatty, G.L., Jhala, N., Clark, C.E., Rhim, A.D., Stanger, B.Z., Vonderheide, R.H., 2012. Tumor-Derived Granulocyte-Macrophage Colony-Stimulating Factor Regulates Myeloid Inflammation and T Cell Immunity in Pancreatic Cancer. Cancer Cell 21, 822–835. https://doi.org/10.1016/j.ccr.2012.04.025

Bellone, G., Turletti, A., Artusio, E., Mareschi, K., Carbone, A., Tibaudi, D., Robecchi, A., Emanuelli, G., Rodeck, U., 1999. Tumor-Associated Transforming Growth Factor-β and Interleukin-10 Contribute to a Systemic Th2 Immune Phenotype in Pancreatic Carcinoma Patients. The American Journal of Pathology 155, 537–547. https://doi.org/10.1016/S0002-9440(10)65149-8

Bertini, I., Cacciatore, S., Jensen, B.V., Schou, J.V., Johansen, J.S., Kruhøffer, M., Luchinat, C., Nielsen, D.L., Turano, P., 2012. Metabolomic NMR Fingerprinting to Identify and Predict Survival of Patients with Metastatic Colorectal Cancer. Cancer Res 72, 356. https://doi.org/10.1158/0008-5472.CAN-11-1543

Bever, K.M., Borazanci, E.H., Thompson, E.A., Durham, J.N., Pinero, K., Jameson, G.S., Vrana, A., Liu, M., Wilt, C., Wu, A.A., Fu, W., Wang, H., Yin, Y., Leal, J.P., Jesus-Acosta, A.D., Zheng, L., Laheru, D.A., Von Hoff, D.D., Jaffee, E.M., Powell, J.D., Le, D.T., 2020. An exploratory study of metformin with or without rapamycin as maintenance therapy after induction chemotherapy in patients with metastatic pancreatic adenocarcinoma. Oncotarget 11, 1929–1941. https://doi.org/10.18632/oncotarget.27586

Bhandari, M., Toouli, J., 2006. Preoperative biliary drainage (stenting) for treatment of obstructive jaundice. HPB (Oxford) 8, 343–345. https://doi.org/10.1080/13651820600804328

Bin, P., Huang, R., Zhou, X., 2017. Oxidation Resistance of the Sulfur Amino Acids: Methionine and Cysteine. BioMed Research International 2017, 9584932. https://doi.org/10.1155/2017/9584932

Boese, A.C., Kang, S., 2021. Mitochondrial metabolism-mediated redox regulation in cancer progression. Redox Biology 42, 101870. https://doi.org/10.1016/j.redox.2021.101870

Bosetti, C., Lucenteforte, E., Silverman, D.T., Petersen, G., Bracci, P.M., Ji, B.T., Negri, E., Li, D., Risch, H.A., Olson, S.H., Gallinger, S., Miller, A.B., Bueno-de-Mesquita, H.B., Talamini, R., Polesel, J., Ghadirian, P., Baghurst, P.A., Zatonski, W., Fontham, E., Bamlet, W.R., Holly, E.A., Bertuccio, P., Gao, Y.T., Hassan, M., Yu, H., Kurtz, R.C., Cotterchio, M., Su, J., Maisonneuve, P., Duell, E.J., Boffetta, P., La Vecchia, C., 2012. Cigarette smoking and pancreatic cancer: an analysis from the International Pancreatic Cancer Case-Control Consortium (Panc4). Annals of Oncology 23, 1880–1888. https://doi.org/10.1093/annonc/mdr541

Braganza, J.M., Lee, S.H., McCloy, R.F., McMahon, M.J., 2011. Chronic pancreatitis. The Lancet 377, 1184–1197. https://doi.org/10.1016/S0140-6736(10)61852-1

Brand, A., Singer, K., Koehl, G.E., Kolitzus, M., Schoenhammer, G., Thiel, A., Matos, C., Bruss, C., Klobuch, S., Peter, K., Kastenberger, M., Bogdan, C., Schleicher, U., Mackensen, A., Ullrich, E., Fichtner-Feigl, S., Kesselring, R., Mack, M., Ritter, U., Schmid, M., Blank, C., Dettmer, K., Oefner, P.J., Hoffmann, P., Walenta, S., Geissler, E.K., Pouyssegur, J., Villunger, A., Steven, A., Seliger, B., Schreml, S., Haferkamp, S., Kohl, E., Karrer, S., Berneburg, M., Herr, W., Mueller-Klieser, W., Renner, K., Kreutz, M., 2016. LDHA-Associated Lactic Acid Production Blunts Tumor Immunosurveillance by T and NK Cells. Cell Metabolism 24, 657–671. https://doi.org/10.1016/j.cmet.2016.08.011

Brandt, E.J., Regnier, S.M., Leung, E.K., Chou, S.H., Baron, B.W., Te, H.S., Davidson, M.H., Sargis, R.M., 2015. Management of lipoprotein X and its complications in a patient with primary sclerosing cholangitis. Clin Lipidol 10, 305–312. https://doi.org/10.2217/clp.15.23

Braudeau, C., Salabert-Le Guen, N., Chevreuil, J., Rimbert, M., Martin, J.C., Josien, R., 2021. An easy and reliable whole blood freezing method for flow cytometry immuno-phenotyping and functional analyses. Cytometry Part B: Clinical Cytometry 100, 652–665. https://doi.org/10.1002/cyto.b.21994

Bray, R., Cacciatore, S., Jiménez, B., Cartwright, R., Digesu, A., Fernando, R., Holmes, E., Nicholson, J.K., Bennett, P.R., MacIntyre, D.A., Khullar, V., 2017. Urinary Metabolic Phenotyping of Women with Lower Urinary Tract Symptoms. J. Proteome Res. 16, 4208–4216. https://doi.org/10.1021/acs.jproteome.7b00568

Brenchley, J.M., Karandikar, N.J., Betts, M.R., Ambrozak, D.R., Hill, B.J., Crotty, L.E., Casazza, J.P., Kuruppu, J., Migueles, S.A., Connors, M., Roederer, M., Douek, D.C., Koup, R.A., 2003. Expression of CD57 defines replicative senescence and antigen-induced apoptotic death of CD8+ T cells. Blood 101, 2711–2720. https://doi.org/10.1182/blood-2002-07-2103

Brune, K.A., Lau, B., Palmisano, E., Canto, M., Goggins, M.G., Hruban, R.H., Klein, A.P., 2010. Importance of Age of Onset in Pancreatic Cancer Kindreds. JNCI: Journal of the National Cancer Institute 102, 119–126. https://doi.org/10.1093/jnci/djp466

Bustin, S.A., Benes, V., Garson, J.A., Hellemans, J., Huggett, J., Kubista, M., Mueller, R., Nolan, T., Pfaffl, M.W., Shipley, G.L., Vandesompele, J., Wittwer, C.T., 2009. The MIQE Guidelines: Minimum Information for Publication of Quantitative Real-Time PCR Experiments. Clinical Chemistry 55, 611–622. https://doi.org/10.1373/clinchem.2008.112797

Cacciatore, S., Tenori, L., Luchinat, C., Bennett, P.R., MacIntyre, D.A., 2017a. KODAMA: an R package for knowledge discovery and data mining. Bioinformatics 33, 621–623. https://doi.org/10.1093/bioinformatics/btw705

Cacciatore, S., Wium, M., Licari, C., Ajayi-Smith, A., Masieri, L., Anderson, C., Salukazana, A.S., Kaestner, L., Carini, M., Carbone, G.M., Catapano, C.V., Loda, M., Libermann, T.A., Zerbini, L.F., 2021. Inflammatory metabolic profile of South African patients with prostate cancer. Cancer & Metabolism 9, 29. https://doi.org/10.1186/s40170-021-00265-6

Cacciatore, S., Zadra, G., Bango, C., Penney, K.L., Tyekucheva, S., Yanes, O., Loda, M., 2017b. Metabolic Profiling in Formalin-Fixed and Paraffin-Embedded Prostate Cancer Tissues. Mol Cancer Res 15, 439. https://doi.org/10.1158/1541-7786.MCR-16-0262

Cai, S.-W., Yang, S.-Z., Gao, J., Pan, K., Chen, J.-Y., Wang, Y.-L., Wei, L.-X., Dong, J.-H., 2011. Prognostic significance of mast cell count following curative resection for pancreatic ductal adenocarcinoma. Surgery 149, 576–584. https://doi.org/10.1016/j.surg.2010.10.009

Cameron, M.E., Yakovenko, A., Trevino, J.G., 2018. Glucose and Lactate Transport in Pancreatic Cancer: Glycolytic Metabolism Revisited. J Oncol 2018, 6214838–6214838. https://doi.org/10.1155/2018/6214838

Canto, M.I., Harinck, F., Hruban, R.H., Offerhaus, G.J., Poley, J.-W., Kamel, I., Nio, Y., Schulick, R.S., Bassi, C., Kluijt, I., Levy, M.J., Chak, A., Fockens, P., Goggins, M., Bruno, M., =International Cancer of Pancreas Screening (CAPS) Consortium, 2013. International Cancer of the Pancreas Screening (CAPS) Consortium summit on the management of patients with increased risk for familial pancreatic cancer. Gut 62, 339–347. https://doi.org/10.1136/gutjnl-2012-303108

Cao, L., Wu, J., Qu, X., Sheng, J., Cui, M., Liu, S., Huang, X., Xiang, Y., Li, B., Zhang, X., Cui, R., 2020. Glycometabolic rearrangements--aerobic glycolysis in pancreatic cancer: causes, characteristics and clinical applications. Journal of Experimental & Clinical Cancer Research 39, 267. https://doi.org/10.1186/s13046-020-01765-x

Carstens, J.L., Correa de Sampaio, P., Yang, D., Barua, S., Wang, H., Rao, A., Allison, J.P., LeBleu, V.S., Kalluri, R., 2017. Spatial computation of intratumoral T cells correlates with survival of patients with pancreatic cancer. Nature Communications 8, 15095. https://doi.org/10.1038/ncomms15095

Cassim, S., Pouyssegur, J., 2020. Tumor Microenvironment: A Metabolic Player that Shapes the Immune Response. International Journal of Molecular Sciences 21. https://doi.org/10.3390/ijms21010157

Castaneda, O.A., Lee, S.-C., Ho, C.-T., Huang, T.-C., 2017. Macrophages in oxidative stress and models to evaluate the antioxidant function of dietary natural compounds. Journal of Food and Drug Analysis 25, 111–118. https://doi.org/10.1016/j.jfda.2016.11.006

Cesmebasi, A., Malefant, J., Patel, S.D., Plessis, M.D., Renna, S., Tubbs, R.S., Loukas, M., 2015. The surgical anatomy of the lymphatic system of the pancreas. Clinical Anatomy 28, 527–537. https://doi.org/10.1002/ca.22461

Chang, J.H., Jiang, Y., Pillarisetty, V.G., 2016. Role of immune cells in pancreatic cancer from bench to clinical application: An updated review. Medicine (Baltimore) 95, e5541–e5541. https://doi.org/10.1097/MD.0000000000005541

Chang, Z.-K., Kou, Z.-P., Li, S.-X., Lou, X.-L., 2018. To evaluate the correlation between the change of immune system function before and after the treatment of malignant obstructive type jaundice treated with biliary stent. Eur Rev Med Pharmacol Sci 22, 1638–1644. https://doi.org/10.26355/eurrev_201803_14570

Chari, S.T., Leibson, C.L., Rabe, K.G., Timmons, L.J., Ransom, J., de Andrade, M., Petersen, G.M., 2008. Pancreatic cancer-associated diabetes mellitus: prevalence and temporal

association with diagnosis of cancer. Gastroenterology 134, 95–101. https://doi.org/10.1053/j.gastro.2007.10.040
Chatterjee, S., Khunti, K., Davies, M.J., 2017. Type 2 diabetes. The Lancet 389, 2239–2251. https://doi.org/10.1016/S0140-6736(17)30058-2
Chattopadhyay, P.K., Betts, M.R., Price, D.A., Gostick, E., Horton, H., Roederer, M., De Rosa, S.C., 2009. The cytolytic enzymes granyzme A, granzyme B, and perforin: expression patterns, cell distribution, and their relationship to cell maturity and bright CD57 expression. J Leukoc Biol 85, 88–97. https://doi.org/10.1189/jlb.0208107
Chen, Huey-Ling, Wu, S.-H., Hsu, S.-H., Liou, B.-Y., Chen, Hui-Ling, Chang, M.-H., 2018. Jaundice revisited: recent advances in the diagnosis and treatment of inherited cholestatic liver diseases. Journal of Biomedical Science 25, 75. https://doi.org/10.1186/s12929-018-0475-8
Chen, Q., Espey, M.G., Sun, A.Y., Pooput, C., Kirk, K.L., Krishna, M.C., Khosh, D.B., Drisko, J., Levine, M., 2008. Pharmacologic doses of ascorbate act as a prooxidant and decrease growth of aggressive tumor xenografts in mice. Proc Natl Acad Sci U S A 105, 11105–11109. https://doi.org/10.1073/pnas.0804226105
Chen, X., Zeh, H.J., Kang, R., Kroemer, G., Tang, D., 2021. Cell death in pancreatic cancer: from pathogenesis to therapy. Nature Reviews Gastroenterology & Hepatology 18, 804–823. https://doi.org/10.1038/s41575-021-00486-6
Chen, Y., Song, Y., Du, W., Gong, L., Chang, H., Zou, Z., 2019. Tumor-associated macrophages: an accomplice in solid tumor progression. Journal of Biomedical Science 26, 78. https://doi.org/10.1186/s12929-019-0568-z
Cheung, E.C., DeNicola, G.M., Nixon, C., Blyth, K., Labuschagne, C.F., Tuveson, D.A., Vousden, K.H., 2020. Dynamic ROS Control by TIGAR Regulates the Initiation and Progression of Pancreatic Cancer. Cancer Cell 37, 168-182.e4. https://doi.org/10.1016/j.ccell.2019.12.012
Choi, S.Y.C., Collins, C.C., Gout, P.W., Wang, Y., 2013. Cancer-generated lactic acid: a regulatory, immunosuppressive metabolite? The Journal of Pathology 230, 350–355. https://doi.org/10.1002/path.4218
Chung, J.C., Oh, M.J., Choi, S.H., Bae, C.D., 2008. PROTEOMIC ANALYSIS TO IDENTIFY BIOMARKER PROTEINS IN PANCREATIC DUCTAL ADENOCARCINOMA. ANZ Journal of Surgery 78, 245–251. https://doi.org/10.1111/j.1445-2197.2008.04429.x
Chung, Y.T., Matkowskyj, K.A., Li, H., Bai, H., Zhang, W., Tsao, M.-S., Liao, J., Yang, G.-Y., 2012. Overexpression and oncogenic function of aldo-keto reductase family 1B10 (AKR1B10) in pancreatic carcinoma. Modern Pathology 25, 758–766. https://doi.org/10.1038/modpathol.2011.191
Cluntun, A.A., Lukey, M.J., Cerione, R.A., Locasale, J.W., 2017. Glutamine Metabolism in Cancer: Understanding the Heterogeneity. Trends in Cancer 3, 169–180. https://doi.org/10.1016/j.trecan.2017.01.005
Colegio, O.R., Chu, N.-Q., Szabo, A.L., Chu, T., Rhebergen, A.M., Jairam, V., Cyrus, N., Brokowski, C.E., Eisenbarth, S.C., Phillips, G.M., Cline, G.W., Phillips, A.J., Medzhitov, R., 2014. Functional polarization of tumour-associated macrophages by tumour-derived lactic acid. Nature 513, 559.
Coleman, R.A., Lewin, T.M., Van Horn, C.G., Gonzalez-Baró, M.R., 2002. Do Long-Chain Acyl-CoA Synthetases Regulate Fatty Acid Entry into Synthetic Versus Degradative Pathways? The Journal of Nutrition 132, 2123–2126. https://doi.org/10.1093/jn/132.8.2123
Commisso, C., Davidson, S.M., Soydaner-Azeloglu, R.G., Parker, S.J., Kamphorst, J.J., Hackett, S., Grabocka, E., Nofal, M., Drebin, J.A., Thompson, C.B., Rabinowitz, J.D.,

Metallo, C.M., Vander Heiden, M.G., Bar-Sagi, D., 2013. Macropinocytosis of protein is an amino acid supply route in Ras-transformed cells. Nature 497, 633.
Costache, M., Ioana, M., Iordache, S., Ene, D., Costache, C.A., Săftoiu, A., 2015. VEGF Expression in Pancreatic Cancer and Other Malignancies: A Review of the Literature. Rom J Intern Med 53, 199–208. https://doi.org/10.1515/rjim-2015-0027
Cruz, A.F., Rohban, R., Esni, F., 2020. Macrophages in the pancreas: Villains by circumstances, not necessarily by actions. Immunity, Inflammation and Disease 8, 807–824. https://doi.org/10.1002/iid3.345
Ćwiklińska, A., Mickiewicz, A., Kowalski, R., Kortas-Stempak, B., Kuchta, A., Mucha, K., Makowiecki, M., Gliwińska, A., Lewandowski, K., Pączek, L., Fijałkowski, M., Gruchała, M., Jankowski, M., 2020. Detection of Lipoprotein X (LpX): A challenge in patients with severe hypercholesterolaemia. J Med Biochem 39, 283–289. https://doi.org/10.2478/jomb-2019-0038
Dadey, R.E., Workman, C.J., Vignali, D.A.A., 2020. Regulatory T Cells in the Tumor Microenvironment. Adv Exp Med Biol 1273, 105–134. https://doi.org/10.1007/978-3-030-49270-0_6
Dallal, R.M., Christakos, P., Lee, K., Egawa, S., Son, Y.-I., Lotze, M.T., 2002. Paucity of dendritic cells in pancreatic cancer. Surgery 131, 135–138. https://doi.org/10.1067/msy.2002.119937
Danai, L.V., Babic, A., Rosenthal, M.H., Dennstedt, E.A., Muir, A., Lien, E.C., Mayers, J.R., Tai, K., Lau, A.N., Jones-Sali, P., Prado, C.M., Petersen, G.M., Takahashi, N., Sugimoto, M., Yeh, J.J., Lopez, N., Bardeesy, N., Fernandez-Del Castillo, C., Liss, A.S., Koong, A.C., Bui, J., Yuan, C., Welch, M.W., Brais, L.K., Kulke, M.H., Dennis, C., Clish, C.B., Wolpin, B.M., Vander Heiden, M.G., 2018. Altered exocrine function can drive adipose wasting in early pancreatic cancer. Nature 558, 600–604. https://doi.org/10.1038/s41586-018-0235-7
Daniel, S.K., Sullivan, K.M., Labadie, K.P., Pillarisetty, V.G., 2019. Hypoxia as a barrier to immunotherapy in pancreatic adenocarcinoma. Clin Transl Med 8, 10–10. https://doi.org/10.1186/s40169-019-0226-9
Dannenberg, A.J., Subbaramaiah, K., 2003. Targeting cyclooxygenase-2 in human neoplasia: rationale and promise. Cancer Cell 4, 431–436. https://doi.org/10.1016/s1535-6108(03)00310-6
Darnell, E.P., Wang, T.J., Lumish, M.A., Hernandez-Barco, Y.G., Weniger, M., Casey, B.W., Qadan, M., Lillemoe, K.D., Ferrone, C.R., Fernandez-Del Castillo, C., Krishnan, K., 2021. Preoperative cholangitis is an independent risk factor for mortality in patients after pancreatoduodenectomy for pancreatic cancer. The American Journal of Surgery 221, 134–140. https://doi.org/10.1016/j.amjsurg.2020.07.025
De Monte, L., Reni, M., Tassi, E., Clavenna, D., Papa, I., Recalde, H., Braga, M., Di Carlo, V., Doglioni, C., Protti, M.P., 2011. Intratumor T helper type 2 cell infiltrate correlates with cancer-associated fibroblast thymic stromal lymphopoietin production and reduced survival in pancreatic cancer. Journal of Experimental Medicine 208, 469–478. https://doi.org/10.1084/jem.20101876
De Oliveira, M.P., Liesa, M., 2020. The Role of Mitochondrial Fat Oxidation in Cancer Cell Proliferation and Survival. Cells 9. https://doi.org/10.3390/cells9122600
De Sanctis, F., Solito, S., Ugel, S., Molon, B., Bronte, V., Marigo, I., 2016. MDSCs in cancer: Conceiving new prognostic and therapeutic targets. Biochimica et Biophysica Acta (BBA) - Reviews on Cancer 1865, 35–48. https://doi.org/10.1016/j.bbcan.2015.08.001
Delaye, J.B., Patin, F., Piver, E., Bruno, C., Vasse, M., Vourc'h, P., Andres, C.R., Corcia, P., Blasco, H., 2017. Low IDL-B and high LDL-1 subfraction levels in serum of ALS

patients. Journal of the Neurological Sciences 380, 124–127. https://doi.org/10.1016/j.jns.2017.07.019

Delimaris, I., Faviou, E., Antonakos, G., Stathopoulou, E., Zachari, A., Dionyssiou-Asteriou, A., 2007. Oxidized LDL, serum oxidizability and serum lipid levels in patients with breast or ovarian cancer. Clinical Biochemistry 40, 1129–1134. https://doi.org/10.1016/j.clinbiochem.2007.06.007

Di Gangi, I.M., Mazza, T., Fontana, A., Copetti, M., Fusilli, C., Ippolito, A., Mattivi, F., Latiano, A., Andriulli, A., Vrhovsek, U., Pazienza, V., 2016. Metabolomic profile in pancreatic cancer patients: a consensus-based approach to identify highly discriminating metabolites. Oncotarget 7, 5815–5829. https://doi.org/10.18632/oncotarget.6808

D'Marco, L., Puchades, M.J., Romero-Parra, M., Gorriz, J.L., 2020. Diabetic Kidney Disease and COVID-19: The Crash of Two Pandemics. Front Med (Lausanne) 7, 199–199. https://doi.org/10.3389/fmed.2020.00199

Drisko, J.A., Serrano, O.K., Spruce, L.R., Chen, Q., Levine, M., 2018. Treatment of pancreatic cancer with intravenous vitamin C: a case report. Anticancer Drugs 29, 373–379. https://doi.org/10.1097/CAD.0000000000000603

Duan, X., Deng, L., Chen, X., Lu, Y., Zhang, Q., Zhang, K., Hu, Y., Zeng, J., Sun, W., 2011a. Clinical significance of the immunostimulatory MHC class I chain-related molecule A and NKG2D receptor on NK cells in pancreatic cancer. Medical Oncology 28, 466–474. https://doi.org/10.1007/s12032-010-9480-9

Duan, X., Deng, L., Chen, X., Lu, Y., Zhang, Q., Zhang, K., Hu, Y., Zeng, J., Sun, W., 2011b. Clinical significance of the immunostimulatory MHC class I chain-related molecule A and NKG2D receptor on NK cells in pancreatic cancer. Medical Oncology 28, 466–474. https://doi.org/10.1007/s12032-010-9480-9

DuBois, R.N., Awad, J., Morrow, J., Roberts, L.J., 2nd, Bishop, P.R., 1994. Regulation of eicosanoid production and mitogenesis in rat intestinal epithelial cells by transforming growth factor-alpha and phorbol ester. J Clin Invest 93, 493–498. https://doi.org/10.1172/JCI116998

Dunn, W.B., Bailey, N.J.C., Johnson, H.E., 2005. Measuring the metabolome: current analytical technologies. Analyst 130, 606–625. https://doi.org/10.1039/B418288J

DuPage, M., Bluestone, J.A., 2016. Harnessing the plasticity of CD4+ T cells to treat immune-mediated disease. Nature Reviews Immunology 16, 149–163. https://doi.org/10.1038/nri.2015.18

Durand, N., Storz, P., 2017. Targeting reactive oxygen species in development and progression of pancreatic cancer. null 17, 19–31. https://doi.org/10.1080/14737140.2017.1261017

El Ansari, R., Craze, M.L., Miligy, I., Diez-Rodriguez, M., Nolan, C.C., Ellis, I.O., Rakha, E.A., Green, A.R., 2018. The amino acid transporter SLC7A5 confers a poor prognosis in the highly proliferative breast cancer subtypes and is a key therapeutic target in luminal B tumours. Breast Cancer Research 20, 21. https://doi.org/10.1186/s13058-018-0946-6

Elebo, N., Omoshoro-Jones, J., Fru, P.N., Devar, J., De Wet van Zyl, C., Vorster, B.C., Smith, M., Cacciatore, S., Zerbini, L.F., Candy, G., Nweke, E.E., 2021. Serum Metabolomic and Lipoprotein Profiling of Pancreatic Ductal Adenocarcinoma Patients of African Ancestry. Metabolites 11. https://doi.org/10.3390/metabo11100663

Epstein, A.S., Soff, G.A., Capanu, M., Crosbie, C., Shah, M.A., Kelsen, D.P., Denton, B., Gardos, S., O'Reilly, E.M., 2012. Analysis of incidence and clinical outcomes in patients with thromboembolic events and invasive exocrine pancreatic cancer. Cancer 118, 3053–3061. https://doi.org/10.1002/cncr.26600

Eriksson, L., Jaworska, J., Worth, A.P., Cronin, M.T.D., McDowell, R.M., Gramatica, P., 2003. Methods for reliability and uncertainty assessment and for applicability evaluations of classification- and regression-based QSARs. Environ Health Perspect 111, 1361–1375. https://doi.org/10.1289/ehp.5758

Ersahin, T., Tuncbag, N., Cetin-Atalay, R., 2015. The PI3K/AKT/mTOR interactive pathway. Mol Biosyst 11, 1946–1954. https://doi.org/10.1039/c5mb00101c

Everts, B., Amiel, E., Huang, S.C.-C., Smith, A.M., Chang, C.-H., Lam, W.Y., Redmann, V., Freitas, T.C., Blagih, J., van der Windt, G.J.W., Artyomov, M.N., Jones, R.G., Pearce, E.L., Pearce, E.J., 2014. TLR-driven early glycolytic reprogramming via the kinases TBK1-IKKε supports the anabolic demands of dendritic cell activation. Nature Immunology 15, 323.

Fahrmann, J.F., Bantis, L.E., Capello, M., Scelo, G., Dennison, J.B., Patel, N., Murage, E., Vykoukal, J., Kundnani, D.L., Foretova, L., Fabianova, E., Holcatova, I., Janout, V., Feng, Z., Yip-Schneider, M., Zhang, J., Brand, R., Taguchi, A., Maitra, A., Brennan, P., Max Schmidt, C., Hanash, S., 2019. A Plasma-Derived Protein-Metabolite Multiplexed Panel for Early-Stage Pancreatic Cancer. JNCI: Journal of the National Cancer Institute 111, 372–379. https://doi.org/10.1093/jnci/djy126

Fan, Z., Fan, K., Gong, Y., Huang, Q., Yang, C., Cheng, H., Jin, K., Ni, Q., Yu, X., Luo, G., Liu, C., 2019. The CRP/Albumin Ratio Predicts Survival And Monitors Chemotherapeutic Effectiveness In Patients With Advanced Pancreatic Cancer. Cancer Manag Res 11, 8781–8788. https://doi.org/10.2147/CMAR.S211363

Feingold, K.R., Grunfeld, C., 2000. The Effect of Inflammation and Infection on Lipids and Lipoproteins. MDText.com, Inc., South Dartmouth (MA).

Fellin, R., Manzato, E., 2019. Lipoprotein-X fifty years after its original discovery. Nutrition, Metabolism and Cardiovascular Diseases 29, 4–8. https://doi.org/10.1016/j.numecd.2018.09.006

Feng, L., Gu, S., Wang, P., Chen, H., Chen, Z., Meng, Z., Liu, L., 2018. Pretreatment values of bilirubin and albumin are not prognostic predictors in patients with advanced pancreatic cancer. Cancer Med 7, 5943–5951. https://doi.org/10.1002/cam4.1848

Fernandez-Zapico, M., Kim, D.W., Philip, P., Vandell, A., Eckard, J., Korn, R., Priore, G.D., Simeone, D., 2019a. Abstract B15: Therapeutic potential of targeting amino acid metabolism in pancreatic cancer. Cancer Res 79, B15. https://doi.org/10.1158/1538-7445.PANCA19-B15

Fernandez-Zapico, M., Kim, D.W., Philip, P., Vandell, A., Eckard, J., Korn, R., Priore, G.D., Simeone, D., 2019b. Abstract B15: Therapeutic potential of targeting amino acid metabolism in pancreatic cancer. Cancer Res 79, B15. https://doi.org/10.1158/1538-7445.PANCA19-B15

Field, K.M., Dow, C., Michael, M., 2008. Part I: Liver function in oncology: biochemistry and beyond. The Lancet Oncology 9, 1092–1101. https://doi.org/10.1016/S1470-2045(08)70279-1

Fischer, K., Hoffmann, P., Voelkl, S., Meidenbauer, N., Ammer, J., Edinger, M., Gottfried, E., Schwarz, S., Rothe, G., Hoves, S., Renner, K., Timischl, B., Mackensen, A., Kunz-Schughart, L., Andreesen, R., Krause, S.W., Kreutz, M., 2007. Inhibitory effect of tumor cell–derived lactic acid on human T cells. Blood 109, 3812–3819. https://doi.org/10.1182/blood-2006-07-035972

Fogar, P., Sperti, C., Basso, D., Sanzari, M.C., Greco, E., Davoli, C., Navaglia, F., Zambon, C.-F., Pasquali, C., Venza, E., Pedrazzoli, S., Plebani, M., 2006. Decreased Total Lymphocyte Counts in Pancreatic Cancer: An Index of Adverse Outcome. Pancreas 32.

Formentini, A., Prokopchuk, O., Sträter, J., Kleeff, J., Grochola, L.F., Leder, G., Henne-Bruns, D., Korc, M., Kornmann, M., 2009. Interleukin-13 exerts autocrine growth-promoting

effects on human pancreatic cancer, and its expression correlates with a propensity for lymph node metastases. International Journal of Colorectal Disease 24, 57–67. https://doi.org/10.1007/s00384-008-0550-9

Foucher, E.D., Ghigo, C., Chouaib, S., Galon, J., Iovanna, J., Olive, D., 2018. Pancreatic Ductal Adenocarcinoma: A Strong Imbalance of Good and Bad Immunological Cops in the Tumor Microenvironment. Front Immunol 9, 1044–1044. https://doi.org/10.3389/fimmu.2018.01044

Franchina, D.G., Dostert, C., Brenner, D., 2018. Reactive Oxygen Species: Involvement in T Cell Signaling and Metabolism. Trends in Immunology 39, 489–502. https://doi.org/10.1016/j.it.2018.01.005

Frankel, T.L., Burns, W., Riley, J., Morgan, R.A., Davis, J.L., Hanada, K., Quezado, M., Rosenberg, S.A., Royal, R.E., 2010. Identification and characterization of a tumor infiltrating CD56+/CD16− NK cell subset with specificity for pancreatic and prostate cancer cell lines. Cancer Immunology, Immunotherapy 59, 1757–1769. https://doi.org/10.1007/s00262-010-0897-y

Frossi, B., De Carli, M., Piemonte, M., Pucillo, C., 2008. Oxidative microenvironment exerts an opposite regulatory effect on cytokine production by Th1 and Th2 cells. Molecular Immunology 45, 58–64. https://doi.org/10.1016/j.molimm.2007.05.008

Fukunaga, A., Miyamoto, M., Cho, Y., Murakami, S., Kawarada, Y., Oshikiri, T., Kato, K., Kurokawa, T., Suzuoki, M., Nakakubo, Y., Hiraoka, K., Itoh, T., Morikawa, T., Okushiba, S., Kondo, S., Hiroyuki, K., 2004a. CD8+tumor-infiltrating lymphocytes together with CD4+tumor-infiltrating lymphocytes and dendritic cells improve the prognosis of patients with pancreatic adenocarcinoma. Pancreas 28, e26–e31. https://doi.org/10.1097/00006676-200401000-00023

Fukunaga, A., Miyamoto, M., Cho, Y., Murakami, S., Kawarada, Y., Oshikiri, T., Kato, K., Kurokawa, T., Suzuoki, M., Nakakubo, Y., Hiraoka, K., Itoh, T., Morikawa, T., Okushiba, S., Kondo, S., Hiroyuki, K., 2004b. CD8+tumor-infiltrating lymphocytes together with CD4+tumor-infiltrating lymphocytes and dendritic cells improve the prognosis of patients with pancreatic adenocarcinoma. Pancreas 28, e26–e31. https://doi.org/10.1097/00006676-200401000-00023

Gabitass, R.F., Annels, N.E., Stocken, D.D., Pandha, H.A., Middleton, G.W., 2011a. Elevated myeloid-derived suppressor cells in pancreatic, esophageal and gastric cancer are an independent prognostic factor and are associated with significant elevation of the Th2 cytokine interleukin-13. Cancer Immunology, Immunotherapy 60, 1419. https://doi.org/10.1007/s00262-011-1028-0

Gabitass, R.F., Annels, N.E., Stocken, D.D., Pandha, H.A., Middleton, G.W., 2011b. Elevated myeloid-derived suppressor cells in pancreatic, esophageal and gastric cancer are an independent prognostic factor and are associated with significant elevation of the Th2 cytokine interleukin-13. Cancer Immunology, Immunotherapy 60, 1419. https://doi.org/10.1007/s00262-011-1028-0

Gabrilovich, D.I., 2017. Myeloid-Derived Suppressor Cells. Cancer Immunol Res 5, 3–8. https://doi.org/10.1158/2326-6066.CIR-16-0297

Gaianigo, N., Melisi, D., Carbone, C., 2017. EMT and Treatment Resistance in Pancreatic Cancer. Cancers 9. https://doi.org/10.3390/cancers9090122

Galdiero, M.R., Varricchi, G., Loffredo, S., Mantovani, A., Marone, G., 2018. Roles of neutrophils in cancer growth and progression. Journal of Leukocyte Biology 103, 457–464. https://doi.org/10.1002/JLB.3MR0717-292R

Gardner, T.B., Adler, D.G., Forsmark, C.E., Sauer, B.G., Taylor, J.R., Whitcomb, D.C., 2020. ACG Clinical Guideline: Chronic Pancreatitis. Official journal of the American College of Gastroenterology | ACG 115.

Garrido, F., Perea, F., Bernal, M., Sánchez-Palencia, A., Aptsiauri, N., Ruiz-Cabello, F., 2017. The Escape of Cancer from T Cell-Mediated Immune Surveillance: HLA Class I Loss and Tumor Tissue Architecture. Vaccines 5. https://doi.org/10.3390/vaccines5010007

Gatenby, R.A., Gillies, R.J., 2004. Why do cancers have high aerobic glycolysis? Nature Reviews Cancer 4, 891–899. https://doi.org/10.1038/nrc1478

Georgila, K., Vyrla, D., Drakos, E., 2019. Apolipoprotein A-I (ApoA-I), Immunity, Inflammation and Cancer. Cancers 11. https://doi.org/10.3390/cancers11081097

Ghesquière, B., Wong, B.W., Kuchnio, A., Carmeliet, P., 2014. Metabolism of stromal and immune cells in health and disease. Nature 511, 167–176. https://doi.org/10.1038/nature13312

Giovanelli, P., Sandoval, T.A., Cubillos-Ruiz, J.R., 2019. Dendritic Cell Metabolism and Function in Tumors. Trends in Immunology 40, 699–718. https://doi.org/10.1016/j.it.2019.06.004

Gnerlich, J.L., Mitchem, J.B., Weir, J.S., Sankpal, N.V., Kashiwagi, H., Belt, B.A., Porembka, M.R., Herndon, J.M., Eberlein, T.J., Goedegebuure, P., Linehan, D.C., 2010a. Induction of Th17 Cells in the Tumor Microenvironment Improves Survival in a Murine Model of Pancreatic Cancer. J. Immunol. 185, 4063. https://doi.org/10.4049/jimmunol.0902609

Gnerlich, J.L., Mitchem, J.B., Weir, J.S., Sankpal, N.V., Kashiwagi, H., Belt, B.A., Porembka, M.R., Herndon, J.M., Eberlein, T.J., Goedegebuure, P., Linehan, D.C., 2010b. Induction of Th17 Cells in the Tumor Microenvironment Improves Survival in a Murine Model of Pancreatic Cancer. J. Immunol. 185, 4063. https://doi.org/10.4049/jimmunol.0902609

Gnerlich, J.L., Mitchem, J.B., Weir, J.S., Sankpal, N.V., Kashiwagi, H., Belt, B.A., Porembka, M.R., Herndon, J.M., Eberlein, T.J., Goedegebuure, P., Linehan, D.C., 2010c. Induction of Th17 Cells in the Tumor Microenvironment Improves Survival in a Murine Model of Pancreatic Cancer. J. Immunol. 185, 4063. https://doi.org/10.4049/jimmunol.0902609

Goulart, M.R., Stasinos, K., Fincham, R.E.A., Delvecchio, F.R., Kocher, H.M., 2021. T cells in pancreatic cancer stroma. World J Gastroenterol 27, 7956–7968. https://doi.org/10.3748/wjg.v27.i46.7956

Grossberg, A.J., Chu, L.C., Deig, C.R., Fishman, E.K., Hwang, W.L., Maitra, A., Marks, D.L., Mehta, A., Nabavizadeh, N., Simeone, D.M., Weekes, C.D., Thomas, C.R., Jr, 2020. Multidisciplinary standards of care and recent progress in pancreatic ductal adenocarcinoma. CA Cancer J Clin 70, 375–403. https://doi.org/10.3322/caac.21626

Gruppen, Eke G., Connelly, M.A., Otvos, J.D., Bakker, S.J.L., Dullaart, R.P.F., 2015. A novel protein glycan biomarker and LCAT activity in metabolic syndrome. European Journal of Clinical Investigation 45, 850–859. https://doi.org/10.1111/eci.12481

Gruppen, Eke G, Riphagen, I.J., Connelly, M.A., Otvos, J.D., Bakker, S.J.L., Dullaart, R.P.F., 2015. GlycA, a Pro-Inflammatory Glycoprotein Biomarker, and Incident Cardiovascular Disease: Relationship with C-Reactive Protein and Renal Function. PLoS One 10, e0139057–e0139057. https://doi.org/10.1371/journal.pone.0139057

Guillaumond, F., Bidaut, G., Ouaissi, M., Servais, S., Gouirand, V., Olivares, O., Lac, S., Borge, L., Roques, J., Gayet, O., Pinault, M., Guimaraes, C., Nigri, J., Loncle, C., Lavaut, M.-N., Garcia, S., Tailleux, A., Staels, B., Calvo, E., Tomasini, R., Iovanna, J.L., Vasseur, S., 2015. Cholesterol uptake disruption, in association with chemotherapy, is a promising combined metabolic therapy for pancreatic adenocarcinoma. Proc Natl Acad Sci U S A 112, 2473–2478. https://doi.org/10.1073/pnas.1421601112

Gullino, P.M., Grantham, F.H., Smith, S.H., Haggerty, A.C., 1965. Modifications of the Acid-Base Status of the Internal Milieu of Tumors. JNCI: Journal of the National Cancer Institute 34, 857–869. https://doi.org/10.1093/jnci/34.6.857

Halabe Bucay, A., 2009. Hypothesis proved...citric acid (citrate) does improve cancer: a case of a patient suffering from medullary thyroid cancer. Medical hypotheses 73, 271. https://doi.org/10.1016/j.mehy.2009.03.018

Halperin, M.L., Hammeke, M., Josse, R.G., Jungas, R.L., 1983. Metabolic acidosis in the alcoholic: A pathophysiologic approach. Metabolism 32, 308–315. https://doi.org/10.1016/0026-0495(83)90197-X

Hanahan, D., Weinberg, R.A., 2011. Hallmarks of Cancer: The Next Generation. Cell 144, 646–674. https://doi.org/10.1016/j.cell.2011.02.013

Hank, T., Sandini, M., Ferrone, C.R., Ryan, D.P., Mino-Kenudson, M., Qadan, M., Wo, J.Y., Klaiber, U., Weekes, C.D., Weniger, M., Hinz, U., Harrison, J.M., Heckler, M., Warshaw, A.L., Hong, T.S., Hackert, T., Clark, J.W., Büchler, M.W., Lillemoe, K.D., Strobel, O., Castillo, C.F., 2022. A Combination of Biochemical and Pathological Parameters Improves Prediction of Postresection Survival After Preoperative Chemotherapy in Pancreatic Cancer: The PANAMA-score. Annals of Surgery 275.

Harris, I.S., DeNicola, G.M., 2020. The Complex Interplay between Antioxidants and ROS in Cancer. Trends in Cell Biology 30, 440–451. https://doi.org/10.1016/j.tcb.2020.03.002

Hart, P.A., Bellin, M.D., Andersen, D.K., Bradley, D., Cruz-Monserrate, Z., Forsmark, C.E., Goodarzi, M.O., Habtezion, A., Korc, M., Kudva, Y.C., Pandol, S.J., Yadav, D., Chari, S.T., 2016. Type 3c (pancreatogenic) diabetes mellitus secondary to chronic pancreatitis and pancreatic cancer. The Lancet Gastroenterology & Hepatology 1, 226–237. https://doi.org/10.1016/S2468-1253(16)30106-6

Hart, P.A., Chari, S.T., 2019. Is Screening for Pancreatic Cancer in High-Risk Individuals One Step Closer or a Fool's Errand? Clin Gastroenterol Hepatol 17, 36–38. https://doi.org/10.1016/j.cgh.2018.09.024

Hart, S.P., Ross, J.A., Ross, K., Haslett, C., Dransfield, I., 2000. Molecular characterization of the surface of apoptotic neutrophils: Implications for functional downregulation and recognition by phagocytes. Cell Death & Differentiation 7, 493–503. https://doi.org/10.1038/sj.cdd.4400680

Harvey, L.A., 2018. REDCap: web-based software for all types of data storage and collection. Spinal Cord 56, 625–625. https://doi.org/10.1038/s41393-018-0169-9

Haschemi, A., Kosma, P., Gille, L., Evans, C.R., Burant, C.F., Starkl, P., Knapp, B., Haas, R., Schmid, J.A., Jandl, C., Amir, S., Lubec, G., Park, J., Esterbauer, H., Bilban, M., Brizuela, L., Pospisilik, J.A., Otterbein, L.E., Wagner, O., 2012. The Sedoheptulose Kinase CARKL Directs Macrophage Polarization through Control of Glucose Metabolism. Cell Metabolism 15, 813–826. https://doi.org/10.1016/j.cmet.2012.04.023

Hashemi, M., Hoshyar, R., Ande, S.R., Chen, Q.M., Solomon, C., Zuse, A., Naderi, M., 2017. Mevalonate Cascade and its Regulation in Cholesterol Metabolism in Different Tissues in Health and Disease. Curr Mol Pharmacol 10, 13–26. https://doi.org/10.2174/1874467209666160112123746

Haslett, C., Savill, J.S., Whyte, M.K.B., Stern, M., Dransfield, I., Meagher, L.C., Dexter, T.M., Raff, M.C., Wyllie, A.H., 1994. Granulocyte apoptosis and the control of inflammation. Philosophical Transactions of the Royal Society of London. Series B: Biological Sciences 345, 327–333. https://doi.org/10.1098/rstb.1994.0113

Hato, T., Dagher, P.C., 2015. How the Innate Immune System Senses Trouble and Causes Trouble. CLIN J AM SOC NEPHROL 10, 1459. https://doi.org/10.2215/CJN.04680514

Hatzivassiliou, G., Zhao, F., Bauer, D.E., Andreadis, C., Shaw, A.N., Dhanak, D., Hingorani, S.R., Tuveson, D.A., Thompson, C.B., 2005. ATP citrate lyase inhibition can suppress tumor cell growth. Cancer Cell 8, 311–321. https://doi.org/10.1016/j.ccr.2005.09.008

Hayashi, I., Morishita, Y., Imai, K., Nakamura, M., Nakachi, K., Hayashi, T., 2007. High-throughput spectrophotometric assay of reactive oxygen species in serum. Mutation Research/Genetic Toxicology and Environmental Mutagenesis 631, 55–61. https://doi.org/10.1016/j.mrgentox.2007.04.006

Hayes, J.D., Dinkova-Kostova, A.T., Tew, K.D., 2020. Oxidative Stress in Cancer. Cancer Cell 38, 167–197. https://doi.org/10.1016/j.ccell.2020.06.001

He, Q., Luo, X., Huang, Y., Sheikh, M.S., 2002. Apo2L/TRAIL differentially modulates the apoptotic effects of sulindac and a COX-2 selective non-steroidal anti-inflammatory agent in Bax-deficient cells. Oncogene 21. https://doi.org/10.1038/sj.onc.1205897

He, S., Fei, M., Wu, Y., Zheng, D., Wan, D., Wang, L., Li, D., 2011a. Distribution and Clinical Significance of Th17 Cells in the Tumor Microenvironment and Peripheral Blood of Pancreatic Cancer Patients. International Journal of Molecular Sciences 12. https://doi.org/10.3390/ijms12117424

He, S., Fei, M., Wu, Y., Zheng, D., Wan, D., Wang, L., Li, D., 2011b. Distribution and Clinical Significance of Th17 Cells in the Tumor Microenvironment and Peripheral Blood of Pancreatic Cancer Patients. International Journal of Molecular Sciences 12. https://doi.org/10.3390/ijms12117424

Herbel, C., Patsoukis, N., Bardhan, K., Seth, P., Weaver, J.D., Boussiotis, V.A., 2016. Clinical significance of T cell metabolic reprogramming in cancer. Clinical and Translational Medicine 5, 29. https://doi.org/10.1186/s40169-016-0110-9

Herlea, V., Mustafa, E.S., Iorgescu, A.C., Pechianu, N.C., Cretoiu, D., Sajin, M., Dima, S.O., Vasilescu, C., Stroescu, C., Ungureanu, C., Dumitrascu, T., Brasoveanu, V., Ghinescu, M., Popescu, I., 2020. A Morphological and Immunohistochemical Study of the Tumoral and Inflammatory Cells in Pancreatic Ductal Adenocarcinoma. Journal of Immunology Research 2020, 6148286. https://doi.org/10.1155/2020/6148286

Hernberg, M., Muhonen, T., Turunen, J.P., Hahka-Kemppinen, M., Pyrhönen, S., 1996. The CD4+/CD8+ ratio as a prognostic factor in patients with metastatic melanoma receiving chemoimmunotherapy. JCO 14, 1690–1696. https://doi.org/10.1200/JCO.1996.14.5.1690

Ho, W.J., Jaffee, E.M., Zheng, L., 2020. The tumour microenvironment in pancreatic cancer — clinical challenges and opportunities. Nature Reviews Clinical Oncology 17, 527–540. https://doi.org/10.1038/s41571-020-0363-5

Höflich, C., Döcke, W.D., Busch, A., Kern, F., Volk, H.D., 1998. CD45RA(bright)/CD11a(bright) CD8+ T cells: effector T cells. International Immunology 10, 1837–1845. https://doi.org/10.1093/intimm/10.12.1837

Hohla, F., Hopfinger, G., Romeder, F., Rinnerthaler, G., Bezan, A., Stättner, S., Hauser-Kronberger, C., Ulmer, H., Greil, R., 2014. Female gender may predict response to FOLFIRINOX in patients with unresectable pancreatic cancer: a single institution retrospective review. Int J Oncol 44, 319–326. https://doi.org/10.3892/ijo.2013.2176

Hosein, A.N., Brekken, R.A., Maitra, A., 2020. Pancreatic cancer stroma: an update on therapeutic targeting strategies. Nature Reviews Gastroenterology & Hepatology 17, 487–505. https://doi.org/10.1038/s41575-020-0300-1

Hossain, F., Al-Khami, A.A., Wyczechowska, D., Hernandez, C., Zheng, L., Reiss, K., Valle, L.D., Trillo-Tinoco, J., Maj, T., Zou, W., Rodriguez, P.C., Ochoa, A.C., 2015. Inhibition of Fatty Acid Oxidation Modulates Immunosuppressive Functions of Myeloid-Derived Suppressor Cells and Enhances Cancer Therapies. Cancer Immunol Res 3, 1236. https://doi.org/10.1158/2326-6066.CIR-15-0036

Houg, D.S., Bijlsma, M.F., 2018. The hepatic pre-metastatic niche in pancreatic ductal adenocarcinoma. Molecular Cancer 17, 95. https://doi.org/10.1186/s12943-018-0842-9

Huang, J., Lok, V., Ngai, C.H., Zhang, L., Yuan, J., Lao, X.Q., Ng, K., Chong, C., Zheng, Z.-J., Wong, M.C.S., 2021. Worldwide Burden of, Risk Factors for, and Trends in Pancreatic Cancer. Gastroenterology 160, 744–754. https://doi.org/10.1053/j.gastro.2020.10.007

Huber, M., Brehm, C.U., Gress, T.M., Buchholz, M., Alashkar Alhamwe, B., von Strandmann, E.P., Slater, E.P., Bartsch, J.W., Bauer, C., Lauth, M., 2020. The Immune Microenvironment in Pancreatic Cancer. Int J Mol Sci 21, 7307. https://doi.org/10.3390/ijms21197307

Hwang, N.R., Yim, S.-H., Kim, Y.M., Jeong, J., Song, E.J., Lee, Y., Lee, J.H., Choi, S., Lee, K.-J., 2009. Oxidative modifications of glyceraldehyde-3-phosphate dehydrogenase play a key role in its multiple cellular functions. Biochemical Journal 423, 253–264. https://doi.org/10.1042/BJ20090854

Inman, K.S., Francis, A.A., Murray, N.R., 2014a. Complex role for the immune system in initiation and progression of pancreatic cancer. World journal of gastroenterology 20, 11160–11181. https://doi.org/10.3748/wjg.v20.i32.11160

Inman, K.S., Francis, A.A., Murray, N.R., 2014b. Complex role for the immune system in initiation and progression of pancreatic cancer. World journal of gastroenterology 20, 11160–11181. https://doi.org/10.3748/wjg.v20.i32.11160

Ito, T., Amakawa, R., Inaba, M., Ikehara, S., Inaba, K., Fukuhara, S., 2001. Differential Regulation of Human Blood Dendritic Cell Subsets by IFNs. J. Immunol. 166, 2961. https://doi.org/10.4049/jimmunol.166.5.2961

Janakiram, N.B., Mohammed, A., Bryant, T., Ritchie, R., Stratton, N., Jackson, L., Lightfoot, S., Benbrook, D.M., Asch, A.S., Lang, M.L., Rao, C.V., 2017. Loss of natural killer T cells promotes pancreatic cancer in LSL-KrasG12D/+ mice. Immunology 152, 36–51. https://doi.org/10.1111/imm.12746

Jellusova, J., 2020. Metabolic control of B cell immune responses. Current Opinion in Immunology 63, 21–28. https://doi.org/10.1016/j.coi.2019.11.002

Jiang, J., Nilsson-Ehle, P., Xu, N., 2006. Influence of liver cancer on lipid and lipoprotein metabolism. Lipids in Health and Disease 5, 4. https://doi.org/10.1186/1476-511X-5-4

Jin, J., Zhao, Q., 2020. Emerging role of mTOR in tumor immune contexture: Impact on chemokine-related immune cells migration. Theranostics 10, 6231–6244. https://doi.org/10.7150/thno.45219

Jomova, K., Baros, S., Valko, M., 2012. Redox active metal-induced oxidative stress in biological systems. Transition Metal Chemistry 37, 127–134. https://doi.org/10.1007/s11243-012-9583-6

Jung, Y.Y., Ko, J.-H., Um, J.-Y., Chinnathambi, A., Alharbi, S.A., Sethi, G., Ahn, K.S., 2021. LDL cholesterol promotes the proliferation of prostate and pancreatic cancer cells by activating the STAT3 pathway. Journal of Cellular Physiology 236, 5253–5264. https://doi.org/10.1002/jcp.30229

Kalinski, P., 2012. Regulation of Immune Responses by Prostaglandin E_2. J. Immunol. 188, 21. https://doi.org/10.4049/jimmunol.1101029

Kamphorst, J.J., Nofal, M., Commisso, C., Hackett, S.R., Lu, W., Grabocka, E., Vander Heiden, M.G., Miller, G., Drebin, J.A., Bar-Sagi, D., Thompson, C.B., Rabinowitz, J.D., 2015. Human pancreatic cancer tumors are nutrient poor and tumor cells actively scavenge extracellular protein. Cancer Res 75, 544–553. https://doi.org/10.1158/0008-5472.CAN-14-2211

Kang, S.W., Lee, S., Lee, E.K., 2015. ROS and energy metabolism in cancer cells: alliance for fast growth. Archives of Pharmacal Research 38, 338–345. https://doi.org/10.1007/s12272-015-0550-6

Kared, H., Martelli, S., Ng, T.P., Pender, S.L.F., Larbi, A., 2016. CD57 in human natural killer cells and T-lymphocytes. Cancer Immunol Immunother 65, 441–452. https://doi.org/10.1007/s00262-016-1803-z

Kared, H., Martelli, S., Tan, S.W., Simoni, Y., Chong, M.L., Yap, S.H., Newell, E.W., Pender, S.L.F., Kamarulzaman, A., Rajasuriar, R., Larbi, A., 2018. Adaptive NKG2C(+)CD57(+) Natural Killer Cell and Tim-3 Expression During Viral Infections. Front Immunol 9, 686–686. https://doi.org/10.3389/fimmu.2018.00686

Keane, M.G., Horsfall, L., Rait, G., Pereira, S.P., 2014. A case–control study comparing the incidence of early symptoms in pancreatic and biliary tract cancer. BMJ Open 4, e005720. https://doi.org/10.1136/bmjopen-2014-005720

Kelada, S.N.P., Aylor, D.L., Peck, B.C.E., Ryan, J.F., Tavarez, U., Buus, R.J., Miller, D.R., Chesler, E.J., Threadgill, D.W., Churchill, G.A., Pardo-Manuel de Villena, F., Collins, F.S., 2012. Genetic analysis of hematological parameters in incipient lines of the collaborative cross. G3 (Bethesda) 2, 157–165. https://doi.org/10.1534/g3.111.001776

Kennel, K.B., Greten, F.R., 2021. Immune cell - produced ROS and their impact on tumor growth and metastasis. Redox Biology 42, 101891. https://doi.org/10.1016/j.redox.2021.101891

Khawja, S.N., Mohammed, S., Silberfein, E.J., Musher, B.L., Fisher, W.E., Van Buren, G.I., 2015. Pancreatic Cancer Disparities in African Americans. Pancreas 44.

Kim, J.S., Park, Y.S., Kim, J.Y., Kim, Y.G., Kim, Y.J., Lee, H.K., Kim, H.S., Hong, J.T., Kim, Y., Han, S.-B., 2012. Inhibition of human pancreatic tumor growth by cytokine-induced killer cells in nude mouse xenograft model. Immune Netw 12, 247–252. https://doi.org/10.4110/in.2012.12.6.247

Klein, A.P., 2021. Pancreatic cancer epidemiology: understanding the role of lifestyle and inherited risk factors. Nature Reviews Gastroenterology & Hepatology 18, 493–502. https://doi.org/10.1038/s41575-021-00457-x

Korangath, P., Teo, W.W., Sadik, H., Han, L., Mori, N., Huijts, C.M., Wildes, F., Bharti, S., Zhang, Z., Santa-Maria, C.A., Tsai, H., Dang, C.V., Stearns, V., Bhujwalla, Z.M., Sukumar, S., 2015. Targeting Glutamine Metabolism in Breast Cancer with Aminooxyacetate. Clin Cancer Res 21, 3263. https://doi.org/10.1158/1078-0432.CCR-14-1200

Kotsafti, A., Scarpa, Marco, Castagliuolo, I., Scarpa, Melania, 2020. Reactive Oxygen Species and Anti-tumor Immunity—From Surveillance to Evasion. Cancers 12. https://doi.org/10.3390/cancers12071748

Krawczyk, C.M., Holowka, T., Sun, J., Blagih, J., Amiel, E., DeBerardinis, R.J., Cross, J.R., Jung, E., Thompson, C.B., Jones, R.G., Pearce, E.J., 2010. Toll-like receptor–induced changes in glycolytic metabolism regulate dendritic cell activation. Blood 115, 4742. https://doi.org/10.1182/blood-2009-10-249540

Kubes, P., Jenne, C., 2018. Immune Responses in the Liver. Annu Rev Immunol 36, 247–277. https://doi.org/10.1146/annurev-immunol-051116-052415

Kumar, N., Mandal, C.C., 2021. Cholesterol-Lowering Drugs on Akt Signaling for Prevention of Tumorigenesis. Front Genet 12, 724149–724149. https://doi.org/10.3389/fgene.2021.724149

Kunk, P.R., Bauer, T.W., Slingluff, C.L., Rahma, O.E., 2016. From bench to bedside a comprehensive review of pancreatic cancer immunotherapy. Journal for ImmunoTherapy of Cancer 4, 14. https://doi.org/10.1186/s40425-016-0119-z

Kurata, Y., Shiraki, T., Ichinose, M., Kubota, K., Imai, Y., 2021. Effect and limitation of neoadjuvant chemotherapy for pancreatic ductal adenocarcinoma: consideration from a new perspective. World Journal of Surgical Oncology 19, 85. https://doi.org/10.1186/s12957-021-02192-8

Kwiterovich, P., 1998. The antiatherogenic role of high-density lipoprotein cholesterol. Am J Cardiol 82, 13Q-21Q. https://doi.org/10.1016/s0002-9149(98)00808-x

Labbé, D.P., Zadra, G., Yang, M., Reyes, J.M., Lin, C.Y., Cacciatore, S., Ebot, E.M., Creech, A.L., Giunchi, F., Fiorentino, M., Elfandy, H., Syamala, S., Karoly, E.D., Alshalalfa, M., Erho, N., Ross, A., Schaeffer, E.M., Gibb, E.A., Takhar, M., Den, R.B., Lehrer, J., Karnes, R.J., Freedland, S.J., Davicioni, E., Spratt, D.E., Ellis, L., Jaffe, J.D., D'Amico, A.V., Kantoff, P.W., Bradner, J.E., Mucci, L.A., Chavarro, J.E., Loda, M., Brown, M., 2019. High-fat diet fuels prostate cancer progression by rewiring the metabolome and amplifying the MYC program. Nature Communications 10, 4358. https://doi.org/10.1038/s41467-019-12298-z

Laffel, L., 1999. Ketone bodies: a review of physiology, pathophysiology and application of monitoring to diabetes. Diabetes/Metabolism Research and Reviews 15, 412–426. https://doi.org/10.1002/(SICI)1520-7560(199911/12)15:6<412::AID-DMRR72>3.0.CO;2-8

Lamiquiz-Moneo, I., Civeira, F., Gómez-Coronado, D., Blanco-Vaca, F., Villafuerte-Ledesma, H.M., Gil, M., Amigó, N., Mateo-Gallego, R., Cenarro, A., 2019. Lipid Profile Rather Than the LCAT Mutation Explains Renal Disease in Familial LCAT Deficiency. Journal of Clinical Medicine 8. https://doi.org/10.3390/jcm8111860

Laurenti, G., Tennant, D.A., 2016. Isocitrate dehydrogenase (IDH), succinate dehydrogenase (SDH), fumarate hydratase (FH): three players for one phenotype in cancer? Biochemical Society Transactions 44, 1111–1116. https://doi.org/10.1042/BST20160099

Lee, H.S., Leem, G., Kang, H., Jo, J.H., Chung, M.J., Jang, S.J., Yoon, D.H., Park, J.Y., Park, S.W., Song, S.Y., Bang, S., 2021. Peripheral natural killer cell activity is associated with poor clinical outcomes in pancreatic ductal adenocarcinoma. Journal of Gastroenterology and Hepatology 36, 516–522. https://doi.org/10.1111/jgh.15265

Lee, J., Lozano-Ruiz, B., Yang, F.M., Fan, D.D., Shen, L., González-Navajas, J.M., 2021. The Multifaceted Role of Th1, Th9, and Th17 Cells in Immune Checkpoint Inhibition Therapy. Front Immunol 12, 625667–625667. https://doi.org/10.3389/fimmu.2021.625667

Lee, J.-S., Oh, S.-J., Choi, H.-J., Kang, J.H., Lee, S.-H., Ha, J.S., Woo, S.M., Jang, H., Lee, H., Kim, S.-Y., 2020. ATP Production Relies on Fatty Acid Oxidation Rather than Glycolysis in Pancreatic Ductal Adenocarcinoma. Cancers (Basel) 12, 2477. https://doi.org/10.3390/cancers12092477

Lemmon, M.A., Schlessinger, J., 2010. Cell Signaling by Receptor Tyrosine Kinases. Cell 141, 1117–1134. https://doi.org/10.1016/j.cell.2010.06.011

Leone, R.D., Emens, L.A., 2018. Targeting adenosine for cancer immunotherapy. Journal for ImmunoTherapy of Cancer 6, 57. https://doi.org/10.1186/s40425-018-0360-8

Levitt, D.G., Levitt, M.D., 2014. Quantitative assessment of the multiple processes responsible for bilirubin homeostasis in health and disease. Clin Exp Gastroenterol 7, 307–328. https://doi.org/10.2147/CEG.S64283

Li, J., Cao, G., Ma, Q., Liu, H., Li, W., Han, L., 2012. The bidirectional interation between pancreatic cancer and diabetes. World J Surg Oncol 10, 171–171. https://doi.org/10.1186/1477-7819-10-171

Li, K.-Y., Yuan, J.-L., Trafton, D., Wang, J.-X., Niu, N., Yuan, C.-H., Liu, X.-B., Zheng, L., 2020. Pancreatic ductal adenocarcinoma immune microenvironment and

immunotherapy prospects. Chronic Dis Transl Med 6, 6–17. https://doi.org/10.1016/j.cdtm.2020.01.002
Li, M., Tan, S.-Y., Wang, X.-F., 2014. Paeonol exerts an anticancer effect on human colorectal cancer cells through inhibition of PGE_2 synthesis and COX-2 expression. Oncology reports 32, 2845–2853. https://doi.org/10.3892/or.2014.3543
Li, R., Wen, A., Lin, J., 2020. Pro-Inflammatory Cytokines in the Formation of the Pre-Metastatic Niche. Cancers 12. https://doi.org/10.3390/cancers12123752
Li, X., Wenes, M., Romero, P., Huang, S.C.-C., Fendt, S.-M., Ho, P.-C., 2019. Navigating metabolic pathways to enhance anti-tumour immunity and immunotherapy. Nature Reviews Clinical Oncology 16, 425–441. https://doi.org/10.1038/s41571-019-0203-7
Li, Y., Li, X., Liu, J., Wang, H., Fan, L., Li, J., Sun, G., 2018. PKM2, a potential target for regulating cancer. Gene 668, 48–53. https://doi.org/10.1016/j.gene.2018.05.038
Li, Y., Zhu, B., 2018. Editorial: Metabolism of Cancer Cells and Immune Cells in the Tumor Microenvironment. Front Immunol 9, 3080–3080. https://doi.org/10.3389/fimmu.2018.03080
Liang, Z.-W., Yu, J., Gu, D.-M., Liu, X.-M., Liu, J., Wu, M.-Y., Xu, M.-D., Shen, M., Duan, W., Li, W., 2022. M2-phenotype tumour-associated macrophages upregulate the expression of prognostic predictors MMP14 and INHBA in pancreatic cancer. Journal of Cellular and Molecular Medicine n/a. https://doi.org/10.1111/jcmm.17191
Liao, F., He, W., Jiang, C., Yin, C., Guo, G., Chen, X., Qiu, H., Rong, Y., Zhang, B., Xu, D., Xia, L., 2015. A high LDL-C to HDL-C ratio predicts poor prognosis for initially metastatic colorectal cancer patients with elevations in LDL-C. Onco Targets Ther 8, 3135–3142. https://doi.org/10.2147/OTT.S90479
Liermann, J., Shinoto, M., Syed, M., Debus, J., Herfarth, K., Naumann, P., 2020. Carbon ion radiotherapy in pancreatic cancer: A review of clinical data. Radiotherapy and Oncology 147, 145–150. https://doi.org/10.1016/j.radonc.2020.05.012
Lim, A.R., Rathmell, W.K., Rathmell, J.C., 2020. The tumor microenvironment as a metabolic barrier to effector T cells and immunotherapy. Elife 9. https://doi.org/10.7554/elife.55185
Lim, D.J., Sharma, Y., Thompson, C.H., 2018. Vitamin C and alcohol: a call to action. BMJ Nutr Prev Health 1, 17–22. https://doi.org/10.1136/bmjnph-2018-000010
Lim, S.A., Kim, J., Jeon, S., Shin, M.H., Kwon, J., Kim, T.-J., Im, K., Han, Y., Kwon, W., Kim, S.-W., Yee, C., Kim, S.-J., Jang, J.-Y., Lee, K.-M., 2019. Defective Localization With Impaired Tumor Cytotoxicity Contributes to the Immune Escape of NK Cells in Pancreatic Cancer Patients. Front Immunol 10, 496. https://doi.org/10.3389/fimmu.2019.00496
Lin, M., Liang, S., Wang, X., Liang, Y., Zhang, M., Chen, J., Niu, L., Xu, K., 2017. Percutaneous irreversible electroporation combined with allogeneic natural killer cell immunotherapy for patients with unresectable (stage III/IV) pancreatic cancer: a promising treatment. Journal of Cancer Research and Clinical Oncology 143, 2607–2618. https://doi.org/10.1007/s00432-017-2513-4
Lin, X., Zhan, B., Wen, S., Li, Z., Huang, H., Feng, J., 2016. Metabonomic alterations from pancreatic intraepithelial neoplasia to pancreatic ductal adenocarcinoma facilitate the identification of biomarkers in serum for early diagnosis of pancreatic cancer. Mol Biosyst 12, 2883–2892. https://doi.org/10.1039/c6mb00381h
Lippitz, B.E., 2013. Cytokine patterns in patients with cancer: a systematic review. The Lancet Oncology 14, e218–e228. https://doi.org/10.1016/S1470-2045(12)70582-X
Lisiecka, U., Kostro, K., 2016. Mechanisms of tumour escape from immune surveillance. Journal of Veterinary Research 60, 453–460. https://doi.org/10.1515/jvetres-2016-0068

Liu, C., Cheng, H., Luo, G., Lu, Y., Jin, K., Guo, M., Ni, Q., Yu, X., 2017. Circulating regulatory T cell subsets predict overall survival of patients with unresectable pancreatic cancer. Int J Oncol 51, 686–694. https://doi.org/10.3892/ijo.2017.4032

Liu, H., Huang, D., McArthur, D.L., Boros, L.G., Nissen, N., Heaney, A.P., 2010. Fructose Induces Transketolase Flux to Promote Pancreatic Cancer Growth. Cancer Res 70, 6368. https://doi.org/10.1158/0008-5472.CAN-09-4615

Liu, K., 2016. Dendritic Cells. Encyclopedia of Cell Biology 741–749. https://doi.org/10.1016/B978-0-12-394447-4.30111-0

Liu, L., Zhao, G., Wu, W., Rong, Y., Jin, D., Wang, D., Lou, W., Qin, X., 2016. Low intratumoral regulatory T cells and high peritumoral CD8(+) T cells relate to long-term survival in patients with pancreatic ductal adenocarcinoma after pancreatectomy. Cancer Immunol Immunother 65, 73–82. https://doi.org/10.1007/s00262-015-1775-4

Liu, W.-R., Tian, M.-X., Yang, L.-X., Lin, Y.-L., Jin, L., Ding, Z.-B., Shen, Y.-H., Peng, Y.-F., Gao, D.-M., Zhou, J., Qiu, S.-J., Dai, Z., He, R., Fan, J., Shi, Y.-H., 2015. PKM2 promotes metastasis by recruiting myeloid-derived suppressor cells and indicates poor prognosis for hepatocellular carcinoma. Oncotarget 6, 846–861. https://doi.org/10.18632/oncotarget.2749

Liu, Z., Kuang, W., Zhou, Q., Zhang, Y., 2018. TGF-β1 secreted by M2 phenotype macrophages enhances the stemness and migration of glioma cells via the SMAD2/3 signalling pathway. Int J Mol Med 42, 3395–3403. https://doi.org/10.3892/ijmm.2018.3923

Liu, Z., Zhou, T., Ziegler, A.C., Dimitrion, P., Zuo, L., 2017. Oxidative Stress in Neurodegenerative Diseases: From Molecular Mechanisms to Clinical Applications. Oxidative Medicine and Cellular Longevity 2017, 2525967. https://doi.org/10.1155/2017/2525967

Lochner, M., Berod, L., Sparwasser, T., 2015. Fatty acid metabolism in the regulation of T cell function. Trends in Immunology 36, 81–91. https://doi.org/10.1016/j.it.2014.12.005

Longo, V., Tamma, R., Brunetti, O., Pisconti, S., Argentiero, A., Silvestris, N., Ribatti, D., 2018. Mast cells and angiogenesis in pancreatic ductal adenocarcinoma. Clinical and Experimental Medicine 18, 319–323. https://doi.org/10.1007/s10238-018-0493-6

Lu, C., Thompson, C.B., 2012. Metabolic Regulation of Epigenetics. Cell Metabolism 16, 9–17. https://doi.org/10.1016/j.cmet.2012.06.001

Lusczek, E.R., Paulo, J.A., Saltzman, J.R., Kadiyala, V., Banks, P.A., Beilman, G., Conwell, D.L., 2013. Urinary 1H-NMR metabolomics can distinguish pancreatitis patients from healthy controls. JOP : Journal of the pancreas 14, 161–170. https://doi.org/10.6092/1590-8577/1294

Ma, Y., Wang, W., Idowu, M.O., Oh, U., Wang, X.-Y., Temkin, S.M., Fang, X., 2019. Ovarian Cancer Relies on Glucose Transporter 1 to Fuel Glycolysis and Growth: Anti-Tumor Activity of BAY-876. Cancers 11. https://doi.org/10.3390/cancers11010033

Macášek, J., Vecka, M., Žák, A., Urbánek, M., Krechler, T., Petruželka, L., Staňková, B., Zeman, M., 2012. Plasma fatty acid composition in patients with pancreatic cancer: correlations to clinical parameters. Nutrition and cancer 64, 946–955. https://doi.org/10.1080/01635581.2012.716138

Macintyre, A.N., Gerriets, V.A., Nichols, A.G., Michalek, R.D., Rudolph, M.C., Deoliveira, D., Anderson, S.M., Abel, E.D., Chen, B.J., Hale, L.P., Rathmell, J.C., 2014a. The Glucose Transporter Glut1 Is Selectively Essential for CD4 T Cell Activation and Effector Function. Cell Metabolism 20, 61–72. https://doi.org/10.1016/j.cmet.2014.05.004

Macintyre, A.N., Gerriets, V.A., Nichols, A.G., Michalek, R.D., Rudolph, M.C., Deoliveira, D., Anderson, S.M., Abel, E.D., Chen, B.J., Hale, L.P., Rathmell, J.C., 2014b. The

Glucose Transporter Glut1 Is Selectively Essential for CD4 T Cell Activation and Effector Function. Cell Metabolism 20, 61–72. https://doi.org/10.1016/j.cmet.2014.05.004
Mackey, J.B.G., Coffelt, S.B., Carlin, L.M., 2019. Neutrophil Maturity in Cancer. Front Immunol 10, 1912–1912. https://doi.org/10.3389/fimmu.2019.01912
Magura, L., Blanchard, R., Hope, B., Beal, J.R., Schwartz, G.G., Sahmoun, A.E., 2008. Hypercholesterolemia and prostate cancer: a hospital-based case–control study. Cancer Causes & Control 19, 1259–1266. https://doi.org/10.1007/s10552-008-9197-7
Mallol, R., Amigó, N., Rodríguez, M.A., Heras, M., Vinaixa, M., Plana, N., Rock, E., Ribalta, J., Yanes, O., Masana, L., Correig, X., 2015. Liposcale: a novel advanced lipoprotein test based on 2D diffusion-ordered 1H NMR spectroscopy. J Lipid Res 56, 737–746. https://doi.org/10.1194/jlr.D050120
Malvezzi, M., Carioli, G., Bertuccio, P., Rosso, T., Boffetta, P., Levi, F., La Vecchia, C., Negri, E., 2016. European cancer mortality predictions for the year 2016 with focus on leukaemias. Annals of Oncology 27, 725–731. https://doi.org/10.1093/annonc/mdw022
Mao, X., Xu, J., Wang, W., Liang, C., Hua, J., Liu, J., Zhang, B., Meng, Q., Yu, X., Shi, S., 2021. Crosstalk between cancer-associated fibroblasts and immune cells in the tumor microenvironment: new findings and future perspectives. Molecular Cancer 20, 131. https://doi.org/10.1186/s12943-021-01428-1
Mao, Z., Zhang, W., 2018. Role of mTOR in Glucose and Lipid Metabolism. International Journal of Molecular Sciences 19. https://doi.org/10.3390/ijms19072043
Marcon, F., Zuo, J., Pearce, H., Nicol, S., Margielewska-Davies, S., Farhat, M., Mahon, B., Middleton, G., Brown, R., Roberts, K.J., Moss, P., 2020. NK cells in pancreatic cancer demonstrate impaired cytotoxicity and a regulatory IL-10 phenotype. null 9, 1845424. https://doi.org/10.1080/2162402X.2020.1845424
Marshall, I., Higinbotham, J., Bruce, S., Freise, A., 1997. Use of voigt lineshape for quantification of in vivo 1H spectra. Magnetic Resonance in Medicine 37, 651–657. https://doi.org/10.1002/mrm.1910370504
Martinez-Bosch, N., Vinaixa, J., Navarro, P., 2018a. Immune Evasion in Pancreatic Cancer: From Mechanisms to Therapy. Cancers 10. https://doi.org/10.3390/cancers10010006
Martinez-Bosch, N., Vinaixa, J., Navarro, P., 2018b. Immune Evasion in Pancreatic Cancer: From Mechanisms to Therapy. Cancers 10. https://doi.org/10.3390/cancers10010006
Martínez-Reyes, I., Chandel, N.S., 2020. Mitochondrial TCA cycle metabolites control physiology and disease. Nature Communications 11, 102. https://doi.org/10.1038/s41467-019-13668-3
Martinez-Useros, J., Li, W., Cabeza-Morales, M., Garcia-Foncillas, J., 2017a. Oxidative Stress: A New Target for Pancreatic Cancer Prognosis and Treatment. J Clin Med 6, 29. https://doi.org/10.3390/jcm6030029
Martinez-Useros, J., Li, W., Cabeza-Morales, M., Garcia-Foncillas, J., 2017b. Oxidative Stress: A New Target for Pancreatic Cancer Prognosis and Treatment. J Clin Med 6, 29. https://doi.org/10.3390/jcm6030029
Mas, L., Schwarz, L., Bachet, J.-B., 2020. Adjuvant chemotherapy in pancreatic cancer: state of the art and future perspectives. Current Opinion in Oncology 32.
Masugi, Y., Abe, T., Ueno, A., Fujii-Nishimura, Y., Ojima, H., Endo, Y., Fujita, Y., Kitago, M., Shinoda, M., Kitagawa, Y., Sakamoto, M., 2019. Characterization of spatial distribution of tumor-infiltrating CD8+ T cells refines their prognostic utility for pancreatic cancer survival. Modern Pathology 32, 1495–1507. https://doi.org/10.1038/s41379-019-0291-z

Matilla, A.J., 2021. Cellular oxidative stress in programmed cell death: focusing on chloroplastic 1O2 and mitochondrial cytochrome-c release. Journal of Plant Research 134, 179–194. https://doi.org/10.1007/s10265-021-01259-7

Mayers, J.R., Wu, C., Clish, C.B., Kraft, P., Torrence, M.E., Fiske, B.P., Yuan, C., Bao, Y., Townsend, M.K., Tworoger, S.S., Davidson, S.M., Papagiannakopoulos, T., Yang, A., Dayton, T.L., Ogino, S., Stampfer, M.J., Giovannucci, E.L., Qian, Z.R., Rubinson, D.A., Ma, J., Sesso, H.D., Gaziano, J.M., Cochrane, B.B., Liu, S., Wactawski-Wende, J., Manson, J.E., Pollak, M.N., Kimmelman, A.C., Souza, A., Pierce, K., Wang, T.J., Gerszten, R.E., Fuchs, C.S., Vander Heiden, M.G., Wolpin, B.M., 2014. Elevation of circulating branched-chain amino acids is an early event in human pancreatic adenocarcinoma development. Nature Medicine 20, 1193–1198. https://doi.org/10.1038/nm.3686

McDonald, O.G., Li, X., Saunders, T., Tryggvadottir, R., Mentch, S.J., Warmoes, M.O., Word, A.E., Carrer, A., Salz, T.H., Natsume, S., Stauffer, K.M., Makohon-Moore, A., Zhong, Y., Wu, H., Wellen, K.E., Locasale, J.W., Iacobuzio-Donahue, C.A., Feinberg, A.P., 2017. Epigenomic reprogramming during pancreatic cancer progression links anabolic glucose metabolism to distant metastasis. Nature Genetics 49, 367–376. https://doi.org/10.1038/ng.3753

McGuigan, A., Kelly, P., Turkington, R.C., Jones, C., Coleman, H.G., McCain, R.S., 2018. Pancreatic cancer: A review of clinical diagnosis, epidemiology, treatment and outcomes. World J Gastroenterol 24, 4846–4861. https://doi.org/10.3748/wjg.v24.i43.4846

McKinnon, K.M., 2018. Flow Cytometry: An Overview. Curr Protoc Immunol 120, 5.1.1-5.1.11. https://doi.org/10.1002/cpim.40

McMillan, D.C., 2013. The systemic inflammation-based Glasgow Prognostic Score: A decade of experience in patients with cancer. Cancer Treatment Reviews 39, 534–540. https://doi.org/10.1016/j.ctrv.2012.08.003

Mehta, K.Y., Wu, H.-J., Menon, S.S., Fallah, Y., Zhong, X., Rizk, N., Unger, K., Mapstone, M., Fiandaca, M.S., Federoff, H.J., Cheema, A.K., 2017. Metabolomic biomarkers of pancreatic cancer: a meta-analysis study. Oncotarget 8, 68899–68915. https://doi.org/10.18632/oncotarget.20324

Méndez-Sánchez, N., Vítek, L., Aguilar-Olivos, N.E., Uribe, M., 2017. Bilirubin as a Biomarker in Liver Disease, in: Patel, V.B., Preedy, V.R. (Eds.), Biomarkers in Liver Disease. Springer Netherlands, Dordrecht, pp. 281–304. https://doi.org/10.1007/978-94-007-7675-3_25

Mentch, S.J., Locasale, J.W., 2016. One-carbon metabolism and epigenetics: understanding the specificity. Ann N Y Acad Sci 1363, 91–98. https://doi.org/10.1111/nyas.12956

Michalek, R.D., Gerriets, V.A., Jacobs, S.R., Macintyre, A.N., MacIver, N.J., Mason, E.F., Sullivan, S.A., Nichols, A.G., Rathmell, J.C., 2011a. Cutting Edge: Distinct Glycolytic and Lipid Oxidative Metabolic Programs Are Essential for Effector and Regulatory $CD4^+$ T Cell Subsets. J. Immunol. 186, 3299. https://doi.org/10.4049/jimmunol.1003613

Michalek, R.D., Gerriets, V.A., Jacobs, S.R., Macintyre, A.N., MacIver, N.J., Mason, E.F., Sullivan, S.A., Nichols, A.G., Rathmell, J.C., 2011b. Cutting Edge: Distinct Glycolytic and Lipid Oxidative Metabolic Programs Are Essential for Effector and Regulatory $CD4^+$ T Cell Subsets. J. Immunol. 186, 3299. https://doi.org/10.4049/jimmunol.1003613

Michálková, L., Horník, Š., Sýkora, J., Habartová, L., Setnička, V., 2018. Diagnosis of pancreatic cancer via ^{1}H NMR metabolomics of human plasma. Analyst 143, 5974–5978. https://doi.org/10.1039/c8an01310a

Michálková, L., Horník, Š., Sýkora, J., Habartová, L., Setnička, V., Bunganič, B., 2021. Early Detection of Pancreatic Cancer in Type 2 Diabetes Mellitus Patients Based on 1H NMR Metabolomics. J. Proteome Res. 20, 1744–1753. https://doi.org/10.1021/acs.jproteome.0c00990

Mielgo, A., Schmid, M.C., 2013. Impact of tumour associated macrophages in pancreatic cancer. BMB Rep 46, 131–138. https://doi.org/10.5483/bmbrep.2013.46.3.036

Mills, E.L., O'Neill, L.A., 2016. Reprogramming mitochondrial metabolism in macrophages as an anti-inflammatory signal. European Journal of Immunology 46, 13–21. https://doi.org/10.1002/eji.201445427

Miyazawa, M., Katsuda, M., Kawai, M., Hirono, S., Okada, K., Kitahata, Y., Yamaue, H., 2021. Advances in immunotherapy for pancreatic ductal adenocarcinoma. Journal of Hepato-Biliary-Pancreatic Sciences 28, 419–430. https://doi.org/10.1002/jhbp.944

Mizrahi, J.D., Surana, R., Valle, J.W., Shroff, R.T., 2020. Pancreatic cancer. The Lancet 395, 2008–2020. https://doi.org/10.1016/S0140-6736(20)30974-0

Mohammad, G.H., Olde Damink, S.W.M., Malago, M., Dhar, D.K., Pereira, S.P., 2016a. Pyruvate Kinase M2 and Lactate Dehydrogenase A Are Overexpressed in Pancreatic Cancer and Correlate with Poor Outcome. PLoS One 11, e0151635–e0151635. https://doi.org/10.1371/journal.pone.0151635

Mohammad, G.H., Olde Damink, S.W.M., Malago, M., Dhar, D.K., Pereira, S.P., 2016b. Pyruvate Kinase M2 and Lactate Dehydrogenase A Are Overexpressed in Pancreatic Cancer and Correlate with Poor Outcome. PLoS One 11, e0151635–e0151635. https://doi.org/10.1371/journal.pone.0151635

Mohelnikova-Duchonova, B., Oliverius, M., Honsova, E., Soucek, P., 2012. Evaluation of reference genes and normalization strategy for quantitative real-time PCR in human pancreatic carcinoma. Dis Markers 32, 203–210. https://doi.org/10.3233/dma-2011-0875

Molina, M.A., Sitja-Arnau, M., Lemoine, M.G., Frazier, M.L., Sinicrope, F.A., 1999. Increased cyclooxygenase-2 expression in human pancreatic carcinomas and cell lines: growth inhibition by nonsteroidal anti-inflammatory drugs. Cancer Res 59.

Moore, H.B., Culp-Hill, R., Reisz, J.A., Lawson, P.J., Sauaia, A., Schulick, R.D., Del Chiaro, M., Nydam, T.L., Moore, E.E., Hansen, K.C., D'Alessandro, A., 2019. The metabolic time line of pancreatic cancer: Opportunities to improve early detection of adenocarcinoma. The American Journal of Surgery 218, 1206–1212. https://doi.org/10.1016/j.amjsurg.2019.08.015

Muñiz, N., 1977. Measurement of plasma lipoproteins by electrophoresis on polyacrylamide gel. Clin Chem 23, 1826–1833.

Muronetz, V.I., Melnikova, A.K., Saso, L., Schmalhausen, E.V., 2020. Influence of Oxidative Stress on Catalytic and Non-glycolytic Functions of Glyceraldehyde-3-phosphate Dehydrogenase. Curr Med Chem 27, 2040–2058. https://doi.org/10.2174/0929867325666180530101057

Murray, P.J., Allen, J.E., Biswas, S.K., Fisher, E.A., Gilroy, D.W., Goerdt, S., Gordon, S., Hamilton, J.A., Ivashkiv, L.B., Lawrence, T., Locati, M., Mantovani, A., Martinez, F.O., Mege, J.-L., Mosser, D.M., Natoli, G., Saeij, J.P., Schultze, J.L., Shirey, K.A., Sica, A., Suttles, J., Udalova, I., van Ginderachter, J.A., Vogel, S.N., Wynn, T.A., 2014. Macrophage Activation and Polarization: Nomenclature and Experimental Guidelines. Immunity 41, 14–20. https://doi.org/10.1016/j.immuni.2014.06.008

Naito, Y., Saito, K., Shiiba, K., Ohuchi, A., Saigenji, K., Nagura, H., Ohtani, H., 1998. $CD8^+$ T Cells Infiltrated within Cancer Cell Nests as a Prognostic Factor in Human Colorectal Cancer. Cancer Res 58, 3491.

Nakchbandi, I.A., Löhr, J.-M., 2008. Coagulation, anticoagulation and pancreatic carcinoma. Nature Clinical Practice Gastroenterology & Hepatology 5, 445–455. https://doi.org/10.1038/ncpgasthep1184

Nandi, A., Yan, L.-J., Jana, C.K., Das, N., 2019. Role of Catalase in Oxidative Stress- and Age-Associated Degenerative Diseases. Oxidative Medicine and Cellular Longevity 2019, 9613090. https://doi.org/10.1155/2019/9613090

Natsuizaka, M., Ozasa, M., Darmanin, S., Miyamoto, M., Kondo, S., Kamada, S., Shindoh, M., Higashino, F., Suhara, W., Koide, H., Aita, K., Nakagawa, K., Kondo, T., Asaka, M., Okada, F., Kobayashi, M., 2007. Synergistic up-regulation of Hexokinase-2, glucose transporters and angiogenic factors in pancreatic cancer cells by glucose deprivation and hypoxia. Experimental Cell Research 313, 3337–3348. https://doi.org/10.1016/j.yexcr.2007.06.013

Nogueira, V., Hay, N., 2013. Molecular Pathways: Reactive Oxygen Species Homeostasis in Cancer Cells and Implications for Cancer Therapy. Clin Cancer Res 19, 4309. https://doi.org/10.1158/1078-0432.CCR-12-1424

Nonnenmacher, Y., Hiller, K., 2018. Biochemistry of proinflammatory macrophage activation. Cellular and Molecular Life Sciences 75, 2093–2109. https://doi.org/10.1007/s00018-018-2784-1

Nordmann, T.M., Dror, E., Schulze, F., Traub, S., Berishvili, E., Barbieux, C., Böni-Schnetzler, M., Donath, M.Y., 2017. The Role of Inflammation in β-cell Dedifferentiation. Scientific Reports 7, 6285. https://doi.org/10.1038/s41598-017-06731-w

Notarstefano, V., Sabbatini, S., Conti, C., Pisani, M., Astolfi, P., Pro, C., Rubini, C., Vaccari, L., Giorgini, E., 2020. Investigation of human pancreatic cancer tissues by Fourier Transform Infrared Hyperspectral Imaging. Journal of Biophotonics 13, e201960071. https://doi.org/10.1002/jbio.201960071

Nzeako, U.C., Gores, G.J., 2002. Increased expression of cyclooxygenase-2 in human pancreatic neoplasms and potential for chemoprevention by cyclooxygenase inhibitors. Cancer 94. https://doi.org/10.1002/cncr.10409

Oberkampf, M., Guillerey, C., Mouriès, J., Rosenbaum, P., Fayolle, C., Bobard, A., Savina, A., Ogier-Denis, E., Enninga, J., Amigorena, S., Leclerc, C., Dadaglio, G., 2018. Mitochondrial reactive oxygen species regulate the induction of CD8(+) T cells by plasmacytoid dendritic cells. Nat Commun 9, 2241–2241. https://doi.org/10.1038/s41467-018-04686-8

Ochi, A., Nguyen, A.H., Bedrosian, A.S., Mushlin, H.M., Zarbakhsh, S., Barilla, R., Zambirinis, C.P., Fallon, N.C., Rehman, A., Pylayeva-Gupta, Y., Badar, S., Hajdu, C.H., Frey, A.B., Bar-Sagi, D., Miller, G., 2012. MyD88 inhibition amplifies dendritic cell capacity to promote pancreatic carcinogenesis via Th2 cells. Journal of Experimental Medicine 209, 1671–1687. https://doi.org/10.1084/jem.20111706

Odegaard, J.I., Chawla, A., 2013. The Immune System as a Sensor of the Metabolic State. Immunity 38, 644–654. https://doi.org/10.1016/j.immuni.2013.04.001

O'Donnell, J.S., Massi, D., Teng, M.W.L., Mandala, M., 2018. PI3K-AKT-mTOR inhibition in cancer immunotherapy, redux. Seminars in Cancer Biology 48, 91–103. https://doi.org/10.1016/j.semcancer.2017.04.015

Olesen, S.S., Poulsen, J.L., Novovic, S., Nøjgaard, C., Kalaitzakis, E., Jensen, N.M., Engjom, T., Tjora, E., Waage, A., Hauge, T., Haas, S.L., Vujasinovic, M., Barauskas, G., Pukitis, A., Ozola-Zālīte, I., Okhlobystin, A., Parhiala, M., Laukkarinen, J., Drewes, A.M., 2020. Multiple risk factors for diabetes mellitus in patients with chronic pancreatitis: A multicentre study of 1117 cases. United European Gastroenterol J 8, 453–461. https://doi.org/10.1177/2050640620901973

O'Neill, L.A.J., Kishton, R.J., Rathmell, J., 2016a. A guide to immunometabolism for immunologists. Nature Reviews Immunology 16, 553.
O'Neill, L.A.J., Kishton, R.J., Rathmell, J., 2016b. A guide to immunometabolism for immunologists. Nature Reviews Immunology 16, 553.
Ostrand-Rosenberg, S., 2010. Myeloid-derived suppressor cells: more mechanisms for inhibiting anti-tumor immunity. Cancer Immunology, Immunotherapy 59, 1593–1600. https://doi.org/10.1007/s00262-010-0855-8
O'Sullivan, D., van der Windt, G.J.W., Huang, S.C.-C., Curtis, J.D., Chang, C.-H., Buck, M.D., Qiu, J., Smith, A.M., Lam, W.Y., DiPlato, L.M., Hsu, F.-F., Birnbaum, M.J., Pearce, E.J., Pearce, E.L., 2014a. Memory CD8+ T Cells Use Cell-Intrinsic Lipolysis to Support the Metabolic Programming Necessary for Development. Immunity 41, 75–88. https://doi.org/10.1016/j.immuni.2014.06.005
O'Sullivan, D., van der Windt, G.J.W., Huang, S.C.-C., Curtis, J.D., Chang, C.-H., Buck, M.D., Qiu, J., Smith, A.M., Lam, W.Y., DiPlato, L.M., Hsu, F.-F., Birnbaum, M.J., Pearce, E.J., Pearce, E.L., 2014b. Memory CD8+ T Cells Use Cell-Intrinsic Lipolysis to Support the Metabolic Programming Necessary for Development. Immunity 41, 75–88. https://doi.org/10.1016/j.immuni.2014.06.005
Otto, L., Rahn, S., Daunke, T., Walter, F., Winter, E., Möller, J.L., Rose-John, S., Wesch, D., Schäfer, H., Sebens, S., 2021. Initiation of Pancreatic Cancer: The Interplay of Hyperglycemia and Macrophages Promotes the Acquisition of Malignancy-Associated Properties in Pancreatic Ductal Epithelial Cells. International Journal of Molecular Sciences 22. https://doi.org/10.3390/ijms22105086
Otvos, J.D., Shalaurova, I., Wolak-Dinsmore, J., Connelly, M.A., Mackey, R.H., Stein, J.H., Tracy, R.P., 2015. GlycA: A Composite Nuclear Magnetic Resonance Biomarker of Systemic Inflammation. Clinical Chemistry 61, 714–723. https://doi.org/10.1373/clinchem.2014.232918
OuYang, D., Xu, J., Huang, H., Chen, Z., 2011. Metabolomic Profiling of Serum from Human Pancreatic Cancer Patients Using 1H NMR Spectroscopy and Principal Component Analysis. Applied Biochemistry and Biotechnology 165, 148–154. https://doi.org/10.1007/s12010-011-9240-0
Padoan, A., Plebani, M., Basso, D., 2019. Inflammation and Pancreatic Cancer: Focus on Metabolism, Cytokines, and Immunity. International Journal of Molecular Sciences 20. https://doi.org/10.3390/ijms20030676
Palmer, C.S., Ostrowski, M., Balderson, B., Christian, N., Crowe, S.M., 2015. Glucose Metabolism Regulates T Cell Activation, Differentiation, and Functions. Frontiers in Immunology 6, 1. https://doi.org/10.3389/fimmu.2015.00001
Palsson-McDermott, E.M., Curtis, A.M., Goel, G., Lauterbach, M.A.R., Sheedy, F.J., Gleeson, L.E., van den Bosch, M.W.M., Quinn, S.R., Domingo-Fernandez, R., Johnston, D.G.W., Jiang, J., Israelsen, W.J., Keane, J., Thomas, C., Clish, C., Vander Heiden, M., Xavier, R.J., O'Neill, L.A.J., 2015. Pyruvate Kinase M2 Regulates Hif-1α Activity and IL-1β Induction and Is a Critical Determinant of the Warburg Effect in LPS-Activated Macrophages. Cell Metabolism 21, 65–80. https://doi.org/10.1016/j.cmet.2014.12.005
Pan, S., Fan, M., Liu, Z., Li, X., Wang, H., 2021. Serine, glycine and one-carbon metabolism in cancer (Review). Int J Oncol 58, 158–170. https://doi.org/10.3892/ijo.2020.5158
Pandol, S.J., Apte, M.V., Wilson, J.S., Gukovskaya, A.S., Edderkaoui, M., 2012. The burning question: Why is smoking a risk factor for pancreatic cancer? Pancreatology 12, 344–349. https://doi.org/10.1016/j.pan.2012.06.002
Pannala, R., Basu, A., Petersen, G.M., Chari, S.T., 2009. New-onset diabetes: a potential clue to the early diagnosis of pancreatic cancer. The Lancet Oncology 10, 88–95. https://doi.org/10.1016/S1470-2045(08)70337-1

Panni, R.Z., Sanford, D.E., Belt, B.A., Mitchem, J.B., Worley, L.A., Goetz, B.D., Mukherjee, P., Wang-Gillam, A., Link, D.C., Denardo, D.G., Goedegebuure, S.P., Linehan, D.C., 2014. Tumor-induced STAT3 activation in monocytic myeloid-derived suppressor cells enhances stemness and mesenchymal properties in human pancreatic cancer. Cancer Immunol Immunother 63, 513–528. https://doi.org/10.1007/s00262-014-1527-x

Park, H.J., Choi, Y.J., Lee, J.H., Nam, M.J., 2017. Naringenin causes ASK1-induced apoptosis via reactive oxygen species in human pancreatic cancer cells. Food and Chemical Toxicology 99, 1–8. https://doi.org/10.1016/j.fct.2016.11.008

Park, S., Ahn, S., Shin, Y., Yang, Y., Yeom, C.H., 2018. Vitamin C in Cancer: A Metabolomics Perspective. Front Physiol 9, 762. https://doi.org/10.3389/fphys.2018.00762

Pasanen, P., Pikkarainen, P., Alhava, E., Partanen, K., Penttilä, I., 1993. Value of serum alkaline phosphatase, aminotransferases, gamma-glutamyl transferase, leucine aminopeptidase, and bilirubin in the distinction between benign and malignant diseases causing jaundice and cholestasis: Results from a prospective study. null 53, 35–39. https://doi.org/10.3109/00365519309092529

Patel, K.K., Kashfi, K., 2022. Lipoproteins and cancer: The role of HDL-C, LDL-C, and cholesterol-lowering drugs. Biochemical Pharmacology 196, 114654. https://doi.org/10.1016/j.bcp.2021.114654

Pathria, P., Louis, T.L., Varner, J.A., 2019. Targeting Tumor-Associated Macrophages in Cancer. Trends in Immunology 40, 310–327. https://doi.org/10.1016/j.it.2019.02.003

Patra, K.C., Hay, N., 2014. The pentose phosphate pathway and cancer. Trends Biochem Sci 39, 347–354. https://doi.org/10.1016/j.tibs.2014.06.005

Patsoukis, N., Bardhan, K., Chatterjee, P., Sari, D., Liu, B., Bell, L.N., Karoly, E.D., Freeman, G.J., Petkova, V., Seth, P., Li, L., Boussiotis, V.A., 2015. PD-1 alters T-cell metabolic reprogramming by inhibiting glycolysis and promoting lipolysis and fatty acid oxidation. Nature Communications 6, 6692. https://doi.org/10.1038/ncomms7692

Paul, S., Lal, G., 2017. The Molecular Mechanism of Natural Killer Cells Function and Its Importance in Cancer Immunotherapy. Front Immunol 8, 1124–1124. https://doi.org/10.3389/fimmu.2017.01124

Pearce, E.J., Pearce, E.L., 2017. Driving immunity: all roads lead to metabolism. Nature Reviews Immunology 18, 81.

Pereira, S.P., Oldfield, L., Ney, A., Hart, P.A., Keane, M.G., Pandol, S.J., Li, D., Greenhalf, W., Jeon, C.Y., Koay, E.J., Almario, C.V., Halloran, C., Lennon, A.M., Costello, E., 2020. Early detection of pancreatic cancer. Lancet Gastroenterol Hepatol 5, 698–710. https://doi.org/10.1016/s2468-1253(19)30416-9

Pergamo, M., Miller, G., 2017. Myeloid-derived suppressor cells and their role in pancreatic cancer. Cancer Gene Therapy 24, 100–105. https://doi.org/10.1038/cgt.2016.65

Phatlhane, D.V., Zemlin, A.E., 2015. Severe hypercholesterolemia mediated by lipoprotein X in a patient with cholestasis. Ann Hepatol 14, 924–928. https://doi.org/10.5604/16652681.1171785

Philip, P.A., Buyse, M.E., Alistar, A.T., Rocha Lima, C.M.S.P., Luther, S., Pardee, T.S., Van Cutsem, E., 2019. Avenger 500, a phase III open-label randomized trial of the combination of CPI-613 with modified FOLFIRINOX (mFFX) versus FOLFIRINOX (FFX) in patients with metastatic adenocarcinoma of the pancreas. JCO 37, TPS479–TPS479. https://doi.org/10.1200/JCO.2019.37.4_suppl.TPS479

Pilotte, L., Larrieu, P., Stroobant, V., Colau, D., Dolušić, E., Frédérick, R., De Plaen, E., Uyttenhove, C., Wouters, J., Masereel, B., Van den Eynde, B.J., 2012. Reversal of tumoral immune resistance by inhibition of tryptophan 2,3-dioxygenase. Proc Natl Acad Sci USA 109, 2497. https://doi.org/10.1073/pnas.1113873109

Polireddy, K., Chen, Q., 2016. Cancer of the Pancreas: Molecular Pathways and Current Advancement in Treatment. J Cancer 7, 1497–1514. https://doi.org/10.7150/jca.14922

Polireddy, K., Dong, R., Reed, G., Yu, J., Chen, P., Williamson, S., Violet, P.-C., Pessetto, Z., Godwin, A.K., Fan, F., Levine, M., Drisko, J.A., Chen, Q., 2017. High Dose Parenteral Ascorbate Inhibited Pancreatic Cancer Growth and Metastasis: Mechanisms and a Phase I/IIa study. Scientific Reports 7, 17188. https://doi.org/10.1038/s41598-017-17568-8

Porta, M., Fabregat, X., Malats, N., Guarner, L., Carrato, A., de Miguel, A., Ruiz, L., Jariod, M., Costafreda, S., Coll, S., Alguacil, J., Corominas, J.M., Solà, R., Salas, A., Real, F.X., the PANKRAS II Study Group, 2005. Exocrine pancreatic cancer: Symptoms at presentation and their relation to tumour site and stage. Clinical and Translational Oncology 7, 189–197. https://doi.org/10.1007/BF02712816

Poruk, K.E., Firpo, M.A., Adler, D.G., Mulvihill, S.J., 2013. Screening for pancreatic cancer: why, how, and who? Ann Surg 257, 17–26. https://doi.org/10.1097/SLA.0b013e31825ffbfb

Previte, D.M., O'Connor, E.C., Novak, E.A., Martins, C.P., Mollen, K.P., Piganelli, J.D., 2017. Reactive oxygen species are required for driving efficient and sustained aerobic glycolysis during CD4+ T cell activation. PLoS One 12, e0175549. https://doi.org/10.1371/journal.pone.0175549

Ravetch, J.V., Perussia, B., 1989. Alternative membrane forms of Fc gamma RIII(CD16) on human natural killer cells and neutrophils. Cell type-specific expression of two genes that differ in single nucleotide substitutions. Journal of Experimental Medicine 170, 481–497. https://doi.org/10.1084/jem.170.2.481

Rawla, P., Sunkara, T., Gaduputi, V., 2019. Epidemiology of Pancreatic Cancer: Global Trends, Etiology and Risk Factors. World J Oncol 10, 10–27. https://doi.org/10.14740/wjon1166

Rayward-smith, V.J., R., A.P. ;Richards, G.;. de la Iglesia, B.;, 2006. Clustering Rules: A Comparison of Partitioning and Hierarchical Clustering Algorithms. J. Math. Model. Algorithms Vol. 5, 475–504. https://doi.org/DOI:10.1007/s10852-005-9022-1

Reyes-Castellanos, G., Masoud, R., Carrier, A., 2020. Mitochondrial Metabolism in PDAC: From Better Knowledge to New Targeting Strategies. Biomedicines 8. https://doi.org/10.3390/biomedicines8080270

Rhee, I., 2016. Diverse macrophages polarization in tumor microenvironment. Archives of Pharmacal Research 39, 1588–1596. https://doi.org/10.1007/s12272-016-0820-y

Ribatti, D., 2016. Mast cells as therapeutic target in cancer. European Journal of Pharmacology 778, 152–157. https://doi.org/10.1016/j.ejphar.2015.02.056

Rodrigues dos Santos, C., Fonseca, I., Dias, S., Mendes de Almeida, J., 2014. Plasma level of LDL-cholesterol at diagnosis is a predictor factor of breast tumor progression. BMC Cancer 14, 132. https://doi.org/10.1186/1471-2407-14-132

Rodríguez-Espinosa, O., Rojas-Espinosa, O., Moreno-Altamirano, M.M.B., López-Villegas, E.O., Sánchez-García, F.J., 2015. Metabolic requirements for neutrophil extracellular traps formation. Immunology 145, 213–224. https://doi.org/10.1111/imm.12437

Rodríguez-Prados, J.-C., Través, P.G., Cuenca, J., Rico, D., Aragonés, J., Martín-Sanz, P., Cascante, M., Boscá, L., 2010. Substrate Fate in Activated Macrophages: A Comparison between Innate, Classic, and Alternative Activation. J. Immunol. 185, 605. https://doi.org/10.4049/jimmunol.0901698

Rousseeuw, P.J., 1987. Silhouettes: A graphical aid to the interpretation and validation of cluster analysis. Journal of Computational and Applied Mathematics 20, 53–65. https://doi.org/10.1016/0377-0427(87)90125-7

Ryan, D.P., Hong, T.S., Bardeesy, N., 2014. Pancreatic Adenocarcinoma. N Engl J Med 371, 1039–1049. https://doi.org/10.1056/NEJMra1404198

Sah, R.P., Sharma, Ayush, Nagpal, S., Patlolla, S.H., Sharma, Anil, Kandlakunta, H., Anani, V., Angom, R.S., Kamboj, A.K., Ahmed, N., Mohapatra, S., Vivekanandhan, S., Philbrick, K.A., Weston, A., Takahashi, N., Kirkland, J., Javeed, N., Matveyenko, A., Levy, M.J., Mukhopadhyay, D., Chari, S.T., 2019. Phases of Metabolic and Soft Tissue Changes in Months Preceding a Diagnosis of Pancreatic Ductal Adenocarcinoma. Gastroenterology 156, 1742–1752. https://doi.org/10.1053/j.gastro.2019.01.039

Saka, D., Gökalp, M., Piyade, B., Cevik, N.C., Arik Sever, E., Unutmaz, D., Ceyhan, G.O., Demir, I.E., Asimgil, H., 2020. Mechanisms of T-Cell Exhaustion in Pancreatic Cancer. Cancers 12. https://doi.org/10.3390/cancers12082274

Sakaguchi, S., Miyara, M., Costantino, C.M., Hafler, D.A., 2010. FOXP3+ regulatory T cells in the human immune system. Nature Reviews Immunology 10, 490–500. https://doi.org/10.1038/nri2785

Sarantis, P., Koustas, E., Papadimitropoulou, A., Papavassiliou, A.G., Karamouzis, M.V., 2020. Pancreatic ductal adenocarcinoma: Treatment hurdles, tumor microenvironment and immunotherapy. World J Gastrointest Oncol 12, 173–181. https://doi.org/10.4251/wjgo.v12.i2.173

Saravia, J., Chapman, N.M., Chi, H., 2019. Helper T cell differentiation. Cellular & Molecular Immunology 16, 634–643. https://doi.org/10.1038/s41423-019-0220-6

Sato, T., Nakajima, H., Fujio, K., Mori, Y., 1997. Enhancement of Prostaglandin E2 Production by Epidermal Growth Factor Requires the Coordinate Activation of Cytosolic Phospholipase A2 and Cyclooxygenase 2 in Human Squamous Carcinoma A431 Cells. Prostaglandins 53, 355–369. https://doi.org/10.1016/S0090-6980(97)00036-1

Scarà, S., Bottoni, P., Scatena, R., 2015. CA 19-9: Biochemical and Clinical Aspects. Adv Exp Med Biol 867, 247–260. https://doi.org/10.1007/978-94-017-7215-0_15

Schlichtholz, B., Turyn, J., Goyke, E., Biernacki, M., Jaskiewicz, K., Sledzinski, Z., Swierczynski, J., 2005a. Enhanced citrate synthase activity in human pancreatic cancer. Pancreas 30, 99–104. https://doi.org/10.1097/01.mpa.0000153326.69816.7d

Schlichtholz, B., Turyn, J., Goyke, E., Biernacki, M., Jaskiewicz, K., Sledzinski, Z., Swierczynski, J., 2005b. Enhanced citrate synthase activity in human pancreatic cancer. Pancreas 30, 99–104. https://doi.org/10.1097/01.mpa.0000153326.69816.7d

Schreiber, R.D., Old, L.J., Smyth, M.J., 2011. Cancer immunoediting: integrating immunity's roles in cancer suppression and promotion. Science 331, 1565–1570. https://doi.org/10.1126/science.1203486

Schumacher, K., Haensch, W., Röefzaad, C., Schlag, P.M., 2001. Prognostic Significance of Activated $CD8^+$ T Cell Infiltrations within Esophageal Carcinomas. Cancer Res 61, 3932.

Sena, L.A., Li, S., Jairaman, A., Prakriya, M., Ezponda, T., Hildeman, D.A., Wang, C.-R., Schumacker, P.T., Licht, J.D., Perlman, H., Bryce, P.J., Chandel, N.S., 2013. Mitochondria Are Required for Antigen-Specific T Cell Activation through Reactive Oxygen Species Signaling. Immunity 38, 225–236. https://doi.org/10.1016/j.immuni.2012.10.020

Serkova, N., Florian Fuller, T., Klawitter, J., Freise, C.E., Niemann, C.U., 2005. 1H-NMR–based metabolic signatures of mild and severe ischemia/reperfusion injury in rat kidney transplants. Kidney International 67, 1142–1151. https://doi.org/10.1111/j.1523-1755.2005.00181.x

Shadhu, K., Xi, C., 2019. Inflammation and pancreatic cancer: An updated review. Saudi J Gastroenterol 25, 3–13. https://doi.org/10.4103/sjg.SJG_390_18

Sharafi, G., He, H., Nikfarjam, M., 2019. Potential Use of Cannabinoids for the Treatment of Pancreatic Cancer. Journal of Pancreatic Cancer 5, 1–7. https://doi.org/10.1089/pancan.2018.0019

Sheng, K.-C., Pietersz, G.A., Tang, C.K., Ramsland, P.A., Apostolopoulos, V., 2010. Reactive Oxygen Species Level Defines Two Functionally Distinctive Stages of Inflammatory Dendritic Cell Development from Mouse Bone Marrow. J. Immunol. 184, 2863. https://doi.org/10.4049/jimmunol.0903458

Shukla, S.K., Purohit, V., Mehla, K., Gunda, V., Chaika, N.V., Vernucci, E., King, R.J., Abrego, J., Goode, G.D., Dasgupta, A., Illies, A.L., Gebregiworgis, T., Dai, B., Augustine, J.J., Murthy, D., Attri, K.S., Mashadova, O., Grandgenett, P.M., Powers, R., Ly, Q.P., Lazenby, A.J., Grem, J.L., Yu, F., Matés, J.M., Asara, J.M., Kim, J., Hankins, J.H., Weekes, C., Hollingsworth, M.A., Serkova, N.J., Sasson, A.R., Fleming, J.B., Oliveto, J.M., Lyssiotis, C.A., Cantley, L.C., Berim, L., Singh, P.K., 2017. MUC1 and HIF-1alpha Signaling Crosstalk Induces Anabolic Glucose Metabolism to Impart Gemcitabine Resistance to Pancreatic Cancer. Cancer Cell 32, 71-87.e7. https://doi.org/10.1016/j.ccell.2017.06.004

Sideras, K., Braat, H., Kwekkeboom, J., van Eijck, C.H., Peppelenbosch, M.P., Sleijfer, S., Bruno, M., 2014. Role of the immune system in pancreatic cancer progression and immune modulating treatment strategies. Cancer Treatment Reviews 40, 513–522. https://doi.org/10.1016/j.ctrv.2013.11.005

Siegel, R.L., Miller, K.D., Fuchs, H.E., Jemal, A., 2022. Cancer statistics, 2022. CA: A Cancer Journal for Clinicians 72, 7–33. https://doi.org/10.3322/caac.21708

Siegel, R.L., Miller, K.D., Fuchs, H.E., Jemal, A., 2021. Cancer Statistics, 2021. CA: A Cancer Journal for Clinicians 71, 7–33. https://doi.org/10.3322/caac.21654

Sies, H., 2017. Hydrogen peroxide as a central redox signaling molecule in physiological oxidative stress: Oxidative eustress. Redox Biology 11, 613–619. https://doi.org/10.1016/j.redox.2016.12.035

Silva, A.S., Yunes, J.A., Gillies, R.J., Gatenby, R.A., 2009. The Potential Role of Systemic Buffers in Reducing Intratumoral Extracellular pH and Acid-Mediated Invasion. Cancer Res 69, 2677. https://doi.org/10.1158/0008-5472.CAN-08-2394

Silverman, D.T., Hoover, R.N., Brown, L.M., Swanson, G.M., Schiffman, M., Greenberg, R.S., Hayes, R.B., Lillemoe, K.D., Schoenberg, J.B., Schwartz, A.G., Liff, J., Pottern, L.M., Fraumeni, J.F.Jr., 2003. Why Do Black Americans Have a Higher Risk of Pancreatic Cancer than White Americans? Epidemiology 14.

Sinclair, L.V., Rolf, J., Emslie, E., Shi, Y.-B., Taylor, P.M., Cantrell, D.A., 2013. Control of amino-acid transport by antigen receptors coordinates the metabolic reprogramming essential for T cell differentiation. Nature Immunology 14, 500.

Singer, K., Cheng, W.-C., Kreutz, M., Ho, P.-C., Siska, P.J., 2018. Immunometabolism in cancer at a glance. Dis Models Mech 11, dmm034272. https://doi.org/10.1242/dmm.034272

Singh, A., Kukreti, R., Saso, L., Kukreti, S., 2019. Oxidative Stress: A Key Modulator in Neurodegenerative Diseases. Molecules 24, 1583. https://doi.org/10.3390/molecules24081583

Singhi, A.D., Koay, E.J., Chari, S.T., Maitra, A., 2019. Early Detection of Pancreatic Cancer: Opportunities and Challenges. Gastroenterology 156, 2024–2040. https://doi.org/10.1053/j.gastro.2019.01.259

Sivakumar, T., Chaidarun, S., Lee, H.K., Cervinski, M., Comi, R., 2011a. Multiple lipoprotein and electrolyte laboratory artifacts caused by lipoprotein X in obstructive biliary cholestasis secondary to pancreatic cancer. Journal of Clinical Lipidology 5, 324–328. https://doi.org/10.1016/j.jacl.2011.04.004

Sivakumar, T., Chaidarun, S., Lee, H.K., Cervinski, M., Comi, R., 2011b. Multiple lipoprotein and electrolyte laboratory artifacts caused by lipoprotein X in obstructive biliary cholestasis secondary to pancreatic cancer. Journal of Clinical Lipidology 5, 324–328. https://doi.org/10.1016/j.jacl.2011.04.004

Smelt, A.H.M., 2010. Triglycerides and gallstone formation. Clinica Chimica Acta 411, 1625–1631. https://doi.org/10.1016/j.cca.2010.08.003

Son, J., Lyssiotis, C.A., Ying, H., Wang, X., Hua, S., Ligorio, M., Perera, R.M., Ferrone, C.R., Mullarky, E., Shyh-Chang, N., Kang, Y., Fleming, J.B., Bardeesy, N., Asara, J.M., Haigis, M.C., DePinho, R.A., Cantley, L.C., Kimmelman, A.C., 2013. Glutamine supports pancreatic cancer growth through a KRAS-regulated metabolic pathway. Nature 496, 101.

Sörös, P., Böttcher, J., Maschek, H., Selberg, O., Müller, M.J., 1998. Lipoprotein-X in patients with cirrhosis: Its relationship to cholestasis and hypercholesterolemia. Hepatology 28, 1199–1205. https://doi.org/10.1002/hep.510280506

Sosa, V., Moliné, T., Somoza, R., Paciucci, R., Kondoh, H., LLeonart, M.E., 2013. Oxidative stress and cancer: An overview. Ageing Research Reviews 12, 376–390. https://doi.org/10.1016/j.arr.2012.10.004

Sousa, C.M., Kimmelman, A.C., 2014. The complex landscape of pancreatic cancer metabolism. Carcinogenesis 35, 1441–1450. https://doi.org/10.1093/carcin/bgu097

Soweid, A.M., 2017. The borderline resectable and locally advanced pancreatic ductal adenocarcinoma: Definition. Endosc Ultrasound 6, S76–S78. https://doi.org/10.4103/eus.eus_66_17

Stein, E., Stender, S., Mata, P., Sager, P., Ponsonnet, D., Melani, L., Lipka, L., Suresh, R., MacCubbin, D., Veltri, E., 2004. Achieving lipoprotein goals in patients at high risk with severe hypercholesterolemia: Efficacy and safety of ezetimibe co-administered with atorvastatin. American Heart Journal 148, 447–455. https://doi.org/10.1016/j.ahj.2004.03.052

Stopa, B.K., Kusiak, A.A., Szopa, D.M., Ferdek, E.P., Jakubowska, A.M., 2020. Pancreatic Cancer and Its Microenvironment—Recent Advances and Current Controversies. International Journal of Molecular Sciences 21. https://doi.org/10.3390/ijms21093218

Sullivan, L.B., Gui, D.Y., Heiden, M.G.V., 2016. Altered metabolite levels in cancer: implications for tumour biology and cancer therapy. Nature Reviews Cancer 16, 680–693. https://doi.org/10.1038/nrc.2016.85

Sullivan, L.B., Martinez-Garcia, E., Nguyen, H., Mullen, A.R., Dufour, E., Sudarshan, S., Licht, J.D., Deberardinis, R.J., Chandel, N.S., 2013. The Proto-oncometabolite Fumarate Binds Glutathione to Amplify ROS-Dependent Signaling. Molecular Cell 51, 236–248. https://doi.org/10.1016/j.molcel.2013.05.003

Sung, H., Ferlay, J., Siegel, R.L., Laversanne, M., Soerjomataram, I., Jemal, A., Bray, F., 2021. Global Cancer Statistics 2020: GLOBOCAN Estimates of Incidence and Mortality Worldwide for 36 Cancers in 185 Countries. CA: A Cancer Journal for Clinicians 71, 209–249. https://doi.org/10.3322/caac.21660

Swierczynski, J., Hebanowska, A., Sledzinski, T., 2014. Role of abnormal lipid metabolism in development, progression, diagnosis and therapy of pancreatic cancer. World J Gastroenterol 20, 2279–2303. https://doi.org/10.3748/wjg.v20.i9.2279

Szkandera, J., Stotz, M., Absenger, G., Stojakovic, T., Samonigg, H., Kornprat, P., Schaberl-Moser, R., AlZoughbi, W., Lackner, C., Ress, A.L., Seggewies, F.S., Gerger, A., Hoefler, G., Pichler, M., 2014. Validation of C-reactive protein levels as a prognostic indicator for survival in a large cohort of pancreatic cancer patients. British Journal of Cancer 110, 183–188. https://doi.org/10.1038/bjc.2013.701

Szymańska, E., Saccenti, E., Smilde, A.K., Westerhuis, J.A., 2012. Double-check: validation of diagnostic statistics for PLS-DA models in metabolomics studies. Metabolomics 8, 3–16. https://doi.org/10.1007/s11306-011-0330-3

Tadros, S., Shukla, S.K., King, R.J., Gunda, V., Vernucci, E., Abrego, J., Chaika, N.V., Yu, F., Lazenby, A.J., Berim, L., Grem, J., Sasson, A.R., Singh, P.K., 2017. De Novo Lipid Synthesis Facilitates Gemcitabine Resistance through Endoplasmic Reticulum Stress in Pancreatic Cancer. Cancer Res 77, 5503–5517. https://doi.org/10.1158/0008-5472.CAN-16-3062

Talib, W.H., AL-ataby, I.A., Mahmod, A.I., Jawarneh, S., Al Kury, L.T., AL-Yasari, I.H., 2020. The Impact of Herbal Infusion Consumption on Oxidative Stress and Cancer: The Good, the Bad, the Misunderstood. Molecules 25. https://doi.org/10.3390/molecules25184207

Tang, R., Liu, X., Liang, C., Hua, J., Xu, J., Wang, W., Meng, Q., Liu, J., Zhang, B., Yu, X., Shi, S., 2021. Deciphering the Prognostic Implications of the Components and Signatures in the Immune Microenvironment of Pancreatic Ductal Adenocarcinoma. Front Immunol 12, 648917–648917. https://doi.org/10.3389/fimmu.2021.648917

Tang, R.-F., Wang, Shu-Xia, Zhang, F.-R., Peng, L., Wang, Shun-Xiang, Xiao, Y., Zhang, M., 2005. Interleukin-1alpha, 6 regulate the secretion of vascular endothelial growth factor A, C in pancreatic cancer. Hepatobiliary Pancreat Dis Int 4, 460–463.

Tempero, M.A., Malafa, M.P., Chiorean, E.G., Czito, B., Scaife, C., Narang, A.K., Fountzilas, C., Wolpin, B.M., Al-Hawary, M., Asbun, H., Behrman, S.W., Benson, A.B., Binder, E., Cardin, D.B., Cha, C., Chung, V., Dillhoff, M., Dotan, E., Ferrone, C.R., Fisher, G., Hardacre, J., Hawkins, W.G., Ko, A.H., LoConte, N., Lowy, A.M., Moravek, C., Nakakura, E.K., O'Reilly, E.M., Obando, J., Reddy, S., Thayer, S., Wolff, R.A., Burns, J.L., Zuccarino-Catania, G., 2019a. Pancreatic Adenocarcinoma, Version 1.2019. J Natl Compr Canc Netw 17, 202–210. https://doi.org/10.6004/jnccn.2019.0014

Tempero, M.A., Malafa, M.P., Chiorean, E.G., Czito, B., Scaife, C., Narang, A.K., Fountzilas, C., Wolpin, B.M., Al-Hawary, M., Asbun, H., Behrman, S.W., Benson, A.B., Binder, E., Cardin, D.B., Cha, C., Chung, V., Dillhoff, M., Dotan, E., Ferrone, C.R., Fisher, G., Hardacre, J., Hawkins, W.G., Ko, A.H., LoConte, N., Lowy, A.M., Moravek, C., Nakakura, E.K., O'Reilly, E.M., Obando, J., Reddy, S., Thayer, S., Wolff, R.A., Burns, J.L., Zuccarino-Catania, G., 2019b. Pancreatic Adenocarcinoma, Version 1.2019. J Natl Compr Canc Netw 17, 202–210. https://doi.org/10.6004/jnccn.2019.0014

Tennant, D.A., Durán, R.V., Gottlieb, E., 2010. Targeting metabolic transformation for cancer therapy. Nature Reviews Cancer 10, 267–277. https://doi.org/10.1038/nrc2817

Terabe, M., Berzofsky, J.A., 2008. Chapter 8 The Role of NKT Cells in Tumor Immunity, in: Advances in Cancer Research. Academic Press, pp. 277–348. https://doi.org/10.1016/S0065-230X(08)00408-9

Tewari, N., Zaitoun, A.M., Arora, A., Madhusudan, S., Ilyas, M., Lobo, D.N., 2013. The presence of tumour-associated lymphocytes confers a good prognosis in pancreatic ductal adenocarcinoma: an immunohistochemical study of tissue microarrays. BMC Cancer 13, 436. https://doi.org/10.1186/1471-2407-13-436

Tímár, J., Ladányi, A., Forster-Horváth, C., Lukits, J., Döme, B., Remenár, É., Gődény, M., Kásler, M., Bencsik, B., Répássy, G., Szabó, G., Velich, N., Suba, Z., Élő, J., Balatoni, Z., Pócza, K., Zemplén, B., Chretien, P., Talor, E., 2005. Neoadjuvant Immunotherapy of Oral Squamous Cell Carcinoma Modulates Intratumoral CD4/CD8 Ratio and Tumor Microenvironment: A Multicenter Phase II Clinical Trial. JCO 23, 3421–3432. https://doi.org/10.1200/JCO.2005.06.005

Treffers, L.W., van Houdt, M., Bruggeman, C.W., Heineke, M.H., Zhao, X.W., van der Heijden, J., Nagelkerke, S.Q., Verkuijlen, P.J.J.H., Geissler, J., Lissenberg-Thunnissen,

S., Valerius, T., Peipp, M., Franke, K., van Bruggen, R., Kuijpers, T.W., van Egmond, M., Vidarsson, G., Matlung, H.L., van den Berg, T.K., 2019. FcγRIIIb Restricts Antibody-Dependent Destruction of Cancer Cells by Human Neutrophils. Front Immunol 9, 3124–3124. https://doi.org/10.3389/fimmu.2018.03124

Tripathi, N., Jialal, I., 2020. Conjugated Hyperbilirubinemia. StatPearls Publishing, Treasure Island (FL).

Tsilimigras, D.I., Brodt, P., Clavien, P.-A., Muschel, R.J., D'Angelica, M.I., Endo, I., Parks, R.W., Doyle, M., de Santibañes, E., Pawlik, T.M., 2021. Liver metastases. Nat Rev Dis Primers 7, 27. https://doi.org/10.1038/s41572-021-00261-6

Unger, K., Mehta, K.Y., Kaur, P., Wang, Y., Menon, S.S., Jain, S.K., Moonjelly, R.A., Suman, S., Datta, K., Singh, R., Fogel, P., Cheema, A.K., 2018. Metabolomics based predictive classifier for early detection of pancreatic ductal adenocarcinoma. Oncotarget 9, 23078–23090. https://doi.org/10.18632/oncotarget.25212

Van Acker, H.H., Capsomidis, A., Smits, E.L., Van Tendeloo, V.F., 2017. CD56 in the Immune System: More Than a Marker for Cytotoxicity? Front Immunol 8, 892–892. https://doi.org/10.3389/fimmu.2017.00892

Van Audenaerde, J.R.M., Roeyen, G., Darcy, P.K., Kershaw, M.H., Peeters, M., Smits, E.L.J., 2018. Natural killer cells and their therapeutic role in pancreatic cancer: A systematic review. Pharmacology & Therapeutics 189, 31–44. https://doi.org/10.1016/j.pharmthera.2018.04.003

Van Coillie, S., Wiernicki, B., Xu, J., 2020. Molecular and Cellular Functions of CTLA-4. Adv Exp Med Biol 1248, 7–32. https://doi.org/10.1007/978-981-15-3266-5_2

Van den Hove, L.E., Vandenberghe, P., Van Gool, S.W., Ceuppens, J.L., Demuynck, H., Verhoef, G.E.G., Boogaerts, M.A., 1998. Peripheral blood lymphocyte subset shifts in patients with untreated hematological tumors: Evidence for systemic activation of the T cell compartment. Leukemia Research 22, 175–184. https://doi.org/10.1016/S0145-2126(97)00152-5

Vander Heiden, M.G., Cantley, L.C., Thompson, C.B., 2009. Understanding the Warburg Effect: The Metabolic Requirements of Cell Proliferation. Science 324, 1029. https://doi.org/10.1126/science.1160809

Vaquero, E.C., Edderkaoui, M., Pandol, S.J., Gukovsky, I., Gukovskaya, A.S., 2004. Reactive Oxygen Species Produced by NAD(P)H Oxidase Inhibit Apoptosis in Pancreatic Cancer Cells*. Journal of Biological Chemistry 279, 34643–34654. https://doi.org/10.1074/jbc.M400078200

Varghese, A.M., Singh, I., Singh, R., Kunte, S., Chou, J.F., Capanu, M., Wong, W., Lowery, M.A., Stadler, Z.K., Salo-Mullen, E., Saadat, L.V., Wei, A.C., Reyngold, M., Basturk, O., Benayed, R., Mandelker, D., Iacobuzio-Donahue, C.A., Kelsen, D.P., Park, W., Yu, K.H., O'Reilly, E.M., 2021. Early-Onset Pancreas Cancer: Clinical Descriptors, Genomics, and Outcomes. JNCI: Journal of the National Cancer Institute 113, 1194–1202. https://doi.org/10.1093/jnci/djab038

Vogel, A., Kullmann, F., Kunzmann, V., Al-Batran, S.-E., Oettle, H., Plentz, R., Siveke, J., Springfeld, C., Riess, H., 2015. Patients with Advanced Pancreatic Cancer and Hyperbilirubinaemia: Review and German Expert Opinion on Treatment with nab-Paclitaxel plus Gemcitabine. Oncology Research and Treatment 38, 596–603. https://doi.org/10.1159/000441310

von Ahrens, D., Bhagat, T.D., Nagrath, D., Maitra, A., Verma, A., 2017. The role of stromal cancer-associated fibroblasts in pancreatic cancer. Journal of Hematology & Oncology 10, 76. https://doi.org/10.1186/s13045-017-0448-5

Vujasinovic, M., Dugic, A., Maisonneuve, P., Aljic, A., Berggren, R., Panic, N., Valente, R., Pozzi Mucelli, R., Waldthaler, A., Ghorbani, P., Kordes, M., Hagström, H., Löhr, J.-

M., 2020. Risk of Developing Pancreatic Cancer in Patients with Chronic Pancreatitis. Journal of Clinical Medicine 9. https://doi.org/10.3390/jcm9113720
Wachsmann, M.B., Pop, L.M., Vitetta, E.S., 2012. Pancreatic Ductal Adenocarcinoma. J Investig Med 60, 643. https://doi.org/10.2310/JIM.0b013e31824a4d79
Waickman, A.T., Powell, J.D., 2012. mTOR, metabolism, and the regulation of T-cell differentiation and function. Immunological Reviews 249, 43–58. https://doi.org/10.1111/j.1600-065X.2012.01152.x
Waitkus, M.S., Diplas, B.H., Yan, H., 2018. Biological Role and Therapeutic Potential of IDH Mutations in Cancer. Cancer Cell 34, 186–195. https://doi.org/10.1016/j.ccell.2018.04.011
Walli, A., Seidel, D., 1984. Role of lipoprotein-X in the pathogenesis of cholestatic hypercholesterolemia. Uptake of lipoprotein-X and its effect on 3-hydroxy-3-methylglutaryl coenzyme A reductase and chylomicron remnant removal in human fibroblasts, lymphocytes, and in the rat. J Clin Invest 74, 867–879. https://doi.org/10.1172/jci111504
Wang, L., Lu, Q., Gao, W., Yu, S., 2021. Recent advancement on development of drug-induced macrophage polarization in control of human diseases. Life Sciences 284, 119914. https://doi.org/10.1016/j.lfs.2021.119914
Wang, Y., Fu, W., Tang, Z., Meng, W., Zhou, W., Li, X., 2018. Effect of preoperative cholangitis on prognosis of patients with hilar cholangiocarcinoma: A systematic review and meta-analysis. Medicine (Baltimore) 97, e12025–e12025. https://doi.org/10.1097/MD.0000000000012025
Wang, Y.-T., Gou, Y.-W., Jin, W.-W., Xiao, M., Fang, H.-Y., 2016. Association between alcohol intake and the risk of pancreatic cancer: a dose–response meta-analysis of cohort studies. BMC Cancer 16, 212. https://doi.org/10.1186/s12885-016-2241-1
Wang, Z., Zhao, J., Zhao, H., A, S., Liu, Z., Zhang, Y., Liu, X., Wang, F., 2017. Infiltrating CD4/CD8 high T cells shows good prognostic impact in pancreatic cancer. Int J Clin Exp Pathol 10, 8820–8828.
Warburg, O., Wind, F., Negelein, E., 1927. THE METABOLISM OF TUMORS IN THE BODY. The Journal of general physiology 8, 519–530.
Wörmann, S.M., Diakopoulos, K.N., Lesina, M., Algül, H., 2013a. The immune network in pancreatic cancer development and progression. Oncogene 33, 2956.
Wörmann, S.M., Diakopoulos, K.N., Lesina, M., Algül, H., 2013b. The immune network in pancreatic cancer development and progression. Oncogene 33, 2956.
Xu, S., Xu, H., Wang, W., Li, S., Li, H., Li, T., Zhang, W., Yu, X., Liu, L., 2019. The role of collagen in cancer: from bench to bedside. Journal of Translational Medicine 17, 309. https://doi.org/10.1186/s12967-019-2058-1
Yachida, S., Jones, S., Bozic, I., Antal, T., Leary, R., Fu, B., Kamiyama, M., Hruban, R.H., Eshleman, J.R., Nowak, M.A., Velculescu, V.E., Kinzler, K.W., Vogelstein, B., Iacobuzio-Donahue, C.A., 2010. Distant metastasis occurs late during the genetic evolution of pancreatic cancer. Nature 467, 1114.
Yadav, D., Lowenfels, A.B., 2013. The Epidemiology of Pancreatitis and Pancreatic Cancer. Gastroenterology 144, 1252–1261. https://doi.org/10.1053/j.gastro.2013.01.068
Yadav, D., Muddana, V., O'Connell, M., 2011. Hospitalizations for Chronic Pancreatitis in Allegheny County, Pennsylvania, USA. Pancreatology 11, 546–552. https://doi.org/10.1159/000331498
Yamamoto, K., Venida, A., Yano, J., Biancur, D.E., Kakiuchi, M., Gupta, S., Sohn, A.S.W., Mukhopadhyay, S., Lin, E.Y., Parker, S.J., Banh, R.S., Paulo, J.A., Wen, K.W., Debnath, J., Kim, G.E., Mancias, J.D., Fearon, D.T., Perera, R.M., Kimmelman, A.C.,

2020. Autophagy promotes immune evasion of pancreatic cancer by degrading MHC-I. Nature. https://doi.org/10.1038/s41586-020-2229-5

Yamamoto, T., Yanagimoto, H., Satoi, S., Toyokawa, H., Hirooka, S., Yamaki, S., Yui, R., Yamao, J., Kim, S., Kwon, A.-H., 2012. Circulating CD4+CD25+ Regulatory T Cells in Patients With Pancreatic Cancer. Pancreas 41.

Yan, D., Adeshakin, A.O., Xu, M., Afolabi, L.O., Zhang, G., Chen, Y.H., Wan, X., 2019. Lipid Metabolic Pathways Confer the Immunosuppressive Function of Myeloid-Derived Suppressor Cells in Tumor. Front Immunol 10, 1399–1399. https://doi.org/10.3389/fimmu.2019.01399

Yan, L., Tonack, S., Smith, R., Dodd, S., Jenkins, R.E., Kitteringham, N., Greenhalf, W., Ghaneh, P., Neoptolemos, J.P., Costello, E., 2009. Confounding Effect of Obstructive Jaundice in the Interpretation of Proteomic Plasma Profiling Data for Pancreatic Cancer. J. Proteome Res. 8, 142–148. https://doi.org/10.1021/pr800451h

Yang, C., Cheng, H., Luo, G., Lu, Y., Guo, M., Jin, K., Wang, Z., Yu, X., Liu, C., 2017. The metastasis status and tumor burden-associated CA125 level combined with the CD4/CD8 ratio predicts the prognosis of patients with advanced pancreatic cancer: A new scoring system. European Journal of Surgical Oncology 43, 2112–2118. https://doi.org/10.1016/j.ejso.2017.07.010

Yang, F., Feng, C., Zhang, X., Lu, J., Zhao, Y., 2017. The Diverse Biological Functions of Neutrophils, Beyond the Defense Against Infections. Inflammation 40, 311–323. https://doi.org/10.1007/s10753-016-0458-4

Yang, J., Ren, B., Yang, G., Wang, H., Chen, G., You, L., Zhang, T., Zhao, Y., 2020. The enhancement of glycolysis regulates pancreatic cancer metastasis. Cellular and Molecular Life Sciences 77, 305–321. https://doi.org/10.1007/s00018-019-03278-z

Yao, W., Maitra, A., Ying, H., 2020. Recent insights into the biology of pancreatic cancer. EBioMedicine 53, 102655–102655. https://doi.org/10.1016/j.ebiom.2020.102655

Yasuda, T., Ishimoto, T., Baba, H., 2021. Conflicting metabolic alterations in cancer stem cells and regulation by the stromal niche. Regenerative Therapy 17, 8–12. https://doi.org/10.1016/j.reth.2021.01.005

Yilmaz, A., Malya, F., Ozturk, G., Citgez, B., Ozdenkaya, Y., Ersavas, C., Agan, A., Senturk, H., Karatepe, O., 2014. Effect of pre-operative red blood cell distribution on cancer stage and morbidity rate in patients with pancreatic cancer. Int J Clin Exp Med 7, 3072–3075.

Yu, C.-P., Fu, S.-F., Chen, X., Ye, J., Ye, Y., Kong, L.-D., Zhu, Z.-M., 2018. The Clinicopathological and Prognostic Significance of IDO1 Expression in Human Solid Tumors: Evidence from a Systematic Review and Meta-Analysis. Cellular Physiology and Biochemistry 49, 134–143. https://doi.org/10.1159/000492849

Yun, J., Mullarky, E., Lu, C., Bosch, K.N., Kavalier, A., Rivera, K., Roper, J., Chio, I.I.C., Giannopoulou, E.G., Rago, C., Muley, A., Asara, J.M., Paik, J., Elemento, O., Chen, Z., Pappin, D.J., Dow, L.E., Papadopoulos, N., Gross, S.S., Cantley, L.C., 2015. Vitamin C selectively kills KRAS and BRAF mutant colorectal cancer cells by targeting GAPDH. Science 350, 1391–1396. https://doi.org/10.1126/science.aaa5004

Zhang, A., Sun, H., Wang, X., 2012. Serum metabolomics as a novel diagnostic approach for disease: a systematic review. Analytical and Bioanalytical Chemistry 404, 1239–1245. https://doi.org/10.1007/s00216-012-6117-1

Zhang, G., He, P., Tan, H., Budhu, A., Gaedcke, J., Ghadimi, B.M., Ried, T., Yfantis, H.G., Lee, D.H., Maitra, A., Hanna, N., Alexander, H.R., Hussain, S.P., 2013. Integration of metabolomics and transcriptomics revealed a fatty acid network exerting growth inhibitory effects in human pancreatic cancer. Clin Cancer Res 19, 4983–4993. https://doi.org/10.1158/1078-0432.CCR-13-0209

Zhang, H., Ren, D., Jin, X., Wu, H., 2020. The prognostic value of modified Glasgow Prognostic Score in pancreatic cancer: a meta-analysis. Cancer Cell International 20, 462. https://doi.org/10.1186/s12935-020-01558-4

Zhang, L., Li, J., Zong, L., Chen, X., Chen, K., Jiang, Z., Nan, L., Li, X., Li, W., Shan, T., Ma, Q., Ma, Z., 2016. Reactive Oxygen Species and Targeted Therapy for Pancreatic Cancer. Oxidative Medicine and Cellular Longevity 2016, 1616781. https://doi.org/10.1155/2016/1616781

Zhang, S., Liu, W., Hu, B., Wang, P., Lv, X., Chen, S., Shao, Z., 2020. Prognostic Significance of Tumor-Infiltrating Natural Killer Cells in Solid Tumors: A Systematic Review and Meta-Analysis. Front Immunol 11, 1242–1242. https://doi.org/10.3389/fimmu.2020.01242

Zhao, H., Yang, L., Baddour, J., Achreja, A., Bernard, V., Moss, T., Marini, J.C., Tudawe, T., Seviour, E.G., San Lucas, F.A., Alvarez, H., Gupta, S., Maiti, S.N., Cooper, L., Peehl, D., Ram, P.T., Maitra, A., Nagrath, D., 2016. Tumor microenvironment derived exosomes pleiotropically modulate cancer cell metabolism. Elife 5, e10250. https://doi.org/10.7554/eLife.10250

Zimmer, V., Lammert, F., 2015. Acute Bacterial Cholangitis. Viszeralmedizin 31, 166–172. https://doi.org/10.1159/000430965

Zou, W., Restifo, N.P., 2010. TH17 cells in tumour immunity and immunotherapy. Nature Reviews Immunology 10, 248–256. https://doi.org/10.1038/nri2742

SUPPLEMENTARY TABLES

Table S1: List of the quantified signal and their relative assignment and multiplicity.

Metabolite	Assignment (multiplicity)	matrix	Metabolite	Assignment (multiplicity)	matrix
Formate	8.45 (s)	serum	cholesterol-derivated 1	0.64 (s)	lipid extracts
Unknown signal at 8.12 ppm	8.12 (d)	serum	cholesterol-derivated 2	0.65 (s)	lipid extracts
Unknown signal at 8.07 ppm	8.07 (d)	serum	cholesterol-derivated 3	0.66 (s)	lipid extracts
Phenylalanine	7.42 (m)	serum	cholesterol-derivated 4	0.66 (s)	lipid extracts
Tyrosine	7.19 (m)	serum	cholesterol-derivated 5	0.67 (s)	lipid extracts
Unknown signal at 7.14 ppm	7.14 (m)	serum	free cholesterol	0.68 (s)	lipid extracts
Histidine	7.05 (d)	serum	esterified cholesterol	0.68 (s)	lipid extracts
Glucose	5.23 (d)	serum	cholesterol-derivated 6	0.69 (s)	lipid extracts
Mannose	5.18 (d)	serum	cholesterol-derivated 7	0.70 (s)	lipid extracts
Unknown signal at 5.15 ppm	5.15 (d)	serum	cholesterol-derivated 8	0.70 (s)	lipid extracts
Unknown signal at 5.09 ppm	5.09 (d)	serum	cholesterol-derivated 9	0.71 (s)	lipid extracts
Unknown signal at 5.01 ppm	5.01 (d)	serum	saturated and omega-9 fatty acid	0.87 (t)	lipid extracts
Ascorbate	4.50 (d)	serum	omega-7 fatty acid	0.87 (t)	lipid extracts
Threonine	4.24 (m)	serum	omega-6 fatty acid	0.88 (t)	lipid extracts
Lactate	4.11 (q)	serum	Unknown signal at 0.91 ppm	0.98 (d)	lipid extracts
Creatinine	4.05 (s)	serum	omega-3 fatty acid	0.99 (t)	lipid extracts
Creatine	3.92 (s)	serum	monounsaturated fatty acid	2.01 (q)	lipid extracts
Glycine	3.55 (s)	serum	polyunsaturated fatty acid 1 (except linoleic)	2.80 (t)	lipid extracts
Methanol	3.35 (s)	serum	polyunsaturated fatty acid 2 (except linoleic)	2.84 (d)	lipid extracts
Unknown signal at 2.55 ppm	2.55 (s)	serum	linoleic acid	2.76 (t)	lipid extracts
Citrate	2.53 (d)	serum	phosphatidylcholine	3.20 (s)	lipid extracts
Glutamine	2.45 (m)	serum	sphingomyelin	3.19 (s)	lipid extracts
Pyruvate	2.36 (s)	serum	triglyceride	5.26 (m)	lipid extracts
Glutamate	2.53 (m)	serum	glycerophospholipid	4.45 (q)	lipid extracts
Acetoacetate	2.22 (s)	serum			
Acetate	1.91 (s)	serum			
Alanine	1.47 (d)	serum			
Unknown signal at 1.45 ppm	1.45 (d)	serum			
Unknown signal at 1.43 ppm	1.43 (d)	serum			
3-Hydroxybutyrate	1.19 (d)	serum			
Ethanol	1.17 (t)	serum			
Unknown signal at 1.16 ppm	1.16 (d)	serum			
Unknown signal at 1.14 ppm	1.14 (d)	serum			
Unknown signal at 1.11 ppm	1.11 (d)	serum			
Unknown signal at 1.06 ppm	1.06 (d)	serum			
Valine	1.04 (d)	serum			
Isoleucine	1.00 (d)	serum			
Leucine	0.95 (dd)	serum			
2-Hydroxybutyrate	0.89 (t)	serum			
Protein NH	10.00-6.00	serum			
Unsaturated lipid -CH=CH-	5.50-5.10	serum			
Lipid alpha-CH2	2.25-2.15	serum			
Cholesterol	0.70-0.60	serum			
Lipid =CH-CH2-CH=	2.85-2.65	serum			
Glycerol phospholipid	4.08-4.03	serum			
Phospholipid	3.68-3.62	serum			
Lipid beta-CH2	1.65-1.40	serum			
Lipid CH2	1.40-1.10	serum			
Lipid CH3	1.10-1.08	serum			
GlycB	2.07 (m)	serum			
GlycA	2.03 (m)	serum			

Table S2: Correlation of concentration of lipid extracts with the stages of Pancreatic Ductal Adenocarcinoma.

Features	rho	p-value	FDR
cholesterol-derivated 1	0.32	0.047	0.154
cholesterol-derivated 2	0.37	0.018	0.089
cholesterol-derivated 3	0.24	0.133	0.195
cholesterol-derivated 4	0.37	0.019	0.089
cholesterol-derivated 5	-0.29	0.065	0.154
free cholesterol	0.28	0.084	0.159
esterified cholesterol	0.09	0.587	0.587
cholesterol-derivated 6	0.38	0.016	0.089
cholesterol-derivated 7	-0.16	0.313	0.327
cholesterol-derivated 8	0.38	0.014	0.089
cholesterol-derivated 9	-0.33	0.037	0.148
saturated and omega-9 fatty acid	0.3	0.062	0.154
omega-7 fatty acid	0.37	0.017	0.089
omega-6 fatty acid	0.24	0.138	0.195
Unknown signal at 0.91 ppm	-0.29	0.071	0.154
omega-3 fatty acid	0.27	0.086	0.159
monounsaturated fatty acid	0.26	0.110	0.180
polyunsaturated fatty acid 1 (except linoleate)	0.18	0.269	0.293
polyunsaturated fatty acid 2 (except linoleate)	0.23	0.149	0.199
Linoleate	0.21	0.194	0.233
Phosphatidylcholine	0.2	0.206	0.235
Sphingomyelin	0.3	0.065	0.154
Triglyceride	0.21	0.189	0.233
Glycerophospholipid	0.25	0.112	0.180

Rho: spearman's correlation coefficient measures the strength of association between two variables; FDR: false discovery rate

Table S3: Selected metabolites ratios and their catalysing enzymes

Ratio	Catalysing enzymes
Glucose/Lactate	Phosphofructokinase
Pyruvate/Lactate	Lactate dehydrogenase
Threonine/Glycine	Threonine dehydrogenase 2-amino-3-ketobutyrate coenzyme A ligase
Glutamine/Glutamate	Glutamine synthetase
3-hydroxybutyrate/acetoacetate	3-hydroxybutyrate dehydrogenase
Glutamate/Alanine	Alanine aminotransferase

Table S4: Correlation of metabolites ratios with the stages of Pancreatic Ductal Adenocarcinoma

Feature	rho	p-value	FDR
Glucose/Lactate	-0.19	0.212	0.424
Pyruvate/Lactate	-0.14	0.360	0.599
Threonine/Glycine	-0.09	0.540	0.674
Glutamine/Glutamate	-0.26	0.089	0.222
3-Hydroxybutyrate/Acetoacetate	-0.05	0.767	0.767
Glutamate/Alanine	0.27	0.073	0.222

Rho: spearman's correlation coefficient measures the strength of association between two variables; FDR: false discovery rate

Table S5: Analysis using Wald Test to evaluate the association of Lipid Extracts levels with survival time in Pancreatic Ductal Adenocarcinoma patients.

Feature	p-value	FDR
cholesterol-derivated 1	0.646	0.948
cholesterol-derivated 2	0.664	0.948
cholesterol-derivated 3	0.745	0.948
cholesterol-derivated 4	0.783	0.948
cholesterol-derivated 5	0.854	0.948
free cholesterol	0.722	0.948
esterified cholesterol	0.425	0.948
cholesterol-derivated 6	0.245	0.948
cholesterol-derivated 7	0.583	0.948
cholesterol-derivated 8	0.785	0.948
cholesterol-derivated 9	0.575	0.948
saturated and omega-9 fatty acid	0.710	0.948
omega-7 fatty acid	0.995	0.995
omega-6 fatty acid	0.486	0.948
Unknown signal at	0.508	0.948
omega-3 fatty acid	0.699	0.948
monounsaturated fatty acid	0.882	0.948
polyunsaturated fatty acid 1 (except linoleic)	0.588	0.948
polyunsaturated fatty acid 2 (except linoleic)	0.619	0.948
linoleic acid	0.908	0.948
phosphatidylcholine	0.697	0.948
sphingomyelin	0.603	0.948
triglyceride	0.682	0.948
glycerophospholipid	0.817	0.948

FDR: false discovery rate

Table S6: Analysis using Wald Test to evaluate the association of Metabolite Ratio levels with survival time in Pancreatic Ductal Adenocarcinoma patients.

Features	p-value	FDR
Glucose/Lactate	0.741	0.873
Pyruvate/Lactate	0.873	0.873
Threonine/Glycine	0.721	0.873
Glutamine/Glutamate	0.473	0.788
3-Hydroxybutyrate/Acetoacetate	0.241	0.783
Glutamate/Alanine	0.313	0.783

FDR: false discovery rate

Table S7: Analysis using Wald Test to evaluate the association of Lipoprotein levels with survival time in Pancreatic Ductal Adenocarcinoma patients.

Features	p-value	FDR
VLDL cholesterol (nmol/L)	0.705	0.971
IDL. cholesterol (nmol/L)	0.699	0.971

LDL cholesterol (nmol/L)	0.174	0.971
HDL cholesterol (nmol/L)	0.666	0.971
VLDL triglyceride (nmol/L)	0.824	0.971
IDL triglyceride (nmol/L)	0.718	0.971
LDL triglyceride (nmol/L)	0.623	0.971
HDL triglyceride (nmol/L)	0.467	0.971
VLDL particle (nmol/L)	0.996	0.996
Large VLDL particle(nmol/L)	0.771	0.971
Medium VLDL particle (nmol/L)	0.581	0.971
Small VLDL particle(nmol/L)	0.935	0.973
LDL particle (nmol/L)	0.250	0.971
Large LDL particle (nmol/L)	0.324	0.971
Medium LDL particle (nmol/L)	0.379	0.971
Small LDL particle (nmol/L)	0.136	0.971
HDL particle (mol/L)	0.815	0.971
Large HDL particle (mol/L)	0.738	0.971
Medium HDL particle (mol/L)	0.884	0.971
Small HDL particle (mol/L)	0.627	0.971
VLDL size (nm)	0.776	0.971
LDL size (nm)	0.871	0.971
HDL size (nm)	0.404	0.971
Non-HDL particle (nmol/L)	0.271	0.971
Total particle / HDL particle (nmol/L)	0.866	0.971
LDL particle / HDL particle (nmol/L)	0.896	0.971

FDR: false discovery rate

Table S8: Comparison of the Full Blood Count of N versus AB Clusters

Features	N, median [IQR]	AB, median [IQR]	log change	p-value	FDR
Haematocrit	0.354 [0.312 0.392]	0.28 [0.261 0.306]	-0.32	0.003	0.015
White cell count (/L^9)	7.315 [5.772 10.12]	10.8 [8.27 15.04]	0.73	0.011	0.040
Haemaglobin (g/DL)	11.2 [10.2 12.95]	9.15 [8.725 9.85]	-0.29	0.002	0.015
Platelet count (/L^9)	352.5 [250.75 450.5]	410 [351.5 460.75]	0.25	0.137	0.250
Prothrombin time (Sec)	13.3 [12.4 14.8]	14.2 [12.8 14.475]	0.05	0.719	0.798
INR	1.08 [0.99 1.19]	1.115 [1.032 1.168]	0.06	0.639	0.798
MCV (fL)	92.3 [87.8 96.5]	89.35 [87.625 95.65]	0	0.826	0.826
MCH (pg)	30.2 [28.1 31.4]	29.8 [28.825 32.1]	0.03	0.725	0.798
MCHC (g/dl)	32.7 [31.3 33.4]	33.5 [32.2 34.15]	0.03	0.131	0.250
MPV (fL)	10.5 [9.475 10.8]	10.75 [9.825 11.2]	0.05	0.172	0.271
Red cell count (/L^12)	3.77 [3.42 4.54]	2.985 [2.75 3.473]	-0.12	0.020	0.055

IQR: Interquartile range; FDR: false discovery rate

Table S9: Comparison of the Blood chemistry of N versus AB components.

Feature	N, median [IQR]	AB, median [IQR]	log change	p-value	FDR
Sodium (mmol/L)	138 [135 140]	136.5 [130.5 138.5]	-0.04	0.063	0.260
Potassium (mmol/L)	3.8 [3.4 4.5]	3.65 [3.35 3.875]	-0.08	0.403	0.448
Chloride (mmol/L)	97 [93 99]	93 [91.25 96]	-0.04	0.078	0.260
Bicarbonate (mmol/L)	21 [19 24]	18.5 [17 24]	-0.14	0.186	0.321
Anion gap (mmol/L)	23 [20 27]	27.5 [21.25 30.75]	0.07	0.395	0.448
Calcium(mmol/L)	2.2 [2.13 2.32]	2.14 [1.997 2.223]	-0.14	0.107	0.267
Magnesium (mmol/L)	0.84 [0.79 0.92]	0.72 [0.673 0.753]	-0.29	0.019	0.190
Inorganic Phosphate (mmol/L)	1.13 [1.03 1.26]	1.02 [0.938 1.198]	-0.16	0.192	0.321
Urea (mmol/L)	4.3 [2.9 5.6]	3.25 [2 8.175]	0.17	0.747	0.747
Creatinine (µmol/L)	75 [63 97]	62.5 [52.75 88.75]	-0.22	0.266	0.380

IQR: Interquartile range; FDR: false discovery rate

Table S10: Comparison of the Liver function tests of N versus AB components.

Feature	N, median [IQR]	AB, median [IQR]	log change	p-val	FDR
Total Protein (g/L)	68 [59 76]	58 [53 64]	-0.23	0.018	0.029
Albumin (g/L)	36 [28 40]	27.5 [26.25 29.75]	-0.34	0.002	0.012

Total Bilirubin (µmol/L)	43 [8 100]	174.5 [143.25 266]	1.32	0.003	0.012
Conjugated Bilirubin (µmol/L)	31 [3 97]	146 [126.75 241.5]	1.34	0.006	0.016
Alanine transaminase (U/L)	28 [18 71]	81.5 [23.25 113.25]	0.2	0.371	0.425
Aspartate transaminase (U/L)	42 [24 92]	115.5 [83 148.5]	0.82	0.009	0.018
Alkaline phosphatase (U/L)	288 [103 683]	696 [330.25 1378.25]	0.62	0.044	0.059
Gamma glutamyl transferase (U/L)	307 [77 1021]	394 [208 926.25]	-0.04	0.650	0.650

IQR: Interquartile range; FDR: false discovery rate

Table S11: Comparison of the metabolite concentration of N versus AB clusters.

Features	N (mM), median [IQR]	AB (mM), median [IQR]	log change	p-value	FDR
Formate	0.016 [0.011 0.019]	0.019 [0.016 0.022]	0.24	0.067	0.225
Unknown signal at 8.12 ppm	0 [0 0.007]	0 [0 0.023]	1.18	0.304	0.550
Unknown signal at 8.07 ppm	0 [0 0.005]	0 [0 0.01]	1	0.193	0.411
Phenylalanine	0.104 [0.069 0.128]	0.113 [0.102 0.143]	0.14	0.080	0.225
Tyrosine	0.046 [0.036 0.052]	0.04 [0.035 0.054]	-0.44	0.585	0.787
Unknown signal at 7.14 ppm	0.026 [0 0.079]	0.034 [0 0.052]	-0.78	0.820	0.889
Histidine	0.064 [0.055 0.082]	0.074 [0.064 0.078]	-0.01	0.313	0.550
Glucose	3.532 [3.029 4.205]	3.549 [2.546 4.962]	0.13	0.952	0.980
Mannose	0.037 [0.028 0.051]	0.078 [0.037 0.115]	1.06	0.005	0.029
Unknown signal at 5.15 ppm	0 [0 0]	0 [0 0]	0.23	0.607	0.787
Unknown signal at 5.09 ppm	0 [0 0.043]	0 [0 0.032]	-0.67	0.696	0.845
Unknown signal at 5.01 ppm	0 [0 0]	0 [0 0]	0.99	0.151	0.340
Ascorbate	0.01 [0 0.019]	0 [0 0.014]	-0.6	0.397	0.621
Threonine	0.079 [0.06 0.091]	0 [0 0.043]	-1.47	0.002	0.013
Lactate	2.253 [2.013 3.114]	2.927 [2.62 3.179]	-0.01	0.153	0.340
Creatinine	0.057 [0.044 0.073]	0.053 [0.031 0.076]	-0.11	0.520	0.781
Creatine	0.012 [0.006 0.035]	0.002 [0 0.028]	-0.56	0.089	0.227
Glycine	0.318 [0.242 0.354]	0.311 [0.273 0.353]	-0.12	0.952	0.980
Methanol	0.027 [0.018 0.036]	0.021 [0.013 0.023]	-0.55	0.054	0.219
Unknown signal at 2.55 ppm	0 [0 0.013]	0 [0 0.013]	-3.27	0.589	0.787
Citrate	0.081 [0 0.103]	0.09 [0 0.123]	-0.11	0.100	0.100
Glutamine	0.4 [0.294 0.424]	0.268 [0.197 0.294]	-0.57	<0.001	0.007
Pyruvate	0.058 [0.048 0.072]	0.061 [0.047 0.091]	0.08	0.762	0.883
Glutamate	0.19 [0.129 0.272]	0.202 [0.155 0.285]	0.09	0.402	0.621
Acetoacetate	0.019 [0.016 0.041]	0.025 [0.017 0.089]	0.09	0.301	0.550
Acetate	0.024 [0.02 0.033]	0.032 [0.026 0.039]	0.09	0.120	0.292
Alanine	0.395 [0.293 0.481]	0.341 [0.273 0.35]	-0.56	0.051	0.219
Unknown signal at 1.45 ppm	0.031 [0.024 0.039]	0.02 [0 0.049]	-0.18	0961	0.980
Unknown signal at 1.43 ppm	0 [0 0]	0 [0 0.405]	1.85	0.005	0.029
3-Hydroxybutyrate	0.046 [0.028 0.1]	0.05 [0.037 0.451]	0.73	0.580	0.787
Ethanol	0.022 [0 0.083]	0 [0 0.084]	-0.81	0.389	0.621
Unknown signal at 1.16 ppm	0.112 [0 0.297]	0.168 [0.026 0.337]	0.08	0.610	0.787
Unknown signal at 1.14 ppm	0.019 [0 0.043]	0.016 [0 0.029]	-0.81	0.729	0.865
Unknown signal at 1.11 ppm	0.053 [0.044 0.061]	0.061 [0.041 0.073]	0.01	0.633	0.787
Unknown signal at 1.06 ppm	0.029 [0.021 0.038]	0.044 [0.026 0.067]	0.24	0.057	0.219
Valine	0.163 [0.127 0.183]	0.139 [0.105 0.161]	-0.35	0.084	0.225
Isoleucine	0.041 [0.033 0.053]	0.046 [0.042 0.054]	0.06	0.391	0.621
Leucine	0.068 [0.055 0.075]	0.05 [0.042 0.067]	-0.59	0.021	0.108
2-Hydroxybutyrate	0 [0 0.021]	0.009 [0 0.048]	1.07	0.312	0.550
Protein NH	144.358 [121.287 154.93]	105.798 [104.188 112.176]	-0.36	<0.001	<0.001
Unsaturated lipid -CH=CH-	11.141 [8.332 14.097]	14.379 [9.344 19.988]	0.36	0.080	0.225
Lipid alpha-CH2	1.863 [1.252 2.379]	6.257 [4.119 8.056]	1.7	<0.001	<0.001
Cholesterol	0.825 [0.644 1.064]	0.516 [0.27 0.934]	-0.37	0.060	0.219
Lipid =CH-CH2-CH=	4.954 [3.999 6.138]	5.02 [3.569 7.556]	0.17	0.818	0.889
Glycerol phospholipid	0.487 [0.243 0.77]	1.663 [1.412 2.797]	1.94	<0.001	<0.001
Phospholipid	3.699 [3.478 4.142]	3.128 [2.95 3.39]	-0.24	<0.001	0.005
Lipid beta-CH2	7.403 [5.083 8.55]	10.095 [6.281 12.356]	0.35	0.084	0.225
Lipid CH2	62.251 [55.441 75.596]	111.18 [73.472 140.862]	0.71	<0.001	0.001
Lipid CH3	26.385 [21.436 29.909]	27.943 [23.387 34.927]	0.14	0.279	0.550
GlycB	0.406 [0.322 0.471]	0.407 [0.366 0.436]	-0.04	0.799	0.889
GlycA	1.996 [1.535 2.186]	1.833 [1.701 2.005]	-0.03	0.619	0.787

IQR: Interquartile range; FDR: false discovery rate

Table S12: Comparison of the lipid extracts concentration of N versus AB clusters.

Feature	N, median [IQR]	AB, median [IQR]	log change	p-value	FDR
cholesterol-derivated 1	0.661 [0.571 0.791]	1.46 [1.158 1.675]	0.88	<0.001	<0.001
cholesterol-derivated 2	0.613 [0.537 0.75]	1.484 [1.15 1.745]	0.97	<0.001	<0.001
cholesterol-derivated 3	0.805 [0.694 0.893]	1.273 [1.118 1.327]	0.48	<0.001	<0.001
cholesterol-derivated 4	0.639 [0.569 0.778]	1.424 [1.185 1.641]	0.85	<0.001	<0.001
cholesterol-derivated 5	1.299 [0.909 1.667]	0.271 [0.241 0.385]	-2.14	<0.001	<0.001

free cholesterol	0.193 [0.055 0.271]	2.095 [0.96 3.516]	2.52	<0.001	<0.001
esterified cholesterol	0.93 [0.572 1.271]	1.073 [0.343 1.437]	-0.03	0.977	0.977
cholesterol-derivated 6	0.608 [0.526 0.828]	1.54 [0.835 2.05]	0.99	0.002	0.002
cholesterol-derivated 7	1.069 [0.907 1.394]	0.713 [0.604 0.784]	-0.67	<0.001	<0.001
cholesterol-derivated 8	0.607 [0.547 0.822]	1.468 [1.162 1.69]	0.9	<0.001	<0.001
cholesterol-derivated 9	1.127 [0.747 1.75]	0.333 [0.31 0.401]	-1.87	<0.001	<0.001
saturated and omega-9 fatty acid	0.667 [0.538 0.833]	1.443 [1.223 1.999]	1.07	<0.001	<0.001
omega-7 fatty acid	0.909 [0.78 1.043]	1.126 [0.982 1.221]	0.36	0.002	0.002
omega-6 fatty acid	0.583 [0.367 1.078]	1.448 [1.256 1.851]	1.07	<0.001	<0.001
Unknown signal at 0.91 ppm	0 [0 0]	0 [0 0]	-	0.230	0.240
omega-3 fatty acid	0.626 [0.397 0.798]	1.748 [1.159 1.915]	1.14	<0.001	<0.001
monounsaturated fatty acid	0.38 [0.193 0.656]	1.898 [1.386 2.441]	2.06	<0.001	<0.001
Polyunsaturated fatty acid 1	0.552 [0.342 0.832]	1.63 [1.211 2.031]	1.46	<0.001	<0.001
Polyunsaturated fatty acid 2	0.536 [0.334 0.812]	1.736 [1.327 2.057]	1.47	<0.001	<0.001
linoleic acid	0.476 [0.228 0.756]	1.582 [1.234 2.454]	1.53	<0.001	<0.001
phosphatidylcholine	0.533 [0.419 0.669]	1.624 [1.108 2.288]	1.52	<0.001	<0.001
sphingomyelin	0.594 [0.499 0.833]	1.205 [0.928 1.719]	0.97	<0.001	<0.001
triglyceride	0.59 [0.474 0.838]	1.643 [1.413 2.011]	1.41	<0.001	<0.001
glycerophospholipid	0.494 [0.393 0.614]	1.704 [1.26 2.384]	1.65	<0.001	<0.001

IQR: Interquartile range; FDR: false discovery rate

Table S13: Comparison of the metabolite concentration ratios of N versus AB clusters.

Feature	N, median [IQR]	AB, median [IQR]	log change	p-value	FDR
Glucose/Pyruvate	1.483 [1.254 1.769]	1.201 [0.975 1.774]	0.10	0.459	0.689
Pyruvate/Lactate	0.023 [0.019 0.031]	0.027 [0.017 0.029]	-0.05	0.799	0.912
Threonine/Glycine	0.248 [0.207 0.31]	0 [0 0.152]	-1.51	0.004	0.019
Glutamine/Glutamate	1.966 [1.23 3.538]	1.378 [0.704 2.113]	-0.80	0.029	0.048
3-Hydroxybutyrate/Acetoacetate	2.566 [1.258 3.729]	2.415 [0.865 4.247]	0.11	0.912	0.912
Glutamate/Alanine	0.52 [0.358 0.606]	0.634 [0.516 0.976]	0.59	0.013	0.031

IQR: Interquartile range; FDR: false discovery rate

Table S14: Comparison of the metabolite concentration ratios of N versus AB clusters

Feature	N, median [IQR]	AB, median [IQR]	log change	p-value	FDR
VLDL cholesterol (nmol/L)	17.81 [11.205 24.26]	24.08 [16.92 34.872]	0.58	0.025	0.030
IDL. cholesterol (nmol/L)	17.31 [10.345 21.475]	73.96 [52.33 82.738]	1.91	<0.001	<0.001
LDL cholesterol (nmol/L)	108.36 [87.245 130.24]	146.94 [119.998 165.042]	0.38	0.008	0.010
HDL cholesterol (nmol/L)	36.31 [28.005 50.43]	1 [1 1]	-4.99	<0.001	<0.001
VLDL triglyceride (nmol/L)	73.84 [47.195 92.89]	108.86 [82.815 141.52]	0.77	<0.001	0.001
IDL triglyceride (nmol/L)	15.4 [11.215 18.165]	50.75 [35.712 57.97]	1.55	<0.001	<0.001

LDL triglyceride (nmol/L)	18.96 [11.86 30.375]	72.13 [48.785 85.205]	1.59	<0.001	<0.001
HDL triglyceride (nmol/L)	17.76 [15.12 22.85]	24.345 [13.485 30.7]	0.25	0.459	0.459
VLDL particle (nmol/L)	50.87 [33.49 65.585]	79.76 [56.802 104.332]	0.75	<0.001	0.001
Large VLDL particle(nmol/L)	1.38 [0.875 1.61]	1.445 [1.375 1.7]	0.39	0.095	0.103
Medium VLDL particle (nmol/L)	5.53 [4.03 7.4]	5.465 [5.07 7.022]	0.31	0.440	0.458
Small VLDL particle(nmol/L)	43.15 [29.4 56.13]	74.645 [50.73 96.23]	0.8	<0.001	<0.001
LDL particle (nmol/L)	1113.73 [848.825 1331.92]	1745.03 [1458.052 2184.075]	0.66	<0.001	<0.001
Large LDL particle (nmol/L)	180.92 [131.475 215.42]	268.655 [194.603 301.295]	0.45	0.002	<0.001
Medium LDL particle (nmol/L)	349.05 [194.215 521.08]	868.56 [666.858 1136.122]	1.12	<0.001	<0.001
Small LDL particle (nmol/L)	577.17 [480.125 661.975]	634.715 [559.785 805.162]	0.29	0.084	0.095
HDL particle (mol/L)	18.54 [14.905 25.96]	4.855 [2.812 5.335]	-2.13	<0.001	<0.001
Large HDL particle (mol/L)	0.28 [0.245 0.305]	0.175 [0.105 0.223]	-0.78	<0.001	<0.001
Medium HDL particle (mol/L)	10.55 [9.295 11.395]	5.735 [3.708 6.16]	-1	<0.001	<0.001
Small HDL particle (mol/L)	8.87 [3.175 15.98]	0 [0 0]	-5.7	<0.001	<0.001
VLDL size (nm)	42.2 [42.175 42.22]	42.16 [42.13 42.18]	0	0.001	0.002
LDL size (nm)	21.27 [21.135 21.46]	21.595 [21.505 21.655]	0.02	<0.001	<0.001
HDL size (nm)	8.5 [8.34 8.9]	9.55 [9.47 9.645]	0.15	<0.001	<0.001
Non-HDL particle (nmol/L)	1130.02 [847.865 1358.64]	1838.72 [1510.072 2274.648]	0.68	<0.001	<0.001
Total particle / HDL particle (nmol/L)	48.14 [35.675 98.015]	437.875 [354.01 539.432]	2.64	<0.001	<0.001
LDL particle / HDL particle (nmol/L)	43.99 [34.045 95.405]	414.975 [333.365 517.24]	2.63	<0.001	<0.001

IQR: Interquartile range; FDR: false discovery rate

Table S15: Correlation of metabolites with GlycA, GlycB, CRP, and Albumin intensity value.

	GlycA			GlycB			CRP			Albumin		
Feature	**rho**	**p-value**	**FDR**	**rho**	**p-value**	**FDR**	**rho**	**p-value**	**FDR**	**rho**	**p-value**	**FDR**
Formate	0.2	0.186	0.389	0.27	0.072	0.334	0.08	0.656	0.910	-0.27	0.101	0.477
Unknown signal at 8.12 ppm	-0.27	0.068	0.233	-0.23	0.122	0.367	-0.08	0.636	0.910	-0.14	0.387	0.658
Unknown signal at 8.07 ppm	-0.26	0.079	0.233	-0.16	0.304	0.583	0.03	0.847	0.910	-0.19	0.237	0.526
Phenylalanine	0.2	0.190	0.389	0.29	0.055	0.280	0.29	0.079	0.808	-0.21	0.197	0.523
Tyrosine	-0.33	0.027	0.175	-0.26	0.079	0.335	0.06	0.727	0.910	0.06	0.702	0.904
Unknown signal at 7.14 ppm	0.34	0.021	0.157	0.26	0.090	0.346	0.08	0.622	0.910	-0.26	0.115	0.477
Histidine	-0.56	<0.001	0.001	-0.49	<0.001	0.008	-0.16	0.358	0.829	0.07	0.662	0.904
Glucose	0.27	0.727	0.233	0.36	0.015	0.095	-0.22	0.184	0.829	0.05	0.740	0.904
Mannose	0.34	0.021	0.157	0.36	0.115	0.095	0.04	0.832	0.910	-0.21	0.192	0.523
Unknown signal at 5.15 ppm	-0.25	0.096	0.233	-0.14	0.358	0.593	-0.06	0.738	0.910	-0.18	0.269	0.553
Unknown signal at 5.09 ppm	0.26	0.086	0.233	0.18	0.233	0.583	-0.01	0.950	0.969	-0.29	0.076	0.477
Unknown signal at 5.01 ppm	-0.28	0.061	0.233	-0.16	0.286	0.583	0.07	0.692	0.910	-0.24	0.140	0.477
Ascorbate	-0.25	0.095	0.233	-0.25	0.099	0.346	-0.05	0.749	0.910	-0.04	0.806	0.909
Threonine	0.04	0.807	0.895	0.02	0.878	0.904	-0.16	0.344	0.829	0.3	0.064	0.477
Lactate	0.32	0.031	0.176	0.38	0.009	0.082	0.4	0.014	0.559	-0.2	0.218	0.523
Creatinine	-0.1	0.506	0.842	-0.06	0.693	0.803	-0.06	0.711	0.910	-0.04	0.820	0.909
Creatine	-0.06	0.675	0.842	-0.03	0.862	0.904	0.2	0.228	0.829	0	0.993	0.993
Glycine	0.07	0.643	0.842	0.13	0.397	0.610	0.16	0.356	0.829	-0.22	0.180	0.523
Methanol	-0.03	0.848	0.920	-0.18	0.237	0.583	0.04	0.830	0.910	0.35	0.028	0.283
Unknown signal at 2.55 ppm	0.08	0.619	0.842	-0.05	0.768	0.851	-0.16	0.341	0.829	0.22	0.169	0.523
Citrate	-0.18	0.237	0.465	-0.06	0.710	0.805	-0.08	0.642	0.910	-0.09	0.599	0.872
Glutamine	-0.06	0.694	0.842	-0.16	0.300	0.583	-0.25	0.137	0.829	0.05	0.773	0.909
Pyruvate	0.15	0.340	0.598	0.24	0.109	0.346	0.19	0.270	0.829	-0.24	0.135	0.477
Glutamate	0.02	0.879	0.934	0.07	0.645	0.783	0.09	0.595	0.910	-0.06	0.733	0.904
Acetoacetate	-0.3	0.049	0.233	-0.16	0.283	0.583	-0.03	0.857	0.910	-0.12	0.455	0.737
Acetate	-0.17	0.277	0.523	-0.08	0.596	0.760	-0.03	0.857	0.910	-0.16	0.318	0.588
Alanine	-0.1	0.531	0.842	-0.12	0.413	0.610	-0.07	0.695	0.910	0.25	0.124	0.477
Unknown signal at 1.45 ppm	0.6	<0.001	<0.001	0.65	<0.001	<0.001	0.36	0.028	0.559	-0.07	0.657	0.904
Unknown signal at 1.43 ppm	-0.29	0.055	0.233	-0.24	0.108	0.346	0.04	0.814	0.910	-0.28	0.087	0.477
3-Hydroxybutyrate	-0.06	0.677	0.842	0	0.977	0.977	0.12	0.475	0.910	-0.06	0.708	0.904
Ethanol	-0.05	0.726	0.842	-0.06	0.673	0.798	0	0.998	0.998	-0.11	0.493	0.761
Unknown signal at 1.16 ppm	0.06	0.713	0.842	0.12	0.430	0.610	-0.16	0.347	0.829	-0.16	0.320	0.588
Unknown signal at 1.14 ppm	0.22	0.149	0.330	0.15	0.338	0.593	0.17	0.321	0.829	0.12	0.462	0.737
Unknown signal at 1.11 ppm	0	0.999	0.999	0.11	0.490	0.657	-0.07	0.697	0.910	0	0.993	0.993
Unknown signal at 1.06 ppm	-0.26	0.090	0.233	-0.17	0.257	0.583	0.12	0.480	0.910	-0.16	0.323	0.588
Valine	-0.08	0.611	0.842	-0.12	0.443	0.611	-0.07	0.682	0.910	0.2	0.226	0.523
Isoleucine	0.25	0.103	0.238	0.15	0.325	0.591	-0.02	0.920	0.957	-0.11	0.510	0.766
Leucine	0.09	0.536	0.842	0.09	0.572	0.748	0.09	0.585	0.910	0.26	0.116	0.477
2-Hydroxybutyrate	-0.28	0.065	0.233	-0.14	0.361	0.593	0.12	0.465	0.910	-0.03	0.880	0.954
Protein NH	0.08	0.610	0.842	-0.03	0.831	0.902	-0.17	0.317	0.829	0.7	<0.001	<0.001
Unsaturated lipid -CH=CH-	-0.09	0.567	0.842	-0.16	0.286	0.583	0.23	0.174	0.829	0.04	0.786	0.909
Lipid alpha-CH2	-0.09	0.567	0.842	-0.13	0.397	0.610	0.33	0.043	0.559	-0.43	0.006	0.157
Cholesterol	0.01	0.926	0.964	-0.02	0.886	0.904	-0.04	0.825	0.910	0.27	0.099	0.477
Lipid =CH-CH2-CH=	0	0.986	0.999	-0.08	0.621	0.773	0.2	0.230	0.829	0.18	0.271	0.553
Glycorol phospholipid	-0.16	0.306	0.557	-0.21	0.172	0.488	0.25	0.143	0.829	-0.37	0.019	0.243
Phospholipid	0.42	0.004	0.041	0.41	0.005	0.055	0.06	0.703	0.910	0.4	0.012	0.198
Lipid beta-CH2	-0.27	0.073	0.233	-0.32	0.031	0.178	0.13	0.458	0.910	-0.02	0.917	0.974
Lipid CH2	-0.07	0.647	0.842	-0.15	0.309	0.583	0.33	0.043	0.559	-0.2	0.213	0.523
Lipid CH3	-0.04	0.801	0.895	-0.12	0.424	0.610	0.19	0.262	0.829	0.16	0.340	0.598
GlycB	0.9	<0.001	<0.001	1	0	0	0.22	0.195	0.829	0.01	0.969	0.993
GlycA	1	0	0	0.9	<0.001	<0.001	0.26	0.115	0.829	0.05	0.744	0.904

Rho: spearman's correlation coefficient measures the strength of association between two variables; FDR: false discovery ratio

Table S16: Correlation of lipid extracts with GlycA, GlycB, CRP, and Albumin intensity value.

	GlycA			GlycB			CRP			Albumin		
Feature	**rho**	**p-value**	**FDR**	**rho**	**p-value**	**FDR**	**rho**	**p-value**	**FDR**	**rho**	**p-value**	**FDR**
cholesterol-derivated 1	-0.17	0.296	0.666	-0.11	0.502	0.788	0.35	0.045	0.123	-0.54	<0.001	0.006
cholesterol-derivated 2	-0.16	0.328	0.666	-0.1	0.525	0.788	0.37	0.035	0.123	-0.53	0.001	0.006
cholesterol-derivated 3	-0.22	0.172	0.666	-0.17	0.282	0.788	0.41	0.019	0.123	-0.5	0.002	0.007
cholesterol-derivated 4	-0.17	0.299	0.666	-0.12	0.458	0.788	0.37	0.035	0.123	-0.54	<0.001	0.006
cholesterol-derivated 5	0.11	0.511	0.756	0.05	0.775	0.829	-0.35	0.044	0.123	0.51	0.002	0.006
free cholesterol	-0.18	0.273	0.666	-0.13	0.440	0.788	0.3	0.094	0.174	-0.39	0.020	0.044
esterified cholesterol	-0.04	0.815	0.857	-0.13	0.414	0.788	-0.09	0.632	0.632	0.34	0.044	0.082
cholesterol-derivated 6	-0.14	0.397	0.666	-0.04	0.798	0.829	0.26	0.146	2.00	-0.56	<0.001	0.060
cholesterol-derivated 7	-0.06	0.701	0.857	-0.04	0.829	0.829	-0.35	0.046	0.123	0.27	0.117	0.165
cholesterol-derivated 8	-0.16	0.338	0.666	-0.11	0.490	0.788	0.37	0.035	0.123	-0.51	0.002	0.006
cholesterol-derivated 9	0.1	0.535	0.756	0.1	0.545	0.788	-0.39	0.027	0.123	0.51	0.002	0.006
saturated and omega-9 fatty acid	-0.23	0.156	0.666	-0.14	0.372	0.788	0.32	0.071	0.172	-0.44	0.009	0.022
omega-7 fatty acid	-0.03	0.857	0.857	-0.05	0.736	0.829	0.18	0.321	0.335	-0.47	0.004	0.011
omega-6 fatty acid	-0.07	0.648	0.857	-0.1	0.558	0.788	0.23	0.196	0.235	-0.19	0.285	0.285
Unknown signal at 0.91 ppm	-0.03	0.837	0.857	-0.11	0.488	0.788	0.19	0.288	0.314	-0.24	0.163	0.218
omega-3 fatty acid	-0.16	0.323	0.666	-0.09	0.602	0.803	0.2	0.273	0.312	-0.29	0.095	0.142
monounsaturated fatty acid	-0.13	0.417	0.666	-0.1	0.539	0.788	0.3	0.093	0.174	-0.36	0.033	0.065
Polyunsaturated fatty acid 1	-0.14	0.376	0.666	-0.13	0.425	0.788	0.28	0.110	0.188	-0.19	0.284	0.285
Polyunsaturated fatty acid 2	-0.19	0.245	0.666	-0.16	0.326	0.788	0.26	0.150	2.00	-0.21	0.233	0.266
linoleic acid	-0.17	0.282	0.666	-0.14	0.390	0.788	0.26	0.147	2.00	-0.22	0.200	0.240
phosphatidylcholine	-0.19	0.237	0.666	-0.16	0.316	0.788	0.27	0.130	2.00	-0.32	0.063	0.100
sphingomyelin	-0.05	0.753	0.857	-0.04	0.814	0.829	0.3	0.091	0.174	-0.19	0.274	0.285
triglyceride	-0.04	0.825	0.857	-0.06	0.724	0.829	0.35	0.043	0.123	-0.23	0.176	0.222
glycerophospholipid	-0.15	0.347	0.666	-0.11	0.481	0.788	0.23	0.196	0.235	-0.33	0.050	0.086

Rho: spearman's correlation coefficient measures the strength of association between two variables; FDR: false discovery ratio

Table S17: Correlation of metabolite concentration ratios with GlycA, GlycB, CRP, and Albumin intensity value.

	GlycA			GlycB			CRP			Albumin		
Feature	**rho**	**p-value**	**FDR**	**rho**	**p-value**	**FDR**	**rho**	**p-value**	**FDR**	**rho**	**p-value**	**FDR**
Glucose/Lactate	-0.03	0.867	0.960	0.01	0.970	0.970	-0.44	0.006	0.004	0.19	0.256	0.683
Pyruvate/Lactate	-0.08	0.622	0.778	-0.07	0.631	0.631	-0.09	0.585	0.585	-0.08	0.644	0.683
Threonine/Glycine	-0.01	0.960	0.960	-0.08	0.584	0.631	-0.36	0.029	0.143	0.48	0.002	0.011
Glutamine/Glutamate	-0.09	0.568	0.778	-0.13	0.381	0.631	-0.18	0.286	0.408	0.07	0.683	0.683
3Hydroxybutyrate/Acetoacetate	0.12	0.431	0.778	0.12	0.450	0.631	0.24	0.160	0.399	-0.07	0.661	0.683
Glutamate/Alanine	0.11	0.473	0.778	0.12	0.417	0.631	0.17	0.326	0.408	-0.13	0.444	0.683

Rho: spearman's correlation coefficient measures the strength of association between two variables; FDR: false discovery ratio

Table S18: Correlation of lipoproteins with GlycA, GlycB, CRP, and Albumin intensity value.

	GlycA			GlycB			CRP			Albumin		
Lipoproteins	**rho**	**p-value**	**FDR**	**rho**	**p-value**	**FDR**	**rho**	**p-value**	**FDR**	**rho**	**p-value**	**FDR**
VLDL cholesterol (nmol/L)	0.18	0.224	0.937	-0.01	0.956	0.965	0.26	0.125	0.181	-0.08	0.684	0.684
IDL. cholesterol (nmol/L)	0.06	0.698	0.957	0.1	0.530	0.927	0.42	0.105	0.049	-0.57	<0.001	<0.001
LDL cholesterol (nmol/L)	-0.16	0.305	0.937	-0.08	0.582	0.927	0.2	0.233	0.275	-0.16	0.316	0.342
HDL cholesterol (nmol/L)	-0.17	0.278	0.937	-0.21	0.175	0.927	-0.44	0.007	0.049	0.66	<0.001	<0.001
VLDL triglyceride (nmol/L)	0.03	0.854	0.957	-0.12	0.431	0.927	0.28	0.938	0.163	-0.21	0.202	0.250
IDL triglyceride (nmol/L)	0.07	0.635	0.957	0.1	0.529	0.927	0.4	0.132	0.049	-0.57	<0.001	<0.001
LDL triglyceride (nmol/L)	0.01	0.996	0.966	0.06	0.713	0.927	0.38	0.189	0.062	-0.54	<0.001	<0.001
HDL triglyceride (nmol/L)	0.02	0.920	0.957	-0.01	0.956	0.965	0.11	0.522	0.565	-0.22	0.185	0.240
VLDL particle (nmol/L)	0.07	0.653	0.957	-0.07	0.630	0.927	0.3	0.762	0.142	-0.23	0.158	0.229
Large VLDL particle(nmol/L)	-0.02	0.872	0.957	-0.17	0.256	0.927	0.09	0.582	0.582	-0.18	0.285	0.322
Medium VLDL particle (nmol/L)	0.17	0.251	0.937	-0.08	0.618	0.927	0.17	0.319	0.361	0.12	0.452	0.470
Small VLDL particle(nmol/L)	0.06	0.711	0.957	-0.09	0.568	0.927	0.31	0.637	0.127	-0.25	0.129	0.197
LDL particle (nmol/L)	-0.16	0.279	0.937	-0.09	0.575	0.927	0.24	0.149	0.185	-0.29	0.760	0.124
Large LDL particle (nmol/L)	-0.03	0.856	0.957	-0.04	0.776	0.961	0.33	0.473	0.112	-0.18	0.268	0.317
Medium LDL particle (nmol/L)	-0.09	0.553	0.957	-0.02	0.901	0.965	0.27	0.104	0.169	-0.31	0.541	0.108
Small LDL particle (nmol/L)	-0.35	0.020	0.524	-0.26	0.904	0.927	0.1	0.568	0.582	-0.22	0.791	0.240
HDL particle (mol/L)	-0.16	0.283	0.937	-0.19	0.209	0.927	-0.42	0.944	0.049	0.67	<0.001	<0.001
Large HDL particle (mol/L)	0.09	0.547	0.957	-0.04	0.813	0.961	-0.26	0.121	0.181	0.49	<0.001	<0.001
Medium HDL particle (mol/L)	-0.05	0.760	0.957	-0.11	0.456	0.927	-0.31	0.625	0.127	0.37	<0.001	<0.001
Small HDL particle (mol/L)	-0.13	0.411	0.957	-0.17	0.267	0.927	-0.42	0.984	0.049	0.72	<0.001	<0.001
VLDL size (nm)	0.06	0.680	0.957	0.01	0.948	0.965	-0.25	0.133	0.181	0.4	<0.001	<0.001
LDL size (nm)	0.27	0.068	0.887	0.21	0.161	0.927	0.36	0.290	0.076	-0.29	0.713	0.124
HDL size (nm)	0.09	0.559	0.957	0.13	0.398	0.927	0.36	0.286	0.076	-0.69	<0.001	<0.001
Non-HDL particle (nmol/L)	-0.15	0.324	0.957	-0.08	0.587	0.927	0.25	0.143	0.185	-0.3	0.634	0.118
Total particle / HDL particle (nmol/L)	0.02	0.896	0.957	0.06	0.678	0.927	0.42	0.877	0.049	-0.59	<0.001	<0.001
LDL particle / HDL particle (nmol/L)	0.02	0.908	0.957	0.07	0.659	0.927	0.41	0.113	0.049	-0.58	<0.001	<0.001

Rho: spearman's correlation coefficient measures the strength of association between two variables; FDR: false discovery rate

Table S19: Comparison of Metabolites of Type 2 Diabetes Mellitus and Non-Type 2 Diabetes Mellitus PDAC patients

Feature	no, median [IQR]	yes, median [IQR]	logchange	p-value	FDR
Formate	0.018 [0.014 0.024]	0.016 [0.014 0.019]	-0.11	0.612	0.954
Phenylalanine	0.112 [0.083 0.136]	0.106 [0.098 0.139]	-0.1	0.914	0.100
Tyrosine	0.041 [0.034 0.049]	0.038 [0.034 0.052]	-0.3	0.100	0.100
Unknown signal at 7.14 ppm	0.03 [0 0.067]	0.051 [0.015 0.081]	0.55	0.315	0.954
Histidine	0.065 [0.057 0.076]	0.07 [0.057 0.079]	-0.04	0.508	0.954
Glucose	3.563 [3.108 4.492]	3.76 [3.557 4.107]	0.1	0.528	0.954
Mannose	0.042 [0.034 0.063]	0.046 [0.033 0.072]	0.03	0.890	0.100
Ascorbate	0.006 [0 0.015]	0 [0 0.006]	-1.16	0.171	0.821
Threonine	0.066 [0 0.09]	0.067 [0.01 0.088]	-0.08	0.987	0.100
Lactate	2.682 [2.109 3.205]	3.028 [2.484 3.152]	-0.06	0.569	0.954
Creatinine	0.056 [0.041 0.076]	0.056 [0.032 0.087]	-0.1	0.890	0.100
Creatine	0.01 [0.005 0.029]	0.003 [0 0.009]	-1.71	0.092	0.718
Glycine	0.328 [0.265 0.374]	0.287 [0.237 0.315]	-0.35	0.089	0.718
Methanol	0.022 [0.013 0.028]	0.023 [0.021 0.036]	0.36	0.177	0.821
Unknown signal at 2.55 ppm	0 [0 0.013]	0.005 [0 0.566]	1.07	0.289	0.954
Citrate	0.09 [0.012 0.121]	0 [0 0.073]	-0.98	0.062	0.718
Glutamine	0.328 [0.269 0.417]	0.283 [0.235 0.385]	-0.24	0.396	0.954
Pyruvate	0.068 [0.047 0.08]	0.06 [0.052 0.068]	-0.19	0.963	0.100
Glutamate	0.201 [0.134 0.282]	0.213 [0.149 0.326]	0.07	0.656	0.954
Acetoacetate	0.029 [0.017 0.079]	0.016 [0.012 0.017]	-2.04	0.010	0.523
Acetate	0.029 [0.021 0.035]	0.025 [0.019 0.028]	-0.24	0.432	0.954
Alanine	0.347 [0.263 0.433]	0.352 [0.336 0.423]	-0.21	0.469	0.954
3-Hydroxybutyrate	0.052 [0.036 0.171]	0.042 [0 0.059]	-2.42	0.113	0.718
Ethanol	0.017 [0 0.248]	0 [0 0.02]	-2.8	0.161	0.821
Valine	0.143 [0.115 0.164]	0.162 [0.138 0.172]	-0.1	0.488	0.954
Isoleucine	0.045 [0.035 0.055]	0.044 [0.037 0.051]	-0.03	0.950	0.100
Leucine	0.055 [0.045 0.071]	0.069 [0.052 0.07]	0.01	0.417	0.954
2-Hydroxybutyrate	0 [0 0.035]	0 [0 0.013]	-2.88	0.274	0.954
Protein NH	121.287 [110.147 144.185]	125.738 [106.732 149.702]	0.05	0.890	0.100
Unsaturated lipid -CH=CH-	11.452 [8.937 15.12]	11.008 [8.385 14.142]	-0.12	0.656	0.954
Lipid alpha-CH2	3.167 [1.68 4.833]	2.012 [1.468 3.611]	-0.07	0.432	0.954
Cholesterol	0.842 [0.603 1.088]	0.536 [0.472 0.659]	-0.52	0.058	0.718
Lipid =CH-CH2-CH=	4.844 [4.03 6.554]	4.509 [3.611 5.98]	-0.18	0.414	0.954
Glycorol phospholipid	1.026 [0.355 1.619]	0.556 [0.458 1.143]	0.12	0.701	0.966
Phospholipid	3.619 [3.222 3.929]	3.485 [2.949 3.781]	-0.04	0.528	0.954
Lipid beta-CH2	7.472 [5.963 10.125]	7.136 [5.252 8.997]	-0.11	0.590	0.954
Lipid CH2	74.209 [60.357 108.095]	66.151 [57.175 71.996]	-0.08	0.548	0.954
Lipid CH3	26.309 [21.235 32.924]	25.705 [21.138 29.265]	-0.1	0.634	0.954
GlycB	0.416 [0.376 0.459]	0.431 [0.333 0.473]	-0.08	0.818	0.100
GlycA	1.986 [1.791 2.073]	2.026 [1.611 2.234]	-0.02	0.963	0.100

IQR: Interquartile range; FDR: false discovery rate, Type2 Diabetes Mellitus (T2DM)

Table S20: Comparison of Lipoproteins of Type 2 Diabetes Mellitus and Non-Type 2 Diabetes Mellitus PDAC patients

Feature	no, median [IQR]	yes, median [IQR]	logchange	p-value	FDR
VLDL.C	20.92 [13.65 28.593]	20.675 [12.652 24.52]	-0.01	0.866	0.866
IDL.C	33.185 [18.238 53.638]	17.14 [10.75 43.74]	-0.38	0.198	0.515
LDL.C	130.235 [101.652 165.042]	104.56 [71.305 122.718]	-0.36	0.089	0.401
HDL.C	25.745 [1 34.135]	30.715 [6.98 41.048]	0.56	0.436	0.667
VLDL.TG	84.935 [56.172 109.148]	79.33 [59.372 95.342]	0.11	0.656	0.735
IDL.TG	24.595 [15.893 36.3]	16.65 [11.02 31.165]	-0.26	0.246	0.533
LDL.TG	34.775 [21.292 49.635]	18.9 [16.882 43.678]	-0.36	0.198	0.515
HDL.TG	18.4 [14.343 24.385]	20.805 [16.738 24.758]	0.05	0.590	0.735
VLDL.P..nmol.L.	58.56 [41.36 82.66]	55.705 [41.465 65.25]	0.02	0.612	0.735
Large.VLDL.P..nmol.L.	1.415 [1.152 1.655]	1.5 [1.197 1.647]	0.16	0.628	0.735
Medium.VLDL.P..nmol.L.	5.425 [4.248 7.058]	6.51 [4.89 8.593]	0.39	0.349	0.593
Small.VLDL.P..nmol.L.	49.415 [36.58 73.048]	48.05 [35.208 55.1]	-0.03	0.678	0.735
LDL.P..nmol.L.	1387.165 [1097.463 1999.575]	995.95 [670 1615.953]	-0.4	0.123	0.401
Large.LDL.P..nmol.L.	209.455 [177.918 299.16]	178.64 [126.795 228.485]	-0.33	0.077	0.401
Medium.LDL.P..nmol.L.	575.865 [364.855 866.215]	286.225 [200.548 797.315]	-0.44	0.246	0.533
Small.LDL.P..nmol.L.	601.97 [533.578 766.985]	496.43 [383.19 575.985]	-0.38	0.036	0.401
HDL.P..Î¼mol.L.	12.88 [5.37 17.915]	15.33 [7.488 24.132]	0.42	0.315	0.586
Large.HDL.P..Î¼mol.L.	0.245 [0.2 0.288]	0.26 [0.23 0.298]	0.06	0.650	0.735
Medium.HDL.P..Î¼mol.L.	8.965 [6.123 10.558]	9.64 [7.01 10.86]	0.15	0.553	0.735
Small.HDL.P..Î¼mol.L.	2.135 [0 6.888]	4.255 [0.66 14.142]	0.8	0.297	0.586
VLDL.Z..nm.	42.18 [42.133 42.2]	42.215 [42.182 42.22]	0	0.041	0.401
LDL.Z..nm.	21.44 [21.202 21.55]	21.455 [21.298 21.512]	0	0.815	0.847
HDL.Z..nm.	8.945 [8.6 9.485]	8.8 [8.362 9.408]	-0.03	0.365	0.593
Non.HDL.P..nmol.L.	1433.85 [1140.635 2069.925]	1008.82 [691.59 1726.787]	-0.39	0.116	0.401
Total.P.HDL.P	141.41 [66.422 393.192]	48.125 [33.44 295.73]	-0.56	0.109	0.401
LDL.P.HDL.P	138.065 [64.638 375.593]	43.95 [31.9 275.938]	-0.58	0.116	0.401

IQR: Interquartile range; FDR: false discovery rate, Type2 Diabetes Mellitus (T2DM)

Table S21: Comparison of Lipid Extracts of Type 2 Diabetes Mellitus and Non-Type 2 Diabetes Mellitus PDAC patients

Feature	no, median [IQR]	yes, median [IQR]	logchange	*p*-value	FDR
cholesterol-derivated 1	1332204.612 [870710.069 1902617.633]	888490.948 [731956.34 1032939.739]	-0.43	0.117	0.499
cholesterol-derivated 2	504433.323 [303978.254 743006.048]	306507.922 [222042.683 424406.439]	-0.52	0.073	0.499
cholesterol-derivated 3	255083.658 [210882.393 343686.673]	209930.22 [184086.972 231440.196]	-0.26	0.192	0.539
cholesterol-derivated 4	1369666.285 [875363.101 1964922.924]	830237.803 [717494.185 1015920.4]	-0.56	0.036	0.499
cholesterol-derivated 5	747567.626 [258196.12 1231683.507]	913403.042 [328890.688 1507419.324]	0.35	0.228	0.539
free cholesterol	5368936.265 [1672835.88 12350261.475]	1410127.91 [453501.951 7008353.376]	-0.2	0.295	0.590
esterified cholesterol	6675226.515 [2535461.488 9740771.238]	6593550.569 [5128438.945 9041894.033]	0.04	0.774	0.886
cholesterol-derivated 6	273597.239 [194014.182 452699.423]	190590.655 [159156.823 259523.193]	-0.57	0.101	0.499
cholesterol-derivated 7	265491.627 [217683.474 308051.79]	270603.118 [210017.586 345407.244]	0.06	0.747	0.886
cholesterol-derivated 8	555840.208 [327978.135 805864.865]	344829.457 [261219.329 395929.103]	-0.57	0.061	0.499
cholesterol-derivated 9	270860.785 [126321.7 447673.102]	355413.992 [175926.368 648537.348]	0.47	0.125	0.499
saturated and omega-9 fatty acid	23068787.119 [16665031.7 34016352.107]	13857291.856 [13035461.901 26814647.265]	-0.14	0.205	0.539
omega-7 fatty acid	9164120.611 [7360223.424 9685477.688]	7991613.618 [7388554.633 8008262.636]	-0.16	0.176	0.539
omega-6 fatty acid	16728006.705 [7946107.124 20615567.233]	11857587.058 [5085601.513 25221047.039]	-0.08	0.715	0.886
Unknown signal at	0 [0 0]	0 [0 0]	-0.44	0.434	0.802
omega-3 fatty acid	1723209.088 [1066881.635 2910180.221]	1328230.444 [975026.424 1981566.024]	-0.25	0.584	0.886
monounsaturate fatty acid	21869585.841 [9330438.555 32288448.408]	9083665.265 [6831261.232 41284045.632]	0.01	0.615	0.886
polyunsaturate fatty acid 1 (except linoleic)	7040948.967 [3930333.852 12026322.483]	4882682.911 [4319077.294 13698800.978]	0.1	0.886	0.886
polyunsaturate fatty acid 2 (except linoleic)	4123176.98 [2830866.275 6852127.55]	2473530.529 [1994100.56 8456592.567]	0.05	0.693	0.886
linoleic acid	8528418.382 [3978643.649 13575696.407]	5431173.466 [3640526.156 13836359.688]	0.03	0.858	0.886
phosphatidylcholine	10720758.528 [6279375.384 17975432.64]	7296037.292 [5403883.027 13651889.081]	0.01	0.886	0.886
sphingomyelin	1804252.686 [1366298.706 3157141.528]	1287269.748 [1169439.217 2534385.902]	-0.3	0.247	0.539
triglyceride	5334849.323 [3368178.363 8351749.562]	4611140.095 [3166847.912 8515446.122]	0.09	0.886	0.886
glycerophospholipid	8163649.219 [4305834.629 14317656.749]	5326823.545 [4520632.311 8656695.015]	-0.04	0.886	0.886

IQR: Interquartile range; FDR: false discovery rate, Type2 Diabetes Mellitus (T2DM)

Table S22: Comparison of Metabolic Ratios of Type 2 Diabetes Mellitus and Non-Type 2 Diabetes Mellitus PDAC patients

Feature	no, median [IQR]	yes, median [IQR]	logchange	*p*-value	FDR
Glucose/Lactate	1.468 [1.018 1.831]	1.517 [1.217 1.648]	-0.1	0.988	0.988
Pyruvate/Lactate	0.024 [0.018 0.03]	0.021 [0.018 0.028]	-0.12	0.528	0.792
Threonine/Glycine	0.209 [0 0.265]	0.296 [0.061 0.352]	0.52	0.102	0.486
Glutamine/Glutamate	1.825 [1.195 2.819]	1.425 [0.668 2.426]	-0.29	0.363	0.725
3-Hydroxybutyrate/Acetoacetate	2.736 [1.377 4.451]	2.377 [0 3.052]	-0.7	0.162	0.486
Glutamate/Alanine	0.565 [0.449 0.69]	0.528 [0.465 0.876]	0.1	0.770	0.924

IQR: Interquartile range; FDR: false discovery rate, Type2 Diabetes Mellitus (T2DM)

Table S23: Comparison of Metabolites of PDAC patients with High and Low Glasgow Prognostic Scores

Feature	high GPS, median [IQR]	low GPS, median [IQR]	logchange	*p*-value	FDR
Formate	0.018 [0.016 0.023]	0.018 [0.013 0.024]	-0.16	0.460	0.815
Phenylalanine	0.118 [0.105 0.142]	0.1 [0.078 0.118]	-0.39	0.074	0.474
Tyrosine	0.038 [0.034 0.05]	0.045 [0.035 0.05]	-0.4	0.577	0.841
Histidine	0.07 [0.062 0.076]	0.063 [0.055 0.078]	-0.23	0.497	0.815
Glucose	3.662 [3.255 4.26]	3.79 [3.37 5.053]	0.09	0.478	0.815
Mannose	0.047 [0.035 0.09]	0.038 [0.033 0.059]	-0.52	0.257	0.727
Ascorbate	0.006 [0 0.014]	0 [0 0.015]	-0.33	0.731	0.935
Threonine	0 [0 0.072]	0.081 [0.067 0.092]	0.93	0.020	0.186
Lactate	2.927 [2.529 3.243]	2.493 [2.122 3.151]	-0.37	0.220	0.727
Creatinine	0.048 [0.038 0.093]	0.06 [0.044 0.073]	-0.04	0.869	0.959
Creatine	0.009 [0 0.051]	0.01 [0.004 0.019]	-1.51	0.926	0.959
Glycine	0.317 [0.278 0.375]	0.327 [0.255 0.348]	-0.2	0.537	0.815
Methanol	0.022 [0.013 0.027]	0.023 [0.015 0.032]	0.14	0.537	0.815
Citrate	0.072 [0 0.119]	0.073 [0 0.104]	0.2	0.742	0.935
Glutamine	0.293 [0.25 0.383]	0.4 [0.273 0.424]	0.1	0.133	0.615
Pyruvate	0.068 [0.047 0.093]	0.058 [0.049 0.071]	-0.4	0.517	0.815
Glutamate	0.202 [0.138 0.313]	0.219 [0.131 0.302]	-0.16	0.707	0.935
Acetoacetate	0.019 [0.016 0.086]	0.021 [0.016 0.035]	0.53	0.869	0.959
Acetate	0.027 [0.022 0.039]	0.025 [0.021 0.033]	0.06	0.641	0.907
Alanine	0.347 [0.267 0.4]	0.396 [0.32 0.473]	-0.23	0.209	0.727
Unknown signal at 1.45 ppm	0.035 [0 0.049]	0.031 [0.026 0.04]	0.08	0.902	0.959
Unknown signal at 1.43 ppm	0 [0 0.088]	0 [0 0]	-4.2	0.112	0.599
3-Hydroxybutyrate	0.044 [0.023 0.256]	0.055 [0.04 0.062]	-0.24	0.902	0.959
Ethanol	0 [0 0.206]	0 [0 0.027]	-1.59	0.490	0.815
Valine	0.139 [0.101 0.163]	0.163 [0.142 0.174]	0.04	0.117	0.599
Isoleucine	0.045 [0.038 0.052]	0.045 [0.037 0.062]	0.06	0.807	0.959
Leucine	0.055 [0.044 0.07]	0.066 [0.055 0.075]	0.04	0.240	0.727
2-Hydroxybutyrate	0 [0 0.043]	0 [0 0.02]	-1.81	0.391	0.815
Protein NH	108.537 [103.949 124.878]	146.281 [127.643 154.61]	0.32	<0.001	0.003
Unsaturated lipid -CH=CH-	11.205 [8.422 18.539]	12.656 [10.199 14.501]	-0.04	0.752	0.935
Lipid alpha-CH2	4.163 [2.397 6.801]	1.965 [1.554 2.411]	-1.01	0.005	0.137
Cholesterol	0.563 [0.291 0.883]	0.959 [0.685 1.093]	0.52	0.022	0.186
Lipid =CH-CH2-CH=	4.46 [3.529 6.47]	5.493 [4.33 6.623]	0.11	0.244	0.727
Glycorol phospholipid	1.472 [0.491 1.897]	0.501 [0.395 0.802]	-1.25	0.022	0.186
Phospholipid	3.171 [3.028 3.759]	3.771 [3.554 4.246]	0.19	0.013	0.186
Lipid beta-CH2	7.273 [5.705 11.198]	7.508 [7.125 9.083]	-0.06	0.940	0.959
Lipid CH2	76.744 [62.021 123.253]	64.949 [58.914 75.226]	-0.33	0.177	0.727
Lipid CH3	25.153 [20.875 32.146]	28.227 [24.144 31.069]	0.06	0.460	0.815
GlycB	0.407 [0.361 0.456]	0.441 [0.402 0.474]	0.08	0.357	0.815
GlycA	1.918 [1.686 2.081]	2.026 [1.782 2.221]	0.04	0.442	0.815

IQR: Interquartile range; FDR: false discovery rate, High GPS=2, Low GPS= 0 and 1

Table S24: Comparison of Lipoproteins of PDAC patients with High and Low Glasgow Prognostic Scores.

Feature	high GPS, median [IQR]	low GPS, median [IQR]	logchange	*p*-value	FDR
VLDL.C	20.575 [14.515 34.378]	22.14 [13.41 25.34]	-0.22	0.775	0.775
IDL.C	47.34 [33.14 76.58]	17.91 [13.45 22.34]	-1.23	<0.001	0.003
LDL.C	136.275 [105.815 161.287]	110.09 [99.19 134.11]	-0.13	0.424	0.479
HDL.C	1 [1 26.078]	38.54 [25.85 41.97]	1.89	<0.001	<0.001
VLDL.TG	85.405 [75.175 122.62]	81.56 [52.26 99.13]	-0.42	0.257	0.337
IDL.TG	32.78 [22.882 53.163]	17.01 [14.33 18.43]	-0.95	0.001	0.004
LDL.TG	47.77 [33.075 74.18]	20.66 [16.98 29.96]	-0.98	0.002	0.004
HDL.TG	19.8 [13.69 28.727]	17.76 [15.56 23.56]	-0.18	0.460	0.498
VLDL.P..nmol.L.	59.155 [52.377 93.702]	58.2 [39.52 67.26]	-0.39	0.232	0.335
Large.VLDL.P..nmol.L.	1.425 [1.272 1.735]	1.45 [1.01 1.54]	-0.29	0.259	0.337
Medium.VLDL.P..nmol.L.	5.24 [4.188 7.327]	6.49 [4.76 7.73]	-0.08	0.737	0.767
Small.VLDL.P..nmol.L.	52.04 [45.842 84.303]	48.77 [34.22 56.74]	-0.42	0.187	0.286
LDL.P..nmol.L.	1681.115 [1303.455 1999.363]	1113.73 [951.63 1529.69]	-0.33	0.110	0.198
Large.LDL.P..nmol.L.	224.005 [180.86 300.945]	196.31 [169.26 260.81]	-0.18	0.326	0.385
Medium.LDL.P..nmol.L.	735.28 [495.52 922.03]	352.62 [219.83 624.83]	-0.55	0.069	0.150
Small.LDL.P..nmol.L.	634.715 [542.95 789.835]	580.82 [473.07 644.05]	-0.18	0.297	0.368
HDL.P..Î¼mol.L.	5.32 [3.615 12.35]	18.54 [15.91 24.72]	1.34	<0.001	<0.001
Large.HDL.P..Î¼mol.L.	0.2 [0.135 0.24]	0.29 [0.25 0.31]	0.51	<0.001	0.003
Medium.HDL.P..Î¼mol.L.	6.16 [4.428 9.383]	10.11 [9.29 10.89]	0.55	0.005	0.011
Small.HDL.P..Î¼mol.L.	0 [0 2.007]	8.87 [5.55 14.87]	2.69	<0.001	<0.001
VLDL.Z..nm.	42.18 [42.13 42.192]	42.21 [42.17 42.22]	0	0.114	0.198
LDL.Z..nm.	21.515 [21.248 21.61]	21.41 [21.27 21.49]	-0.01	0.165	0.269
HDL.Z..nm.	9.48 [8.948 9.635]	8.5 [8.37 8.7]	-0.13	<0.001	<0.001
Non.HDL.P..nmol.L.	1756.69 [1351.162 2087.395]	1154.21 [983.29 1611.01]	-0.35	0.097	0.194
Total.P.HDL.P	358.12 [142.53 505.893]	64.65 [43.18 83.21]	-2.13	<0.001	<0.001
LDL.P.HDL.P	335.29 [139.507 485.98]	62.98 [40.82 80.21]	-2.12	<0.001	<0.001

IQR: Interquartile range; FDR: false discovery rate, High GPS=2, Low GPS= 0 and 1

Table S25: Comparison of Lipid Extracts of PDAC patients with High and Low Glasgow Prognostic Scores.

Feature	high GPS, median [IQR]	low GPS, median [IQR]	logchange	p-value	FDR
cholesterol-derivated 1	1838877.733 [1399339.415 2188856.806]	845445.831 [734251.9 990116.729]	-1.02	<0.001	<0.001
cholesterol-derivated 2	713976.393 [514211.961 840433.144]	295324.957 [241317.314 341673.253]	-1.12	<0.001	<0.001
cholesterol-derivated 3	341402.677 [257651.261 377678.363]	196520.631 [183571.723 228268.595]	-0.69	<0.001	<0.001
cholesterol-derivated 4	1848984.481 [1388162.536 2127545.293]	813954.541 [720695.795 993423.177]	-1.04	<0.001	<0.001
cholesterol-derivated 5	258665.006 [235818.206 445270.256]	1231683.507 [928151.912 1458790.961]	1.37	<0.001	<0.001
free cholesterol	11179652.452 [5670212.397 25234377.254]	1621004.841 [1114147.174 2123380.266]	-2.67	0.001	0.003
esterified cholesterol	5516304.87 [1960045.877 9221473.944]	7450489.175 [6558690.801 10139285.423]	0.37	0.212	0.221
cholesterol-derivated 6	405417.504 [264242.514 645307.797]	181794.127 [139078.351 201800.976]	-1.37	<0.001	<0.001
cholesterol-derivated 7	217782.943 [204792.198 278609.246]	297300.737 [263408.439 341489.188]	0.33	0.009	0.012
cholesterol-derivated 8	778831.454 [566540.977 889325.177]	320104.12 [271078.905 409045.39]	-1.08	<0.001	<0.001
cholesterol-derivated 9	133677.674 [108613.443 220788.834]	447673.102 [364168.257 625121.379]	1.19	<0.001	0.001
saturated and omega-9 fatty acid	32283878.454 [24303752.167 43948583.442]	16665031.7 [13998277.304 20611821.637]	-0.97	<0.001	0.001
omega-7 fatty acid	9164120.611 [7991613.618 9882570.015]	7395660.712 [6312502.551 8133738.356]	-0.27	0.005	0.009
omega-6 fatty acid	18520413.701 [15296215.925 25501845.741]	11804748.615 [7649449.43 17830871.134]	-0.58	0.055	0.062
omega-3 fatty acid	2877566.692 [1680420.016 3131650.842]	1186179.04 [1065022.677 1425389.228]	-0.82	0.008	0.013
monounsaturate fatty acid	34436085.175 [22445245.744 47172167.399]	9584302.124 [7123235.817 16219376.588]	-1.49	0.003	0.006
polyunsaturate fatty acid 1 (except linoleic)	12023949.658 [6030773.712 14244873.606]	5307607.746 [4353586.177 6751348.439]	-0.96	0.016	0.020
polyunsaturate fatty acid 2 (except linoleic)	6461707.873 [3878870.149 9208559.993]	3129180.122 [2508022.18 3759142.062]	-0.86	0.021	0.026
linoleic acid	13756390.864 [7784537.979 18614168.382]	5278754.888 [3887379.441 7893981.975]	-1.02	0.013	0.017
phosphatidylcholine	16626493.809 [11152424.435 27658546.682]	6980321.698 [5540573.628 8413805.235]	-1.29	0.001	0.003
sphingomyelin	2609927.697 [1854266.235 3784736.393]	1366298.706 [1269139.277 1780004.99]	-0.86	0.009	0.013
triglyceride	8199897.623 [3961621.536 10801769.759]	4437030.69 [3241239.674 5502530.259]	-0.63	0.114	0.124
glycerophospholipid	12698782.626 [8260574.038 22260606.406]	5283917.432 [4440401.46 6627363.29]	-1.34	0.003	0.006

IQR: Interquartile range; FDR: false discovery rate, High GPS=2, Low GPS= 0 and 1

Table S26: Comparison of Metabolic Ratios of PDAC patients with High and Low Glasgow Prognostic Scores.

Feature	high GPS, median [IQR]	low GPS, median [IQR]	logchange	*p*-value	FDR
Glucose/Lactate	1.201 [0.916 1.63]	1.594 [1.42 1.805]	0.16	0.091	0.273
Pyruvate/Lactate	0.024 [0.016 0.029]	0.021 [0.018 0.029]	0.03	0.821	0.854
Threonine/Glycine	0 [0 0.215]	0.277 [0.242 0.343]	1.34	<0.001	0.005
Glutamine/Glutamate	1.464 [1.109 2.201]	2.299 [0.841 3.237]	0.41	0.220	0.440
3-Hydroxybutyrate/Acetoacetate	2.415 [0.352 4.8]	2.726 [1.32 3.31]	-0.21	0.854	0.854
Glutamate/Alanine	0.549 [0.477 0.909]	0.554 [0.422 0.609]	-0.26	0.390	0.584

IQR: Interquartile range; FDR: false discovery rate, High GPS=2, Low GPS= 0 and 1

Table S27: 6-colour Flow Cytometry Immunophenotyping Panel

Laser Name	Filter	Parameter	Em	lymphocytes	T Cells	NK Cells	B cells, monos & granulocytes	Vol per test (µl)	Optimised volume(µl)	Catalogue #/Clone (2019)
Red 640										
	730/45 BP	Alexa Fluor 700	720		CD4			5		561030, Clone; RPA-T4
Blue 488										
A	780/60 BP	PE-Cy7	780			CD56		5		560916; Clone; B159
C	660/20	PE-Cy5	670			CD16				561725, Clone; 3 G8
D	530/30BP	BB515	515		CD57			5		565285, Clone; NK 1
Violet 405										
Power 50	605/12	BV605	605		CD8			5		564115, Clone; SK1
UV 355										
	530/30	BUV496	496	CD3				5		612941, Clone; UCHT1

BUV: BD Horizon Brilliant™ Ultraviolet; BV: Brilliant Violet™; PE-CY: Phycoerythrin Cyanine; BB515: BD Horizon Brilliant™ Blue;

Table S28: 6-colour Flow Cytometry Immunophenotyping Fluorescence Minus One (FMO) panel

ANTIBODY	**MINUS** **Alexa Flour 700** **CD4**	**MINUS** **PE-Cy 7 CD56**	**MINUS** **PE-Cy5 CD16**	**MINUS** **BB515/FITC CD57**	**MINUS** **BV605 CD8**	**MINUS** **BUV496 CD3**
Alexa Flour 700 CD4		Alexa Flour 700 CD4	Alexa Flour 700 CD4	Alexa Flour 700 CD4	Alexa Flour 700 CD4	Alexa Flour 700 CD4
PE-Cy 7 CD56	PE-Cy 7 CD56		PE-Cy 7 CD56	PE-Cy 7 CD56	PE-Cy 7 CD56	PE-Cy 7 CD56
PE-Cy5 CD16	PE-Cy5 CD16	PE-Cy5 CD16		PE-Cy5 CD16	PE-Cy5 CD16	PE-Cy5 CD16
BB515/FITC CD57	BB515/FITC CD57	BB515/FITC CD57	BB515/FITC CD57		BB515/FITC CD57	BB515/FITC CD57
BV605CD8	BV605CD8	BV605CD8	BV605 CD8	BV605CD8		BV605CD8
BUV496 CD3	BUV496 CD3	BUV496 CD3	BUV496 CD3	BUV496 CD3	BUV496 CD3	

BUV: BD Horizon Brilliant™ Ultraviolet; BV: Brilliant Violet™; PE-CY: Phycoerythrin Cyanine; BB515: BD Horizon Brilliant™ Blue;

Table S29: Comparisons of LAPC01, LAPC02 and RPC01 with the rest of the PDAC groups

Feature	FALSE, median [IQR]	TRUE, median [IQR]	Total, median [IQR]	logchange	*p*-value	FDR
CD16 Granulocytes	73.2 [62.175 81.775]	73 [64.05 77.125]	73.2 [62.175 80.575]	-0.08	0.607	0.639
Lymphs in Leukocytes	66.2 [57.825 74.175]	63.95 [56.725 66.475]	65.3 [57.825 73.8]	-0.12	0.414	0.487
$CD3^+$ in Lymphs	63.3 [52.5 69.575]	78.1 [72.325 80.55]	65.8 [58.075 73.6]	0.27	0.070	0.125
$CD3^-$ in Lymphs	36.1 [29.825 47.5]	21.4 [19.175 26.575]	33.55 [26.25 41.8]	-0.63	0.036	0.090
$CD4^+$ in $CD3^+$	52.9 [50.8 65.5]	11.8 [10.373 23.45]	52.45 [50.625 64.4]	-1.34	0.025	0.084
$CD8^+$ in $CD3^+$	37.95 [29.75 45.625]	82.05 [68.575 85.4]	39.4 [29.95 46.875]	0.89	0.025	0.084
NKTs in $CD3^+$	10.68 [5.417 39.4]	54.7 [16.025 94.85]	13.95 [5.627 45.625]	1.1	0.069	0.125
$CD57^+$ NKTs	41.4 [28.85 50]	58.55 [56.8 65.575]	46.7 [30.25 57.325]	0.62	0.030	0.086
MFI CD57	318 [291.5 399.25]	573 [466.25 794.5]	329 [295 623]	0.38	0.051	0.112
$CD57^+$ NKs	14.85 [3.648 23.15]	64.95 [60.275 68.775]	18.65 [4.613 28.025]	2.04	<0.001	0.003
MFI CD57	218 [155 297.75]	603 [581 650.5]	260.5 [158.75 331.5]	1.43	0.002	0.020

IQR: Interquartile range; FDR: false discovery rate

Table S30: Correlation of Metabolites and Immune cell marker CD57+ NKTs in PDAC

Feature	rho	p-value	FDR
Formate	0.25	0.220	0.602
Unknown signal at 8.12 ppm	0.05	0.803	0.921
Unknown signal at 8.07 ppm	0.02	0.925	0.969
Phenylalanine	0.13	0.535	0.853
Tyrosine	-0.24	0.235	0.602
Unknown signal at 7.14 ppm	0.43	0.029	0.419
Histidine	-0.06	0.764	0.921
Glucose	0.29	0.152	0.602
Mannose	0.27	0.175	0.602
Unknown signal at 5.15 ppm	0.13	0.526	0.853
Unknown signal at 5.09 ppm	0.24	0.247	0.602
Unknown signal at 5.01 ppm	-0.02	0.931	0.969
Ascorbate	-0.5	0.010	0.419
Threonine	0.23	0.248	0.602
Lactate	0.27	0.188	0.602
Creatinine	0.04	0.833	0.921
Creatine	-0.12	0.567	0.876
Glycine	0.45	0.021	0.419
Methanol	-0.14	0.479	0.853
Unknown signal at 2.55 ppm	0.07	0.742	0.921
Citrate	-0.18	0.388	0.733
Glutamine	0.19	0.355	0.714
Pyruvate	0.26	0.194	0.602
Glutamate	0.08	0.681	0.914
Acetoacetate	-0.06	0.774	0.921
Acetate	0.18	0.364	0.714
Alanine	-0.13	0.524	0.853
Unknown signal at 1.45 ppm	0.26	0.197	0.602
Unknown signal at 1.43 ppm	0.09	0.645	0.914
3-Hydroxybutyrate	0	0.983	0.983
Ethanol	0.01	0.965	0.983
Unknown signal at 1.16 ppm	0.13	0.511	0.853
Unknown signal at 1.14 ppm	-0.27	0.185	0.602
Unknown signal at 1.11 ppm	0.09	0.657	0.914
Unknown signal at 1.06 ppm	-0.05	0.820	0.921
Valine	-0.28	0.168	0.602
Isoleucine	0.2	0.324	0.688
Leucine	-0.24	0.229	0.602
2-Hydroxybutyrate	-0.05	0.792	0.921
Protein NH	-0.41	0.041	0.419
Unsaturated lipid -CH=CH-	-0.22	0.290	0.643
Lipid alpha-CH2	0.1	0.630	0.914
Cholesterol	-0.23	0.266	0.616
Lipid =CH-CH2-CH=	-0.32	0.112	0.602
Glycorol phospholipid	0.09	0.668	0.914
Phospholipid	0.06	0.781	0.921
Lipid beta-CH2	-0.31	0.126	0.602
Lipid CH2	-0.04	0.849	0.921
Lipid CH3	-0.41	0.039	0.419
GlycB	0.32	0.110	0.602
GlycA	0.31	0.122	0.602

Rho: spearman's correlation coefficient measures the strength of association between two variables; FDR: false discovery rate

Table S31: Correlation of Metabolites and Immune cell marker CD3+ CD56- NKTs in Pancreatic Ductal Adenocarcinoma

Feature	rho	*p*-value	FDR
Formate	0.4	0.040	0.194
Unknown signal at 8.12 ppm	-0.29	0.152	0.432
Unknown signal at 8.07 ppm	0.47	0.017	0.194
Phenylalanine	0.43	0.028	0.194
Tyrosine	-0.12	0.564	0.774
Unknown signal at 7.14 ppm	0.13	0.513	0.774
Histidine	-0.36	0.069	0.295
Glucose	0.27	0.189	0.507
Mannose	0.25	0.227	0.550
Unknown signal at 5.15 ppm	0.03	0.897	0.934
Unknown signal at 5.09 ppm	0.16	0.431	0.710
Unknown signal at 5.01 ppm	0.11	0.604	0.774
Ascorbate	-0.41	0.036	0.194
Threonine	-0.13	0.537	0.774
Lactate	0.45	0.020	0.194
Creatinine	-0.24	0.231	0.550
Creatine	-0.3	0.137	0.411
Glycine	0.01	0.952	0.952
Methanol	-0.17	0.412	0.710
Unknown signal at 2.55 ppm	0.11	0.607	0.774
Citrate	-0.18	0.376	0.685
Glutamine	-0.43	0.027	0.194
Pyruvate	0.23	0.248	0.550
Glutamate	0.52	0.006	0.194
Acetoacetate	-0.12	0.554	0.774
Acetate	0.12	0.563	0.774
Alanine	-0.07	0.725	0.818
Unknown signal at 1.45 ppm	0.33	0.105	0.357
Unknown signal at 1.43 ppm	0.07	0.737	0.818
3-Hydroxybutyrate	0.07	0.737	0.818
Ethanol	-0.17	0.419	0.710
Unknown signal at 1.16 ppm	0.18	0.367	0.685
Unknown signal at 1.14 ppm	0.07	0.721	0.818
Unknown signal at 1.11 ppm	0.08	0.699	0.818
Unknown signal at 1.06 ppm	-0.11	0.604	0.774
Valine	-0.3	0.137	0.411
Isoleucine	-0.19	0.341	0.685
Leucine	-0.19	0.358	0.685
2-Hydroxybutyrate	0.06	0.786	0.853
Protein NH	-0.41	0.036	0.194
Unsaturated lipid -CH=CH-	0.03	0.877	0.932
Lipid alpha-CH2	0.47	0.016	0.194
Cholesterol	-0.13	0.516	0.774
Lipid =CH-CH2-CH=	-0.19	0.347	0.685
Glycorol phospholipid	0.35	0.077	0.305
Phospholipid	-0.24	0.245	0.550
Lipid beta-CH2	0.08	0.683	0.818
Lipid CH2	0.34	0.087	0.316
Lipid CH3	-0.02	0.931	0.950
GlycB	0.48	0.014	0.194
GlycA	0.4	0.042	0.194

Rho: spearman's correlation coefficient measures the strength of association between two variables; FDR: false discovery rate

Table S32: Correlation of Lipid Extracts and Immune cell marker CD57+NKTs in Pancreatic Ductal Adenocarcinoma.

Feature	rho	*p*-value	FDR
cholesterol-derivated 1	0.61	0.002	0.004
cholesterol-derivated 2	0.67	<0.001	0.003
cholesterol-derivated 3	0.57	0.004	0.007
cholesterol-derivated 4	0.64	0.001	0.003
cholesterol-derivated 5	-0.64	<0.001	0.003
free cholesterol	0.64	0.001	0.003
esterified cholesterol	0.22	0.322	0.336
cholesterol-derivated 6	0.65	<0.001	0.003
cholesterol-derivated 7	-0.53	0.010	0.013
cholesterol-derivated 8	0.64	0.001	0.003
cholesterol-derivated 9	-0.63	0.001	0.003
saturated and omega-9 fatty acid	0.59	0.003	0.006
omega-7 fatty acid	0.42	0.046	0.051
omega-6 fatty acid	0.6	0.003	0.005
Unknown signal at 0.91 ppm	-0.06	0.776	0.776
omega-3 fatty acid	0.68	<0.001	0.003
monounsaturated fatty acid	0.61	0.002	0.004
polyunsaturated fatty acid 1 (except linoleate)	0.56	0.005	0.008
polyunsaturated fatty acid 2 (except linoleate)	0.48	0.021	0.026
Linoleate	0.55	<0.001	0.009
Phosphatidylcholine	0.52	0.010	0.013
Sphingomyelin	0.72	<0.001	0.003
Triglyceride	0.47	0.025	0.029
Glycerophospholipid	0.61	0.002	0.004

Rho: spearman's correlation coefficient measures the strength of association between two variables; FDR: false discovery rate

SUPPLEMENTARY FIGURES

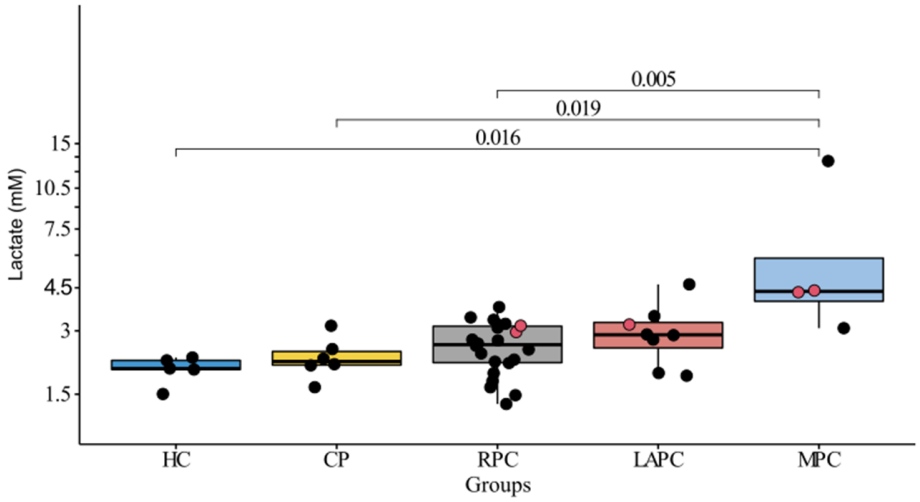


Figure S1: Correlation of Lactate with Cholangitis in PDAC patients: Red dots represent PDAC patients with cholangitis. The cholangitis patients did not have the highest levels of lactate across the PDAC groups. Also, no significant correlation was observed between the elevated lactate levels and cholangitis and this could be due to the sample size limitation. CP: Chronic pancreatitis; RPC: Resectable Pancreatic Ductal Adenocarcinoma; LAPC: Locally Advanced Pancreatic Ductal Adenocarcinoma; MPC: Metastatic Pancreatic Ductal Adenocarcinoma.

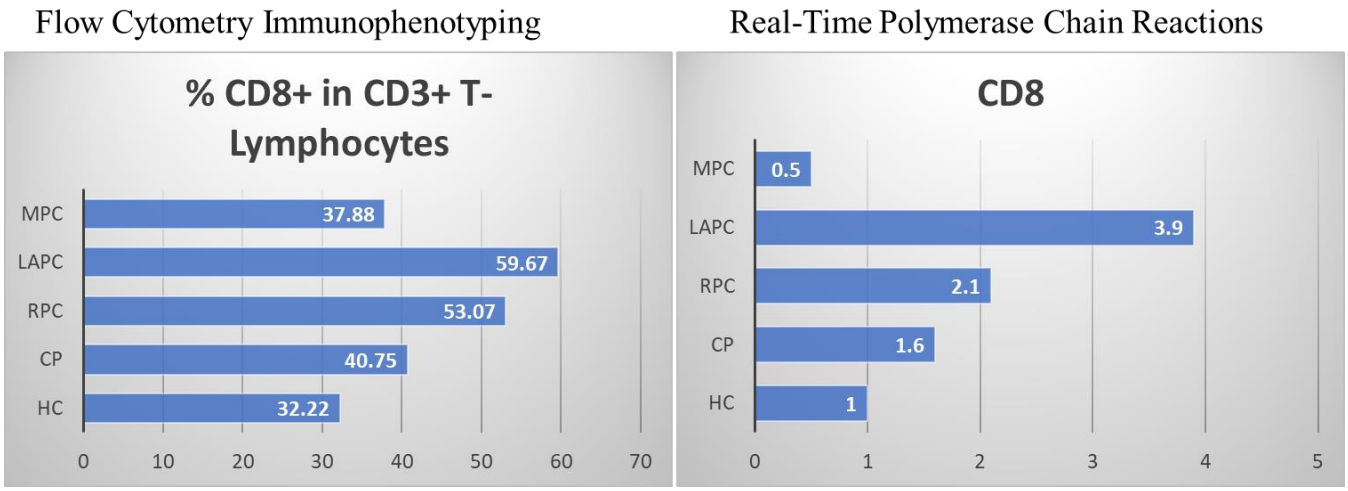
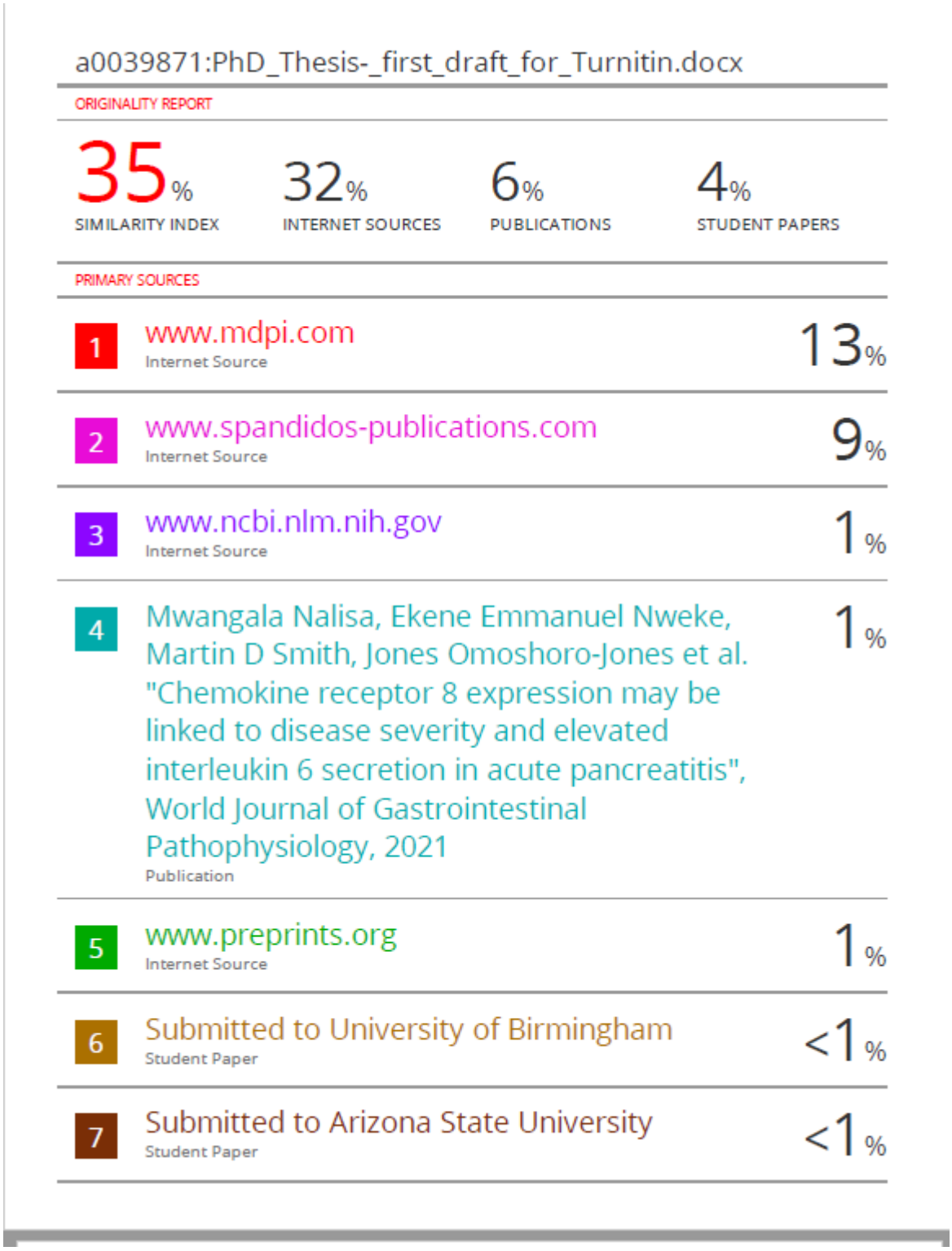


Figure S2: Comparison of Immunophenotyping and Real-Time Polymerase Chain Reactions. The expression of CD8 in both assays was very similar. CD8 was most upregulated in LAPC followed by RPC and then CP. MPC: Metastatic Pancreatic Ductal Adenocarcinoma, LAPC: Locally Advanced Pancreatic Adenocarcinoma, RPC: Resectable Pancreatic Ductal Adenocarcinoma, CP; Chronic Pancreatitis and HC: Healthy Controls.

APPENDIX A: TURNITIN REPORT



a0039871:PhD_Thesis-_first_draft_for_Turnitin.docx

ORIGINALITY REPORT

35%	32%	6%	4%
SIMILARITY INDEX	INTERNET SOURCES	PUBLICATIONS	STUDENT PAPERS

PRIMARY SOURCES

1	www.mdpi.com Internet Source	13%
2	www.spandidos-publications.com Internet Source	9%
3	www.ncbi.nlm.nih.gov Internet Source	1%
4	Mwangala Nalisa, Ekene Emmanuel Nweke, Martin D Smith, Jones Omoshoro-Jones et al. "Chemokine receptor 8 expression may be linked to disease severity and elevated interleukin 6 secretion in acute pancreatitis", World Journal of Gastrointestinal Pathophysiology, 2021 Publication	1%
5	www.preprints.org Internet Source	1%
6	Submitted to University of Birmingham Student Paper	<1%
7	Submitted to Arizona State University Student Paper	<1%

From: Ekene Nweke
To: "Nnenna Elebo"
Subject: RE: Turnitin Report for PhD
Date: Friday, 18 March 2022 13:05:37

Dear Ms Elebo,

Herewith your MMed plagiarism report is attached. Your overall similarity index is 35% with a maximum single matches of 13% and 9% which were from your already published articles from your PhD. All other matches are ≤ 1%. Therefore, your similarity index is **ACCEPTABLE** within our Department.

For PG submissions - Please only submit the Turnitin report PDF pages in the attached report showing the similarity index, as well as this email stating that your plagiarism report is **ACCEPTABLE** within the Department of Surgery.

Kind regards
Emmanuel

From: Nnenna Elebo <500688@students.wits.ac.za>
Sent: Friday, 04 March 2022 11:18
To: Ekene Nweke <Ekene.Nweke@wits.ac.za>
Subject: Turnitin Report for PhD

Good morning Doc, please could you kindly send a turnitin report for my PhD thesis. Thanks

Kind Regards

APPENDIX B: ETHICS CLEARANCE CERTIFICATE

UNIVERSITY OF THE WITWATERSRAND JOHANNESBURG

HUMAN RESEARCH ETHICS COMMITTEE (MEDICAL)

Office of the Deputy Vice-Chancellor (Research & Post Graduate Affairs)

TO: Ms N Elebo
School of Clinical Medicine
Department of Surgery
Medical School
University

E-mail: 500689@students.wits.ac.za

CC: Supervisor: Professor G Candy, et al <Geoffrey.Candy@wits.ac.za>
and <HREC-Medical.ResearchOffice@wits.ac.za>

FROM: Iain Burns
Human Research Ethics Committee (Medical)
Tel: 011 717 1252

E-mail: Iain.Burns@wits.ac.za

DATE: 2019/09/30

REF: *R14/49*

PROTOCOL NO: **M190681** *(This is your ethics application study reference number. Please quote this reference number in all correspondence relating to this study)*

PROJECT TITLE: *Role of metabolites in the immunopathogenesis of Pancreatic Ductal Adenocarcinoma cancer*

Please find attached the Clearance Certificate for the above project. I hope it goes well and that an article in a recognized publication comes out of it. This will reflect well on your professional standing and contribute to the Government funding of the University.

MSWorks2000/Iain2007/Clearscan.wps

APPENDIX C: STUDY INFORMATION DOCUMENT (HEALTHY CONTROLS)

Study title: Metabolites and lipoproteins profiles of a cohort of Pancreatic Ductal Adenocarcinoma patients and associated immune responses.

Greetings Sir/Madam:

Introduction:
Good day, we, Prof. Geoffrey Candy and Nnenna Elebo are carrying out a research study on Pancreatic cancer. Research is a process used in seeking new knowledge. In this study, we want to learn the role of metabolites in Pancreatic Ductal Adenocarcinoma cancer progression. This will be done by drawing blood samples from patients for the three stages of PDAC which are resectable, non-metastatic, and metastatic as well as patients with chronic pancreatitis and healthy volunteers. This will allow us to study the role metabolites play in each stage and compare it with that of the controls (chronic pancreatitis and healthy controls).

Invitation to Participate: For us to study PDAC, we are asking you to take part in this research study.

What is involved in the study: You are among the healthy volunteers we would like to recruit for this study. We are asking for your permission to draw a blood sample, and this will be carried out by qualified persons.

Risks of being involved in the study: There is no risk to you directly, but you might feel some pains during the blood extraction.

Benefits of being in the study: This is a research study. We do not know at this time what we will find if anything. Research studies like this can take years to complete and we need samples from several patients to make sure we are seeing the same differences in all the patients. So, at this time you will not benefit from taking part in this study. However, if you do take part, we may find better ways to treat or diagnose other patients in the future. However, should there be a discovery that may benefit you we would contact your treating doctor who would contact you through your clinic.

Participation is voluntary: If you decide to not participate in the study, this is your right and this will not influence the way you are treated while in hospital. If you decline to take part, we simply will not take the samples indicated. If you change your mind later, we will destroy the samples we have taken. Again, there will be no penalty or loss of benefits or care that you receive. Either way, you will need to contact Prof. Geoffrey Candy to ensure that this happens

– the contact details are below. Finally, your participation in this study will not cost you anything.

Reimbursements: Participation in the study is entirely voluntary and you would not be paid for taking part in the study. None of the scientists or doctors are being paid if you decide to participate in the study.

Confidentiality: As with any medical records, every effort will be made to keep all your personal information confidential. Your name will not be disclosed to any external third parties. In order to keep your identity confidential, a specialised identity code will be assigned to you; only the investigators of this study will have access to the files which link your name to the specialised identity code. However, absolute confidentiality cannot be guaranteed, and personal information may be disclosed if required by law. Organisations such as the Research Ethics Committee of the University of the Witwatersrand may inspect and/or copy your research records for quality assurance and data analysis where this is required (this includes groups such as the Medicines Control Council.
For this study, we are only interested in cancer and diagnosis, not in names and personal information. It is the intention to publish the data, showing proteins that may be of interest for all the patients in the group – not that of individuals participating in the study.

Contact details of researcher/s: If you have further queries or questions, Prof. Geoffrey Candy can be contacted on 011-717 2574 or 083-226 2436

Outputs: As previously mentioned, it is the intention to publish the data, showing proteins that may be of interest for all the patients in the group – not that of individuals participating in the study.

Contact details of HREC administrator and chair:
This study has been approved by the Human Research Ethics Committee (Medical) of the University of the Witwatersrand, Johannesburg ("Committee"). A principal function of this Committee is to safeguard the rights and dignity of all human subjects who agree to participate in a research project and the integrity of the research.
If you have any concerns over the way the study is being conducted, please contact the Chairperson of this Committee who is Professor Clement Penny, who may be contacted on telephone number 011 717 2301, or by e-mail at Clement.Penny@wits.ac.za. The telephone numbers for the Committee secretariat are 011 717 2700/1234 and the e-mail addresses are Zanele.Ndlovu@wits.ac.za and Rhulani.Mukansi@wits.ac.za

Thank you for reading this Study Information Sheet.

Date: February 2019

APPENDIX D: STUDY INFORMATION DOCUMENT (PDAC/CHRONIC PANCREATITIS PATIENTS)

Study title: Metabolites and lipoproteins profiles of a cohort of Pancreatic Ductal Adenocarcinoma patients and associated immune responses.

Greetings Sir/Madam:

Introduction:
Good day, we, Prof. Geoffrey Candy and Nnenna Elebo are researching Pancreatic cancer. Research is a process used in seeking new knowledge. In this study, we want to learn the role of metabolites in Pancreatic Ductal Adenocarcinoma cancer progression. This will be done by drawing blood samples from patients for the three stages of PDAC which are resectable, non-metastatic, and metastatic patients. This will allow us to study the role metabolites play in each stage and compare it with that of the control which will be chronic pancreatitis

This is a research study and is not part of the normal and routine care which you will receive while in hospital. The study hopes to find out why cancer starts, what makes it different, and hopefully, find ways to best kill it by using drugs or other treatment therapies.

Invitation to Participate: In order for us to study pancreatic adenocarcinoma cancer, we are asking you to take part in this research study.

What is involved in the study: You have been diagnosed with one of the three classes of PDAC or chronic pancreatitis disease which would be used as a control group in this study. In this study only your blood samples would be required, and they will be taken once. About 16 ml of your blood will be extracted in two different tubes: purple cap tube (10 ml) and red cap tube (6 ml). The blood samples collected will be processed into serum, plasma, and cells. Various techniques will be used to analyse the metabolites present in the blood at each stage of cancer and compared with each other as well as with the control blood samples.

Risks of being involved in the study: We are extracting the blood through your veins, and this could cause some discomfort and pains but there is no risk to you. Furthermore, this extraction will be done by the interns in the surgery division unit 1, that are trained to do so safely.

Benefits of being in the study: This is a research study. We do not know at this time what we will find if anything. Research studies like this can take years to complete and we need samples from a number of patients to make sure we are seeing the same differences in all the patients. So, at this time, you will not benefit from taking part in this study. However, if you do take part, we may find better ways to treat or diagnose other chronic pancreatitis patients in the future by discovering ways of preventing its progression to cancer. However, should there be

a discovery that may benefit you we would contact your treating doctor who would contact you through your clinic.

Participation is voluntary: If you decide not to participate in the study, this is your right and this will not influence the way you are treated while in hospital. If you decline to take part, we simply will not take the samples indicated. If you change your mind later, we will destroy the samples we have taken. Again, there will be no penalty or loss of benefits or care that you receive. Either way, you will need to contact Prof. Geoffrey Candy to ensure that this happens – the contact details are below. Finally, your participation in this study will not cost you anything.

Reimbursements: Participation in the study is entirely voluntary and you would not be paid for taking part in the study. None of the scientists or doctors are being paid if you decide to participate in the study.

Confidentiality: As with any medical records, every effort will be made to keep all your personal information confidential. Your name will not be disclosed to any external third parties. In order to keep your identity confidential, a specialised identity code will be assigned to you; only the investigators of this study will have access to the files which link your name to the specialised identity code. However, absolute confidentiality cannot be guaranteed, and personal information may be disclosed if required by law. Organisations such as the Research Ethics Committee of the University of the Witwatersrand may inspect and/or copy your research records for quality assurance and data analysis where this is required (this includes groups such as the Medicines Control Council.
For this study, we are only interested in the pancreatic ductal adenocarcinoma cancer and diagnosis, not in names and personal information. We intend to publish the data, showing blood samples that may be of interest for all the patients in the group – not that of individuals participating in the study.

Contact details of researcher/s: If you have further queries or questions, Prof. Geoffrey Candy can be contacted on 011-717 2574 or 083-226 2436

Outputs: As previously mentioned, we intend to publish the data, showing blood samples that may be of interest to all the patients in the group – not that of individuals participating in the study, and these articles would be shown to you if interested.

Contact details of HREC administrator and chair:
This study has been approved by the Human Research Ethics Committee (Medical) of the University of the Witwatersrand, Johannesburg ("Committee"). A principal function of this Committee is to safeguard the rights and dignity of all human subjects who agree to participate in a research project and the integrity of the research.
If you have any concerns over the way the study is being conducted, please contact the Chairperson of this Committee who is Professor Clement Penny, who may be contacted on telephone number 011 717 2301, or by e-mail at Clement.Penny@wits.ac.za. The telephone numbers for the Committee secretariat are 011 717 2700/1234 and the e-mail addresses are Zanele.Ndlovu@wits.ac.za and Rhulani.Mukansi@wits.ac.za

Thank you for reading this Study Information Sheet
Date: May 2019

APPENDIX E: INFORMED CONSENT

UNIVERSITY OF THE WITWATERSRAND, JOHANNESBURG

Consent Form: Metabolites and lipoproteins profiles of a cohort of Pancreatic Ductal Adenocarcinoma patients and associated immune responses.

Dear Patient,
You are currently admitted to our hospital and have been diagnosed with Pancreatic Ductal Adenocarcinoma Cancer (PDAC). The Hospital not only renders treatment but is also actively involved in conducting research aimed at improving the quality of care that we deliver. From time to time such research involves the use of patient records from which information is extracted. We will also be using samples taken through your vein for this research study. This sample extraction will not jeopardize your safety and there will be no risk at all. The use of such information and sample is subject to the following:

1. Approval from the Human Research Ethics Committee (Medical) of the University of the Witwatersrand.
2. As with any medical records, every effort will be made to keep all your personal information confidential. Your name will not be disclosed to any external third parties. In order to keep your identity confidential, a specialised identity code will be assigned to you; only the investigators of this study will have access to the files which link your name to the specialised identity code. However, absolute confidentiality cannot be guaranteed, and personal information may be disclosed if required by law. Organisations such as the Research Ethics Committee of the University of the Witwatersrand may inspect and/or copy your research records for quality assurance and data analysis where this is required for this study we are only interested in cancer and diagnosis, not in names and personal information. It is the intention to publish the data, showing metabolites that may be of interest for all the patients in the group – not that of individuals participating in the study.

We would like to obtain your consent to use information from your file for this research, subject to the aforementioned conditions. If you choose not to give consent, this will not compromise your treatment in any way. If at any time you choose to withdraw consent, you are free to do so and will not be prejudiced in any way.

Should you wish to contact us at any stage regarding consent, contact Dr. Jones Omoshoro at (011) 9339267 or Professor Geoffrey Candy 011-7172574

A. Consent Given

I_____ hereby give consent for my records to be used as per the above-mentioned conditions for the purposes of research:

PATIENT: _____
Name Signature Date

RESEARCHER: _____
Name Signature Date

WITNESS: _____
Name Signature Date

APPENDIX F: PERMISSION TO CONDUCT RESEARCH



PERMISSION TO CONDUCT RESEARCH

Date: 11th, May 2019

TITLE OF PROJECT: Metabolites and lipoproteins profiles of a cohort of Pancreatic Ductal Adenocarcinoma patients and associated immune responses.

UNIVERSITY: Witwatersrand

Principal Investigator: Nnenna Elebo

Department: Surgery

Supervisor: Dr JAO Omoshoro-Jones

Permission Head Department (where research conducted): Yes

The Medical Advisory Committee recommends that the said research be conducted at Chris HaniBaragwanath Academic Hospital. The CEO/ management of Chris Hani Baragwanath Academic Hospital is accordingly informed and the study issue, subject to:-

- **Permission having been granted by the Committee for Research on Human Subjects of the University of the Witwatersrand.**
- The Hospital will not incur extra costs as a result of the research being conducted on its patients within the hospital
- The MAC will be informed of any serious adverse events as soon as they occur

Permission is granted for the duration of the Ethics Committee Approval: ·

Recommended
(On behalf of the MAC)
Date: 17/05/2019

Approved/Not Approved
Hospital Management
Date: 25/05/2019